



Universiteit  
Leiden  
The Netherlands

## **Modulation of the canonical Wnt signaling pathway in bone and cartilage**

Miclea, R.L.

### **Citation**

Miclea, R. L. (2011, November 30). *Modulation of the canonical Wnt signaling pathway in bone and cartilage*. Retrieved from <https://hdl.handle.net/1887/18153>

Version: Corrected Publisher's Version

License: [Licence agreement concerning inclusion of doctoral thesis in the Institutional Repository of the University of Leiden](#)

Downloaded from: <https://hdl.handle.net/1887/18153>

**Note:** To cite this publication please use the final published version (if applicable).





**Modulation of the  
canonical Wnt signaling pathway  
in bone and cartilage**

**Răzvan Lucian Miclea**

The studies presented in this thesis were financially supported by an unrestricted educational grant from Ipsen Farmaceutica BV, by a research fellowship from the European Society for Pediatric Endocrinology, by a research grant from The Human Growth Foundation, and by a research grant from the Association for International Cancer Research.

Financial support for the costs associated with the publication of this thesis from the Department of Pediatrics of the Leiden University Medical Centre, the Jurriaanse Foundation, the Dutch Arthritis Association, Ipsen Farmaceutica BV, the Dutch Society for Calcium and Bone Metabolism, Ferring BV (Hoofddorp), Goodlife, Guerbet, Novo Nordisk, Oldelft, Pfizer, Servier, Toshiba and Greiner Bio – One is gratefully acknowledged.

Graphic design: dr. P.D. Feitsma.

Cover: Marleen de Jager.

Printed by: Off Page.

ISBN:

© 2011 R.L. Miclea, Leiderdorp, the Netherlands.

All rights reserved. No part of this publication may be reproduced in any form or by any means without prior permission of the author.

# **Modulation of the canonical Wnt signaling pathway in bone and cartilage**

Proefschrift

ter verkrijging van  
de graad van Doctor aan de Universiteit Leiden,  
op gezag van Rector Magnificus prof. mr. P.F. van der Heijden,  
volgens besluit van het College voor Promoties  
te verdedigen op  
woensdag 30 november 2011  
klokke 11.15 uur

door

**Răzvan Lucian Miclea**

geboren te Oradea, Roemenië  
in 1979

## **PROMOTIECOMMISSIE**

### **Promotor**

Prof. dr. J. M. Wit

### **Co-promotoren**

Dr. H. B. J. Karperien (Universiteit van Twente)

Dr. E. C. Robanus-Maandag

### **Overige leden**

Prof. dr. P. ten Dijke

Prof. dr. J. P. T. M. van Leeuwen (Erasmus Universiteit Rotterdam)

Prof. dr. M. Richardson

*Celor două mele pupile*





# Contents

<b>Chapter 1</b>	General introduction	11
<b>Chapter 2</b>	Adenomatous polyposis coli-mediated control of $\beta$ -catenin is essential for both chondrogenic and osteogenic differentiation of skeletal precursors	39
<b>Chapter 3</b>	Adenomatous polyposis coli-gene dosage controls $\beta$ -catenin-mediated differentiation of skeletal precursors	63
<b>Chapter 4</b>	Apc bridges Wnt/ $\beta$ -catenin and BMP signaling during osteoblast differentiation of KS483 cells	85
<b>Chapter 5</b>	<i>APC</i> mutations are associated with increased bone mineral density in patients with familial adenomatous polyposis	107
<b>Chapter 6</b>	Inhibition of Gsk3 $\beta$ in cartilage induces osteoarthritic features through activation of the canonical Wnt signaling pathway	127
<b>Chapter 7</b>	Summary, conclusions, directions for future research	157
	Samenvatting	167
	List of publications	175
	Curriculum vitae	179
	Dankwoord	183



# **Chapter 1**

## **General introduction**



# General introduction

## I. DEVELOPMENT OF THE ENDOCHONDRAL SKELETON

The formation of most of the vertebrate skeleton occurs via endochondral bone formation, a process which begins with the aggregation, proliferation and condensation of mesenchymal cells (MCs) at specific locations within the embryo where the skeletal elements will arise. MCs can be of three origins: the neural crest (forming some craniofacial bones), the sclerotome of the paraxial mesoderm (forming the axial skeleton), or the lateral plate mesoderm (forming the appendicular skeleton). MCs commit to the skeletal lineage once they differentiate into skeletal precursor cells (SPCs), cells from which both chondrocytes and osteoblasts can derive. At the periphery of these condensations, SPCs form a perichondrial layer, while in the core they differentiate into chondrocytes that start producing cartilage-specific extracellular matrix (ECM) proteins and continue to proliferate. Continuous division of chondrocytes and further secretion of ECM together contribute to the elongation of the cartilage template, which prefigures the shape of the future bone. Once the cartilaginous template is formed, the innermost chondrocytes mature, exit from the cell cycle, and become hypertrophic, secreting a progressively calcified ECM. Simultaneously with the onset of hypertrophic chondrocyte differentiation, perichondrial SPCs differentiate into osteoblasts, forming a tight, yet adaptable sheath (later called periosteum), which modulates the final size and shape of the cartilage template. When the cartilage ECM is mineralized, concurrent vascular invasion and apoptosis of terminal hypertrophic chondrocytes together contribute to the formation of the primary ossification centre, the first region of the cartilaginous anlage that will be replaced by bone. This complex differentiation program radiates centrifugally, leading to the development of trabecular bone (the primary spongiosa) (1-6) (Figure 1).

Vascular invasion of the primary spongiosa continues via the so-called “periosteal buds” that provide SPCs (later forming osteoblasts), hematopoietic cells (later forming osteoclasts) and blood vessels, which grow from the periosteum to reach the primary ossification center. Osteoblasts attach to spicules of calcified scaffolds left behind by dying chondrocytes and begin producing osteoid, a gelatinous substance made up of collagen and mucopolysaccharide. Soon after the osteoid is laid down, inorganic salts are deposited in it to form mineralized bone. In turn, osteoclasts break down spongy bone to form the medullary cavity filled with bone marrow, the main site for haematopoiesis in post-natal life (7;8).

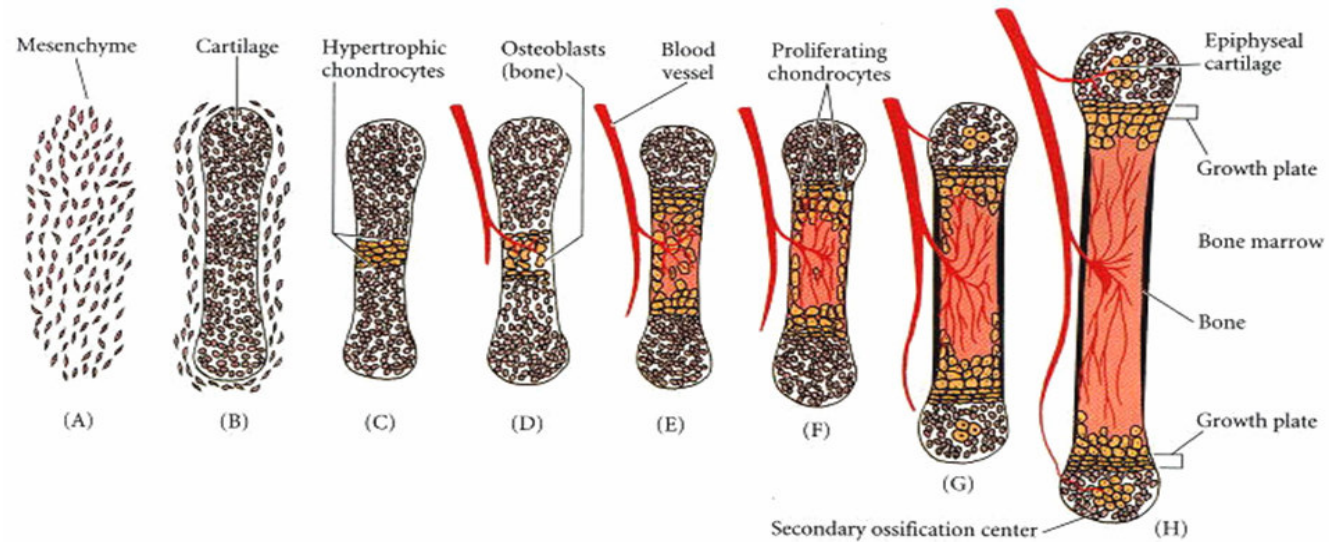


**Figure 1. Schematic diagram of endochondral ossification.** (A, B) Mesenchymal cells condense and differentiate into chondrocytes to form the cartilaginous model of the bone. (C) Chondrocytes in the center of the shaft undergo hypertrophy and apoptosis while they change and mineralize their extracellular matrix. Their death allows blood vessels to enter. (D, E) Blood vessels bring in osteoblasts, which bind to the degenerating cartilaginous matrix and deposit bone matrix. (F-H) Bone formation and growth consist of ordered arrays of proliferating, hypertrophic, and mineralizing chondrocytes. Secondary ossification centers also form as blood vessels enter near the tips of the bone, physically separating AC from GP. Reprinted with permission from Gilbert SF, *Developmental Biology*, 6th edition, Sunderland (MA): Sinauer Associates; 2000

The fascinating multi-step process of endochondral bone formation described above, continues postnatally in the growth plates (GP). This highly specialized cartilage structure develops at the distal ends of any growing endochondral bone, secondary to the ordered buildup of the diaphyseal bone from the primary ossification centre. GP activity leads to the persistent formation of chondrocytes and cartilage ECM. This does not, however, lead to a perpetual increase in GP height, since the process of tissue production is balanced by a tightly regulated process of tissue resorption at the epiphyseal/metaphyseal interface (9). GPs are spatially polarized biological structures, comprising several distinct chondrocyte layers: resting, proliferating, prehypertrophic, and hypertrophic, proceeding from the cartilaginous epiphysis to the bony diaphysis (Figure 2). Chondrocyte proliferation, matrix production and hypertrophy in the GP is responsible for the rate of longitudinal growth as well as for the ultimate length of all endochondral bones until the end of puberty, when GPs disappear and bone growth ceases (10;11).

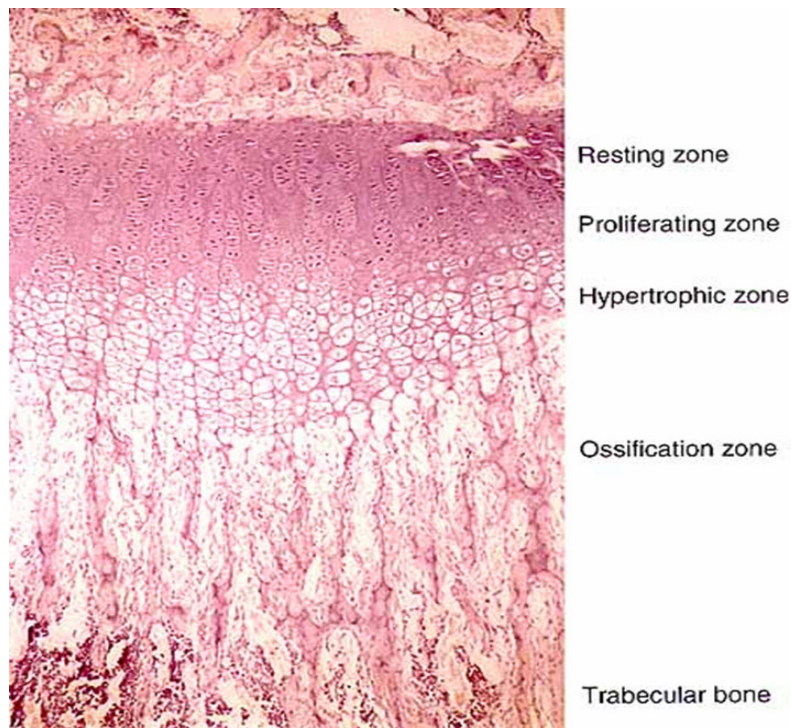


**Figure 2.** Section of the epiphyseal growth plate from the proximal tibia of a three-week-old mouse depicts the different chondrocyte layers within the growth plate.



Upon a certain trigger, MCs from the resting zone differentiate into chondrocytes assuming a flattened shape and organizing into longitudinal columns. These chondrocytes proliferate at a high rate until they exit the cell cycle and start to mature and increase in size, undergoing prehypertrophy followed by full hypertrophy. Ultimately, hypertrophic chondrocytes undergo cell death allowing primary ossification centers to expand. During the development and growth of endochondral bones, most of the skeletal cartilage is therefore an ephemeral tissue, with two main functions: 1) to compute the size and the shape of the future bone, and 2) to provide the scaffold in which bone will form.

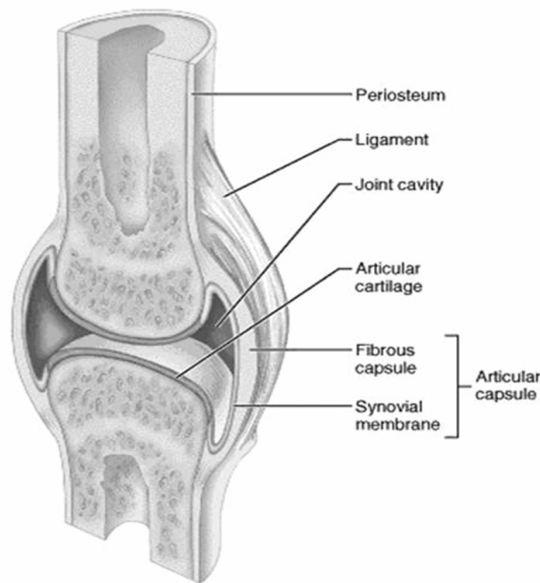


**Figure 3.** Longitudinal section through a synovial joint depicts its main components.

On the surfaces of diarthrodial joints permanent articular cartilage (AC) maintains joint function throughout life (Figure 3). In marked contrast with the GP, AC retains a stable phenotype, providing the tissue with functional adaptability. During embryogenesis, joint development begins at specific skeletal sites before any chondrocyte differentiation occurs from MCs. At the site of the future joint, condensed MCs do not differentiate into chondrocytes, become highly packed and flattened to form the so-called “interzone”. In the middle of the interzone, a cavity will shape via apoptosis, separating the two skeletal elements to be articulated. On each epiphyseal end of these skeletal elements, chondrocytes start differentiating from a layer of perichondrium-like cells to give rise to AC. These articular chondrocytes are responsible for the initial longitudinal lengthening of the elements through appositional growth, until GPs are fully functional and become the source of self-renewing proliferating chondrocytes and the main mechanism of longitudinal growth. Through a process of endochondral

bone formation, chondrocytes in the centre of the epiphysis will form the scaffold for the second ossification centre, so that only the most epiphyseal among them will survive to become authentic articular chondrocytes (12-14).

## II. DEVELOPMENTAL REGULATION OF SKELETOGENESIS

The vertebrate skeleton contains three different cell types spread within the ECM: chondrocytes (cartilage cells), osteoblasts (bone cells) and osteoclasts (cartilage- and bone-resorbing cells). Once differentiated, chondrocytes, osteoblasts and osteoclasts complete one another's functions to accomplish longitudinal bone growth, and maintain skeletal remodeling (formation following resorption), matrix mineralization and bone mass. Regulation of the various steps of skeletal cell differentiation, proliferation and survival is the result of a very complex and formidable interaction between transcription factors, systemic hormones, growth factors, the surrounding matrix, but also environmental and mechanical signals.

### II. a. Transcriptional regulation of skeletogenesis

Initially identified due to its inactivating mutations in patients with campomelic dysplasia, Sex determining region Y (SRY)-box 9 (Sox9) is generally accepted as the master transcription factor for the commitment of MCs to the chondrogenic lineage (15;16). *Sox9* can first be detected in MCs condensing at the site of the future endochondral bone and continues to be expressed by chondrocytes throughout their subsequent differentiation steps until they become hypertrophic (17). Although this spatio-temporal expression pattern resembles the one of  $\alpha 1(II)$  collagen (*Col2a1*), *Sox9* expression begins scarcely earlier (18). Besides stimulating and coordinating the formation of mesenchymal condensations, Sox9 also regulates the expression of *Col2a1*, but also of other chondrocyte markers, like *Aggrecan (Acan)*, and  $\alpha 1(XI)$  collagen (*Col11a1*) (19-24). Furthermore, it has been shown that Sox9 not only controls proliferation and differentiation of chondrocytes, but it also prevents them from entering hypertrophy (25-27). L-Sox5 and Sox6, two other high-mobility group (HMG) domain-containing transcription factors, are also expressed in all precartilaginous condensations and in nonhypertrophic chondrocytes (28). Like Sox9, they are essential for chondrogenesis and together promote the expression of chondrocytic genes, like *Col2a1* and *Acan* (22;29).

Hypertrophy, the last chondrocytic differentiation step during endochondral bone formation, is induced by a member of the Runt domain family of transcription factors (RunX2), also known as core binding factor  $\alpha 1$  (Cbfa1). *RunX2*, which is transiently expressed by prehypertrophic chondrocytes, is essential for chondrocytes to enter maturation and for the expression of  $\alpha 1(X)$  collagen (*Col10a1*), a typical marker for hypertrophic chondrocytes (30-33). However, RunX2 is not the sole transcription factor known to stimulate chondrocyte hypertrophy, as genetic studies indicate similar roles

for RunX3, another member of the Runt domain family of transcription factors, and also for Twist-1 (34;35).

Already introduced as a dominant regulator of chondrocyte hypertrophy, RunX2/Cbfa1 was originally identified and described as the critical transcription factor for the commitment of MCs to the osteogenic lineage (36). During development, *RunX2* begins to be expressed in mesenchymal condensations, while later during development it is expressed at high levels in osteoblasts and at much lower levels in pre-hypertrophic chondrocytes, but never in other cells (37). Osteoblasts do not develop in *RunX2* null mice, while heterozygous *RunX2* mutants display skeletal anomalies similar to those observed in patients with cleidocranial dysplasia: hypoplastic clavicles and delayed closure of the fontanelles (37-40). RunX2 promotes osteogenesis, by positively regulating nearly all osteogenic genes, like *Osteocalcin* (*Ocn*) and bone sialoproteins (36).

Besides Runx2, Osterix (*Osx*), a zinc finger-containing transcription factor, is also essential for osteoblast differentiation (41). Specifically expressed in osteoblasts, *Osx* acts downstream of RunX2 during osteoblast differentiation and its expression is regulated by RunX2 (42). *Osx* inactivation in mice leads to perinatal lethality due to a complete absence of bone formation (41). Unlike Runx2-deficient mice whose skeleton is entirely nonmineralized, the *Osx*-deficient mice lack a mineralized matrix in intramembranous bones only. This suggests that *Osx*, unlike Runx2, is not required for chondrocyte hypertrophy, thereby demonstrating that *Osx* specifically induces osteoblast differentiation and bone formation *in vivo*.

## II. b. Paracrine regulation of skeletogenesis

Besides transcription factors, a wide variety of locally produced growth factors play a crucial role during skeletal development and maintenance. Such regulating growth factors are Indian Hedgehog (Ihh), parathyroid related hormone (PTHrP), bone morphogenetic proteins (BMPs) and members of the Wnt family of morphogens.

Within the growth plate, chondrocyte proliferation and maturation are tightly regulated by a negative feedback loop between Ihh and PTHrP. PTHrP inhibits the rate at which chondrocytes proliferate and are converted to post-proliferative hypertrophic chondrocytes. PTHrP's expression in periarticular chondrocytes is dependent on Ihh, which is expressed at the prehypertrophic-hypertrophic boundary so that cells that escape the inhibitory action of PTHrP signaling in the growth plate express Ihh, which in turn will stimulate PTHrP expression (43-46).

BMPs are members of the TGF $\beta$  superfamily of growth factors initially isolated from demineralized bone and osteosarcomas. They are best known for their chondro- and osteoinductive effects during skeletal development and patterning (47;48). BMPs bind to type II and type I serine/threonine kinase receptors, thereby initiating intracellular signaling by activating Smad proteins. Early in skeletal development, BMPs promote the condensation step of MCs by stimulating cell-cell interaction through upregulation of N-cadherin function and expression (49). Studies have demonstrated the requirement of BMPs for Sox gene expression in chondrogenesis (50;51) and their stimulatory effect on *Sox9* and *Col2a1* in multipotential mesenchymal C3H10T1/2 cells

and monopotential chondroprogenitor MC615 cells (52). Additionally, BMPs increase the expression of the specific hypertrophic chondrocyte marker *Col10a1* by inducing its promoter activity (53-55). BMPs also induce osteoblastogenesis from MCs to promote osteoblastic maturation and function (56;57), a process that requires interactions of Smad 1/5 and RunX2 (58;59).

Wnts are a family of highly conserved secreted glycoproteins with important roles during cell specification, formation of the body plan, cell growth, differentiation and apoptosis (60). Up to date 19 human Wnt genes have been identified in humans and mice. Wnts can activate a number of different signal transduction pathways, the so-called non-canonical pathways, which include the planar cell polarity and  $Ca^{2+}$  pathways, and the canonical Wnt/ $\beta$ -catenin pathway (61). Several members of this growth factor family have inhibitory effects on chondrogenesis (62-66), while their effect on osteoblastogenesis remains heterogeneous. Wnt3a promotes osteoblast proliferation, but suppresses osteoblastogenesis from human mesenchymal stem cells *in vitro* (67;68). Furthermore, Wnt3a and Wnt5a prevent osteoblast apoptosis (69). At the same time, Wnt-10b stimulates osteoblast differentiation from bi-potential skeletal precursor cells (SPCs) by activating RunX2, Osterix and Dlx5 and inhibits adipocyte formation (70).

### III. SKELETAL PATHOLOGY

#### III. a. Growth disorders

Growth is the key characteristic that distinguishes children from adults, and growth disturbances are frequently presented to health personnel at all levels (youth health care, general practitioners, paediatricians, paediatric endocrinologists). Disturbances of longitudinal bone growth occur quite frequently with a high diversity in etiology. Both short and tall stature disorders are divided into primary (skeletal defect), secondary (non-skeletal defect), or idiopathic (cause unknown) (71). Whereas primary growth disorders may have a prenatal onset and may be of chromosomal or genetic origin, secondary growth syndromes are frequently the result of hormonal disturbances. Although growth disorders do not necessarily lead to clinical problems, relatively often they are considered a disability by the affected individuals resulting in psychological, social, educational and professional consequences in childhood, adolescence, but also adulthood. Exposure of patients to gluten prevents healing of gut mucosa, reactivation of specific T cells and reappearance of symptoms. Although not every patient is equally sensitive to gluten exposure, it was reported that exposure to 1 mg of gluten prevented mucosal recovery (35). Therefore, to safeguard patients from gluten exposure, sensitive methods for gluten detection are required and have been developed.

### **III. b. Osteoarthritis**

Osteoarthritis (OA) represents one of the two most frequent chronic skeletal diseases and is undoubtedly by far the most common cause limiting the daily activities of the elderly population (72). OA is characterized by a progressive loss of articular cartilage, synovial proliferation, osteophyte formation and subchondral sclerosis that may culminate in pain, loss of joint function, and disability (73). A variety of risk factors and pathophysiologic processes contribute to the progressive nature of the disease and serve as targets for behavioral and pharmacologic interventions. Risk factors such as age, sex, trauma, overuse, genetics, and obesity can each make contributions to the process of injury in different compartments of the joint (74;75). Although the etiology of OA is not completely understood, it appears to be the result of mechanical, biochemical and enzymatic factors. The final common pathway of these interactions is the failure of the chondrocytes to maintain a homeostatic balance between cartilage formation and resorption (76;77). Loss of articular cartilage is mainly due to proteolytic enzymes that can degrade both proteoglycans (aggrecanases) and collagen (collagenases) (78). Cartilage collagen is cleaved by matrix metalloproteinase (MMP) 1, 8, and 13 (79). Of these three MMPs, MMP13 appears to be the most important in OA because it preferentially degrades type II collagen (80) and its expression is significantly increased in OA (81). Typical phenotypic changes in OA cartilage include the development of the hypertrophic chondrocyte phenotype normally not present in articular cartilage, characterized by increased production of MMP-13, type X collagen, and alkaline phosphatase (ALP) (75).

### **III. c. Osteoporosis**

Osteoporosis is the other most frequent chronic skeletal disease, characterized by low bone mass, concurrent disruption of the bone micro-architecture, and decreased bone strength. Consequently, osteoporotic bones are more fragile and there is increased risk of fracture, particularly of the spine, hip, wrist, humerus, and pelvis (82). Osteoporosis affects an estimated 300 million people worldwide (83). About one in two white women will experience an osteoporotic fracture in her lifetime (84), while older men affected by osteoporosis have a higher mortality from hip fractures and a lower frequency of screening and treatment (85). The risk of fractures increases dramatically with age and most of those affected are over 75 (86). Since the elderly constitute the fastest-growing age group in the world, the number of osteoporotic fractures is predicted to increase considerably with the continued aging of this population in future decades (87;88). Physiological age-related bone loss starts in the 4<sup>th</sup> or 5<sup>th</sup> decade of life, as a result of increased bone breakdown by osteoclasts and decreased bone formation by osteoblasts (89). The role of oestrogen deficiency in menopausal bone loss in women is well documented, and bone mass in elderly men is also related to oestrogen levels. Vitamin D insufficiency and secondary hyperparathyroidism are common in elderly people and may also contribute. Other possible factors are reduced physical activity with ageing and decreased production of insulin-like growth factors. As described above, osteoporosis installs due to involutinal changes of aging and to

hormonal changes of menopause, being thereby classified as primary. However, osteoporosis can also be caused or worsened by other diseases or medications, when it is referred to as secondary (90).

Bone mineral density (BMD) represents the average concentration of minerals per unit area of bone (measured in  $\text{g}/\text{cm}^2$ ). In 1994, the World Health Organization established operational definitions of osteoporosis and osteopenia based on BMD (91). According to this classification normal BMD is defined above -1.0 SD of the young adult reference mean (T-score above -1.0), osteopenia is defined between -1.0 and -2.5 SD of the young adult reference mean (T-score between -1.0 and -2.5), osteoporosis is defined below -2.5 SD of the young adult reference mean (T-score at or below -2.5), while severe osteoporosis requires an osteoporotic BMD in the presence of 1 or more fragility fractures. Different treatments for osteoporosis are available, all aimed at reducing the risk of fractures. Estrogen treatment in post-menopausal women, selective modulators of estrogen receptors (especially raloxifene), calcitonin, a recombinant form of parathormone (teriparatide), strontium ralenate, and especially bisphosphonates, are drugs widely used in clinical practice (92).

#### **IV. CANONICAL WNT SIGNALING DURING SKELETOGENESIS**

Increasing amount of evidence points out to the important role of the canonical Wnt/ $\beta$ -catenin signaling in essentially all aspects of skeletal development and maintenance. This pathway is composed of evolutionarily-conserved cellular components, and controls cell proliferation and cell fate determination by inducing changes in gene expression (93). Signaling through this pathway depends on the intracellular levels of its core component,  $\beta$ -catenin.  $\beta$ -catenin is a molecule involved in cell adhesion via its interaction with E-cadherin and  $\alpha$ -catenin (94). In the absence of the Wnt ligand,  $\beta$ -catenin is phosphorylated at the  $\text{NH}_2$ -terminus by glycogen synthase kinase 3 beta (GSK3 $\beta$ ) and casein kinase 1 (CK1) in a “destruction” complex brought together by two scaffolding proteins, Axin and Adenomatous polyposis coli (APC). This phosphorylation ultimately results in the ubiquitylation and proteasomal degradation of  $\beta$ -catenin (Figure 4A). When Wnts bind to the 7 transmembrane Frizzled receptors and LDL related protein 5 or 6 (LRP5/6) co-receptors, Dishevelled (Dsh) is activated, leading to suppression of GSK3 $\beta$  activity. As a result,  $\beta$ -catenin will not undergo phosphorylation anymore. Cytoplasmic  $\beta$ -catenin stabilizes and upon reaching a certain level it will translocate into the nucleus where it interacts with transcription factors such as lymphoid enhancer-binding factor 1/T cell-specific transcription factor (LEF/TCF) to initiate the transcription of target genes (95) (Figure 4B). Cells also secrete several Wnt antagonists like secreted frizzled-related proteins (SFRPs), Dickkopf (DKK) and Sclerostin (SOST) (96-98).

APC is involved in a wide variety of cellular processes such as signal transduction, cytoskeletal organization, apoptosis, cell adhesion and motility, cell fate determination and chromosomal stability (99). However, biochemical and genetic evidence was provided showing that APC's main suppressor activity resides in its ability to bind to  $\beta$ -

catenin and induce its degradation, thereby acting as a strong negative regulator of the canonical Wnt pathway (100). The failure of mutated *APC* to direct cytosolic  $\beta$ -catenin to degradation causes cytoplasmic accumulation of  $\beta$ -catenin and, subsequently, its translocation to the nucleus. *Apc* influences the differentiation capacity of mouse embryonic stem (ES) cells in a quantitative and qualitative fashion depending on the dose of  $\beta$ -catenin signalling (101;102). The differentiation ability and sensitivity of ES cells is inhibited by increasing dosages of  $\beta$ -catenin signaling, ranging from a severe differentiation blockade in severely truncated *Apc* alleles, to more specific neuroectodermal, dorsal mesodermal and endodermal defects in more hypomorphic alleles. Exclusive levels of APC/ $\beta$ -catenin signaling differentially affect stem cell differentiation (100).

Identified originally as a regulator of glycogen metabolism, GSK3 $\beta$  is now a well-established negative modulator of the canonical Wnt signaling pathway, by inducing degradation of  $\beta$ -catenin (103;104). It also plays important roles in protein synthesis, cell proliferation, cell differentiation, microtubule dynamics and cell motility by phosphorylating initiation factors, components of the cell-division cycle, transcription factors and proteins involved in microtubule function and cell adhesion (105). It is constitutively active and unlike many kinases that are activated following stimulus-dependent phosphorylation, GSK3 $\beta$  is inactivated following phosphorylation (106).

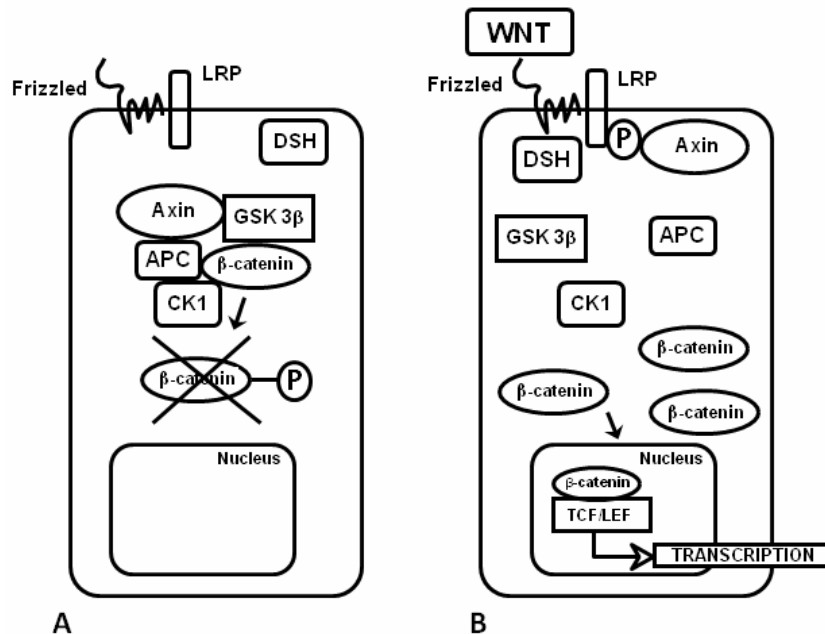


**Figure 4. The canonical Wnt/ $\beta$ -catenin pathway.** (A) In the absence of a Wnt signal,  $\beta$ -catenin is phosphorylated and targeted for proteasomemediated degradation (details in the text). (B) Upon binding of Wnt to the receptors Fz and LRP, the destruction complex does not form anymore leading to stabilization of  $\beta$ -catenin (details in the text).

The role of canonical Wnt/ $\beta$ -catenin signaling at subsequent stages of skeletogenesis has been suggested based on the expression patterns of many Wnt pathway members, as well as Wnt reporter expression in the mouse (107-113). It is well established that many members of the Wnt family of growth factors, like Wnt1, Wnt3a, Wnt4, Wnt7a, Wnt9a and Wnt 11 inhibit chondrogenesis *ex vivo*, while stabilization of  $\beta$ -catenin has similar effects *in vivo* (62-66;107;110;114-117). However, the detrimental effect of increased canonical Wnt signaling on chondrogenesis is not universal since mouse embryonic fibroblasts (MEFs) lacking the Wnt inhibitor *Sfrp1* display an increased potential to form chondrocytes (118). Besides inhibiting differentiation of MCs into chondrocytes, activation of Wnt/ $\beta$ -catenin signaling also leads to dedifferentiation of chondrocytes, a process associated with downregulation of *Col2a1* and decrease in glycosaminoglycans (GAGs) in the cartilage matrix (64;115;116;119-121). Not only does the canonical Wnt/ $\beta$ -catenin signaling pathway control chondrocyte differentiation and maintenance, it is also highly active in promoting chondrocyte maturation. In this fashion, *in vivo* overexpression of *Wnt4* and *Wnt8* or of a stabilized form of  $\beta$ -catenin accelerates chondrocyte hypertrophy (122;123). Moreover, *Sfrp1*<sup>-/-</sup> MEFs display increased chondrocyte hypertrophy and mineralization, while Wnt9a positively regulates *Ihh* expression, known for its stimulating role on chondrocyte proliferation and inhibiting role on maturation (116;118;124). Interestingly, overexpression of *Wnt9a*, besides positively regulating chondrocyte hypertrophy, also increases osteoblast differentiation in the surrounding perichondrium, suggesting thereby a stimulating effect of Wnt/ $\beta$ -catenin pathway on this step of endochondral bone formation (108).

In the past decade many studies have identified an important role for the canonical Wnt/ $\beta$ -catenin pathway in joint formation as well. Wnt9a is the molecular marker currently viewed as the earliest “inducer” of joint formation since its expression has been validated *in vivo* at day 5 of embryonic development in a single stripe of the future diarthroidal joint (4). Interestingly, *Wnt9a* misexpression *in vivo* induces the formation of ectopic joints through up-regulation of articular chondrocyte markers like *Col3a1*, and joint specific markers such as *Chordin* (*Chdr*), *Autotaxin* (*Atx*), and *growth differentiation factor 5* (*Gdf5*), together with down-regulation of non-articular chondrocyte markers like *Col2a1*, *Col9a1*, *Aggrecan* (*Acan*), *Sox9* and *Bmp4* (4;123). Knock-out of both *Wnt9a* and *Wnt4* results in limited joint fusions indicating that possibly *Wnt16* (the 3<sup>rd</sup> Wnt growth factor known to be expressed in joint interzones) may compensate for the absence of Wnt9a and Wnt4 (116). When no signal is possible through the canonical Wnt/ $\beta$ -catenin signaling pathway at various stages of limb development and joint induction, a severe skeletal phenotype occurs, including chondrodysplasia, ectopic cartilage formation, together with absent or delayed endochondral ossification (107;108;114). Surprisingly, inactivation of  $\beta$ -catenin only in the joints leads to limited fusions in hip joints (125). It is very well possible that joint induction is regulated in a  $\beta$ -catenin-dependent (via Wnt9a and Wnt16) and -independent way (via Wnt4) (62). Alternatively, Wnt/ $\beta$ -catenin signaling might not be exclusively required for the initial induction of joint formation. This observation is sustained by expression of early joint interzone markers in the limbs of conditional mouse embryos lacking  $\beta$ -catenin function in the whole limb mesenchyme (126).



Not less fascinating is the concert regulation of osteoblastogenesis by the multi-potent Wnt/ $\beta$ -catenin signaling pathway. LRP5 has a crucial role in BMD accrual and bone metabolism (127). In bone, LRP5 expression is restricted to osteoblasts of the endosteal and trabecular bone surface and regulates osteoblast proliferation, survival and activity (128). Targeted disruption of *Lrp5* in mice leads to a significant reduction in the osteoblast surface density in both primary and secondary spongiosa (129). Surprisingly, although Wnt3a upregulates the levels of canonical Wnt signaling in human mesenchymal stem cells (hMSCs) *in vitro*, it inhibits their osteoblast differentiation, but it stimulates the proliferation of already differentiated osteoblasts (67;68;130). Signaling through Wnt10b induces osteoblast formation from SPCs, while inhibiting adipogenesis; *Wnt10b*<sup>-/-</sup> mice have a decreased trabecular bone volume and serum osteocalcin levels (70). In agreement with this, *Sfrp*<sup>-/-</sup> adult mice display enhanced trabecular bone accrual, as a result of increased osteoblast proliferation and differentiation and decreased osteoblast apoptosis (96). Similarly *Sfrp4* was shown to be a negative regulator of BMD in mice, by inhibiting Wnt signaling (131). By antagonizing the levels of Wnt/ $\beta$ -catenin transduced signal, *Dkk-1* and *Dkk-2* are also established regulators of osteoblastogenesis *in vitro* (132). *In vitro* knock-down of *Dkk-1* and *Dkk-2* results in a complete blockade of osteoblast differentiation and matrix mineralization. Another well established antagonist of the Wnt/ $\beta$ -catenin is sclerostin, encoded by the *SOST* gene, whose expression is confined to osteocytes (133). Sclerostin was shown to negatively regulate bone formation both *in vitro* and *in vivo* (133-136).

By far the most investigated component of the canonical Wnt signaling pathway during skeletal development remains its central molecule,  $\beta$ -catenin. Several lines of evidence, especially generated by observation in conditional mouse lines, indicate an indubitable role for  $\beta$ -catenin in the differentiation of osteoblasts from SPCs (107;110-112;117;137;138). Lack of  $\beta$ -catenin in precursor cells impairs osteoblastogenesis and affected SPCs will follow instead the chondrogenic pathway, regardless of the time when  $\beta$ -catenin is inactivated, prior (*Prx1-Cre*) or after (*Dermo1-Cre*, *Col2a1-Cre*) cartilage condensation has occurred (107;110;112). Interestingly, the shift to the chondrogenic lineage of the osteoblast precursors also takes place when  $\beta$ -catenin is deleted in *Osx*-expressing, and therefore committed osteoblasts (137). One would imagine based on these data that activation of  $\beta$ -catenin would have beneficial impact on osteoblast differentiation. This is however not entirely true, since stabilization of  $\beta$ -catenin in *Osx*-positive osteoblast precursors leads to a marked increase in proliferation and an accelerated bone matrix accumulation, yet these osteoblasts fail to express the mature osteoblast marker *Osc* (137). Moreover, the constitutive expression of a stabilized form of  $\beta$ -catenin in the limbs using *Prx1-Cre* mice also negatively affects osteoblastogenesis, leading to the formation of tiny remnants of skeletal elements (110). All these data suggest that  $\beta$ -catenin levels must be finely tuned during subsequent stages of skeletal development for proper osteoblast formation.

## V. CANONICAL WNT SIGNALING DURING SKELETAL PATHOLOGY

Initial evidence for a role of the canonical Wnt signaling pathway in skeletal pathology was provided by the identification of mutations in the *LRP5* gene inducing either the Osteoporosis-Pseudoglioma Syndrome (OPPG) or the hereditary High Bone Mass Syndrome (HBMS) in humans. OPPG is a rare autosomal recessive disorder affecting the skeleton and the eye associated with loss-of function mutations in the *LRP5* gene, which prevents Wnt from binding to the receptor (127). Children with the OPPG have a very low BMD and easily develop fractures and deformations. In agreement with this, *Lrp5*<sup>-/-</sup> mice have a low BMD due to reduced proliferation of precursor cells (129). Interestingly, low bone mass in *Lrp5*<sup>-/-</sup> mice is further exacerbated by loss of an *Lrp6* allele, suggesting that Wnts signal through both the LRP5 and LRP6 co-receptors to influence bone mass (139). Recently, LRP-6 mutations have been found to cause metabolic syndrome with osteoporosis (140). In contrast, gain-of-function mutations in *LRP5* are associated with increased BMD in the autosomal dominant HBM trait (141-143). These individuals display not only increased BMD, but also increased bone synthesis and excessive bone accrual, yet normal bone resorption, bone architecture, serum calcium, phosphate, PTH and vitamin D levels (128;143;144). These human bone phenotypes were later confirmed by animal models with overexpression of LRP5. For instance, mice that overexpress the HBM LRP5 variant LRP5G171V in osteoblasts have enhanced osteoblast activity, reduced osteoblast apoptosis, and a high BMD supporting the observations in humans with this mutation (145).

Mutations in the *SOST* gene have been shown to result in high bone mass (146). *SOST* truncation abolishes its inhibitory effect, leading to hyperactivation of canonical Wnt signaling, resulting in the disease sclerosteosis. Furthermore, a 52-kb deletion downstream of the *SOST* gene gives rise to Van Buchem disease. In both these rare and related diseases there is overproduction of bone (147;148). Clinical features of sclerosteosis include: syndactyly as well as very thick and dense bones, particularly in the skull. This can lead to cranial nerve entrapment, resulting in deafness and facial nerve palsy, increased intracranial pressure, and greater risk of stroke (134;149). Patients with Van Buchem disease have similar characteristics, yet in this syndrome syndactyly was not described (134;149). Nevertheless, some Van Buchem patients carry mutations in the *LRP5* gene (149). The HBM LRP5 variant LRP5G171V exhibits reduced *SOST* binding, suggesting that *LRP5* HBM mutations render LRP5 more resistant to *SOST* inhibition (147;150). Importantly, this resistance to *SOST* inhibition may be responsible for most of the pathogenesis associated with increased Wnt signaling in the *LRP5* mutants. The relationship between *SOST* and LRP5 represents the hope of many researchers in the area of anti-osteoporotic drugs, since the administration of a therapeutic agent that could alter the ability of *SOST* to bind to LRP5 might lead to increased bone formation (151;152). That this approach is a very attractive basis for developing future osteoporosis therapeutics is proven by the increased bone formation, BMD, and bone strength in several animal models of osteoporosis after administration of sclerostin-neutralizing monoclonal antibodies (153-155).

Another major skeletal disease on which the canonical Wnt signaling lays its fingerprint is osteoarthritis. Recent findings indicate that this pathway responds to mechanical injury to cartilage and is associated with postnatal cartilage matrix degradation, chondrocyte dedifferentiation and apoptosis (119;121;156;157). Upon several whole genome studies, the Wnt antagonist FRZB has emerged as a candidate gene associated with an increased risk for OA (158-161). Although not developing a noteworthy developmental phenotype, *Frzb*<sup>-/-</sup> mice display greater cartilage loss in comparison to wild-type controls when exposed to factors known to induce OA, like enzymatic treatment (papain-induced osteoarthritis), accelerated instability (collagenase-induced ligament and meniscal damage) or inflammation (mBSA induced monoarthritis) (96;162). Cartilage degradation in the *Frzb*<sup>-/-</sup> mice is associated with up-regulation of  $\beta$ -catenin and Mmp9. Interestingly, it was also shown *in vitro* that cartilage injury results in increased Wnt activity and lower expression of FRZB (163). While Wnt-7a is associated with cartilage destruction by regulating the maintenance of differentiation status and the apoptosis of articular chondrocytes (119), Wnt-7b expression is upregulated in OA cartilage (164). Mechanical stress resulting in acutely injured cartilage, leads to upregulation of Wnt16, downregulation of FrzB, upregulation of Wnt target genes, and nuclear localization of  $\beta$ -catenin (157). Once canonical Wnt signaling was associated with OA, the question arose whether an animal model with abnormal  $\beta$ -catenin in AC would show an OA phenotype. For this purpose, Zhu and colleagues have generated conditional mice carrying either lower (ICAT) or higher ( $\beta$ -catenin cAct) levels of  $\beta$ -catenin in *Col2a1*-expressing chondrocytes (165;166). Interestingly, both conditional mouse lines displayed OA features, suggesting that precisely regulated canonical Wnt levels are mandatory during AC maintenance. While conditional  $\beta$ -catenin inactivation led to AC destruction and chondrocyte apoptosis, forced expression of a stabilized form of  $\beta$ -catenin resulted in a time-dependent AC degeneration and upregulation of Mmp13. Nevertheless,  $\beta$ -catenin protein expression is upregulated in knee joint samples from patients with OA (165).

## VI. OUTLINE OF THIS THESIS

In view of the complex roles of the canonical Wnt signaling during skeletal development and disease, it is important to accurately distinguish the specific roles of this signaling cascade at specific time windows during embryogenesis as well as postnatally in the maintenance of the skeleton. Moreover, a proper understanding of these multifaceted roles will ultimately aid us in identifying new therapeutic targets for the treatment of growth disorders, osteoporosis and osteoarthritis.

Most of the animal models that furnish our knowledge of the effects of canonical Wnt signaling during skeletal development and maintenance use the forced expression of a stabilized and thereby oncogenic  $\beta$ -catenin. The roles of intracellular  $\beta$ -catenin regulators and thereby of wild type  $\beta$ -catenin levels during skeletogenesis, bone mass accrual or AC maintenance are largely unknown. The research described in this thesis aimed at describing the role of two major intracellular regulators of  $\beta$ -catenin, namely Apc and Gsk3 $\beta$  in regulation of SPC differentiation, bone mass accrual and cartilage maintenance.

To investigate whether Apc is involved in lineage commitment of SPCs, we generated conditional knockout mice lacking functional Apc in *Col2a1*-expressing cells (115). Our data presented in **chapter 2** indicate that a tight Apc-mediated control of  $\beta$ -catenin levels is essential for differentiation of skeletal precursors as well as for the maintenance of a chondrocytic phenotype in a spatio-temporal regulated manner. Next we investigated the skeletal development of compound Apc mutant embryos with one conditional mutant allele (*Apc*<sup>15lox</sup>) and one hypomorphic Apc mutant allele (*Apc*<sup>1638N</sup> or *Apc*<sup>1572T</sup>) resulting in differential levels of transduced canonical Wnt signaling in SPC (167). We show in **chapter 3** that precise dosages of Wnt/ $\beta$ -catenin signaling distinctly influence the differentiation of SPC. In order to reveal the molecular mechanisms by which Apc regulates the differentiation of SPCs *in vitro*, we have knocked down Apc in the murine mesenchymal stem cell-like KS483 cells by stable expression of Apc-specific small interfering RNA (168). Our results described in **chapter 4** demonstrate that Apc is essential for the proliferation, survival and differentiation of KS483 cells. We next conducted a cross-sectional study evaluating skeletal status in FAP patients with a documented APC mutation to determine if APC mutations affect bone mass (169). We demonstrate in **chapter 5** that FAP patients display a significantly higher than normal mean BMD compared to age- and sex-matched healthy controls in the presence of a balanced bone turnover. Finally, to investigate the role of Gsk3 $\beta$  in cartilage maintenance we conducted *ex vivo* and *in vivo* experiments in which we treated chondrocytes with GIN, a selective GSK3 $\beta$  inhibitor (170). Our results described in **chapter 6** suggest that, by down-regulating  $\beta$ -catenin, Gsk3 $\beta$  preserves the chondrocytic phenotype, and is involved in maintenance of the cartilage extracellular matrix. In **chapter 7** we summarize the major findings comprised in this thesis. At the same time several possible future research lines are hypothesized, that might help us in more profoundly understanding the function of APC and GSK3 $\beta$  during skeletal development and maintenance.

## REFERENCES

1. Olsen BR, Reginato AM, Wang W. Bone development. *Annu Rev Cell Dev Biol* 2000; 16:191-220.
2. Cohen MM, Jr. The new bone biology: pathologic, molecular, and clinical correlates. *Am J Med Genet A* 2006; 140(23):2646-706.
3. Karsenty G. Genetics of skeletogenesis. *Dev Genet* 1998; 22(4):301-13.
4. Karsenty G, Wagner EF. Reaching a genetic and molecular understanding of skeletal development. *Dev Cell* 2002; 2(4):389-406.
5. Zelzer E, Olsen BR. The genetic basis for skeletal diseases. *Nature* 2003; 423(6937):343-8.
6. Hall BK, Miyake T. All for one and one for all: condensations and the initiation of skeletal development. *Bioessays* 2000; 22(2):138-47.
7. Land C, Schoenau E. Fetal and postnatal bone development: reviewing the role of mechanical stimuli and nutrition. *Best Pract Res Clin Endocrinol Metab* 2008; 22(1):107-18.
8. Kronenberg HM. The role of the perichondrium in fetal bone development. *Ann N Y Acad Sci* 2007; 1116:59-64.
9. Hunziker EB. Mechanism of longitudinal bone growth and its regulation by growth plate chondrocytes. *Microsc Res Tech* 1994; 28(6):505-19.
10. Kronenberg HM. Developmental regulation of the growth plate. *Nature* 2003; 423(6937):332-6.
11. van der Eerden BC, Karperien M, Wit JM. Systemic and local regulation of the growth plate. *Endocr Rev* 2003; 24(6):782-801.
12. Pacifici M, Koyama E, Iwamoto M. Mechanisms of synovial joint and articular cartilage formation: recent advances, but many lingering mysteries. *Birth Defects Res C Embryo Today* 2005; 75(3):237-48.
13. Pacifici M, Koyama E, Shibukawa Y, Wu C, Tamamura Y, Enomoto-Iwamoto M et al. Cellular and molecular mechanisms of synovial joint and articular cartilage formation. *Ann N Y Acad Sci* 2006; 1068:74-86.
14. Pacifici M, Koyama E, Iwamoto M, Gentili C. Development of articular cartilage: what do we know about it and how may it occur? *Connect Tissue Res* 2000; 41(3):175-84.
15. Wagner T, Wirth J, Meyer J, Zabel B, Held M, Zimmer J et al. Autosomal sex reversal and campomelic dysplasia are caused by mutations in and around the SRY-related gene SOX9. *Cell* 1994; 79(6):1111-20.
16. Foster JW, Dominguez-Steglich MA, Guioli S, Kwok C, Weller PA, Stevanovic M et al. Campomelic dysplasia and autosomal sex reversal caused by mutations in an SRY-related gene. *Nature* 1994; 372(6506):525-30.
17. Wright E, Hargrave MR, Christiansen J, Cooper L, Kun J, Evans T et al. The Sry-related gene Sox9 is expressed during chondrogenesis in mouse embryos. *Nat Genet* 1995; 9(1):15-20.

18. Cheah KS, Lau ET, Au PK, Tam PP. Expression of the mouse alpha 1(II) collagen gene is not restricted to cartilage during development. *Development* 1991; 111(4):945-53.
19. Lefebvre V, Huang W, Harley VR, Goodfellow PN, de Crombrughe B. SOX9 is a potent activator of the chondrocyte-specific enhancer of the pro alpha1(II) collagen gene. *Mol Cell Biol* 1997; 17(4):2336-46.
20. Sekiya I, Tsuji K, Koopman P, Watanabe H, Yamada Y, Shinomiya K et al. SOX9 enhances aggrecan gene promoter/enhancer activity and is up-regulated by retinoic acid in a cartilage-derived cell line, TC6. *J Biol Chem* 2000; 275(15):10738-44.
21. Hall BK, Miyake T. All for one and one for all: condensations and the initiation of skeletal development. *Bioessays* 2000; 22(2):138-47.
22. Bell DM, Leung KK, Wheatley SC, Ng LJ, Zhou S, Ling KW et al. SOX9 directly regulates the type-II collagen gene. *Nat Genet* 1997; 16(2):174-8.
23. Ng LJ, Wheatley S, Muscat GE, Conway-Campbell J, Bowles J, Wright E et al. SOX9 binds DNA, activates transcription, and coexpresses with type II collagen during chondrogenesis in the mouse. *Dev Biol* 1997; 183(1):108-21.
24. Bridgewater LC, Lefebvre V, de Crombrughe B. Chondrocyte-specific enhancer elements in the Col11a2 gene resemble the Col2a1 tissue-specific enhancer. *J Biol Chem* 1998; 273(24):14998-5006.
25. Bi W, Deng JM, Zhang Z, Behringer RR, de Crombrughe B. Sox9 is required for cartilage formation. *Nat Genet* 1999; 22(1):85-9.
26. Bi W, Huang W, Whitworth DJ, Deng JM, Zhang Z, Behringer RR et al. Haploinsufficiency of Sox9 results in defective cartilage primordia and premature skeletal mineralization. *Proc Natl Acad Sci U S A* 2001; 98(12):6698-703.
27. Huang W, Chung UI, Kronenberg HM, de Crombrughe B. The chondrogenic transcription factor Sox9 is a target of signaling by the parathyroid hormone-related peptide in the growth plate of endochondral bones. *Proc Natl Acad Sci U S A* 2001; 98(1):160-5.
28. Lefebvre V, Li P, de Crombrughe B. A new long form of Sox5 (L-Sox5), Sox6 and Sox9 are coexpressed in chondrogenesis and cooperatively activate the type II collagen gene. *EMBO J* 1998; 17(19):5718-33.
29. Smits P, Li P, Mandel J, Zhang Z, Deng JM, Behringer RR et al. The transcription factors L-Sox5 and Sox6 are essential for cartilage formation. *Dev Cell* 2001; 1(2):277-90.
30. Ueta C, Iwamoto M, Kanatani N, Yoshida C, Liu Y, Enomoto-Iwamoto M et al. Skeletal malformations caused by overexpression of Cbfa1 or its dominant negative form in chondrocytes. *J Cell Biol* 2001; 153(1):87-100.
31. Takeda S, Bonnamy JP, Owen MJ, Ducy P, Karsenty G. Continuous expression of Cbfa1 in nonhypertrophic chondrocytes uncovers its ability to induce hypertrophic chondrocyte differentiation and partially rescues Cbfa1-deficient mice. *Genes Dev* 2001; 15(4):467-81.
32. Kim IS, Otto F, Zabel B, Mundlos S. Regulation of chondrocyte differentiation by Cbfa1. *Mech Dev* 1999; 80(2):159-70.
33. Enomoto H, Enomoto-Iwamoto M, Iwamoto M, Nomura S, Himeno M, Kitamura Y et al. Cbfa1 is a positive regulatory factor in chondrocyte maturation. *J Biol Chem* 2000; 275(12):8695-702.
34. Bialek P, Kern B, Yang X, Schrock M, Susic D, Hong N et al. A twist code determines the onset of osteoblast differentiation. *Dev Cell* 2004; 6(3):423-35.

35. Yoshida CA, Yamamoto H, Fujita T, Furuichi T, Ito K, Inoue K et al. Runx2 and Runx3 are essential for chondrocyte maturation, and Runx2 regulates limb growth through induction of Indian hedgehog. *Genes Dev* 2004; 18(8):952-63.
36. Ducy P, Zhang R, Geoffroy V, Ridall AL, Karsenty G. *Osf2/Cbfa1*: a transcriptional activator of osteoblast differentiation. *Cell* 1997; 89(5):747-54.
37. Ducy P. *Cbfa1*: a molecular switch in osteoblast biology. *Dev Dyn* 2000; 219(4):461-71.
38. Lee B, Thirunavukkarasu K, Zhou L, Pastore L, Baldini A, Hecht J et al. Missense mutations abolishing DNA binding of the osteoblast-specific transcription factor OSF2/CBFA1 in cleidocranial dysplasia. *Nat Genet* 1997; 16(3):307-10.
39. Mundlos S, Otto F, Mundlos C, Mulliken JB, Aylsworth AS, Albright S et al. Mutations involving the transcription factor CBFA1 cause cleidocranial dysplasia. *Cell* 1997; 89(5):773-9.
40. Otto F, Thornell AP, Crompton T, Denzel A, Gilmour KC, Rosewell IR et al. *Cbfa1*, a candidate gene for cleidocranial dysplasia syndrome, is essential for osteoblast differentiation and bone development. *Cell* 1997; 89(5):765-71.
41. Nakashima K, Zhou X, Kunkel G, Zhang Z, Deng JM, Behringer RR et al. The novel zinc finger-containing transcription factor osterix is required for osteoblast differentiation and bone formation. *Cell* 2002; 108(1):17-29.
42. Nishio Y, Dong Y, Paris M, O'Keefe RJ, Schwarz EM, Drissi H. Runx2-mediated regulation of the zinc finger *Osterix/Sp7* gene. *Gene* 2006; 372:62-70.
43. Vortkamp A, Lee K, Lanske B, Segre GV, Kronenberg HM, Tabin CJ. Regulation of rate of cartilage differentiation by Indian hedgehog and PTH-related protein. *Science* 1996; 273(5275):613-22.
44. Karp SJ, Schipani E, St-Jacques B, Hunzelman J, Kronenberg H, McMahon AP. Indian hedgehog coordinates endochondral bone growth and morphogenesis via parathyroid hormone related-protein-dependent and -independent pathways. *Development* 2000; 127(3):543-8.
45. Lanske B, Karaplis AC, Lee K, Luz A, Vortkamp A, Pirro A et al. PTH/PTHrP receptor in early development and Indian hedgehog-regulated bone growth. *Science* 1996; 273(5275):663-6.
46. St-Jacques B, Hammerschmidt M, McMahon AP. Indian hedgehog signaling regulates proliferation and differentiation of chondrocytes and is essential for bone formation. *Genes Dev* 1999; 13(16):2072-86.
47. Urist MR. Bone: formation by autoinduction. *Science* 1965; 150(698):893-9.
48. Rosen V, Thies RS. The BMP proteins in bone formation and repair. *Trends Genet* 1992; 8(3):97-102.
49. Haas AR, Tuan RS. Chondrogenic differentiation of murine C3H10T1/2 multipotential mesenchymal cells: II. Stimulation by bone morphogenetic protein-2 requires modulation of N-cadherin expression and function. *Differentiation* 1999; 64(2):77-89.
50. Zehentner BK, Dony C, Burtscher H. The transcription factor Sox9 is involved in BMP-2 signaling. *J Bone Miner Res* 1999; 14(10):1734-41.
51. Chimal-Monroy J, Rodriguez-Leon J, Montero JA, Ganan Y, Macias D, Merino R et al. Analysis of the molecular cascade responsible for mesodermal limb chondrogenesis: Sox genes and BMP signaling. *Dev Biol* 2003; 257(2):292-301.
52. Hatakeyama Y, Nguyen J, Wang X, Nuckolls GH, Shum L. Smad signaling in mesenchymal and chondroprogenitor cells. *J Bone Joint Surg Am* 2003; 85-A Suppl 3:13-8.

53. Volk SW, Luvalle P, Leask T, Leboy PS. A BMP responsive transcriptional region in the chicken type X collagen gene. *J Bone Miner Res* 1998; 13(10):1521-9.
54. Shukunami C, Ohta Y, Sakuda M, Hiraki Y. Sequential progression of the differentiation program by bone morphogenetic protein-2 in chondrogenic cell line ATDC5. *Exp Cell Res* 1998; 241(1):1-11.
55. Grimsrud CD, Romano PR, D'Souza M, Puzas JE, Reynolds PR, Rosier RN et al. BMP-6 is an autocrine stimulator of chondrocyte differentiation. *J Bone Miner Res* 1999; 14(4):475-82.
56. Yamaguchi A, Ishizuya T, Kintou N, Wada Y, Katagiri T, Wozney JM et al. Effects of BMP-2, BMP-4, and BMP-6 on osteoblastic differentiation of bone marrow-derived stromal cell lines, ST2 and MC3T3-G2/PA6. *Biochem Biophys Res Commun* 1996; 220(2):366-71.
57. Gitelman SE, Kirk M, Ye JQ, Filvaroff EH, Kahn AJ, Derynck R. Vgr-1/BMP-6 induces osteoblastic differentiation of pluripotential mesenchymal cells. *Cell Growth Differ* 1995; 6(7):827-36.
58. Lee KS, Kim HJ, Li QL, Chi XZ, Ueta C, Komori T et al. Runx2 is a common target of transforming growth factor beta1 and bone morphogenetic protein 2, and cooperation between Runx2 and Smad5 induces osteoblast-specific gene expression in the pluripotent mesenchymal precursor cell line C2C12. *Mol Cell Biol* 2000; 20(23):8783-92.
59. Leboy P, Grasso-Knight G, D'Angelo M, Volk SW, Lian JV, Drissi H et al. Smad-Runx interactions during chondrocyte maturation. *J Bone Joint Surg Am* 2001; 83-A Suppl 1(Pt 1):S15-S22.
60. Macsai CE, Foster BK, Xian CJ. Roles of Wnt signalling in bone growth, remodelling, skeletal disorders and fracture repair. *J Cell Physiol* 2008; 215(3):578-87.
61. Logan CY, Nusse R. The Wnt signaling pathway in development and disease. *Annu Rev Cell Dev Biol* 2004; 20:781-810.
62. Church V, Nohno T, Linker C, Marcelle C, Francis-West P. Wnt regulation of chondrocyte differentiation. *J Cell Sci* 2002; 115(Pt 24):4809-18.
63. Hartmann C, Tabin CJ. Wnt-14 plays a pivotal role in inducing synovial joint formation in the developing appendicular skeleton. *Cell* 2001; 104(3):341-51.
64. Hwang SG, Yu SS, Lee SW, Chun JS. Wnt-3a regulates chondrocyte differentiation via c-Jun/AP-1 pathway. *FEBS Lett* 2005; 579(21):4837-42.
65. Rudnicki JA, Brown AM. Inhibition of chondrogenesis by Wnt gene expression in vivo and in vitro. *Dev Biol* 1997; 185(1):104-18.
66. Tufan AC, Daumer KM, DeLise AM, Tuan RS. AP-1 transcription factor complex is a target of signals from both Wnt-7a and N-cadherin-dependent cell-cell adhesion complex during the regulation of limb mesenchymal chondrogenesis. *Exp Cell Res* 2002; 273(2):197-203.
67. de Boer J, Siddappa R, Gaspar C, van Apeldoorn A, Fodde R, van Blitterswijk C. Wnt signaling inhibits osteogenic differentiation of human mesenchymal stem cells. *Bone* 2004; 34(5):818-26.
68. Boland GM, Perkins G, Hall DJ, Tuan RS. Wnt 3a promotes proliferation and suppresses osteogenic differentiation of adult human mesenchymal stem cells. *J Cell Biochem* 2004; 93(6):1210-30.
69. Almeida M, Han L, Bellido T, Manolagas SC, Kousteni S. Wnt proteins prevent apoptosis of both uncommitted osteoblast progenitors and differentiated osteoblasts by beta-catenin-



- dependent and -independent signaling cascades involving Src/ERK and phosphatidylinositol 3-kinase/AKT. *J Biol Chem* 2005; 280(50):41342-51.
70. Bennett CN, Longo KA, Wright WS, Suva LJ, Lane TF, Hankenson KD et al. Regulation of osteoblastogenesis and bone mass by Wnt10b. *Proc Natl Acad Sci U S A* 2005; 102(9):3324-9.
  71. Drop SL, Greggio N, Cappa M, Bernasconi S. Current concepts in tall stature and overgrowth syndromes. *J Pediatr Endocrinol Metab* 2001; 14 Suppl 2:975-84.
  72. Verbrugge LM, Patrick DL. Seven chronic conditions: their impact on US adults' activity levels and use of medical services. *Am J Public Health* 1995; 85(2):173-82.
  73. Aigner T, Zien A, Gehrsitz A, Gebhard PM, McKenna L. Anabolic and catabolic gene expression pattern analysis in normal versus osteoarthritic cartilage using complementary DNA-array technology. *Arthritis Rheum* 2001; 44(12):2777-89.
  74. Creamer P, Hochberg MC. Osteoarthritis. *Lancet* 1997; 350(9076):503-8.
  75. Goldring MB, Goldring SR. Osteoarthritis. *J Cell Physiol* 2007; 213(3):626-34.
  76. Aigner T, Kurz B, Fukui N, Sandell L. Roles of chondrocytes in the pathogenesis of osteoarthritis. *Curr Opin Rheumatol* 2002; 14(5):578-84.
  77. Loeser RF. Molecular mechanisms of cartilage destruction: mechanics, inflammatory mediators, and aging collide. *Arthritis Rheum* 2006; 54(5):1357-60.
  78. Hamerman D. The biology of osteoarthritis. *N Engl J Med* 1989; 320(20):1322-30.
  79. Rengel Y, Ospelt C, Gay S. Proteinases in the joint: clinical relevance of proteinases in joint destruction. *Arthritis Res Ther* 2007; 9(5):221.
  80. Knauper V, Lopez-Otin C, Smith B, Knight G, Murphy G. Biochemical characterization of human collagenase-3. *J Biol Chem* 1996; 271(3):1544-50.
  81. Tetlow LC, Adlam DJ, Woolley DE. Matrix metalloproteinase and proinflammatory cytokine production by chondrocytes of human osteoarthritic cartilage: associations with degenerative changes. *Arthritis Rheum* 2001; 44(3):585-94.
  82. Dolan P, Torgerson DJ. The cost of treating osteoporotic fractures in the United Kingdom female population. *Osteoporos Int* 1998; 8(6):611-7.
  83. Cummings SR, Bates D, Black DM. Clinical use of bone densitometry: scientific review. *JAMA* 2002; 288(15):1889-97.
  84. Elliott ME, Meek PD, Kanous NL, Schill GR, Weinswig PA, Bohlman JP et al. Osteoporosis screening by community pharmacists: use of National Osteoporosis Foundation resources. *J Am Pharm Assoc (Wash )* 2002; 42(1):101-10.
  85. Bone fractures after menopause. *Hum Reprod Update* 2010; 16(6):761-73.
  86. Makras P, Hamdy NA, Zwinderman AH, Ballieux BE, Papapoulos SE. Bisphosphonate dose and incidence of fractures in postmenopausal osteoporosis. *Bone* 2009; 44(5):766-71.
  87. Kanis JA, Brazier JE, Stevenson M, Calvert NW, Lloyd JM. Treatment of established osteoporosis: a systematic review and cost-utility analysis. *Health Technol Assess* 2002; 6(29):1-146.
  88. O'Neill TW, Felsenberg D, Varlow J, Cooper C, Kanis JA, Silman AJ. The prevalence of vertebral deformity in European men and women: the European Vertebral Osteoporosis Study. *J Bone Miner Res* 1996; 11(7):1010-8.
  89. Compston JE. Sex steroids and bone. *Physiol Rev* 2001; 81(1):419-47.

90. Osteoporosis prevention, diagnosis, and therapy. *JAMA* 2001; 285(6):785-95.
91. Assessment of fracture risk and its application to screening for postmenopausal osteoporosis. Report of a WHO Study Group. *World Health Organ Tech Rep Ser* 1994; 843:1-129.
92. Cosman F. The prevention and treatment of osteoporosis: a review. *MedGenMed* 2005; 7(2):73.
93. Miller JR. The Wnts. *Genome Biol* 2002; 3(1):REVIEWS3001.
94. Hirohashi S, Kanai Y. Cell adhesion system and human cancer morphogenesis. *Cancer Sci* 2003; 94(7):575-81.
95. Clevers H. Wnt/beta-catenin signaling in development and disease. *Cell* 2006; 127(3):469-80.
96. Bodine PV, Zhao W, Kharode YP, Bex FJ, Lambert AJ, Goad MB et al. The Wnt antagonist secreted frizzled-related protein-1 is a negative regulator of trabecular bone formation in adult mice. *Mol Endocrinol* 2004; 18(5):1222-37.
97. Tian E, Zhan F, Walker R, Rasmussen E, Ma Y, Barlogie B et al. The role of the Wnt-signaling antagonist DKK1 in the development of osteolytic lesions in multiple myeloma. *N Engl J Med* 2003; 349(26):2483-94.
98. Staehling-Hampton K, Proll S, Paepfer BW, Zhao L, Charmley P, Brown A et al. A 52-kb deletion in the SOST-MEOX1 intergenic region on 17q12-q21 is associated with van Buchem disease in the Dutch population. *Am J Med Genet* 2002; 110(2):144-52.
99. Fodde R. The multiple functions of tumour suppressors: it's all in APC. *Nat Cell Biol* 2003; 5(3):190-2.
100. Gaspar C, Fodde R. APC dosage effects in tumorigenesis and stem cell differentiation. *Int J Dev Biol* 2004; 48(5-6):377-86.
101. Kielman MF, Rindapaa M, Gaspar C, van Poppel N, Breukel C, van Leeuwen S et al. Apc modulates embryonic stem-cell differentiation by controlling the dosage of beta-catenin signaling. *Nat Genet* 2002; 32(4):594-605.
102. Fodde R, Smits R. Cancer biology. A matter of dosage. *Science* 2002; 298(5594):761-3.
103. Embi N, Rylatt DB, Cohen P. Glycogen synthase kinase-3 from rabbit skeletal muscle. Separation from cyclic-AMP-dependent protein kinase and phosphorylase kinase. *Eur J Biochem* 1980; 107(2):519-27.
104. Wodarz A, Nusse R. Mechanisms of Wnt signaling in development. *Annu Rev Cell Dev Biol* 1998; 14:59-88.
105. Doble BW, Woodgett JR. GSK-3: tricks of the trade for a multi-tasking kinase. *J Cell Sci* 2003; 116(Pt 7):1175-86.
106. Gao C, Chen YG. Dishevelled: The hub of Wnt signaling. *Cell Signal*. 2010 May;22(5):717-27.
107. Day TF, Guo X, Garrett-Beal L, Yang Y. Wnt/beta-catenin signaling in mesenchymal progenitors controls osteoblast and chondrocyte differentiation during vertebrate skeletogenesis. *Dev Cell* 2005; 8(5):739-50.
108. Guo X, Day TF, Jiang X, Garrett-Beal L, Topol L, Yang Y. Wnt/beta-catenin signaling is sufficient and necessary for synovial joint formation. *Genes Dev* 2004; 18(19):2404-17.

109. Hens JR, Wilson KM, Dann P, Chen X, Horowitz MC, Wysolmerski JJ. TOPGAL mice show that the canonical Wnt signaling pathway is active during bone development and growth and is activated by mechanical loading in vitro. *J Bone Miner Res* 2005; 20(7):1103-13.
110. Hill TP, Spater D, Taketo MM, Birchmeier W, Hartmann C. Canonical Wnt/beta-catenin signaling prevents osteoblasts from differentiating into chondrocytes. *Dev Cell* 2005; 8(5):727-38.
111. Hill TP, Taketo MM, Birchmeier W, Hartmann C. Multiple roles of mesenchymal beta-catenin during murine limb patterning. *Development* 2006; 133(7):1219-29.
112. Hu H, Hilton MJ, Tu X, Yu K, Ornitz DM, Long F. Sequential roles of Hedgehog and Wnt signaling in osteoblast development. *Development* 2005; 132(1):49-60.
113. Parr BA, McMahon AP. Dorsalizing signal Wnt-7a required for normal polarity of D-V and A-P axes of mouse limb. *Nature* 1995; 374(6520):350-3.
114. Akiyama H, Lyons JP, Mori-Akiyama Y, Yang X, Zhang R, Zhang Z et al. Interactions between Sox9 and beta-catenin control chondrocyte differentiation. *Genes Dev* 2004; 18(9):1072-87.
115. Miclea RL, Karperien M, Bosch CA, van der Horst G, van der Valk MA, Kobayashi T et al. Adenomatous polyposis coli-mediated control of beta-catenin is essential for both chondrogenic and osteogenic differentiation of skeletal precursors. *BMC Dev Biol* 2009; 9:26.
116. Spater D, Hill TP, O'sullivan RJ, Gruber M, Conner DA, Hartmann C. Wnt9a signaling is required for joint integrity and regulation of Ihh during chondrogenesis. *Development* 2006; 133(15):3039-49.
117. Tamamura Y, Otani T, Kanatani N, Koyama E, Kitagaki J, Komori T et al. Developmental regulation of Wnt/beta-catenin signals is required for growth plate assembly, cartilage integrity, and endochondral ossification. *J Biol Chem* 2005; 280(19):19185-95.
118. Gaur T, Rich L, Lengner CJ, Hussain S, Trevant B, Ayers D et al. Secreted frizzled related protein 1 regulates Wnt signaling for BMP2 induced chondrocyte differentiation. *J Cell Physiol* 2006; 208(1):87-96.
119. Hwang SG, Ryu JH, Kim IC, Jho EH, Jung HC, Kim K et al. Wnt-7a causes loss of differentiated phenotype and inhibits apoptosis of articular chondrocytes via different mechanisms. *J Biol Chem* 2004; 279(25):26597-604.
120. Hwang SG, Yu SS, Ryu JH, Jeon HB, Yoo YJ, Eom SH et al. Regulation of beta-catenin signaling and maintenance of chondrocyte differentiation by ubiquitin-independent proteasomal degradation of alpha-catenin. *J Biol Chem* 2005; 280(13):12758-65.
121. Ryu JH, Kim SJ, Kim SH, Oh CD, Hwang SG, Chun CH et al. Regulation of the chondrocyte phenotype by beta-catenin. *Development* 2002; 129(23):5541-50.
122. Enomoto-Iwamoto M, Kitagaki J, Koyama E, Tamamura Y, Wu C, Kanatani N et al. The Wnt antagonist Frzb-1 regulates chondrocyte maturation and long bone development during limb skeletogenesis. *Dev Biol* 2002; 251(1):142-56.
123. Hartmann C, Tabin CJ. Dual roles of Wnt signaling during chondrogenesis in the chicken limb. *Development* 2000; 127(14):3141-59.
124. Lai LP, Mitchell J. Indian hedgehog: its roles and regulation in endochondral bone development. *J Cell Biochem* 2005; 96(6):1163-73.
125. Koyama E, Shibukawa Y, Nagayama M, Sugito H, Young B, Yuasa T et al. A distinct cohort of progenitor cells participates in synovial joint and articular cartilage formation during mouse limb skeletogenesis. *Dev Biol* 2008; 316(1):62-73.

126. Spater D, Hill TP, Gruber M, Hartmann C. Role of canonical Wnt-signalling in joint formation. *Eur Cell Mater* 2006; 12:71-80.
127. Gong Y, Slee RB, Fukai N, Rawadi G, Roman-Roman S, Reginato AM et al. LDL receptor-related protein 5 (LRP5) affects bone accrual and eye development. *Cell* 2001; 107(4):513-23.
128. Koay MA, Brown MA. Genetic disorders of the LRP5-Wnt signalling pathway affecting the skeleton. *Trends Mol Med* 2005; 11(3):129-37.
129. Kato M, Patel MS, Levasseur R, Lobov I, Chang BH, Glass DA et al. Cbfa1-independent decrease in osteoblast proliferation, osteopenia, and persistent embryonic eye vascularization in mice deficient in Lrp5, a Wnt coreceptor. *J Cell Biol* 2002; 157(2):303-14.
130. de Boer J, Wang HJ, van Blitterswijk C. Effects of Wnt signaling on proliferation and differentiation of human mesenchymal stem cells. *Tissue Eng* 2004; 10(3-4):393-401.
131. Nakanishi R, Shimizu M, Mori M, Akiyama H, Okudaira S, Otsuki B et al. Secreted frizzled-related protein 4 is a negative regulator of peak BMD in SAMP6 mice. *J Bone Miner Res* 2006; 21(11):1713-21.
132. van der Horst G., van der Werf SM, Farih-Sips H, van Bezooijen RL, Lowik CW, Karperien M. Downregulation of Wnt signaling by increased expression of Dickkopf-1 and -2 is a prerequisite for late-stage osteoblast differentiation of KS483 cells. *J Bone Miner Res* 2005; 20(10):1867-77.
133. van Bezooijen RL, Roelen BA, Visser A, van der Wee-Pals L, de Wilt E, Karperien M et al. Sclerostin is an osteocyte-expressed negative regulator of bone formation, but not a classical BMP antagonist. *J Exp Med* 2004; 199(6):805-14.
134. van Bezooijen RL, ten Dijke P, Papapoulos SE, Lowik CW. SOST/sclerostin, an osteocyte-derived negative regulator of bone formation. *Cytokine Growth Factor Rev* 2005; 16(3):319-27.
135. Winkler DG, Sutherland MS, Ojala E, Turcott E, Geoghegan JC, Shpektor D et al. Sclerostin inhibition of Wnt-3a-induced C3H10T1/2 cell differentiation is indirect and mediated by bone morphogenetic proteins. *J Biol Chem* 2005; 280(4):2498-502.
136. Winkler DG, Sutherland MK, Geoghegan JC, Yu C, Hayes T, Skonier JE et al. Osteocyte control of bone formation via sclerostin, a novel BMP antagonist. *EMBO J* 2003; 22(23):6267-76.
137. Rodda SJ, McMahon AP. Distinct roles for Hedgehog and canonical Wnt signaling in specification, differentiation and maintenance of osteoblast progenitors. *Development* 2006; 133(16):3231-44.
138. Mak KK, Chen MH, Day TF, Chuang PT, Yang Y. Wnt/beta-catenin signaling interacts differentially with Ihh signaling in controlling endochondral bone and synovial joint formation. *Development* 2006; 133(18):3695-707.
139. Holmen SL, Giambernardi TA, Zylstra CR, Buckner-Berghuis BD, Resau JH, Hess JF et al. Decreased BMD and limb deformities in mice carrying mutations in both Lrp5 and Lrp6. *J Bone Miner Res* 2004; 19(12):2033-40.
140. Mani A, Radhakrishnan J, Wang H, Mani A, Mani MA, Nelson-Williams C et al. LRP6 mutation in a family with early coronary disease and metabolic risk factors. *Science* 2007; 315(5816):1278-82.

141. Gong Y, Vikkula M, Boon L, Liu J, Beighton P, Ramesar R et al. Osteoporosis-pseudoglioma syndrome, a disorder affecting skeletal strength and vision, is assigned to chromosome region 11q12-13. *Am J Hum Genet* 1996; 59(1):146-51.
142. Boyden LM, Mao J, Belsky J, Mitzner L, Farhi A, Mitnick MA et al. High bone density due to a mutation in LDL-receptor-related protein 5. *N Engl J Med* 2002; 346(20):1513-21.
143. Little RD, Carulli JP, Del Mastro RG, Dupuis J, Osborne M, Folz C et al. A mutation in the LDL receptor-related protein 5 gene results in the autosomal dominant high-bone-mass trait. *Am J Hum Genet* 2002; 70(1):11-9.
144. Levasseur R, LaCombe D, de Vernejoul MC. LRP5 mutations in osteoporosis-pseudoglioma syndrome and high-bone-mass disorders. *Joint Bone Spine* 2005; 72(3):207-14.
145. Babij P, Zhao W, Small C, Kharode Y, Yaworsky PJ, Bouxsein ML et al. High bone mass in mice expressing a mutant LRP5 gene. *J Bone Miner Res* 2003; 18(6):960-74.
146. Balemans W, Ebeling M, Patel N, van Hul E, Olson P, Dioszegi M et al. Increased bone density in sclerosteosis is due to the deficiency of a novel secreted protein (SOST). *Hum Mol Genet* 2001; 10(5):537-43.
147. Semenov M, Tamai K, He X. SOST is a ligand for LRP5/LRP6 and a Wnt signaling inhibitor. *J Biol Chem* 2005; 280(29):26770-5.
148. Lowik CW, van Bezooijen RL. Wnt signaling is involved in the inhibitory action of sclerostin on BMP-stimulated bone formation. *J Musculoskelet Neuronal Interact* 2006; 6(4):357.
149. Ott SM. Sclerostin and Wnt signaling--the pathway to bone strength. *J Clin Endocrinol Metab* 2005; 90(12):6741-3.
150. Ellies DL, Viviano B, McCarthy J, Rey JP, Itasaki N, Saunders S et al. Bone density ligand, Sclerostin, directly interacts with LRP5 but not LRP5G171V to modulate Wnt activity. *J Bone Miner Res* 2006; 21(11):1738-49.
151. Semenov MV, He X. LRP5 mutations linked to high bone mass diseases cause reduced LRP5 binding and inhibition by SOST. *J Biol Chem* 2006; 281(50):38276-84.
152. Baron R, Rawadi G. Wnt signaling and the regulation of bone mass. *Curr Osteoporos Rep* 2007; 5(2):73-80.
153. Li X, Warmington KS, Niu QT, Asuncion FJ, Barrero M, Grisanti M et al. Inhibition of sclerostin by monoclonal antibody increases bone formation, bone mass, and bone strength in aged male rats. *J Bone Miner Res* 2010; 25(12):2371-80.
154. Li X, Ominsky MS, Warmington KS, Morony S, Gong J, Cao J et al. Sclerostin antibody treatment increases bone formation, bone mass, and bone strength in a rat model of postmenopausal osteoporosis. *J Bone Miner Res* 2009; 24(4):578-88.
155. Ominsky MS, Vlasseros F, Jolette J, Smith SY, Stouch B, Doellgast G et al. Two doses of sclerostin antibody in cynomolgus monkeys increases bone formation, bone mineral density, and bone strength. *J Bone Miner Res* 2010; 25(5):948-59.
156. Yuasa T, Otani T, Koike T, Iwamoto M, Enomoto-Iwamoto M. Wnt/beta-catenin signaling stimulates matrix catabolic genes and activity in articular chondrocytes: its possible role in joint degeneration. *Lab Invest* 2008; 88(3):264-74.
157. Dell'accio F, De Bari C, Eltawil NM, Vanhummelen P, Pitzalis C. Identification of the molecular response of articular cartilage to injury, by microarray screening: Wnt-16 expression and signaling after injury and in osteoarthritis. *Arthritis Rheum* 2008; 58(5):1410-21.

158. Valdes AM, Loughlin J, Oene MV, Chapman K, Surdulescu GL, Doherty M et al. Sex and ethnic differences in the association of ASPN, CALM1, COL2A1, COMP, and FRZB with genetic susceptibility to osteoarthritis of the knee. *Arthritis Rheum* 2007; 56(1):137-46.
159. Loughlin J, Dowling B, Chapman K, Marcelline L, Mustafa Z, Southam L et al. Functional variants within the secreted frizzled-related protein 3 gene are associated with hip osteoarthritis in females. *Proc Natl Acad Sci U S A* 2004; 101(26):9757-62.
160. Lane NE, Lian K, Nevitt MC, Zmuda JM, Lui L, Li J et al. Frizzled-related protein variants are risk factors for hip osteoarthritis. *Arthritis Rheum* 2006; 54(4):1246-54.
161. Min JL, Meulenbelt I, Riyazi N, Kloppenburg M, Houwing-Duistermaat JJ, Seymour AB et al. Association of the Frizzled-related protein gene with symptomatic osteoarthritis at multiple sites. *Arthritis Rheum* 2005; 52(4):1077-80.
162. Lories RJ, Peeters J, Bakker A, Tylzanowski P, Derese I, Schrooten J et al. Articular cartilage and biomechanical properties of the long bones in Frzb-knockout mice. *Arthritis Rheum* 2007; 56(12):4095-103.
163. Dell'accio F, De Bari C, El Tawil NM, Barone F, Mitsiadis TA, O'Dowd J et al. Activation of WNT and BMP signaling in adult human articular cartilage following mechanical injury. *Arthritis Res Ther* 2006; 8(5):R139.
164. Nakamura Y, Nawata M, Wakitani S. Expression profiles and functional analyses of Wnt-related genes in human joint disorders. *Am J Pathol* 2005; 167(1):97-105.
165. Zhu M, Tang D, Wu Q, Hao S, Chen M, Xie C et al. Activation of beta-catenin signaling in articular chondrocytes leads to osteoarthritis-like phenotype in adult beta-catenin conditional activation mice. *J Bone Miner Res* 2009; 24(1):12-21.
166. Zhu M, Chen M, Zuscik M, Wu Q, Wang YJ, Rosier RN et al. Inhibition of beta-catenin signaling in articular chondrocytes results in articular cartilage destruction. *Arthritis Rheum* 2008; 58(7):2053-64.
167. Miclea RL, Robanus-Maandag EC, Löwik CW, Fodde R, Oostdijk W, Wit JM et al. Adenomatous Polyposis Coli-Gene Dosage Controls beta-catenin-Mediated Differentiation of Skeletal Precursors. (*in preparation*).
168. Miclea RL, van der Horst G, Robanus-Maandag EC, Löwik CW, Oostdijk W, Wit JM et al. Apc bridges the Wnt/beta-catenin to BMP signaling pathway during osteoblast differentiation of KS483 cells. *Exp Cell Res*. 2011; 317(10):1411-21.
169. Miclea RL, Karperien M, Langers AM, Robanus-Maandag EC, van Lierop A, van der Hiel B et al. APC mutations are associated with increased bone mineral density in patients with familial adenomatous polyposis. *J Bone Miner Res* 2010; 25(12):2348-56.
170. Miclea RL, Robanus-Maandag EC, Goeman JJ, Finos L, Bloys H, Löwik CW et al. Inhibition of Gsk3 $\beta$  in cartilage induces osteoarthritic features through activation of the canonical Wnt signaling pathway. *Osteoarthritis Cartilage* 2011.



# Chapter 2

## Adenomatous polyposis coli-mediated control of $\beta$ -catenin is essential for both chondrogenic and osteogenic differentiation of skeletal precursors

R.L. Miclea<sup>#1</sup>, M. Karperien<sup>#2</sup>, C.A. Bosch<sup>3</sup>, G. van der Horst<sup>4</sup>, M.A. van der Valk<sup>5</sup>, T. Kobayashi<sup>6</sup>, H.M. Kronenberg<sup>6</sup>, G. Rawadi<sup>7</sup>, P. Akçakaya<sup>3</sup>, C.W. Löwik<sup>8</sup>, R. Fodde<sup>9</sup>, J.M. Wit<sup>1</sup>, E.C. Robanus-Maandag<sup>3</sup>

<sup>1</sup>Department of Pediatrics, Leiden University Medical Centre (LUMC), Leiden, The Netherlands, <sup>2</sup>Department of Tissue Regeneration, Institute for Biomedical Technology, University of Twente, Enschede, The Netherlands, <sup>3</sup>Department of Human Genetics, LUMC, Leiden, The Netherlands, <sup>4</sup>Department of Urology, LUMC, Leiden, The Netherlands, <sup>5</sup>Department of Animal Pathology, The Netherlands Cancer Institute, Amsterdam, The Netherlands, <sup>6</sup>Department of Medicine, Endocrine Unit, Massachusetts General Hospital, Harvard Medical School, Boston, Massachusetts, USA, <sup>7</sup>Galapagos, Romainville, France, <sup>8</sup>Department of Endocrinology and Metabolic Diseases, LUMC, Leiden, The Netherlands, <sup>9</sup>Department of Pathology, Josephine Nefkens Institute, Erasmus Medical Centre, Rotterdam, The Netherlands, <sup>#</sup>Equal contribution

BMC Dev Biol. 2009 Apr 8;9:26.





# Adenomatous polyposis coli-mediated control of $\beta$ -catenin is essential for both chondrogenic and osteogenic differentiation of skeletal precursors

R.L. Miclea, M. Karperien, C.A. Bosch, G. van der Horst, M.A. van der Valk, T. Kobayashi, H.M. Kronenberg, G. Rawadi, P. Akçakaya, C.W. Löwik, R. Fodde, J.M. Wit, E.C. Robanus-Maandag

## ABSTRACT

### Background

During skeletogenesis, protein levels of  $\beta$ -catenin in the canonical Wnt signaling pathway determine lineage commitment of skeletal precursor cells to osteoblasts and chondrocytes. Adenomatous polyposis coli (*Apc*) is a key controller of  $\beta$ -catenin turnover by down-regulating intracellular levels of  $\beta$ -catenin.

### Results

To investigate whether *Apc* is involved in lineage commitment of skeletal precursor cells, we generated conditional knockout mice lacking functional *Apc* in *Col2a1*-expressing cells. In contrast to other models in which an oncogenic variant of  $\beta$ -catenin was used, our approach resulted in the accumulation of wild type  $\beta$ -catenin protein due to functional loss of *Apc*. Conditional homozygous *Apc* mutant mice died perinatally showing greatly impaired skeletogenesis. All endochondral bones were misshaped and lacked structural integrity. Lack of functional *Apc* resulted in a pleiotropic skeletal cell phenotype. The majority of the precursor cells lacking *Apc* failed to differentiate into chondrocytes or osteoblasts. However, skeletal precursor cells in the proximal ribs were able to escape the noxious effect of functional loss of *Apc* resulting in formation of highly active osteoblasts. Inactivation of *Apc* in chondrocytes was associated with dedifferentiation of these cells.

### Conclusion

Our data indicate that a tight *Apc*-mediated control of  $\beta$ -catenin levels is essential for differentiation of skeletal precursors as well as for the maintenance of a chondrocytic phenotype in a spatio-temporal regulated manner.

## INTRODUCTION

During vertebrate embryogenesis, the axial and appendicular skeleton develop through endochondral bone formation. In this process, mesenchymal cells aggregate to form a chondrocytic template that prefigures the shape of the future bone. At the periphery of this cartilaginous mold, osteoblasts differentiate to form the bone collar. The cartilaginous mold is eventually replaced by bone in a step-wise program. Besides chondrocytes and osteoblasts, the skeleton also contains osteoclasts, which are of haematopoietic origin and play pivotal roles in both cartilage and bone resorption and remodelling (1-3).

Every step in the proliferation, differentiation, maturation, apoptosis, and resorption of both chondrocytes and osteoblasts is characterized by a specific transcriptional guideline (4). Sox9, a high-mobility-group transcription factor, and Runx2, a Runt domain transcription factor, are both expressed in bi-potential skeletal precursor cells differentiating into either chondrocytes or osteoblasts (5-7). Sox9 and Runx2 play leading roles in lineage commitment of these precursors: upregulation of Sox9 leads to chondrogenic differentiation (8), while activation of Runx2 is required for their osteogenic commitment (9).

Recently, based on mouse models, the canonical Wnt/ $\beta$ -catenin signaling pathway was found to act upstream of Sox9 and Runx2. In this pathway, in the absence of a Wnt signal, cytosolic  $\beta$ -catenin is degraded by the ubiquitination/proteasome system upon its phosphorylation at specific Ser-Thr residues by a destruction complex consisting of scaffold proteins such as Axin1, Axin2 (also known as Conductin) and the adenomatous polyposis coli (APC) tumor suppressor, and two kinases, namely glycogen synthase kinase 3 $\beta$  (GSK3 $\beta$ ) and casein-kinase 1 $\alpha$  (CK1 $\alpha$ ). Binding of Wnt to a complex composed of the transmembrane frizzled receptor and low-density lipoprotein receptor-related protein 5 or 6 (LRP5 or 6) co-receptor results in inactivation of the destruction complex and accumulation of cytoplasmic  $\beta$ -catenin. Upon its nuclear translocation,  $\beta$ -catenin acts as transcriptional co-activator in complex with transcription factors of the TCF/LEF family, leading to transcriptional activation of Wnt target genes (10). In wild type mouse embryos, high levels of  $\beta$ -catenin and activation of canonical Wnt signaling have been found in osteoblastic precursors in developing skull and limb bones (11). Accumulating evidence suggests that increased levels of canonical Wnt/ $\beta$ -catenin signaling inhibit Sox9 expression and activity, and stimulate Runx2 expression, leading to decreased chondrocyte differentiation and increased osteoblast differentiation, respectively (12-15). Similar results have been found in transgenic mice with *Wnt14* overexpression in *Collagen 2a1* (*Col2a1*)-expressing cells (11).

It has been also demonstrated that  $\beta$ -catenin is required at an early stage to repress chondrocytic differentiation (15). Upon conditional inactivation of  *$\beta$ -catenin* in the limb and head mesenchyme before or during early mesenchymal condensations, *Prx1*-expressing and *Dermo1*-expressing skeletal precursors, respectively, differentiate into chondrocytes instead of osteoblasts (11;15). Finally, results on both constitutively

active and inactivated  $\beta$ -catenin in *Osterix (Osx)*-, *Collagen 1a1 (Col1a1)*- or *Osteocalcin (Osc)*-expressing osteoblasts suggest that Wnt/ $\beta$ -catenin signaling coordinates bone formation by controlling the differentiation and activity of both osteoblasts and osteoclasts in a sequential, stage-specific manner (16;17).

Little is known about the mechanisms regulating  $\beta$ -catenin activity in skeletal precursors. Through its wide range of specific motifs and domains, APC is involved in multiple cellular processes such as signal transduction, cytoskeletal organization, apoptosis, cell adhesion and motility, cell fate determination, and chromosomal stability (18). However, biochemical and genetic evidence has been provided showing that APC's main tumor suppressing activity resides in its ability to bind to  $\beta$ -catenin and induce its degradation, thereby acting as a strong negative regulator of the canonical Wnt pathway (19-21).

Familial adenomatous polyposis (FAP) patients heterozygous for an APC mutation frequently develop osteomas and dental anomalies (22). Heterozygous *Apc*<sup>1638N</sup> mutant mice occasionally develop osteomas (R. Fodde, personal communication). Homozygosity for the severely truncated *Apc*<sup>Min</sup> and for the more hypomorphic *Apc*<sup>1638N</sup> allele in the mouse results in a failure of primitive ectoderm development shortly after implantation, leading to lethality prior to gastrulation (23;24). Mutant Apc disturbs the differentiation capacity of mouse embryonic stem (ES) cells in a quantitative and qualitative fashion depending on the dose of  $\beta$ -catenin signaling. Aberrant differentiation capacity of ES cells ranges from a strong differentiation blockade in case of two severely truncated *Apc*<sup>Min</sup> alleles, to more specific neuroectodermal, dorsal mesodermal, and endodermal defects (e.g., no differentiation in bone or cartilage) in case of two hypomorphic *Apc*<sup>1638N</sup> alleles (25;26). Osteoblast-specific loss of Apc in the mouse leads to early onset of dramatically increased bone deposition and to lethality early in life (17). However, Apc has not yet been linked with a role in the differentiation of skeletal precursor cells.

Here, we report that skeletal precursors of the axial and appendicular skeleton, when exposed to an uncontrolled rise of the  $\beta$ -catenin level due to conditional inactivation of *Apc*, lose their differentiation capacity to both the chondrogenic and osteogenic lineage. Moreover, conditional *Apc* mutant ribs show enhanced osteoblast activity, while the mutant nasal septum displays chondrocyte dedifferentiation. These results provide the first genetic evidence that Apc plays a crucial role throughout mouse skeletogenesis by regulating the differentiation of skeletal progenitor cells and maintenance of chondrocytes.

## MATERIALS AND METHODS

### Transgenic mice

All animal studies were approved by the ethical committee of the Leiden University Medical Centre and complied with national laws relating to the conduct of animal experiments. The *Apc*<sup>15lox/+</sup> mouse was generated by gene targeting in IB10 embryonic stem cells, using a 22.5 kb targeting vector containing loxP sites flanking the last exon

of *Apc*, i.e. exon 15. *LoxP* sites were inserted in the *Bgl*III site of intron 14 and in the *Apal* site approximately 350 bp downstream of the *Apc* polyadenylation signal. Exon 15 of the *Apc* gene encodes for codons 660 to 2842 of the Apc protein and harbours all the functional domains of Apc involved in  $\beta$ -catenin regulation as well as the C-terminal domains binding to microtubules, DLG, and EB1. Therefore, following Cre-mediated deletion of exon 15, functionality of the remaining protein will be fully impaired with respect to the main function of Apc, i.e.  $\beta$ -catenin regulating. Moreover, as deletion of exon 15 also removes the polyadenylation signal, no stable mRNA is produced and as a consequence no stable truncated protein will be generated. A full description of this new conditional *Apc* mouse model is currently in preparation (Robanus-Maandag et al., in preparation). Col2a1-*Cre* mice (27) were mated with *Apc*<sup>15lox/15lox</sup> mice. Of the offspring, Col2a1-*Cre*<sup>+/-</sup>; *Apc*<sup>15lox/+</sup> mice were mated with *Apc*<sup>15lox/15lox</sup> mice to obtain Col2a1-*Cre*<sup>+/-</sup>; *Apc*<sup>15lox/15lox</sup> mice. *LacZ* reporter mice were obtained from Dr. Xiaohong Mao (28). Routine mouse genotyping was performed on tail DNAs by PCR (Robanus-Maandag et al., in preparation).

### **Skeletal analysis**

Skeletons of mouse embryos were stained with Alcian blue and Alizarin red for cartilaginous and mineralized tissues, respectively, according to standard procedures (47). For micro-computed tomography ( $\mu$ CT) analysis, femora were recovered from 12-week-old mice after death and processed as described (48).

### **$\beta$ -galactosidase staining, Histology, Immunohistochemistry, In situ hybridization**

Whole mount  $\beta$ -galactosidase staining was performed as described (49), from E16.5 on after removal of the skin. For histology, immunohistochemistry, and in situ hybridization, specimens were fixed in phosphate-buffered formalin, embedded in paraffin, and sectioned at 6  $\mu$ m. Hematoxylin/eosin, Nuclear red, Toluidine blue, and von Kossa stainings were performed according to standard procedures. For immunohistochemistry, sections were treated with 1% H<sub>2</sub>O<sub>2</sub> in 40% methanol/60% TBS for 30 minutes to reduce endogenous peroxidase activity. For antigen retrieval the sections were boiled in Tris-EDTA pH 9.0 for 20 minutes. Blocking was performed with 5% blocking buffer for 30 minutes at 37°C (Boehringer Ingelheim). Sections were incubated with the primary mouse monoclonal antibody against  $\beta$ -catenin (1:100; BD Transduction Laboratories) overnight at 4°C, followed by incubation with the second antibody biotin-conjugated rabbit anti-mouse IgG (1:300; Amersham Biosciences) for 45 minutes at 37°C. The biotinylated proteins were detected by incubation with horseradish peroxidase-conjugated streptavidin (1:200; Amersham Biosciences) for 30 minutes at 37°C and visualized with DAB (Sigma). After counterstaining with Alcian blue for 15 minutes and hematoxylin for 1 minute, sections were dehydrated and embedded in Histomount (BDH). For in situ hybridization, digoxigenin-labeled single-stranded RNA probes were prepared using a DIG RNA labeling kit (Boehringer) following the manufacturers' instructions. All probes are available upon request. In situ hybridization was carried out as described (15;50). Images were taken with a DXM-1200 digital camera (Nikon).

## RESULTS

### Conditional *Apc*<sup>15lox</sup> mice and transgenic *Col2a1-Cre* mice

Recently, we (ECR-M and RF) generated a novel mouse model carrying a conditional *Apc*<sup>15lox</sup> allele where exon 15, encoding the majority of the coding region of *Apc* and the polyadenylation signal, is flanked by *loxP* sites. Mice heterozygous and homozygous for the conditional *Apc*<sup>15lox</sup> allele did not show any major abnormalities or susceptibility to tumors. *Apc*<sup>Δ15/+</sup> mice, heterozygous for the *Apc*<sup>Δ15</sup> mutant allele obtained by germline Cre-mediated deletion of exon 15, developed multiple intestinal tumors at an early age similar to *Apc*<sup>Min/+</sup> animals. These results indicate that Cre-mediated recombination of the *Apc*<sup>15lox</sup> allele leads to inactivation of the *Apc* protein and to the constitutive activation of Wnt/ $\beta$ -catenin signaling (Robanus-Maandag et al., in preparation).

Next, we investigated the temporal and spatial expression pattern of *Cre* in transgenic *Col2a1-Cre* mice (27) using *LacZ* reporter mice ("Rosaflox") (28). *Col2a1-Cre*;Rosaflox embryos expressed *Cre* specifically at all sites of endochondral bone formation (Fig. 1A). In accordance with previous studies suggesting that *Col2a1* is already expressed at E9.5 in the sclerotome of the somites (29), we detected *Cre* activity (based on positive LacZ staining) in mesenchymal condensations forming the sclerotome at E9.5 (Fig. 1B). At E12.5, LacZ-positive cells were identified in cartilage primordia later forming the vertebrae, long bones, sternum and cranial bones (Fig. 1C; data not shown). As reported in other *Col2a1-Cre* mouse lines (11;30), we found LacZ staining in the perichondrium at E14.5 (data not shown), and in the periosteum and primary spongiosa of long bones at E16.5, sites where osteoblasts normally differentiate (Fig. 1D,D'). The early onset (E9.5) of the *LacZ* expression in the sclerotome as well as its presence at later developmental stages (E14.5 and E16.5) in cells of the osteogenic lineage prompted us to conclude that the *Col2a1-Cre*-mediated recombination occurred in skeletal precursors characterized by both a chondrogenic and osteogenic differentiation potential.

### Heterozygous *Apc*<sup>15lox/+</sup> mice do not show any skeletal defect upon *Col2a1*-driven *Cre* expression

*Apc*<sup>15lox/15lox</sup> mice were bred with *Col2a1-Cre* mice to generate conditional heterozygous *Col2a1-Cre*;*Apc*<sup>15lox/+</sup> mice. Microscopical analysis performed on *Col2a1-Cre*;*Apc*<sup>15lox/+</sup> and control *Apc*<sup>15lox/+</sup> embryos at various developmental stages (E12.5, E14.5, E16.5) displayed a normal spatio-temporal expression of all chondrogenic and osteogenic markers investigated (data not shown).

To study postnatal growth and bone acquisition, 18 *Col2a1-Cre*;*Apc*<sup>15lox/+</sup> mice (7 males, 11 females) and 11 *Apc*<sup>15lox/+</sup> mice (7 males, 4 females) were monitored for 12 weeks after birth. Mice of both genotypes were healthy, similar in appearance, size, body length/weight ratio and growth rate (data not shown). We next assessed bone architecture in these animals by micro-computed tomography ( $\mu$ CT) of the distal femora. No difference was detected between *Col2a1-Cre*;*Apc*<sup>15lox/+</sup> mice and gender-matched *Apc*<sup>15lox/+</sup> control littermates with respect to bone mineral density, trabecular

bone volume fraction, trabecular number, trabecular thickness, and trabecular separation (Fig. 2A-D; data not shown). We further wanted to study whether conditional heterozygous *Apc* inactivation would lead to skeletal anomalies later in life. For this purpose, 10 *Col2a1-Cre;Apc<sup>15lox/+</sup>* mice (5 males and 5 females) and 5 *Apc<sup>15lox/+</sup>* male mice were followed for 24 months. At the end of this period, animals were sacrificed and tissues were analyzed microscopically using hematoxiline/eosine-stained sections. No important abnormalities could be distinguished in the skull, ribs, vertebral column and long bones. We evenly detected in both groups signs of cartilage degradation, fibrosis, and osteochondritis, pathological findings which most likely were all age-related (data not shown). Altogether, we considered conditional heterozygous *Apc* mutant embryos as controls for the next experiments.

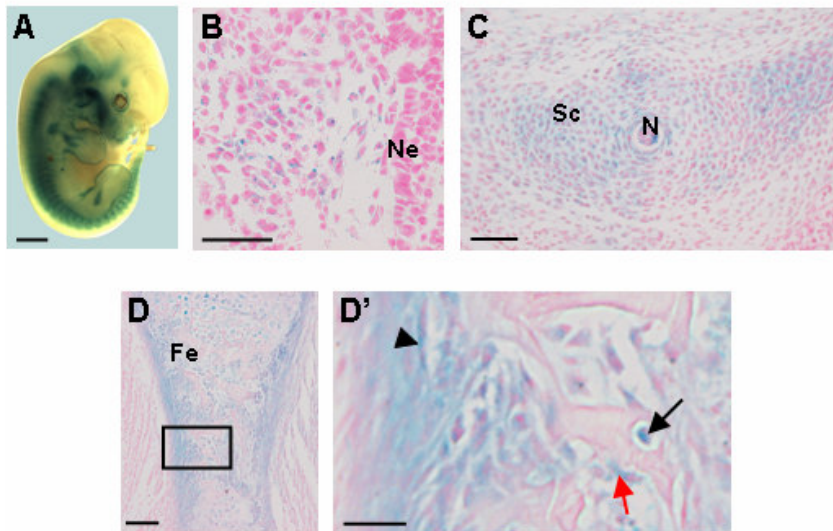


**Figure 1. *Col2a1-Cre;Rosaflox* mice express *Cre* at sites of endochondral bone formation.** (A-D) *LacZ* expression in *Col2a1-Cre;Rosaflox* embryos following *Cre* recombination, detected by whole-mount X-Gal staining. (A) Macroscopic picture of E12.5 *Col2a1-Cre;Rosaflox* embryo. (B) Transversal section of E9.5 embryo showing  $\beta$ -galactosidase-positive sclerotomal cells adjacent to the neural tube. (C) Transversal section of E12.5 embryo showing *LacZ* expression in vertebrae primordia. (D) Sagittal section of E16.5 embryo showing *LacZ* expression in the femur. The boxed region in D is magnified in D' showing *LacZ* expression in the periosteum (arrow head), osteoblasts (red arrow) and osteocytes (black arrow). Ne, neuroepithelium; Sc, sclerotome; N, notochord; Fe, femur. Scale bars: 1 mm in A; 50  $\mu$ m in B,D'; 100  $\mu$ m in C,D.

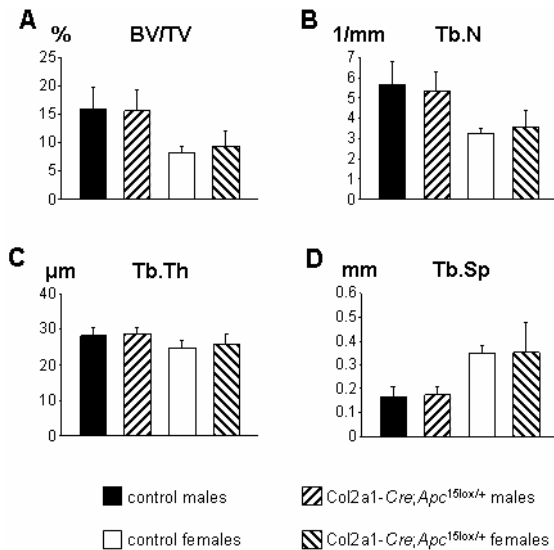


**Figure 2. Skeletal development occurs normally in Col2a1-Cre;Apc<sup>15lox/+</sup> mice.** (A-D)  $\mu$ CT analysis of the distal diaphysis of the femur did not reveal significant differences between 12-week-old Col2a1-Cre;Apc<sup>15lox/+</sup> mice and control littermates in any of the parameters investigated: (A) trabecular bone volume [BV/TV (%)], (B) number of trabeculae [Tb.N (1/mm)], (C) trabecular thickness [Tb.Th ( $\mu$ m)], and (D) trabecular separation [Tb.Sp (mm)]. All data represent mean values  $\pm$  s.d..

### Homozygous Col2a1-Cre;Apc<sup>15lox/15lox</sup> mice die perinatally due to severe defects in skeletogenesis

Col2a1-Cre;Apc<sup>15lox/+</sup> mice were crossed with Apc<sup>15lox/15lox</sup> mice to generate conditional homozygous Col2a1-Cre;Apc<sup>15lox/15lox</sup> mice (1:4). None of these mice were found at one month of age among 77 liveborn offspring. Of 27 dead pups found within the first month after delivery, only 5 pups on the day after delivery were Col2a1-Cre;Apc<sup>15lox/15lox</sup>. To further investigate the Col2a1-Cre;Apc<sup>15lox/15lox</sup> phenotype, embryonic litters at various developmental stages were isolated. Eight of 31 embryos isolated between E16.5 and E19.5 were Col2a1-Cre;Apc<sup>15lox/15lox</sup> (26%). We concluded that conditional homozygosity for this Apc mutant allele was perinatally lethal.

At E12.5, Col2a1-Cre;Apc<sup>15lox/15lox</sup> embryos, although normal in size, displayed poor mandible and limb outgrowth compared to control littermates (Fig. 3A). At E14.5 and E16.5, Col2a1-Cre;Apc<sup>15lox/15lox</sup> embryos were much smaller in comparison to controls, displayed craniofacial abnormalities, short trunk, and an incomplete closure of both thoracic and abdominal cavities (Fig. 3B,C). Gross analysis further indicated a severe truncation of both upper and lower limbs. Already at E14.5, but more significantly at E16.5, Col2a1-Cre;Apc<sup>15lox/15lox</sup> embryos presented large skin blisters especially in the dorso-lumbar region (Fig. 3C).



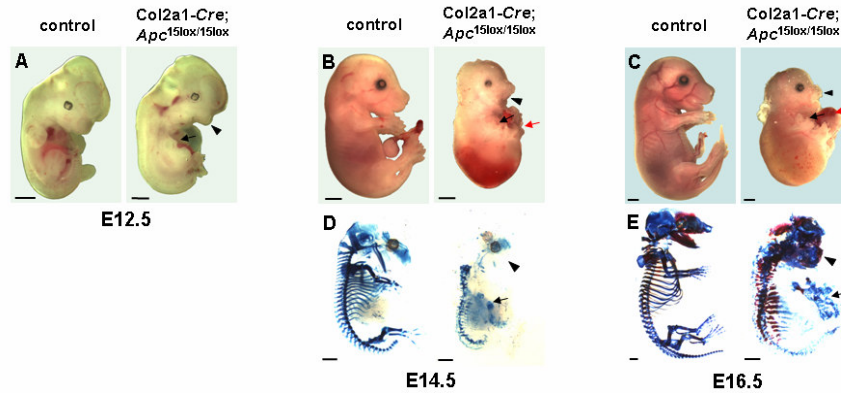


**Figure 3. Skeletogenesis is severely impaired in *Col2a1-Cre;Apc<sup>15lox/15lox</sup>* embryos.** (A-E) Greatly impaired skeletal development and growth arrest of *Col2a1-Cre;Apc<sup>15lox/15lox</sup>* embryos. Gross appearance (A-C) and Alizarin red and Alcian blue and Alizarin red staining (D-E) of skeletal preparations of *Col2a1-Cre;Apc<sup>15lox/15lox</sup>* embryos and control littermates at indicated developmental stages. Conditional *Apc* mutants showed lack of mandible outgrowth (arrowheads), poor limb development (black arrows), and an open thoracic and abdominal cavity (red arrows). Scale bars: 1 mm.

Skeletal preparations of mouse embryos stained with Alcian blue (chondrocyte matrix) and Alizarin red (mineralized matrix) of embryos at E14.5 revealed a clear difference in size between *Col2a1-Cre;Apc<sup>15lox/15lox</sup>* mutants and control littermates (Fig. 3D). All mutant structures were severely misshaped and fragmented. Mutants failed to develop a cartilaginous mold of both the mandibles and the occipital bone. The axial skeleton contained patchy and irregular cartilaginous structures that did not organize in vertebrae. All 13 rib pairs could be individually distinguished, however, due to their inadequate orientation, size, and shape and due to lack of a sternum, no thoracic basket was formed (Fig. 4A,B). Distorted cartilage rudiments were found where forelimbs should normally arise (Fig. 4E,F), while no signs of bone formation were found in hindlimb rudiments. Furthermore, no cartilaginous primordia of pelvic bones were observed. Similar observations were made in *Col2a1-Cre;Apc<sup>15lox/15lox</sup>* embryos at E16.5 (Fig. 3E). At this developmental stage however, distinct areas of mineralization were observed in most parts of the mutant skeleton. The mutant hind skull showed mineralized regions, whereas the control occipital and temporal bone primordia stained only with Alcian blue (Fig. 4I,J). Mutant proximal ribs in these *Col2a1-Cre;Apc<sup>15lox/15lox</sup>* embryos were much thicker and shorter in comparison to those in control embryos, and stained intensively with Alizarin red (Fig. 4C,D). In the mutant forelimb, a hypoplastic scapula could be identified, whereas more distal components were agenetic and replaced by an irregular cartilaginous structure (Fig. 4G,H).

### Loss of functional *Apc* inhibits differentiation of skeletal precursors

Lack of functional *Apc* results in accumulation of cytoplasmic  $\beta$ -catenin, translocates into the nucleus. This process can be well detected by immunohistochemistry

(IHC). To investigate endochondral bone formation in *Col2a1-Cre;Apc<sup>15lox/15lox</sup>* embryos, we analyzed vertebra formation at E12.5 and E14.5, and humerus development at E16.5 using IHC for  $\beta$ -catenin in combination with Alcian blue staining, and *in situ* hybridization (ISH) for several chondrocyte- and osteoblast-specific genes. Strongly elevated levels of  $\beta$ -catenin were seen at all sites of endochondral ossification in the *Col2a1-Cre;Apc<sup>15lox/15lox</sup>* embryos at E12.5, E14.5 and E16.5, indicating efficient *Col2a1-Cre*-mediated *Apc* inactivation.

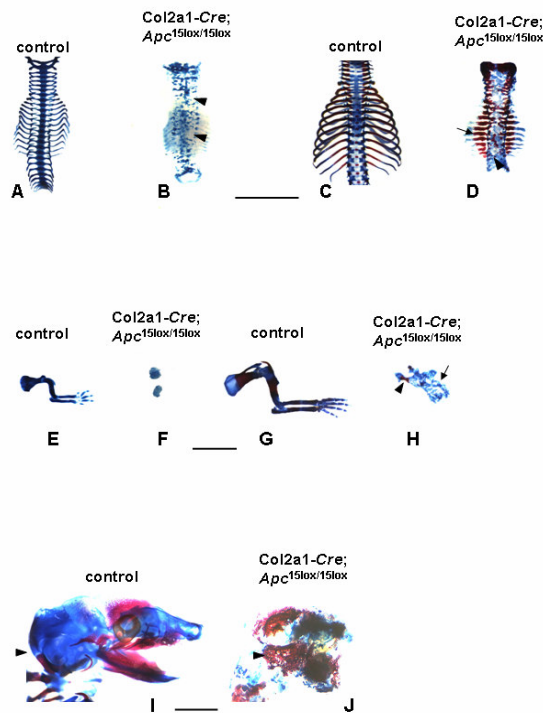


**Figure 4. Details of skeletal preparations.** (A-D) Vertebral column of control and mutant littermates at E14.5 (A,B) and E16.5 (C,D). Mutant vertebrae lacked structural integrity (arrowheads). At E16.5, mineralization was enhanced in the proximal part of the mutant rib (arrow). (E-H) Forelimb of control and mutant littermates at E14.5 (E,F) and E16.5 (G,H). At E16.5, only the scapula was identified (arrowhead), while more distal parts were represented by patchy cartilage aggregations (arrow). (I,J) Skull of control and mutant littermates at E16.5. The mutant displayed mineral deposition in the back skull corresponding to the cartilaginous structure in the control (arrowheads). Scale bars: 3 mm in A-H; 1 mm in I,J.

At E12.5, transversal sections of control vertebral primordia showed normal mesenchymal cell condensation and subsequent chondrogenic differentiation (Fig. 5A-C). Chondrocytes stained negatively for  $\beta$ -catenin, started to deposit an Alcian blue-stained matrix, and expressed the nascent chondrocyte markers *Sox9* and *Col2a1*. In marked contrast, mutant sclerotomal cells failed to condense into skeletal primordias.

They showed strong nuclear  $\beta$ -catenin staining and displayed a mesenchymal-like spindle shape morphology. These cells expressed neither *Sox9*, nor *Col2a1*, implying that conditional loss of functional *Apc* in skeletal precursors inhibited mesenchymal cell condensation and chondrogenic differentiation. Next, we investigated whether these cells had switched their commitment to the osteogenic lineage due to the accumulation of  $\beta$ -catenin. Surprisingly, they did not express the early osteoblast markers *Runx2* and *Col1a1*, suggesting that  $\beta$ -catenin accumulation due to *Apc* inactivation impaired osteogenic differentiation of skeletal precursors as well (Fig. 5D,E).

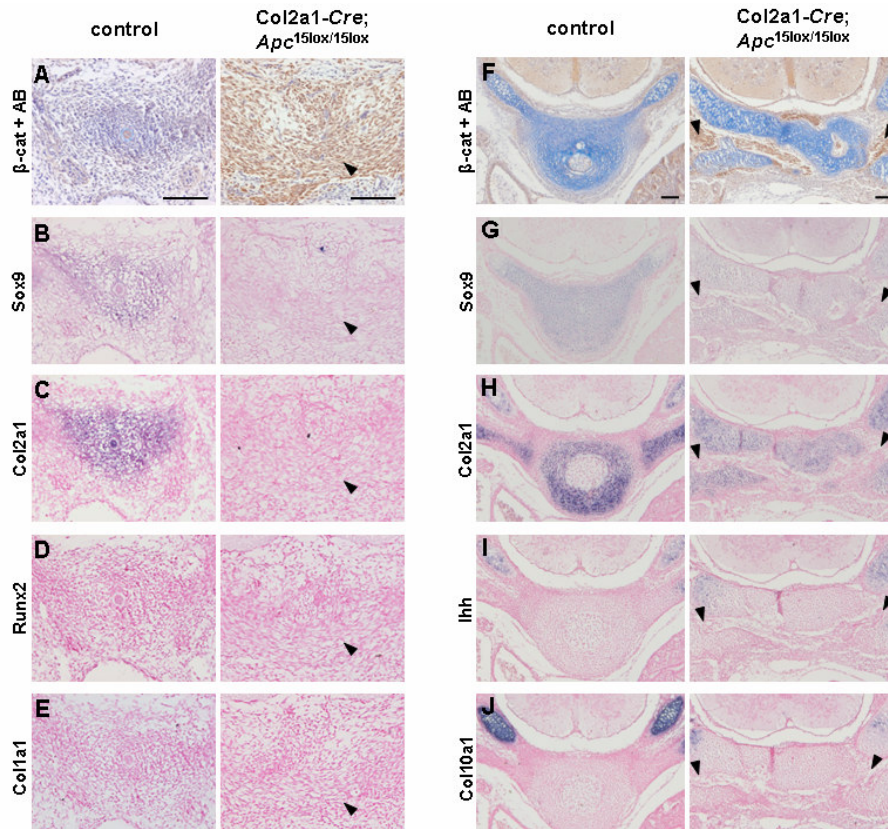


**Figure 5. Abnormal axial skeleton formation of *Col2a1-Cre;Apc<sup>15lox/15lox</sup>* embryos already detectable at E12.5.** (A) Immunostaining for  $\beta$ -catenin combined with Alcian blue (AB) staining, and (B-E) gene expression analysis by in situ hybridization with indicated probes on consecutive transversal sections of the sclerotome of a *Col2a1-Cre;Apc<sup>15lox/15lox</sup>* embryo and control littermate at E12.5. (F-J) Similar analysis of vertebrae primordia at E14.5.  $\beta$ -Catenin-positive spindle-shaped cells lacked expression of all indicated chondrogenic and osteogenic markers (arrowheads). Scale bars: 100  $\mu$ m.

At E14.5, chondrocytes in the control vertebrae did not stain positively for  $\beta$ -catenin, displayed an intensely Alcian blue-stained matrix and expressed both early (*Sox9*, *Col2a1*) and mature chondrocyte markers, like *Indian hedgehog* (*Ihh*) and *Collagen 10a1* (*Col10a1*), indicating a normal progression of endochondral ossification (Fig. 5F-J). Although somite formation was present, mutant vertebrae were heavily crumbled and failed to organize in a cartilaginous anlage. Occasionally Alcian blue-positive clusters of chondrocytes were seen, which lacked detectable  $\beta$ -catenin immunostaining and were positive for chondrogenic marker expression. These cells were probably derived from non-recombined cells due to mosaicism of *Cre* expression. Surrounding these cartilage islands, mesenchymal-like spindle-shaped cells were observed. Comparable to the defects observed at E12.5, these cells expressed high levels of nuclear  $\beta$ -catenin due to *Apc* inactivation and lacked not only an Alcian blue-positive matrix but also expression of both chondrogenic and osteogenic markers (Fig. 5F-J; data not shown).

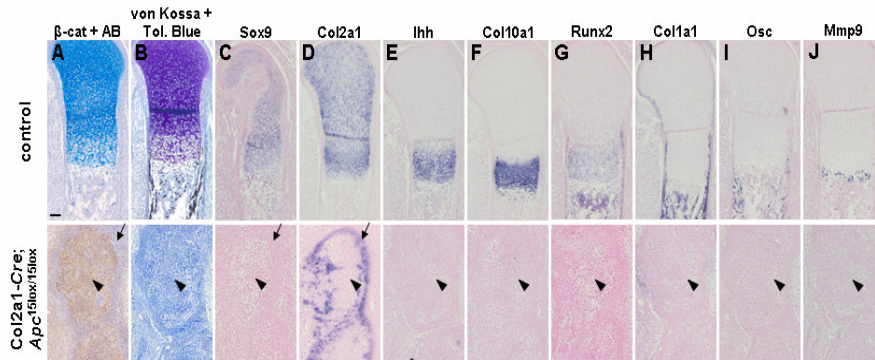


**Figure 6. No chondrogenic and osteogenic differentiation in the developing humerus due to lack of functional *Apc*.** (A-B) Immunostaining for  $\beta$ -catenin combined with Alcian blue (AB) staining (A), combined von Kossa-Toluidine blue staining (B), and (C-J) gene expression analysis by in situ hybridization with indicated probes for (C-F) chondrocytes, (G-I) osteoblasts and (J) osteoclasts on consecutive transversal sections of the developing humerus of a *Col2a1-Cre;Apc*<sup>15lox/15lox</sup> embryo and control littermate at E16.5.  $\beta$ -Catenin-positive spindle-shaped cells organized in clusters and failed to express chondrogenic and osteogenic markers (arrowheads).  $\beta$ -Catenin-negative cells at the periphery of these clusters expressed early chondrogenic markers only (arrows), probably due to lack of *Cre*-mediated loss of functional *Apc*. Scale bars: 100  $\mu$ m.

At E16.5, chondrocytes of control proximal humeri did not express detectable  $\beta$ -catenin protein levels and were surrounded by a proteoglycan-rich matrix, which stained positively with both Alcian blue and Toluidine blue (Fig. 6A,B). They were organized in growth plates with a characteristic spatial expression pattern of the chondrogenic markers *Sox9*, *Col2a1*, *Ihh*, and *Col10a1* (Fig. 6C-F). Young osteoblasts in the perichondrium, periosteum and primary spongiosa were surrounded by a mineralized osteoid as detected by von Kossa staining (Fig. 6B) and expressed *Runx2* and *Col1a1* (Fig. 6G,H). Mature osteoblasts expressed *Osc* (Fig. 6I), while osteoclasts expressed

Matrix metalloproteinase 9 (*Mmp9*) (Fig. 6J). In contrast, mutant humeri were completely misshaped and contained nuclear  $\beta$ -catenin-positive cells that were organized in clusters, showing a mesenchymal-like shape (Fig. 6A). Similar to our observations at E12.5 and E14.5, these cells expressed neither chondrogenic, nor osteogenic markers (Fig. 6C-I). In addition, no *Mmp9* expression could be detected (Fig. 6J), suggesting that differentiation of bone-resorbing cells was impaired as well. These  $\beta$ -catenin-positive cell clusters were surrounded by chondrocytes expressing *Sox9* and *Col2a* and lacked positive staining for  $\beta$ -catenin. These cell most likely have not undergone a recombination event as observed at E14.5 (Fig. 6A,C,D).

### **Increased osteoblastogenesis in proximal ribs of *Col2a1-Cre;Apc<sup>15lox/15lox</sup>* embryos**

Despite the inhibitory effect of *Apc* inactivation on differentiation of skeletal precursors in long bones and vertebrae, proximal ribs of *Col2a1-Cre;Apc<sup>15lox/15lox</sup>* embryos at E16.5 showed clearly enhanced mineralization upon skeletal staining (Fig. 4D). Therefore, we analyzed the development of these skeletal structures in more detail. The ribs develop through endochondral ossification from the paired lateral sclerotomic areas (31). Formation of the proximal rib depends on the notochord and the ventral neural tube, whereas development of the distal part depends on the surface ectoderm (32). At E14.5, proximal ribs of control embryos were cartilaginous and contained mature chondrocytes that did not stain for  $\beta$ -catenin (Fig. 7A-C). Mutant proximal ribs were severely misshaped and contained  $\beta$ -catenin negatively stained cartilage islands, accounting for the positive Alcian blue staining observed upon skeletal preparation (Fig. 4B,7A).  $\beta$ -Catenin-positive cells were negative for chondrogenic and osteogenic markers (Fig. 7A-D). At E16.5, the  $\beta$ -catenin-negative proximal ribs of control embryos consisted of cartilage and mineralized bone matrix as indicated by combined von Kossa-Toluidine blue staining (Fig. 7E,F; data not shown). They contained chondrocytes, osteoblasts, and osteoclasts as assessed by ISH (Fig. 7H-K; data not shown). In contrast, proximal ribs of mutant littermates stained strongly positive for  $\beta$ -catenin and were significantly thicker and shorter compared to those of control embryos (Fig. 4C,D and 7E-G). They consisted of a massive mineralized bone matrix and a poorly developed bone marrow cavity, although osteoclast differentiation and activity were normal as assessed by ISH for *Mmp9* and TRAP staining, respectively (Fig. 7K,L,L').

Interestingly,  $\beta$ -catenin-positive cells expressed all osteogenic markers analyzed (*Runx2*, *Col1a1*, and *Osc*), indicating that, unlike in the long bones and vertebrae, *Apc* inactivation in skeletal precursors of the proximal ribs did not impair osteoblastogenesis (Fig. 7H-J). Since *Ihh* is a critical regulator of osteoblastogenesis, we subsequently tested whether the increased ossification might be due to increased *Ihh* expression in the non-recombined neighbouring chondrocytes. The  $\beta$ -catenin-negative cells, however, matured normally expressing all chondrocyte markers investigated (*Sox9*, *Col2a1*, *Ihh* and *Col10a1*) at similar levels compared to control cartilage (data not shown). The abundant presence of a bone matrix combined with evidence of functional osteoclasts suggested that the  $\beta$ -catenin-positive osteoblasts were sclerotic.

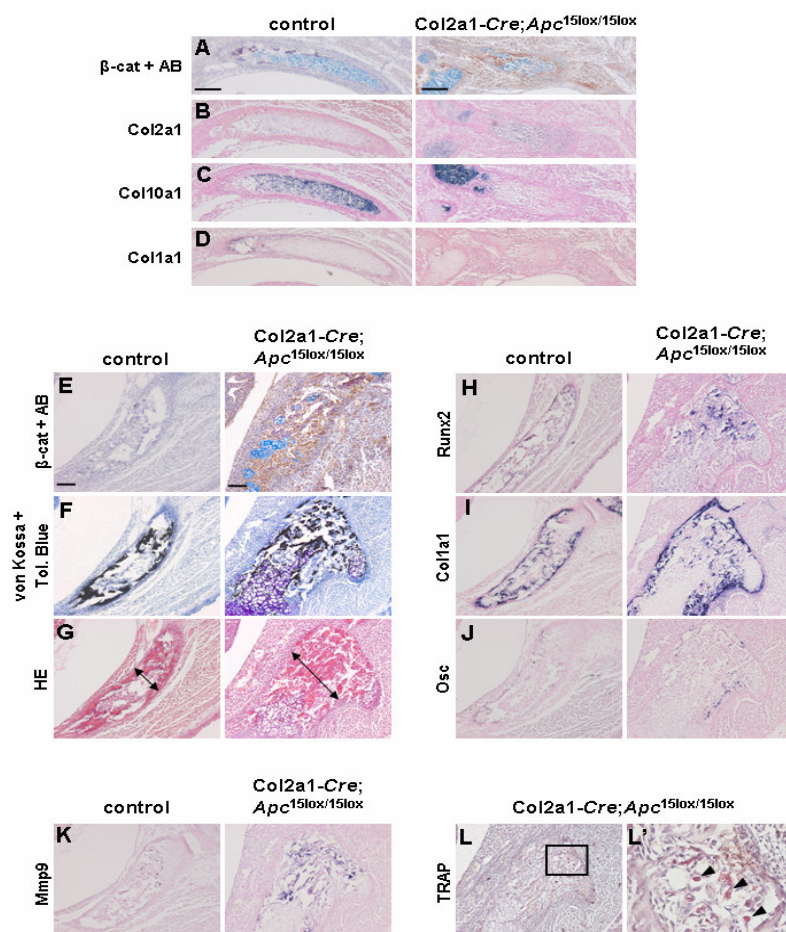


**Figure 7. Conditional *Apc* inactivation enhances osteoblast formation and mineral deposition in the developing proximal rib.** (A-L) Immunostaining for  $\beta$ -catenin combined with Alcian blue (AB) staining (A,E), combined von Kossa-Toluidine blue staining (F), hematoxylin/eosin staining (G), gene expression analysis by in situ hybridization with indicated probes for chondrogenic (B,C), osteogenic (D,H-J) and osteoclastogenic differentiation (K) on consecutive transversal sections of the developing proximal rib of a *Col2a1-Cre;Apc<sup>15lox/15lox</sup>* embryo and control littermate at E14.5 (A-D) and E16.5 (E-K). The double-headed arrows in G indicate the thickness of the rib. (L) Tartrate-resistant acid phosphatase (TRAP) staining of the developing proximal rib of a *Col2a1-Cre;Apc<sup>15lox/15lox</sup>* embryo at E16.5. The boxed region in L is magnified in L' showing multinucleated osteoclasts (arrowheads) staining positive for TRAP. Scale bars: 100  $\mu$ m in A-L; 50  $\mu$ m in L'.

### Chondrocyte dedifferentiation in the nasal septum of *Col2a1-Cre;Apc<sup>15lox/15lox</sup>* embryos

The nasal septum is a midline vertical plate of hyaline cartilage, which undergoes endochondral ossification in postnatal life (33). Endochondral ossification of the caudal and dorsal borders of the septum, when combined with interstitial expansion, has the effect of displacing the facial skeleton away from the neurocranium and thus enlarging the skull (34). At E16.5, chondrocytes forming the nasal septum of control mice did not stain for  $\beta$ -catenin, were surrounded by an Alcian blue-positive matrix, and expressed *Sox9* and *Col2a1* (Fig. 8A-D). In the mutant nasal cartilage we distinguished crumbled chondrogenic islands surrounded by  $\beta$ -catenin-positive cells with an undifferentiated mesenchymal-like phenotype (Fig. 8F-H). The chondrogenic islands consisted of round cells embedded in chondrons surrounded by extracellular matrix (ECM) (Fig. 8E). Interestingly, molecular analysis of these chondrogenic islands revealed the presence of two cell populations:  $\beta$ -catenin-negative and  $\beta$ -catenin-positive cells. The former expressed chondrogenic markers like *Sox9* and *Col2a1*, and their ECM stained positive with Alcian blue, whereas the latter did not express any chondrogenic or osteogenic markers, while their ECM stained significantly less with Alcian blue (Fig. 8F-I; data not shown).

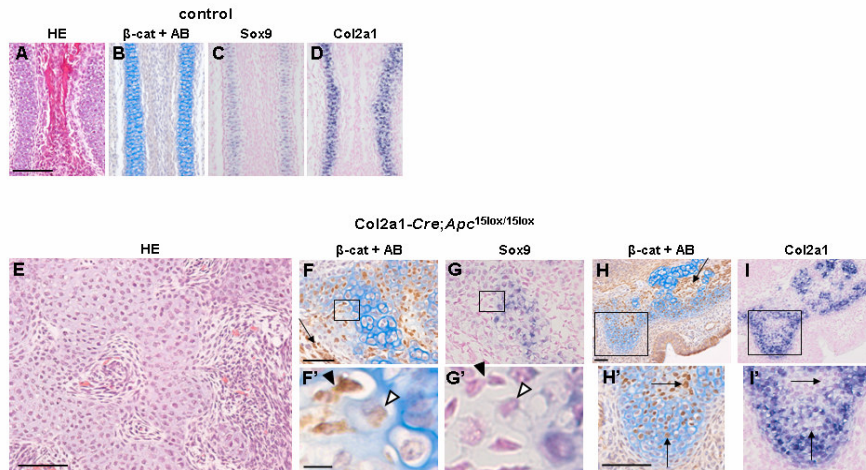


**Figure 8. Dedifferentiation in the nasal septum of *Col2a1-Cre;Apc<sup>15lox/15lox</sup>* embryos at E16.5.** (A,E) Hematoxylin/eosin staining, (B,F,H) immunostaining for  $\beta$ -catenin combined with Alcian blue (AB) staining, and (C-D,G,I) gene expression analysis by in situ hybridization with indicated probes for chondrogenic differentiation on consecutive transversal sections of the developing nasal septum of a *Col2a1-Cre;Apc<sup>15lox/15lox</sup>* embryo and control littermate at E16.5. (F',G',H',I') High magnification pictures of the boxed regions in F, G, H, and I, respectively. Mesenchymal-like  $\beta$ -catenin-positive cells (arrow in F,H) were present between crumbled cartilage islands. Within these cartilage islands, although displaying chondrocytic morphology and an Alcian blue stained matrix, most of the  $\beta$ -catenin-positive cells did not express *Sox9* (arrowheads in G') or *Col2a1* (arrows in I'). Scale bars: 100  $\mu$ m in A,E,F,H; 5  $\mu$ m in F',H'.

The presence of  $\beta$ -catenin-positive cells in the chondrogenic islands suggested that these cells, due to mosaicism of *Cre* expression, had initiated normal chondrocyte differentiation before undergoing *Apc* inactivation. Subsequently, the increased level of  $\beta$ -catenin triggered the loss of expression of the early chondrogenic markers and initiated degradation of the ECM. These observations were indicative of dedifferentiated chondrocytes. Similar observations were made in cartilaginous rudiments at other sites of endochondral bone formation, but the effect was most pronounced in the nasal septum (data not shown).

## DISCUSSION

### Conditional homozygous loss of functional *Apc* severely disrupts mouse skeletogenesis via stabilized $\beta$ -catenin

According to most of the transgenic mouse studies reported, levels of  $\beta$ -catenin, the effector of the canonical Wnt ligands, need to be downregulated in skeletal precursor cells to enable chondrogenic differentiation, whereas elevated  $\beta$ -catenin levels promote differentiation into osteoblasts (11;12;15;35;36). This theory is partly based on observations in heterozygous gain-of-function models in which *Cre*-mediated recombination results in the expression of oncogenic  $\beta$ -catenin. The cellular mechanisms controlling the biological effects of oncogenic  $\beta$ -catenin in the presence of wild type  $\beta$ -catenin are largely unknown. In addition, there are no reports on the role of *Apc* in regulation of skeletal precursor differentiation via control of  $\beta$ -catenin in the mouse. Here, we have focused on this important role of the multifunctional protein *Apc*, binding to and downregulating  $\beta$ -catenin. We have selectively inactivated one or both alleles of *Apc* in murine *Col2a1*-expressing cells. Our data indicate that the *Col2a1* promoter is suitable for this study, since *Cre*-mediated recombination starts very early (E9.5) in skeletal precursor cells that have not yet committed to the chondrogenic or the osteogenic lineage, consistent with previous findings in other *Col2a1-Cre* lines (11;30).

Conditional heterozygous inactivation of *Apc* does not result in a detectable level of its target  $\beta$ -catenin as determined by IHC. Moreover, heterozygous *Col2a1-Cre*-mediated *Apc* inactivation does not interfere with embryonic skeletal development, postnatal growth or bone acquisition up to 24 months of age, as determined by histological and  $\mu$ CT analysis. Our data imply that the level of *Apc* protein produced by a single functional *Apc* allele is sufficient to mediate appropriate  $\beta$ -catenin degradation. This is in agreement with normal body weight, size, and growth of young *Apc*<sup>Min/+</sup> mice (37).

In marked contrast, conditional inactivation of *Apc* results in a strongly elevated level of (wild type)  $\beta$ -catenin in skeletal precursors, leading to greatly impaired embryogenesis and perinatal lethality. The significantly reduced size and the vast range of skeletal malformations in these embryos is most likely due to the specific *Col2a1-Cre* activity in skeletal primordias at a very early embryonic stage starting at E9.5 resulting in massive  $\beta$ -catenin accumulation in the developing endochondral skeleton. Probably



several factors, like the open rib cage and the severe malformation, from E14.5 on have led to the perinatal lethality. The loss of the multiple  $\beta$ -catenin-independent functions of the Apc protein might have contributed to the gravity and complexity of the skeletal phenotype observed in *Col2a1-Cre;Apc<sup>15lox/15lox</sup>* mice as well (18). Moreover, since *Col2a1* expression is not completely restricted to skeletal tissues during mouse embryogenesis (29), we can not exclude that the severity of the phenotype might have been partly due to loss of functional Apc in other *Col2a1-Cre*-expressing cell types.

### **Apc is crucial for both chondrogenic and osteogenic differentiation of skeletal precursors**

Wnt/ $\beta$ -catenin signaling represents a mechanism in mesenchymal precursor cells for selecting between chondrocytic and osteoblastic fates. This key regulating role in lineage commitment has been attributed to  $\beta$ -catenin. Indeed, conditional gain-of-function mutation of  *$\beta$ -catenin* leads to decreased chondrocyte differentiation in *Prx1*-expressing and *Col2a1*-expressing cells (12;15). However, corresponding increased osteoblast differentiation has not been observed in these models, instead, a decreased osteoblast marker expression has been seen in case of *Prx1*-expressing cells, suggesting that activation of  $\beta$ -catenin negatively affects skeletogenesis (12;15). In addition, conditional loss-of-function mutation of  *$\beta$ -catenin* in *Prx1*-expressing cells leads to increased expression of not only chondrocyte but also early osteoblast markers (15). These data strongly suggest that  $\beta$ -catenin negatively regulates the differentiation of mesenchymal cells into a common skeletal precursor (38).

We report here that in the vast majority of endochondral skeletal elements, precursor cells lacking functional Apc express strong nuclear  $\beta$ -catenin staining and fail to differentiate into both chondrogenic and osteogenic lineages. These data are in line with the inability of mouse embryonic stem cells carrying specific bi-allelic Apc mutations to differentiate into bone and cartilage (25). Our data are also consistent with those based on conditional stabilization of  $\beta$ -catenin in mesenchymal skeletal precursors which had an undifferentiated appearance (15). This consistency strongly suggests that, notwithstanding the multiple functions of Apc, its  $\beta$ -catenin-controlling role is the most important during skeletogenesis. We conclude that Apc plays a crucial role in differentiation of skeletal precursors in vertebrae and long bones: it enables the differentiation into both skeletal lineages by decreasing the level of  $\beta$ -catenin.

### **Loss of functional Apc in skeletal precursors of the proximal rib stimulates osteogenesis**

Although in the vast majority of the endochondral skeleton both chondrogenic and osteogenic differentiation is inhibited due to loss of functional Apc in skeletal precursors, we find a different phenotype in the proximal ribs. Notwithstanding the cartilaginous structure at E14.5, proximal ribs of *Col2a1-Cre;Apc<sup>15lox/15lox</sup>* mutants at E16.5 show abundant bone matrix deposited by osteoblasts, invariably expressing high levels of nuclear  $\beta$ -catenin. Since osteoblasts do not express *Col2a1*, these cells are most likely derived from *Col2a1*-expressing skeletal precursors lacking functional Apc. This implies that, in contrast to other skeletal elements, skeletal precursors of the proximal

ribs are able to escape from the noxious effects of strongly elevated  $\beta$ -catenin levels on differentiation of precursor cells by an as yet unknown mechanism. Since *lhh* expression is normal in the non-recombined neighbouring chondrocytes, we speculate that *lhh* may be a prime target for inducing osteoblastogenesis in the recombined precursor cells counteracting the noxious effect of  $\beta$ -catenin.

Despite the evidence of functional osteoclasts, the intensely ossified proximal ribs show a strongly diminished bone marrow cavity, rendering it likely that the increased bone formation is due to osteosclerosis. These observations are in agreement with other data, showing that enhanced canonical Wnt signaling can increase bone mass through stimulation of osteoblast activity rather than inhibition of osteoclast formation and activity (39-41). Such an osteopetrotic phenotype has only been seen in mice with conditional loss of functional *Apc* or constitutively active  $\beta$ -catenin in already differentiated osteoblasts, resulting in dramatically increased bone deposition (17;42).

### **Functional *Apc* is required to maintain the chondrocyte phenotype**

We have found clear evidence for the occurrence of chondrocyte dedifferentiation due to  $\beta$ -catenin accumulation in the nasal septum. Morphologically characterized chondrocytes, which were nuclear  $\beta$ -catenin-positive, lacked expression of typical chondrocyte markers. Furthermore, they were imbedded in an ECM containing significantly less proteoglycans.

Given the noxious effect of increased  $\beta$ -catenin levels on chondrocyte formation (our data and 12;15), these cells most likely have undergone Cre-mediated loss of functional *Apc* after completion of the initial stages of chondrocyte differentiation. Mouse models with an increased level of  $\beta$ -catenin in *Col2a1*-expressing cells show accelerated chondrocyte maturation (11;12). We have found no indication for this phenomenon, implying that the high level of  $\beta$ -catenin due to loss of *Apc* does not result in chondrocyte maturation but in chondrocyte dedifferentiation. Our data suggest that accumulated  $\beta$ -catenin triggers this dedifferentiation program not only through inhibition of chondrogenic marker expression but also by enhancing the loss of ECM presumably through stimulation of matrix-degrading enzymes. It has been demonstrated that  $\beta$ -catenin increases expression and activity of a number of enzymes involved in matrix degradation (43-45).  $\beta$ -Catenin stabilization has been associated with dedifferentiation of articular chondrocytes in vitro upon serial monolayer culture, or treatment with retinoic acid or IL1 $\beta$  (46). Dedifferentiated chondrocytes have also been observed at other sites of endochondral bone formation in the *Col2a1-Cre;Apc<sup>15lox/15lox</sup>* embryos, however, the presence of these cells was most pronounced in the nasal septum. Altogether, our data indicate that *Apc* is required to suppress  $\beta$ -catenin for maintenance of the chondrocytic phenotype.

## **CONCLUSION**

We show here for the first time that *Apc*, by negatively controlling the levels of  $\beta$ -catenin, is a critical regulator of the differentiation of skeletal progenitor cells. Conditional inactivation of the mouse *Apc* gene results in a heterogeneous skeletal pheno-

type. Based on our results, we postulate that Apc-mediated control of the dosage of transcriptionally active  $\beta$ -catenin protein is directive for the differentiation program of skeletal precursor cells. In the vast majority of the skeletal precursors, loss of functional *Apc* leads to a strongly increased  $\beta$ -catenin level, resulting in the formation of an undifferentiated mesenchymal cell, which lacks differentiation potential for both osteogenic and chondrogenic lineages. When the inhibitory effect of a strongly increased  $\beta$ -catenin level in the skeletal precursors is reduced, highly active osteoblasts arise. Strong repression of  $\beta$ -catenin in these precursors is required for chondrogenesis. Support for our hypothesis on the importance of the dosage of Apc and  $\beta$ -catenin is provided by observations in *Col2a1-Wnt14* transgenic mice (11). Higher levels of *Wnt14* expression resulting in a high level of  $\beta$ -catenin block differentiation of skeletal precursors into chondrocytes or osteoblasts, whereas lower levels of *Wnt14* expression result in enhanced ossification. We provide evidence that Apc plays a crucial role in modulating the  $\beta$ -catenin level during mouse skeletogenesis in a spatio-temporal regulated manner. In skeletal precursor cells, Apc is required for differentiation into both chondrocytes and osteoblasts. In addition, Apc is essential in chondrocytes to maintain their phenotype and enable their maturation.

## AUTHORS' CONTRIBUTIONS

*The studies were designed and initiated by MK as principal investigator, with the help of RF and ECR-M; Col2a1-Cre mice were provided by TK and HMK; mutant mice were generated and genotyped by CAJB and ECR-M; embryo experimental work and analysis were performed by RLM;  $\mu$ CT analysis was performed by GR; data interpretation was carried out by RLM assisted by MK, GH, MAV, PA, CWL, RF, JMW, and ECR-M; the manuscript was written by RLM with the assistance of all co-authors. All authors read and approved the final manuscript.*

## ACKNOWLEDGEMENTS

*We thank Christine Hartmann (IMP, Vienna, Austria) for the mouse *Runx2*, *Sox9*, *Osc*, and *Ihh* probes, Eero Vuorio (University of Turku, Finland) for the mouse *Col1a1* and *Col2a1* probes, and Willy Hofstetter (University of Bern, Switzerland) for the mouse *Col10a1* probe.*

*This work was financially supported by a short-term research fellowship from the European Society for Pediatric Endocrinology (RLM), an unrestricted educational grant from IPSEN FARMACEUTICA BV (RLM), a research grant from The Human Growth Foundation (MK), and a research grant from the Association for International Cancer Research (CAJB).*

## REFERENCES

1. Karsenty G, Wagner EF. Reaching a genetic and molecular understanding of skeletal development. *Dev Cell* 2002; 2(4):389-406.
2. Tuan RS. Biology of developmental and regenerative skeletogenesis. *Clin Orthop Relat Res* 2004;(427 Suppl):S105-S117.
3. Olsen BR, Reginato AM, Wang W. Bone development. *Annu Rev Cell Dev Biol* 2000; 16:191-220.
4. Akiyama H, Chaboissier MC, Martin JF, Schedl A, de Crombrughe B. The transcription factor Sox9 has essential roles in successive steps of the chondrocyte differentiation pathway and is required for expression of Sox5 and Sox6. *Genes Dev* 2002; 16(21):2813-28.
5. Smith N, Dong Y, Lian JB, Pratap J, Kingsley PD, van Wijnen AJ et al. Overlapping expression of Runx1(Cbfa2) and Runx2(Cbfa1) transcription factors supports cooperative induction of skeletal development. *J Cell Physiol* 2005; 203(1):133-43.
6. Zhou G, Zheng Q, Engin F, Munivez E, Chen Y, Sebald E et al. Dominance of SOX9 function over RUNX2 during skeletogenesis. *Proc Natl Acad Sci U S A* 2006; 103(50):19004-9.
7. Lefebvre V, Smits P. Transcriptional control of chondrocyte fate and differentiation. *Birth Defects Res C Embryo Today* 2005; 75(3):200-12.
8. Kobayashi T, Kronenberg H. Minireview: transcriptional regulation in development of bone. *Endocrinology* 2005; 146(3):1012-7.
9. Clevers H. Wnt/beta-catenin signaling in development and disease. *Cell* 2006; 127(3):469-80.
10. Day TF, Guo X, Garrett-Beal L, Yang Y. Wnt/beta-catenin signaling in mesenchymal progenitors controls osteoblast and chondrocyte differentiation during vertebrate skeletogenesis. *Dev Cell* 2005; 8(5):739-50.
11. Akiyama H, Lyons JP, Mori-Akiyama Y, Yang X, Zhang R, Zhang Z et al. Interactions between Sox9 and beta-catenin control chondrocyte differentiation. *Genes Dev* 2004; 18(9):1072-87.
12. Gaur T, Lengner CJ, Hovhannisyan H, Bhat RA, Bodine PV, Komm BS et al. Canonical WNT signaling promotes osteogenesis by directly stimulating Runx2 gene expression. *J Biol Chem* 2005; 280(39):33132-40.
13. Dong YF, Soung DY, Schwarz EM, O'Keefe RJ, Drissi H. Wnt induction of chondrocyte hypertrophy through the Runx2 transcription factor. *J Cell Physiol* 2006; 208(1):77-86.
14. Hill TP, Spater D, Taketo MM, Birchmeier W, Hartmann C. Canonical Wnt/beta-catenin signaling prevents osteoblasts from differentiating into chondrocytes. *Dev Cell* 2005; 8(5):727-38.
15. Rodda SJ, McMahon AP. Distinct roles for Hedgehog and canonical Wnt signaling in specification, differentiation and maintenance of osteoblast progenitors. *Development* 2006; 133(16):3231-44.
16. Holmen SL, Zylstra CR, Mukherjee A, Sigler RE, Faugere MC, Bouxsein ML et al. Essential role of beta-catenin in postnatal bone acquisition. *J Biol Chem* 2005; 280(22):21162-8.

17. Fodde R. The multiple functions of tumour suppressors: it's all in APC. *Nat Cell Biol* 2003; 5(3):190-2.
18. Korinek V, Barker N, Morin PJ, van Wichen D, de Weger R, Kinzler KW et al. Constitutive transcriptional activation by a beta-catenin-Tcf complex in APC-/- colon carcinoma. *Science* 1997; 275(5307):1784-7.
19. Morin PJ, Sparks AB, Korinek V, Barker N, Clevers H, Vogelstein B et al. Activation of beta-catenin-Tcf signaling in colon cancer by mutations in beta-catenin or APC. *Science* 1997; 275(5307):1787-90.
20. Smits R, van der Houven van Oordt W, Luz A, Zurcher C, Jagmohan-Changur S, Breukel C et al. *Apc1638N*: a mouse model for familial adenomatous polyposis-associated desmoid tumors and cutaneous cysts. *Gastroenterology* 1998; 114(2):275-83.
21. Bertario L, Russo A, Sala P, Varesco L, Giarola M, Mondini P et al. Multiple approach to the exploration of genotype-phenotype correlations in familial adenomatous polyposis. *J Clin Oncol* 2003; 21(9):1698-707.
22. Fodde R, Edelmann W, Yang K, van Leeuwen C, Carlson C, Renault B et al. A targeted chain-termination mutation in the mouse *Apc* gene results in multiple intestinal tumors. *Proc Natl Acad Sci U S A* 1994; 91(19):8969-73.
23. Moser AR, Shoemaker AR, Connelly CS, Clipson L, Gould KA, Luongo C et al. Homozygosity for the *Min* allele of *Apc* results in disruption of mouse development prior to gastrulation. *Dev Dyn* 1995; 203(4):422-33.
24. Kielman MF, Rindapaa M, Gaspar C, van Poppel N, Breukel C, van Leeuwen S. et al. *Apc* modulates embryonic stem-cell differentiation by controlling the dosage of beta-catenin signaling. *Nat Genet* 2002; 32(4):594-605.
25. Fodde R, Smits R. Cancer biology. A matter of dosage. *Science* 2002; 298(5594):761-3.
26. Schipani E, Ryan HE, Didrickson S, Kobayashi T, Knight M, Johnson RS. Hypoxia in cartilage: HIF-1alpha is essential for chondrocyte growth arrest and survival. *Genes Dev* 2001; 15(21):2865-76.
27. Mao X, Fujiwara Y, Orkin SH. Improved reporter strain for monitoring Cre recombinase-mediated DNA excisions in mice. *Proc Natl Acad Sci U S A* 1999; 96(9):5037-42.
28. Cheah KS, Lau ET, Au PK, Tam PP. Expression of the mouse alpha 1(II) collagen gene is not restricted to cartilage during development. *Development* 1991; 111(4):945-53.
29. Long F, Chung UI, Ohba S, McMahon J, Kronenberg HM, McMahon AP. *Ihh* signaling is directly required for the osteoblast lineage in the endochondral skeleton. *Development* 2004; 131(6):1309-18.
30. Christ B, Wilting J. From somites to vertebral column. *Ann Anat* 1992; 174(1):23-32.
31. Aoyama H, Mizutani-koseki S, Koseki H. Three developmental compartments involved in rib formation. *Int J Dev Biol* 2005; 49(2-3):325-33.
32. Wealthall RJ, Herring SW. Endochondral ossification of the mouse nasal septum. *Anat Rec A Discov Mol Cell Evol Biol* 2006; 288(11):1163-72.
33. Roberts GJ, Lucas VS. Growth of the nasal septum in the Snell strain of hypopituitary dwarf mouse. *Eur J Orthod* 1994; 16(2):138-48.
34. Hu H, Hilton MJ, Tu X, Yu K, Ornitz DM, Long F. Sequential roles of Hedgehog and Wnt signaling in osteoblast development. *Development* 2005; 132(1):49-60.

35. Tamamura Y, Otani T, Kanatani N, Koyama E, Kitagaki J, Komori T et al. Developmental regulation of Wnt/beta-catenin signals is required for growth plate assembly, cartilage integrity, and endochondral ossification. *J Biol Chem* 2005; 280(19):19185-95.
36. Moser AR, Pitot HC, Dove WF. A dominant mutation that predisposes to multiple intestinal neoplasia in the mouse. *Science* 1990; 247(4940):322-4.
37. Hartmann C. A Wnt canon orchestrating osteoblastogenesis. *Trends Cell Biol* 2006; 16(3):151-8.
38. Kato M, Patel MS, Levasseur R, Lobov I, Chang BH, Glass DA et al. Cbfa1-independent decrease in osteoblast proliferation, osteopenia, and persistent embryonic eye vascularization in mice deficient in Lrp5, a Wnt coreceptor. *J Cell Biol* 2002; 157(2):303-14.
39. Bodine PV, Zhao W, Kharode YP, Bex FJ, Lambert AJ, Goad MB et al. The Wnt antagonist secreted frizzled-related protein-1 is a negative regulator of trabecular bone formation in adult mice. *Mol Endocrinol* 2004; 18(5):1222-37.
40. Bennett CN, Longo KA, Wright WS, Suva LJ, Lane TF, Hankenson KD et al. Regulation of osteoblastogenesis and bone mass by Wnt10b. *Proc Natl Acad Sci U S A* 2005; 102(9):3324-9.
41. Glass DA, Bialek P, Ahn JD, Starbuck M, Patel MS, Clevers H et al. Canonical Wnt signaling in differentiated osteoblasts controls osteoclast differentiation. *Dev Cell* 2005; 8(5):751-64.
42. Yuasa T, Otani T, Koike T, Iwamoto M, Enomoto-Iwamoto M. Wnt/beta-catenin signaling stimulates matrix catabolic genes and activity in articular chondrocytes: its possible role in joint degeneration. *Lab Invest* 2008.
43. Enomoto-Iwamoto M, Otani T, Koike T, Iwamoto M. Wnt/ $\beta$ -Catenin Signaling in Chondrocyte Function and Cartilage Matrix Disruption. *Current rheumatology reviews* 2006; 2(1):31-8.
44. Zhu M, Tang D, Wu Q, Hao S, Chen M, Xie C et al. Activation of beta-catenin signaling in articular chondrocytes leads to osteoarthritis-like phenotype in adult beta-catenin conditional activation mice. *J Bone Miner Res* 2009; 24(1):12-21.
45. Ryu JH, Kim SJ, Kim SH, Oh CD, Hwang SG, Chun CH et al. Regulation of the chondrocyte phenotype by beta-catenin. *Development* 2002; 129(23):5541-50.
46. McLeod MJ. Differential staining of cartilage and bone in whole mouse fetuses by alcian blue and alizarin red S. *Teratology* 1980; 22(3):299-301.
47. Clement-Lacroix P, Ai M, Morvan F, Roman-Roman S, Vayssiere B, Belleville C et al. Lrp5-independent activation of Wnt signaling by lithium chloride increases bone formation and bone mass in mice. *Proc Natl Acad Sci U S A* 2005; 102(48):17406-11.
48. Dannenberg JH, Schuijff L, Dekker M, van der Valk M, te Riele H. Tissue-specific tumor suppressor activity of retinoblastoma gene homologs p107 and p130. *Genes Dev* 2004; 18(23):2952-62.
49. van der Eerden BC, van Til NP, Brinkmann AO, Lowik CW, Wit JM, Karperien M. Gender differences in expression of androgen receptor in tibial growth plate and metaphyseal bone of the rat. *Bone* 2002; 30(6):891-6.



# Chapter 3

## Adenomatous polyposis coli-gene dosage controls $\beta$ -catenin-mediated differentiation of skeletal precursors

R.L. Miclea<sup>1</sup>, E.C. Robanus-Maandag<sup>2</sup>, C.W. Löwik<sup>3</sup>, W. Oostdijk<sup>1</sup>, R. Fodde<sup>4</sup>, J.M. Wit<sup>1</sup>, M. Karperien<sup>5</sup>

<sup>1</sup>Department of Pediatrics, Leiden University Medical Center (LUMC), Leiden, The Netherlands, <sup>2</sup>Department of Human Genetics, LUMC, Leiden, The Netherlands, <sup>3</sup>Department of Endocrinology and Metabolic Diseases, LUMC, Leiden, The Netherlands, <sup>4</sup>Department of Pathology, Josephine Nefkens Institute, Erasmus MC, Rotterdam, The Netherlands, <sup>5</sup>MIRA Institute for Biomedical Technology and Technical Medicine, Department of Tissue Regeneration, University of Twente, Enschede, The Netherlands

Manuscript in preparation





# Adenomatous polyposis coli-gene dosage controls $\beta$ -catenin-mediated differentiation of skeletal precursors

R.L. Miclea, E.C. Robanus-Maandag, C.W. Löwik, W. Oostdijk, R. Fodde, J.M. Wit, M. Karperien

## ABSTRACT

The canonical Wnt signaling pathway determines lineage commitment of skeletal precursor cells (SPC) into either osteoblasts or chondrocytes via levels of transcriptionally active  $\beta$ -catenin. So far only the on/off effects of  $\beta$ -catenin on the differentiation of SPC have been investigated. No data is available reporting the effects of intermediate  $\beta$ -catenin levels during skeletogenesis. Adenomatous polyposis coli (Apc) represents the key intracellular regulator of the dosage of transcriptionally active  $\beta$ -catenin.

To be able to investigate the effect of different  $\beta$ -catenin dosages on SPC differentiation, we generated compound *Apc* mutant embryos with one conditional mutant allele (*Apc*<sup>15lox</sup>) and one hypomorphic *Apc* mutant allele (*Apc*<sup>1638N</sup> or *Apc*<sup>1572T</sup>) resulting in differential levels of transduced canonical Wnt signaling in SPC. A relatively high increase in  $\beta$ -catenin in the SPC of *Col2a1-Cre;Apc*<sup>15lox/1638N</sup> embryos led to a complete inhibition of chondrocyte and osteoblast differentiation. Intermediate levels of  $\beta$ -catenin in SPC of *Col2a1-Cre;Apc*<sup>15lox/1572T</sup> embryos resulted in a skeletal phenotype characterized by highly active osteoblasts, precocious mineralization and no osteoclast formation.

We show here for the first time that precise dosages of Wnt/ $\beta$ -catenin signaling distinctly influence the differentiation of SPC. These data further point to the critical role of *Apc* in regulating lineage commitment of SPC by controlling the levels of  $\beta$ -catenin.

## INTRODUCTION

Endochondral bone formation occurs during embryogenesis at specific locations within the embryo where the axial and appendicular skeleton will develop. In this process, the primordial step is represented by the condensation of uncommitted mesenchymal cells that differentiate into chondrocytes to form a cartilaginous template of the future bone. Chondrocytes then undergo a tightly regulated program of proliferation, maturation, hypertrophy, calcification, and cell death, ultimately leaving behind a scaffold for bone formation. At the periphery of this cartilaginous mold, mesenchymal cells give rise to the perichondrium (later called periosteum), from which osteoblasts will differentiate. When the perichondrium and its subjacent hypertrophic cartilage begin to calcify, blood vessels invade, bringing blood supply as well as osteoclast progenitors of the monocyte–macrophage lineage. Endochondral bones continue to elongate due to the activity of the growth plates that are responsible for longitudinal bone growth (1;2).

During endochondral bone formation, differentiation and activity of chondrocytes, osteoblasts and osteoclasts, are controlled through an intricate network of genetic, transcriptional, hormonal and growth factor signals. Among the latter, Wnts, bone morphogenetic proteins (BMPs), hedgehog proteins, fibroblast growth factors (FGFs), and insulin-like growth factors (IGFs) are the most investigated (1;3). Wnts are highly conserved secreted glycoproteins known to activate at least four signaling pathways, out of which the canonical  $\beta$ -catenin pathway is best understood (4-7). Increasing amount of evidence points out to the great importance of the canonical Wnt signaling pathway in the regulation of subsequent steps of endochondral ossification (8;9).

In the canonical Wnt signaling pathway, in the absence of the Wnt signal, cytoplasmic  $\beta$ -catenin is targeted for degradation in the proteasome upon its phosphorylation at specific Ser-Thr residues by a destruction complex consisting of Axin, Adenomatous Polyposis Coli (APC), Glycogen synthase kinase 3 $\beta$  (GSK3 $\beta$ ) and Casein-kinase 1 $\alpha$  (CK1 $\alpha$ ). Binding of Wnts to their receptor Frizzled leads to inactivation of the  $\beta$ -catenin destruction complex, via Dishevelled (DVL). Non-degraded  $\beta$ -catenin accumulates in the cytoplasm and subsequently translocates into the nucleus, where it stimulates transcription of target genes together with members of the T cell factor/lymphoid enhancer factor (TCF/LEF) family (10).

Early during skeletogenesis, mesenchymal cells differentiate first into SPCs, which are bi-potential and can differentiate into chondrocytes and osteoblasts. The differentiation choice for either cell type is at least in part controlled by Wnt/ $\beta$ -catenin signaling. Studies in several mouse models have indicated that high  $\beta$ -catenin levels in SPCs stimulate osteoblastogenesis and inhibit chondrogenesis, whereas down-regulation of this pathway has opposite effects (11-15). However, little evidence is available regarding the role of intracellular  $\beta$ -catenin regulators in lineage commitment of SPC.

Much of our understanding about the role of Apc in negatively controlling the intracellular levels of  $\beta$ -catenin has been revealed by experiments using mouse *Apc* mutant alleles that differentially affect the dosage of  $\beta$ -catenin-driven transcriptional activity (16). The *Apc* <sup>$\Delta$ 15</sup> allele encodes low levels (5%) of a truncated 74 kDa protein in the presence of the *Cre* recombinase (17). This mutant Apc protein lacks all  $\beta$ -catenin-downregulating domains, resulting in extensive canonical Wnt signaling. The *Apc*<sup>1638N</sup> allele encodes very low levels (1-2%) of a truncated 182 kDa protein, which is almost entirely defective in  $\beta$ -catenin regulation and thus results in relatively high Wnt/ $\beta$ -catenin signaling (18;19). The *Apc*<sup>1572T</sup> allele encodes intermediate Wnt/ $\beta$ -catenin signaling levels, much lower than the ones induced by *Apc* <sup>$\Delta$ 15</sup> and *Apc*<sup>1638N</sup>, yet higher than wild type Apc (19-21). We have previously shown that Apc regulates differentiation of SPC and mouse embryonic stem cells (ES) by controlling the dosage of  $\beta$ -catenin signaling. *Apc* alleles with no  $\beta$ -catenin downregulating activity (*Apc* <sup>$\Delta$ 15</sup>) completely block the differentiation of SPC (22). Alleles with some  $\beta$ -catenin downregulating capacity (*Apc*<sup>1638N</sup> and *Apc*<sup>1572T</sup>) inhibit ES differentiation only to specific tissues, like bone and cartilage (20).

So far, only the effects of oncogenic  $\beta$ -catenin gain-of-function mutations and of massive wild type  $\beta$ -catenin levels on the differentiation of SPC have been reported (11-15;22). Little data is available investigating the effect of intermediate levels of wild type  $\beta$ -catenin on the differentiation of SPC into chondrocytes and osteoblasts (11). To further address this issue, we have generated conditional *Apc* mutant mouse embryos, compound heterozygous for the conditional *Apc*<sup>15lox</sup> allele and the constitutional *Apc*<sup>1638N</sup> or *Apc*<sup>1572T</sup> allele in SPC. Our results indicate that distinct levels of  $\beta$ -catenin have different effects on SPC differentiation. Relatively high levels of  $\beta$ -catenin signaling arising upon expression of *Apc* <sup>$\Delta$ 15/1638N</sup> blocked the differentiation of SPC to both chondrocytes and osteoblasts, whereas intermediate upregulation of  $\beta$ -catenin secondary to conditional expression of *Apc* <sup>$\Delta$ 15/1572T</sup> resulted in increased osteoblastogenesis and absence of osteoclasts.

## MATERIALS AND METHODS

### Transgenic mice

All animal studies were approved by the ethical committee of the LUMC and complied with national laws relating to the conduct of animal experiments. The *Apc*<sup>15lox/15lox</sup> (17;22), *Apc*<sup>1638N/+</sup> (18) and *Apc*<sup>1572T/+</sup> (21) mice were previously generated in our laboratories. *Col2a1-Cre* mice (22;23) were a generous gift from Prof. Dr. Henry Kronenberg (Harvard Medical School, Massachusetts General Hospital, Boston, MA, USA). *Apc*<sup>1638N/+</sup> and *Apc*<sup>1572T/+</sup> mice were crossed with *Col2a1-Cre* mice to generate *Col2a1-Cre;Apc*<sup>1638N/+</sup> and *Col2a1-Cre;Apc*<sup>1572T/+</sup> mice, respectively. Next, *Apc*<sup>15lox/15lox</sup> mice were crossed with *Col2a1-Cre;Apc*<sup>1638N/+</sup> and *Col2a1-Cre;Apc*<sup>1572T/+</sup> mice to generate compound *Col2a1-Cre;Apc*<sup>15lox/1638N</sup> and *Col2a1-Cre;Apc*<sup>15lox/1572T</sup> mouse embryos, respectively. Routine mouse genotyping was performed on tail DNAs by PCR.

### Skeletal analysis

Skeletons of mouse embryos were stained with Alcian Blue and Alizarin Red for cartilaginous and mineralized tissues, respectively, as previously described (22).

### Histology, Immunohistochemistry, In situ hybridization

For histology, immunohistochemistry, and in situ hybridization, specimens were fixed in phosphate-buffered formalin, embedded in paraffin, and sectioned at 6  $\mu\text{m}$ . Combined Toluidine Blue - von Kossa staining was performed according to standard procedures. Immunohistochemistry for  $\beta$ -catenin using rabbit polyclonal anti- $\beta$ -catenin (1:100; Abcam) coupled with Alcian Blue staining was performed and analyzed as previously described (22). For in situ hybridization, digoxigenin-labeled single-stranded RNA probes were prepared using a DIG RNA labeling kit (Roche) following the manufacturers' instructions. All probes are available upon request. In situ hybridization was carried out and analyzed as previously described (22).

### RNA isolation and real-time RT-PCR

Total RNA was extracted from Polytron-homogenized forelimbs, ribs and thoracic vertebrae using Trizol LS Reagent (Invitrogen) followed by RNA cleanup with the RNeasy mini kit (Qiagen). For real-time quantitative RT-PCR, RNA was reverse-transcribed into cDNA using random hexamer primers (Fermentas). Quantitative RT-PCR was performed using the iCycler (Bio-Rad). QuantiTect real-time PCR primers (Qiagen) were used for the following genes: *Mmp2*, *Mmp3*, *Mmp9*, *Mmp13*, *Adamts5*, *Hyal1*, *Galns*, *CtsK* and *Actb*. 5 ng cDNA was amplified in triplicate using the Quantitect SYBR Green PCR kit (Qiagen) under the following conditions: cDNA was denatured for 15 min at 95°C, followed by 40 cycles, consisting of 15 sec at 95°C, 30 sec at 60°C (at 56.5°C for the Qiagen primers), and 30 sec at 72°C. From each sample, a melting curve was generated to test for the absence of primer dimer formation and DNA contamination. Fold changes, adjusted for the expression of  $\beta$ -actin, were calculated and log-transformed using the comparative method (24).

## RESULTS

### Compound conditional *Col2a1-Cre;Apc*<sup>15lox/1638N</sup> and *Col2a1-Cre;Apc*<sup>15lox/1572T</sup> mouse embryos are embryonic lethal and display abnormal skeletogenesis

*Apc*<sup>15lox/+</sup>, *Apc*<sup>15lox/15lox</sup>, *Apc*<sup>1638N/+</sup>, and *Apc*<sup>1572T/+</sup> mice were previously reported and showed no skeletal developmental defects (17;21;22 and R. Fodde, unpublished). To generate conditional *Apc* mutant mouse lines expressing hypomorphic *Apc* alleles in SPC, we bred *Apc*<sup>15lox/15lox</sup> mice with *Col2a1-Cre;Apc*<sup>1638N/+</sup> and *Col2a1-Cre;Apc*<sup>1572T/+</sup> mice to obtain compound conditional *Col2a1-Cre;Apc*<sup>15lox/1638N</sup> and *Col2a1-Cre;Apc*<sup>15lox/1572T</sup> mice, respectively. No live newborn mice carrying the two desired genotypes could be isolated, indicating that conditional *Col2a1-Cre*-mediated expression of the compound *Apc* <sup>$\Delta$ 15/1638N</sup> and *Apc* <sup>$\Delta$ 15/1572T</sup> alleles is embryonic lethal.

*Col2a1-Cre;Apc*<sup>15lox/1638N</sup> mouse embryos at E12.5 and E13.5 were slightly smaller in comparison to control littermates and displayed shortened mandibles, protruding tongue, incomplete closure of the snout, thoracic cavity and abdomen, and no limb bud outgrowth (Figure 1A-B). The latest developmental stage at which *Col2a1-Cre;Apc*<sup>15lox/1638N</sup> mutants could be isolated was E14.5. At this stage, they already showed signs of significant resorption (Figure 1C<sub>i</sub>, 1C<sub>ii</sub>). Skeletal preparations of control embryos at E13.5 documented the presence of unmineralized cartilaginous skeletal structures at all sites of endochondral bone formation (Figure 1B<sub>iii</sub>). In marked contrast, no skeletal elements could be identified in the *Col2a1-Cre;Apc*<sup>15lox/1638N</sup> mutants (Figure 1B<sub>iv</sub>).

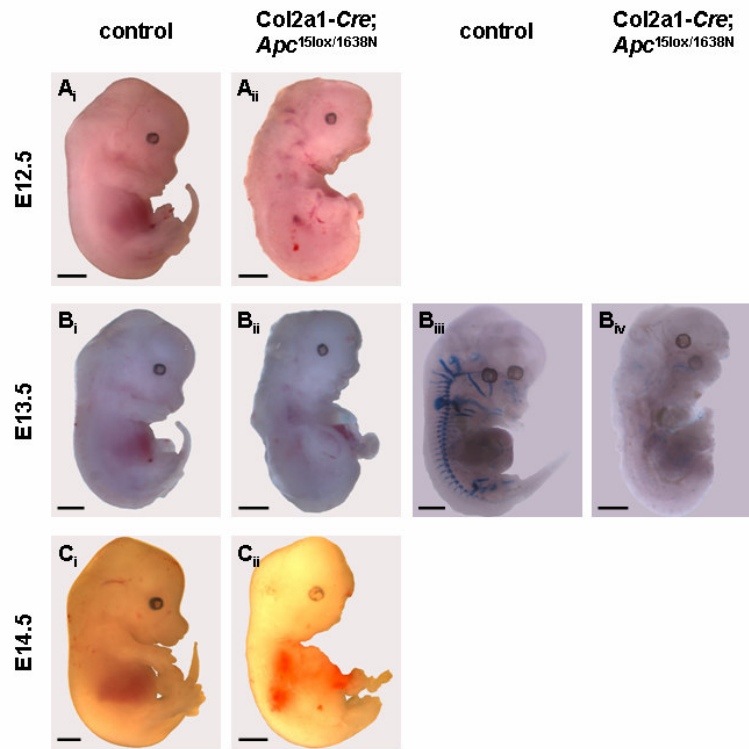


**Figure 1. *Col2a1-Cre;Apc*<sup>15lox/1638N</sup> mouse embryos display severely altered skeletal development.** Lateral gross appearance of control (A<sub>i</sub>-C<sub>i</sub>) and *Col2a1-Cre;Apc*<sup>15lox/1638N</sup> (A<sub>ii</sub>-C<sub>ii</sub>) embryos at indicated developmental stages. Conditional *Apc* mutants show obvious craniofacial and limb malformations already at E12.5 (A<sub>ii</sub>). *Col2a1-Cre;Apc*<sup>15lox/1638N</sup> embryos at E13.5 (B<sub>ii</sub>) and E14.5 (C<sub>ii</sub>) show signs of tissue resorption in the snout, limbs and tail. Skeletal preparations using Alcian Blue and Alizarin Red of *Col2a1-Cre;Apc*<sup>15lox/1638N</sup> (B<sub>iii</sub>) and control (B<sub>iv</sub>) embryos at E13.5 indicate no skeletal tissue formation in the conditional *Apc* mutants. Scale bars: 1 mm.

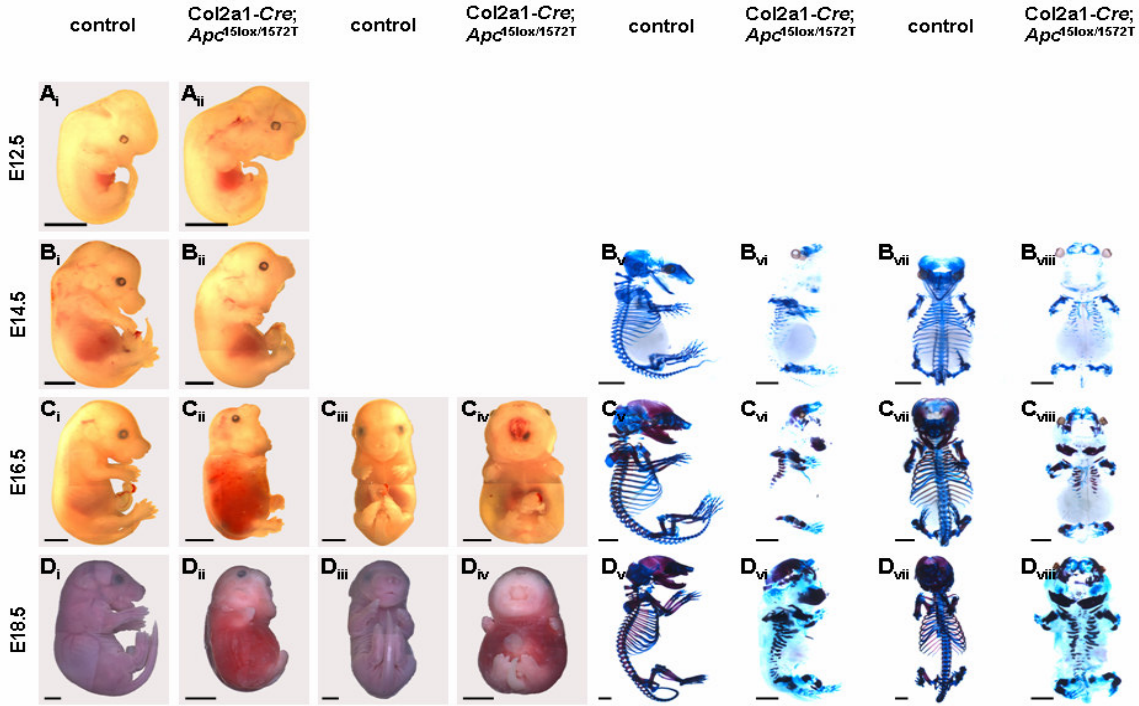


**Figure 2. Greatly impaired skeletogenesis in *Col2a1-Cre;Apc*<sup>15lox/1572T</sup> mouse embryos.** Lateral (A<sub>i</sub>-D<sub>i</sub>, A<sub>ii</sub>-D<sub>ii</sub>) and anterior (C<sub>iii</sub>-D<sub>iii</sub>, C<sub>iv</sub>-D<sub>iv</sub>) pictures displaying gross appearance of control (A<sub>i</sub>-D<sub>i</sub>, C<sub>iii</sub>-D<sub>iii</sub>) and *Col2a1-Cre;Apc*<sup>15lox/1572T</sup> (A<sub>ii</sub>-D<sub>ii</sub>, C<sub>iv</sub>-D<sub>iv</sub>) embryos at indicated developmental stages. *Apc* transgenic mutants show distinct snout malformations and poor fore- and hindlimb outgrowth. Lateral (B<sub>v</sub>-D<sub>v</sub>, B<sub>vi</sub>-D<sub>vi</sub>) and anterior (B<sub>vii</sub>-D<sub>vii</sub>, B<sub>viii</sub>-D<sub>viii</sub>) pictures displaying skeletal preparations of control (B<sub>v</sub>-D<sub>v</sub>, B<sub>vi</sub>-D<sub>vi</sub>) and *Col2a1-Cre;Apc*<sup>15lox/1572T</sup> (B<sub>vi</sub>-D<sub>vi</sub>, B<sub>viii</sub>-D<sub>viii</sub>) embryos at indicated developmental stages. In comparison to control littermates, *Apc* transgenics display shorter and stronger mineralized long bones. Scale bars = 2 mm.

Macroscopic analysis of *Col2a1-Cre;Apc*<sup>15lox/1572T</sup> mutants indicated significant growth retardation at E16.5 and E18.5 in comparison to control littermates (Figure 2A-2A<sub>ii</sub>, 2B-2B<sub>ii</sub>, 2C-2C<sub>ii</sub>, 2D-2D<sub>ii</sub>). Gross abnormalities in the *Col2a1-Cre;Apc*<sup>15lox/1572T</sup> mutants were identified already at E12.5 and included shortened mandibles, wide open mouth, and significantly shortened limbs with hypoplastic autopods. As indicated by

skeletal preparations, besides the vertebral column all other endochondral skeletal elements were present in *Col2a1-Cre;Apc<sup>15lox/1572T</sup>* mouse embryos at E14.5, E16.5 and E18.5 (Figure 2B<sub>v</sub>-2B<sub>viii</sub>, 2C<sub>v</sub>-2C<sub>viii</sub>, 2D<sub>v</sub>-2D<sub>viii</sub>). However, they were shorter, thicker and malformed in comparison to control skeletal elements. Characteristic for the *Col2a1-Cre;Apc<sup>15lox/1572T</sup>* embryos was the presence of severely truncated mandibles already at E14.5. In addition, although failing to outgrow, the inferior mandible showed intense mineral deposition at E16.5 and E18.5 resulting in the formation of a thick bone structure. Thoracic malformations in the *Col2a1-Cre;Apc<sup>15lox/1572T</sup>* embryos included failure of sternum to fuse, absence of vertebrae, and short, thick and intensely mineralized proximal ribs. At E16.5 and E18.5, long bones forming the stylopod and zeugopod of the *Col2a1-Cre;Apc<sup>15lox/1572T</sup>* conditional mutants displayed poorly developed cartilaginous ends and smaller, thicker and stronger mineralized midshaft regions. We occasionally identified fused or extra-numerary digits in the *Col2a1-Cre;Apc<sup>15lox/1572T</sup>* conditional mutants at all developmental stages investigated.

### Impairment of both chondrogenic and osteogenic differentiation of SPC in *Col2a1-Cre;Apc<sup>15lox/1638N</sup>* mouse embryos

Alterations in skeletal development in *Col2a1-Cre;Apc<sup>15lox/1638N</sup>* embryos were examined at the microscopical level by  $\beta$ -catenin immunohistochemistry coupled with Alcian Blue, combined Toluidine Blue - von Kossa staining, and gene expression analysis through in situ hybridization for the  $\beta$ -catenin-target gene *Axin2* and a wide range of established chondrocyte, osteoblast and osteoclast markers.

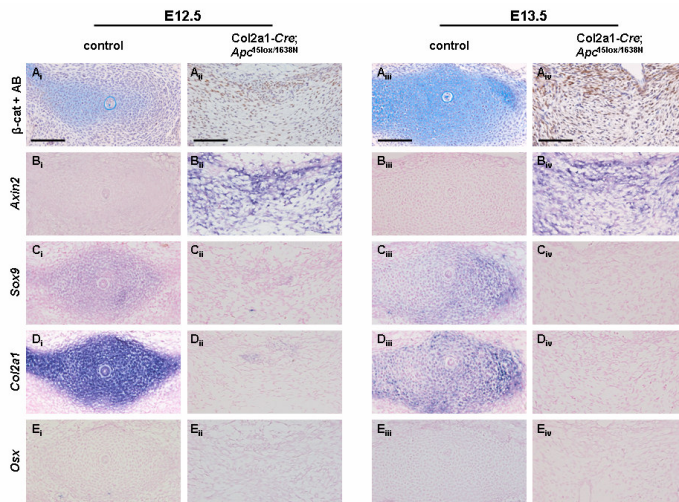


**Figure 3. Microscopical analysis of sclerotome development in *Col2a1-Cre;Apc<sup>15lox/1638N</sup>* mouse embryos.** Immunostaining for  $\beta$ -catenin coupled with Alcian Blue (AB) staining (A<sub>i</sub>-A<sub>iv</sub>) and in situ gene expression analysis for *Axin2* (B<sub>i</sub>-B<sub>iv</sub>), *Sox9* (C<sub>i</sub>-C<sub>iv</sub>), *Col2a1* (D<sub>i</sub>-D<sub>iv</sub>), and *Osx* (E<sub>i</sub>-E<sub>iv</sub>) on consecutive transversal sclerotome sections of control (A<sub>i</sub>-E<sub>i</sub>, A<sub>iii</sub>-E<sub>iii</sub>) and *Col2a1-Cre;Apc<sup>15lox/1638N</sup>* (A<sub>ii</sub>-E<sub>ii</sub>, A<sub>iv</sub>-E<sub>iv</sub>) embryos at indicated developmental stages. Upregulation of the canonical Wnt signaling pathway is associated with inhibition of chondrogenic and osteogenic differentiation already at E12.5. Scale bars: 100  $\mu$ m.



Consecutive transversal sclerotome sections of control embryos at E12.5 depicted condensation of  $\beta$ -catenin- and *Axin2*-negative SPC committed to the chondrogenic lineage (Figure 3A<sub>i</sub>-E<sub>i</sub>). By E13.5, these cells were still  $\beta$ -catenin- and *Axin2*-negative and clearly differentiated into chondrocytes as confirmed by an Alcian Blue-positive extracellular matrix, expression of the early chondrogenic markers *Sox9* and *Col2a1*, and no expression of the osteoblast marker *Osx* (Figure 3A<sub>iii</sub>-E<sub>iii</sub>). The conditional expression of the compound *Apc*<sup>Δ15/1638N</sup> allele resulted in relatively high levels of cytoplasmic and nuclear  $\beta$ -catenin levels indicative for increased canonical Wnt signaling. This was confirmed by the strong upregulation of the established  $\beta$ -catenin target gene, *Axin2* (Figure 3A<sub>ii</sub>, 3B<sub>ii</sub>, 3A<sub>iv</sub>, 3B<sub>iv</sub>). These cells showed a spindle, mesenchymal-like morphology, failed to condensate and did not express *Sox9*, *Col2a1*, and *Osx*, suggesting that chondrogenic and osteogenic differentiation was almost completely inhibited (Figure 3C<sub>ii</sub>-E<sub>ii</sub>, 3C<sub>iv</sub>-E<sub>iv</sub>). In addition we did not detect any sign of notochord formation in these conditional mutants at all developmental stages investigated.

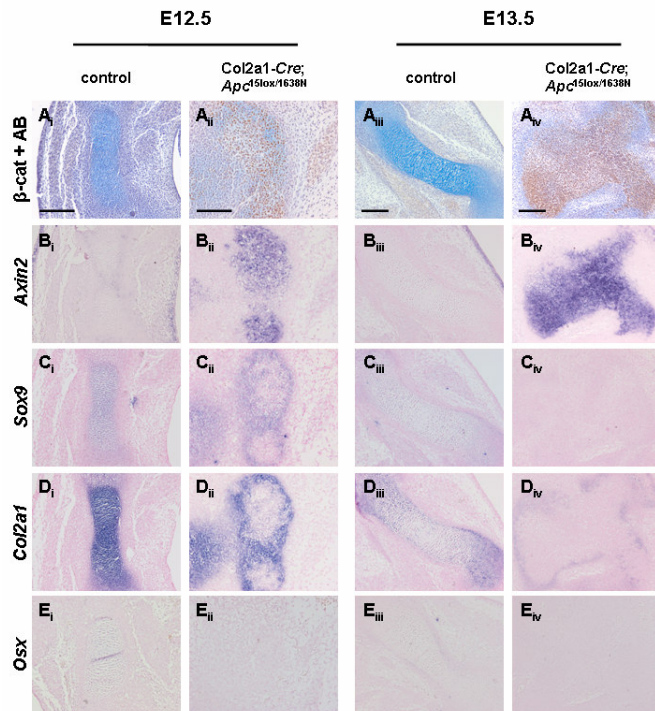


**Figure 4. Microscopical analysis of humerus development in *Col2a1-Cre;Apc*<sup>15lox/1638N</sup> mouse embryos.** Immunostaining for  $\beta$ -catenin coupled with Alcian Blue (AB) staining (A<sub>i</sub>-A<sub>iv</sub>) and in situ gene expression analysis for *Axin2* (B<sub>i</sub>-B<sub>iv</sub>), *Sox9* (C<sub>i</sub>-C<sub>iv</sub>), *Col2a1* (D<sub>i</sub>-D<sub>iv</sub>), and *Osx* (E<sub>i</sub>-E<sub>iv</sub>) on consecutive longitudinal sections of the humerus of control (A<sub>i</sub>-E<sub>i</sub>, A<sub>iii</sub>-E<sub>iii</sub>) and *Col2a1-Cre;Apc*<sup>15lox/1638N</sup> (A<sub>ii</sub>-E<sub>ii</sub>, A<sub>iv</sub>-E<sub>iv</sub>) embryos at E12.5 (A<sub>i</sub>-E<sub>i</sub>, A<sub>ii</sub>-E<sub>ii</sub>) and E13.5 (A<sub>iii</sub>-E<sub>iii</sub>, A<sub>iv</sub>-E<sub>iv</sub>). SPC expressing the compound *Apc*<sup>15lox/1638N</sup> allele fail to differentiate into chondrocytes and osteoblasts. Scale bars: 200  $\mu$ m (A<sub>i</sub>-E<sub>i</sub>, A<sub>iii</sub>-E<sub>iii</sub>, A<sub>iv</sub>-E<sub>iv</sub>), 100  $\mu$ m (A<sub>ii</sub>-E<sub>ii</sub>).

We next investigated chondrogenesis and osteoblastogenesis in the humerus of *Col2a1-Cre;Apc<sup>15lox/1638N</sup>* conditional mutants and control littermates at E12.5 and E13.5 (Figure 4). Control humeri contained chondrocytes embedded in an Alcian Blue-positive matrix (Figure 4A<sub>i</sub>, 4A<sub>iii</sub>). These cells were negative for  $\beta$ -catenin and *Axin2*, and positive for *Sox9* and *Col2a1* (Figure 4A<sub>i</sub>-D<sub>i</sub>, 4A<sub>iii</sub>-D<sub>iii</sub>). In the control perichondrium, *Osx*-positive osteoblasts began to differentiate (Figure 4E<sub>i</sub>, 4E<sub>iii</sub>). In agreement with the role of the canonical Wnt signaling in initiating osteoblastogenesis, these cells displayed endogenous levels of cytoplasmic  $\beta$ -catenin protein and *Axin2* mRNA (Figure 4A<sub>i</sub>, 4B<sub>i</sub>, 4A<sub>iii</sub>, 4B<sub>iii</sub>). In marked contrast, the humerus of *Col2a1-Cre;Apc<sup>15lox/1638N</sup>* conditional mutants at E12.5 was fragmented in cell clusters expressing relatively high levels of  $\beta$ -catenin, suggestive for increased canonical Wnt signal transduction (Figure 4A<sub>ii</sub>, 4B<sub>ii</sub>, 4A<sub>iv</sub>, 4B<sub>iv</sub>). As observed in the sclerotome of *Col2a1-Cre;Apc<sup>15lox/1638N</sup>* conditional embryos, nuclear  $\beta$ -catenin- and *Axin2*-positive cells failed to express any of the chondrogenic and osteogenic markers investigated, suggesting that both chondrocyte and osteoblast differentiation was impaired at this skeletal site as well (Figure 4C<sub>ii</sub>-E<sub>ii</sub>, 4C<sub>iv</sub>-E<sub>iv</sub>). Microscopical analysis indicated only a few cells with low  $\beta$ -catenin and *Axin2* levels, roughly corresponding to the position of *Sox9*- and *Col2a1*-positive chondrocytes on consecutive sections. These cells have most likely not undergone *Cre*-mediated recombination and thus were able to differentiate into chondrocytes.

We next investigated the mRNA expression of several proteases known to be involved in tissue remodeling/destruction in the *Col2a1-Cre;Apc<sup>15lox/1638N</sup>* mouse embryos, by performing quantitative RT-PCR on RNA isolated from E12.5 embryos. Whereas *Mmp2*, *Mmp3*, *Mmp13*, *Adamts5*, *CtsK* and *Galns* showed similar levels in the control and conditional mutant embryos, *Mmp9* and *Hyal1* were significantly upregulated 3.5- and 2.2-fold, respectively, in the *Col2a1-Cre;Apc<sup>15lox/1638N</sup>* mouse embryos as compared to control littermates ( $p < 0.05$ ; Figure 5).

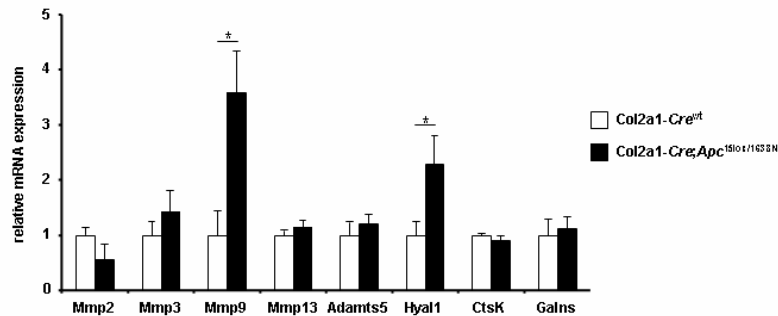


**Figure 5.** Quantitative RT-PCR analysis for the expression of *Mmp2*, *Mmp3*, *Mmp9*, *Mmp13*, *Adamts5*, *Hyal1*, *CtsK*, and *Galns* in the *Col2a1-Cre;Apc<sup>15lox/1638N</sup>* mouse embryos at E12.5. *Mmp9* and *Hyal1* are significantly upregulated 3.5- and 2.2-fold, respectively, in the *Col2a1-Cre;Apc<sup>15lox/1638N</sup>* mouse embryos at E12.5 as compared to control littermates. \* $p < 0.05$ .

### Impairment of both chondrogenic and osteogenic differentiation of SPC in *Col2a1-Cre;Apc<sup>15lox/1572T</sup>* mouse embryos

To investigate SPC differentiation in the sclerotome of *Col2a1-Cre;Apc<sup>15lox/1572T</sup>* mutants at E12.5, E14.5 and E16.5, we performed a microscopical analysis similar to the one conducted in the *Col2a1-Cre;Apc<sup>15lox/1638N</sup>* embryos. Activation of canonical Wnt signaling was detected in the sclerotome of *Col2a1-Cre;Apc<sup>15lox/1572T</sup>* mutants at E12.5, E14.5 and E16.5 as indicated by upregulation of  $\beta$ -catenin and expression of *Axin2* in virtually all cells (Figure 6A<sub>ii</sub>, 6B<sub>ii</sub>, 6A<sub>iv</sub>, 6B<sub>iv</sub>, 6A<sub>vi</sub>, 6B<sub>vi</sub>). Although the notochord was present, the expression of both chondrogenic (*Sox9* and *Col2a1*) and osteogenic (*Osx*) markers was significantly inhibited, suggesting that conditional expression of the compound *Apc<sup>Δ15/1572T</sup>* allele in sclerotomal SPC impairs both chondrocyte and osteoblast differentiation (Figure 6C<sub>ii</sub>-E<sub>ii</sub>, 6C<sub>iv</sub>-E<sub>iv</sub>, 6C<sub>vi</sub>-E<sub>vi</sub>).

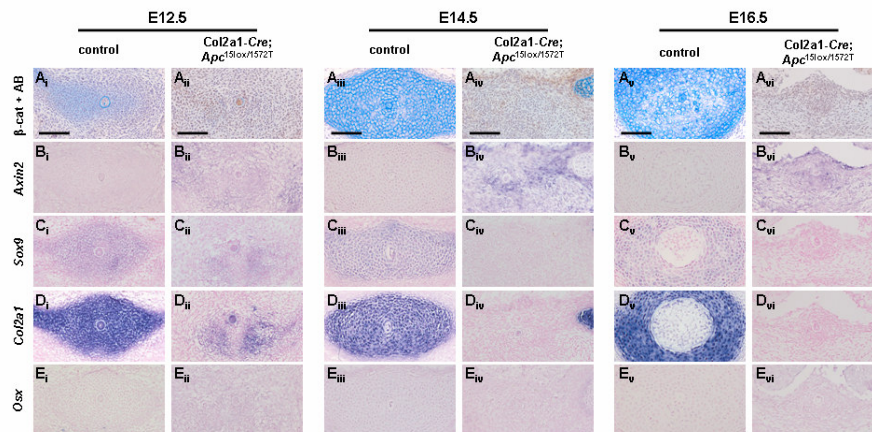


**Figure 6. Microscopical analysis of sclerotome development in *Col2a1-Cre;Apc<sup>15lox/1572T</sup>* mouse embryos.** Immunostaining for  $\beta$ -catenin coupled with Alcian Blue (AB) staining (A<sub>i</sub>-A<sub>vi</sub>), in situ gene expression analysis for *Axin2* (B<sub>i</sub>-B<sub>vi</sub>), *Sox9* (C<sub>i</sub>-C<sub>vi</sub>), *Col2a1* (D<sub>i</sub>-D<sub>vi</sub>), and *Osx* (E<sub>i</sub>-E<sub>vi</sub>) on consecutive transversal sclerotome sections of control (A<sub>i</sub>-E<sub>i</sub>, A<sub>iii</sub>-E<sub>iii</sub>, A<sub>v</sub>-E<sub>v</sub>) and *Col2a1-Cre;Apc<sup>15lox/1572T</sup>* (A<sub>ii</sub>-E<sub>ii</sub>, A<sub>iv</sub>-E<sub>iv</sub>, A<sub>vi</sub>-E<sub>vi</sub>) embryos at indicated developmental stages. Conditional expression of the compound *Apc<sup>15lox/1572T</sup>* allele is associated with inhibition of chondrogenic and osteogenic differentiation. Scale bars: 100  $\mu$ m.

### Increased osteoblastogenesis in long bones of compound *Col2a1-Cre;Apc<sup>15lox/1572T</sup>* conditional mutants

We next analyzed microscopically the long bones of the *Col2a1-Cre;Apc<sup>15lox/1572T</sup>* mouse. Microscopical analysis of control humeri at E12.5 depicted normal initiation of endochondral bone formation (Figure 7A<sub>i</sub>-7G<sub>i</sub>). As observed in the sclerotome, the vast majority of SPC in the humeri of *Col2a1-Cre;Apc<sup>15lox/1572T</sup>* mutants at E12.5 were displaying accumulated  $\beta$ -catenin and *Axin2* expression, indicating activation of the ca-

nonical Wnt signal (Figure 7A<sub>ii</sub>, 7B<sub>ii</sub>). These cells were not expressing *Sox9* and *Col2a1*, suggesting that SPC expressing the compound *Apc*<sup>Δ15lox/1572T</sup> allele cannot differentiate into chondrocytes (Figure 7C<sub>ii</sub>, 7D<sub>ii</sub>). No expression of the prehypertrophic chondrocyte marker *Ihh* was observed, indicating that maturation of chondrocytes arising from non-recombined SPC was delayed (Figure 7E<sub>ii</sub>). However, at the periphery of the humerus of E12.5 *Col2a1-Cre;Apc*<sup>15lox/1572T</sup> mutants, we detected increased expression of *Osx* and *Col1a1*, implying augmented osteoblastogenesis in the perichondrium (Figure 7F<sub>ii</sub>, 7G<sub>ii</sub>).

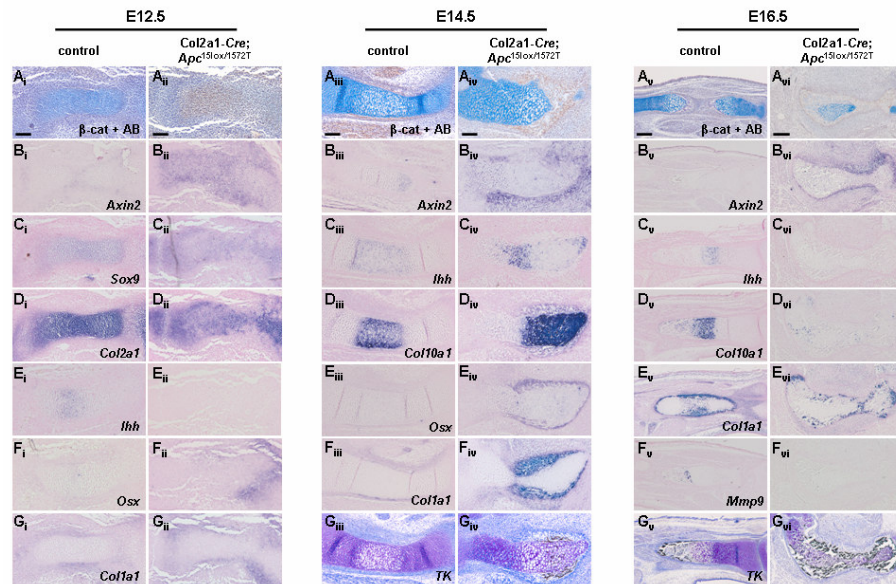


**Figure 7. Microscopical analysis of forelimb development in *Col2a1-Cre;Apc*<sup>15lox/1572T</sup> mouse embryos.** Immunostaining for β-catenin coupled with Alcian Blue (AB) staining (A<sub>i</sub>-A<sub>vi</sub>), in situ gene expression analysis for indicated probes (B<sub>i</sub>-B<sub>vi</sub>, C<sub>i</sub>-C<sub>vi</sub>, D<sub>i</sub>-D<sub>vi</sub>, E<sub>i</sub>-E<sub>vi</sub>, F<sub>i</sub>-F<sub>vi</sub>, G<sub>i</sub>-G<sub>ii</sub>), and combined Toluidine Blue - von Kossa staining (G<sub>iii</sub>-G<sub>vi</sub>) on consecutive longitudinal sections of humerus (E12.5, E14.5) and radius (E16.5) from control (A<sub>i</sub>-G<sub>i</sub>, A<sub>iii</sub>-G<sub>iii</sub>, A<sub>v</sub>-G<sub>v</sub>) and *Col2a1-Cre;Apc*<sup>15lox/1572T</sup> (A<sub>ii</sub>-G<sub>ii</sub>, A<sub>iv</sub>-G<sub>iv</sub>, A<sub>vi</sub>-G<sub>vi</sub>) embryos at indicated developmental stages. At E12.5, a decrease in chondrogenic- and an increase in osteogenic marker expression can be observed in the humerus of *Col2a1-Cre;Apc*<sup>15lox/1572T</sup> mouse embryos. In contrast to controls, matrix mineralization is present already at E14.5 in the humerus of *Col2a1-Cre;Apc*<sup>15lox/1572T</sup> mouse embryos. Intense mineral deposition is associated with absence of *Mmp9*-positive osteoclasts in the radius of transgenic *Apc* mouse embryos at E16.5. Scale bars: 100 μm (A<sub>i</sub>-G<sub>i</sub>, A<sub>iii</sub>-G<sub>iii</sub>, A<sub>v</sub>-G<sub>v</sub>), 200 μm (A<sub>v</sub>-G<sub>v</sub>), 50 μm (A<sub>ii</sub>-G<sub>ii</sub>, A<sub>iv</sub>-G<sub>iv</sub>).

Analysis of control humeri at E14.5 indicated normal progress of endochondral bone formation (Figure 7A<sub>iii</sub>-G<sub>iii</sub>). In agreement with its role in final steps of chondrocyte maturation and osteoblastogenesis, endogenous levels of canonical Wnt signal were detected in the terminal hypertrophic chondrocytes (*Axin2*) and perichondrial osteoblasts (β-catenin) (Figure 7A<sub>iii</sub>, 7B<sub>iii</sub>). Characteristic for this developmental stage, in the core of the humeral cartilaginous mold, chondrocytes began to mature and

became hypertrophic as indicated by expression of *Ihh* and *Col10a1*, respectively, while in the perichondrium we found *Osx*- and *Col1a1*-positive osteoblasts (Figure 7E<sub>iii</sub>, 7F<sub>iii</sub>). Combined Toluidine Blue - von Kossa staining indicated that no mineralization occurred in the control humeri by E14.5 (Figure 7G<sub>iii</sub>). The humerus of compound *Col2a1-Cre;Apc*<sup>15lox/1572T</sup> conditional mutants was shorter and thicker in comparison to controls and displayed chondrocytes that did not stain for  $\beta$ -catenin and *Axin2* (Figure 7A<sub>iv</sub>, 7B<sub>iv</sub>). Whereas expression of early chondrogenic markers seemed unaffected (data not shown), expression of late chondrogenic markers, like *Ihh* and *Col10a1*, was increased in the conditional mutants (Figure 7C<sub>iv</sub>, 7D<sub>iv</sub>). At the periphery of the mutant humerus, we detected a thick perichondrium containing  $\beta$ -catenin- and *Axin2*-positive cells (Figure 7A<sub>iv</sub>, 7B<sub>iv</sub>). These cells exhibited strong expression of *Osx* and *Col1a1* and were entrapped in a bone matrix composed of lacuna-like spaces (Figure 7A<sub>iv</sub>, 7B<sub>iv</sub>). In contrast to control humeri that showed no mineral deposition at this developmental stage, humeri of *Col2a1-Cre;Apc*<sup>15lox/1572T</sup> conditional mutants displayed mineralization in the matrix surrounding the hypertrophic chondrocytes as well as in the perichondrium (Figure 7G<sub>iv</sub>).

At E16.5, the radius of *Col2a1-Cre;Apc*<sup>15lox/1572T</sup> conditional mutants contained islands of  $\beta$ -catenin- and *Axin2*-negative chondrocytes minimally expressing late chondrogenic markers (Figure 7A<sub>vi</sub>, 7C<sub>vi</sub>, 7D<sub>vi</sub>). Surrounding these chondrocytes, thick bone trabeculae were present containing  $\beta$ -catenin- and *Col1a1*-positive osteoblasts (Figure 7A<sub>vi</sub>, 7E<sub>vi</sub>). Subjacent to these bone trabeculae, most of the cells were positive for *Axin2* (Figure 7B<sub>vi</sub>). To detect if osteoclastogenesis occurs normally in the *Col2a1-Cre;Apc*<sup>15lox/1572T</sup> mutants, we next analyzed the presence of osteoclasts by in situ hybridization for *Mmp9*. Whereas *Mmp9*-positive osteoclasts were detected in the control radii at the interface between terminal chondrocytes and primary spongiosa, no *Mmp9* expression was found in the compound *Col2a1-Cre;Apc*<sup>15lox/1572T</sup> mutants, suggesting absence of osteoclasts (Figure 7F<sub>v</sub>, 7F<sub>vi</sub>). As indicated by combined Toluidine Blue - von Kossa staining, mineralization in the control humeri by E16.5 was confined to the hypertrophic chondrocyte matrix and periosteum (Figure 7G<sub>v</sub>). In marked contrast, *Col2a1-Cre;Apc*<sup>15lox/1572T</sup> mutants showed strong mineral deposition in the whole skeletal element, barely leaving any space for bone marrow formation (Figure 7G<sub>vi</sub>). Most likely the absence of osteoclasts was responsible for no remodeling of the cartilaginous matrix and failure of primary spongiosa formation.

### Increased *Bmp7* expression in all endochondral skeletal elements of compound *Col2a1-Cre;Apc*<sup>15lox/1638N</sup> and *Col2a1-Cre;Apc*<sup>15lox/1572T</sup> conditional mutants

We previously reported *in vitro*, that murine mesenchymal-like cells carrying a knockdown of the *Apc* gene not only express higher levels of *Bmp7* mRNA, but are also more responsive to recombinant human BMP-7 during osteoblastogenesis (25). We next tested whether the conditional expression of the compound *Apc* <sup>$\Delta$ 15/1638N</sup> or *Apc* <sup>$\Delta$ 15/1572T</sup> mutant alleles alters the *in situ* *Bmp7* expression levels in our conditional mutant embryos. *Col2a1-Cre;Apc*<sup>15lox/1638N</sup> mutants displayed increased *Bmp7* expression as compared to controls in both the sclerotome and the forelimb at E12.5 and E13.5 in SPC exhibiting relatively high levels of canonical Wnt signal (Figure 8A<sub>i</sub>-A<sub>iv</sub>, 8B<sub>i</sub>-

B<sub>iv</sub>). At the same time, *Col2a1-Cre;Apc*<sup>15lox/1572T</sup> mutants also displayed increased *Bmp7* expression in comparison to controls at all developmental stages investigated in SPC expressing intermediate levels of canonical Wnt signal (Figure 8C<sub>i</sub>-C<sub>vi</sub>, 8D<sub>i</sub>-D<sub>vi</sub>). However, the intensity and the spatial expression pattern of *Bmp7* in the two compound conditional mouse lines were not similar: whereas in the *Col2a1-Cre;Apc*<sup>15lox/1638N</sup> mutants, *Bmp7* was strongly increased at the core of the skeletal structures, *Col2a1-Cre;Apc*<sup>15lox/1572T</sup> mutants showed a slight increase of *Bmp7* expression mainly at the periphery of the endochondral bones.

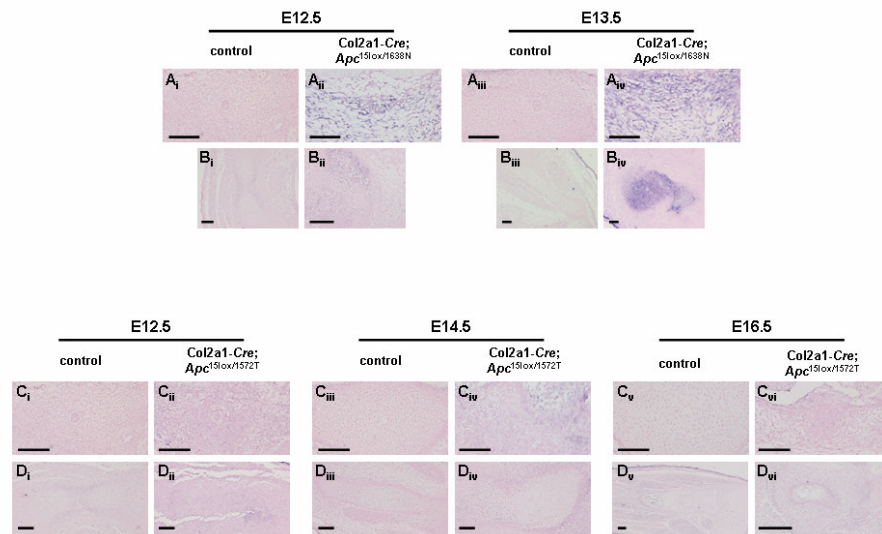


**Figure 8. Increased in situ expression of *Bmp7* in the *Col2a1-Cre;Apc*<sup>15lox/1638N</sup> and *Col2a1-Cre;Apc*<sup>15lox/1572T</sup> mouse embryos.** In situ gene expression analysis for *Bmp7* on transversal sclerotome (A<sub>i</sub>-A<sub>iv</sub>, C<sub>i</sub>-C<sub>vi</sub>) and longitudinal forelimb (B<sub>i</sub>-B<sub>iv</sub>, D<sub>i</sub>-D<sub>vi</sub>) sections of control (A<sub>i</sub>-D<sub>iv</sub>, A<sub>iii</sub>-D<sub>iii</sub>, C<sub>v</sub>, D<sub>v</sub>), *Col2a1-Cre;Apc*<sup>15lox/1638N</sup> (A<sub>ii</sub>, B<sub>ii</sub>, A<sub>iv</sub>, B<sub>iv</sub>), and *Col2a1-Cre;Apc*<sup>15lox/1572T</sup> (C<sub>ii</sub>, D<sub>ii</sub>, C<sub>iv</sub>, D<sub>iv</sub>, C<sub>vi</sub>, D<sub>vi</sub>) mouse embryos at indicated developmental stages. Both *Apc* transgenic mice show increased *Bmp7* expression at all developmental stages investigated. Scale bars: 100 μm.

## DISCUSSION

We report here the generation of compound conditional *Col2a1-Cre;Apc*<sup>15lox/1638N</sup> and *Col2a1-Cre;Apc*<sup>15lox/1572T</sup> mutant embryos, in which distinct levels of Wnt/β-catenin signaling differentially affect the chondrogenic and osteogenic differentiation of SPC. Using these unique *in vivo* experimental models we prove that specific dosages of functional *Apc* direct the differentiation of SPC by regulating the “just-right” dosage of transcriptionally active β-catenin (26). Relatively high levels of β-catenin in the SPC of *Col2a1-Cre;Apc*<sup>15lox/1638N</sup> embryos led to a complete blockade of both chondrocyte and

osteoblast formation, while intermediate levels of  $\beta$ -catenin in the SPC of *Col2a1-Cre;Apc<sup>15lox/1572T</sup>* embryos led to regional-specific modulation of SPC differentiation. Whereas sclerotomal SPC expressing *Apc <sup>$\Delta$ 15/1572T</sup>* failed to differentiate into chondrocytes and osteoblasts, in the inferior mandible and long bones these cells differentiated into highly active osteoblasts. Taken together, these data provide evidence that unique dosages of Wnt/ $\beta$ -catenin signaling distinctly influence the differentiation of SPC in a spatiotemporal regulated manner.

Various *Apc* mutant mouse models carrying different *Apc* mutant alleles that lead to specific levels of transduced Wnt/ $\beta$ -catenin signaling have been investigated on their modulating effect on tumor formation and on differentiation of embryonic stem cells (16;18-21;26). Here we present 2 novel compound conditional mouse embryos, expressing one constitutional mutant *Apc* allele in all cells (*Apc<sup>1638N</sup>* or *Apc<sup>1572T</sup>*), and one conditional *Apc* mutant allele (*Apc<sup>15lox</sup>*) which resulted in a mutant allele (*Apc <sup>$\Delta$ 15</sup>*) only in SPC through *Col2a1-Cre*-mediated excision of exon 15, encoding nearly all functional domains of *Apc* (17;22). It is generally accepted that, in *Col2a1-Cre* mouse lines, *Cre* induces recombination in SPC that still retain a bi-potential differentiation capacity to chondrocytes and osteoblasts (11;22;27-29). In agreement with our previous results in the *Col2a1-Cre;Apc<sup>15lox/15lox</sup>* mutant embryos, one functional *Apc* allele was sufficient to prevent up-regulation of the canonical Wnt signal, so that only skeletal elements of *Col2a1-Cre;Apc<sup>15lox/1638N</sup>* and *Col2a1-Cre;Apc<sup>15lox/1572T</sup>* mutant mice displayed increased levels of Wnt signaling at the mRNA (*Axin2*) and protein ( $\beta$ -catenin) level (22). Although encompassing all 3  $\beta$ -catenin-binding-domains, 3 of the 7  $\beta$ -catenin-down-regulating repeats, and 1 of the 3 axin/conductin-binding motifs, expression of the 'leaky' *Apc<sup>1638N</sup>* allele results in relatively high up-regulation of canonical Wnt signaling due to its minimal transcription levels (1-2%) (18). In agreement with this, almost all SPC of the compound conditional *Col2a1-Cre;Apc<sup>15lox/1638N</sup>* mouse embryos displayed nuclear translocation of  $\beta$ -catenin and strong *Axin2* expression. The *Apc<sup>1572T</sup>* allele is a truncated allele that is fully expressed and that differs from the *Apc<sup>1638N</sup>* allele by the lack of the only one axin/conductin-binding site still present in the *Apc<sup>1638N</sup>* allele. Accordingly, SPC of the compound conditional *Col2a1-Cre;Apc<sup>15lox/1572T</sup>* mutants expressed high levels of *Axin2* mRNA, and intermediate levels of  $\beta$ -catenin protein that was mainly detectable in the cytoplasm and rarely in the nucleus. Our results indicate that distinct levels of  $\beta$ -catenin have particular effects on the differentiation of SPC: a relatively high increase of  $\beta$ -catenin levels in the SPC of *Col2a1-Cre;Apc<sup>15lox/1638N</sup>* embryos led to a complete inhibition of chondrocyte and osteoblast differentiation, while intermediate levels of  $\beta$ -catenin in SPC of *Col2a1-Cre;Apc<sup>15lox/1572T</sup>* embryos resulted in highly active osteoblasts, no osteoclast formation and precocious mineralization. This suggests that *Apc* is essential during lineage commitment of SPC by determining the proper dosage of transcriptionally active  $\beta$ -catenin.

Through its main tumor suppressor function of binding to and downregulating  $\beta$ -catenin, *Apc* represents the key intracellular gate-keeper controlling the levels of transduced canonical Wnt signal (30). By using the same *Col2a1-Cre* transgene, we recently showed that complete lack of any *Apc* activity in SPC has heterogeneous effects on their differentiation capacity in close relation to their developmental stage and location in the skeleton (22). Whereas the vast majority of SPC lacking *Apc* did not

differentiate into chondrocytes or osteoblasts, these cells formed highly active osteoblasts in the proximal ribs. Surprisingly, *Col2a1-Cre;Apc<sup>15lox/1638N</sup>* mouse embryos, although comprising some  $\beta$ -catenin regulating activity in SPC, display a more severe skeletal phenotype than *Col2a1-Cre;Apc<sup>15lox/15lox</sup>* mutants. Not only was there no sign of skeletal formation in the *Col2a1-Cre;Apc<sup>15lox/1638N</sup>* transgenic mice, but these mutants were also lethal at an earlier age showing signs of intense tissue resorption at E14.5, most likely due to upregulation of the 2 proteases *Mmp9* and *Hyal1*. This might occur because in *Col2a1-Cre;Apc<sup>15lox/1638N</sup>* mutants all cells are expressing the *Apc<sup>1638N</sup>* allele and only the SPC also lack the second *Apc* allele, suggesting that, by regulating  $\beta$ -catenin levels, *Apc* is involved in the regulation of SPC in a non-cell-autonomous manner.

Interestingly, a heterogeneous skeletal phenotype was found in *Col2a1-Cre;Apc<sup>15lox/1572T</sup>* mutants, implying that a moderate  $\beta$ -catenin increase induces regional dependent effects on the differentiation of SPC. We found no difference in the levels of canonical Wnt signaling at both the protein ( $\beta$ -catenin) and mRNA (*Axin2*) level between the axial and the appendicular skeleton. However, no axial skeletal formation was observed in these mutants, whereas a combination of accelerated chondrocyte maturation, increased osteoblastogenesis, decreased osteoclastogenesis, and precocious mineralization resulted in the formation of short, thick and intensely mineralized appendicular skeletal elements. This suggests that SPC from the axial and the appendicular skeleton respond differently to increased Wnt/ $\beta$ -catenin signaling. The differential sensitivity of the axial and appendicular skeleton to certain levels of signaling molecules has also been reported in other conditional mouse lines. In this fashion, the axial skeleton was more responsive to a dominant negative PTHrP receptor than the limbs, the expression of a constitutively active form of Akt led to accelerated chondrocyte maturation in the axial skeleton and to opposite effects in the limbs, and forced expression of *Dlx5* resulted in accelerated chondrocyte hypertrophy only in the axial and not in the appendicular skeleton (31-33). Altogether these data suggest that anatomically distinct SPC populations can respond diversely to the same stimulus most likely due to particularities in their surrounding molecular habitats. Nevertheless, our results could also be due to a more pronounced non-cell-autonomous component for skeletal formation in the sclerotome, whereas in the limbs this component would be of minimal importance for endochondral bone formation.

Like the canonical Wnt signaling pathway, the bone morphogenetic protein (BMP) signaling cascade is involved in many biological events such as maintenance and fate specification of precursor cells, organogenesis, and carcinogenesis (10;34;35). BMPs were originally identified as factors promoting bone formation, hence their name (36). During vertebrate skeletogenesis, Wnt and BMP ligands are expressed in overlapping or complementary manners, spatially or temporarily, resulting in a multifaceted cross-talk through which they can either stimulate or inhibit each other, thus causing effects that cannot be achieved by either alone (37). We previously reported that *Apc* knockdown in a murine mesenchymal-like cell line indirectly leads to up-regulation of the BMP signaling pathway through increased *Bmp7* expression (25). In agreement with this, SPC of both *Col2a1-Cre;Apc<sup>15lox/1638N</sup>* and *Col2a1-Cre;Apc<sup>15lox/1572T</sup>* transgenic mutants displayed increased *Bmp7* mRNA expression. *Bmp7*, represents a strong in-



ducer of bone formation both *in vivo* and *in vitro* (38-40), and thus its overexpression should stimulate osteoblastogenesis in both  $Apc^{\Delta15/1638N}$ - and  $Apc^{\Delta15/1572T}$ -expressing SPC. However, we did not find signs of increased osteoblastogenesis in the  $Col2a1-Cre;Apc^{15lox/1638N}$  transgenic mutants, suggesting that *Bmp7* is not sufficient to induce bone formation and that levels of  $\beta$ -catenin must be permissive to osteoblast differentiation. Irrespectively of the presence of the osteoinductive factor *Bmp7*, SPC exposed to massive  $\beta$ -catenin levels fail to form osteoblasts. Nevertheless, when the “opportune” *Apc* mutation determines the “just-right” dosage of  $\beta$ -catenin, this can have stimulatory effects on osteoblast differentiation as observed in the appendicular skeleton of  $Col2a1-Cre;Apc^{15lox/1572T}$  mutants.

Gradients of soluble growth factors regulate many developmental processes such as tissue organization, patterning and segmentation (41). By generating conditional compound  $Col2a1-Cre;Apc^{15lox/1638N}$  and  $Col2a1-Cre;Apc^{15lox/1572T}$  transgenic mice, we prove here that different *Apc* mutations resulting in different levels of canonical Wnt signaling have distinct effects on the differentiation of SPC. This implies that a tight regulation of the dosage of functional *Apc* is directive for the lineage commitment of SPC via modulation of  $\beta$ -catenin.

## ACKNOWLEDGMENTS

*We are grateful to Prof. Dr. Henry Kronenberg (Harvard Medical School, Massachusetts General Hospital, Boston, MA, USA) for the Col2a1-Cre mice. We thank Dr. Christine Hartmann (IMP, Vienna, Austria) for the mouse Runx2, Sox9, Osx, Ihh, and Bmp7 probes; Prof. Dr. Eero Vuorio (University of Turku, Finland) for the mouse Col1a1 and Col2a1 probes; Prof. Dr. Wilhelm Hofstetter (University of Bern, Switzerland) for the mouse Col10a1 probe; Prof. Dr. Franklin Costantini (Columbia University, New York, NY, USA) for the mouse Axin2 probe; and Dr. Tatsuya Kobayashi (Massachusetts General Hospital, Boston, MA, USA) for the mouse Mmp9 probe.*

*This work was financially supported by an unrestricted educational grant from IP-SEN FARMACEUTICA BV (RLM).*

## REFERENCES

1. Kronenberg HM. Developmental regulation of the growth plate. *Nature* 2003; 423(6937):332-6.
2. van der Eerden BC, Karperien M, Wit JM. Systemic and local regulation of the growth plate. *Endocr Rev* 2003; 24(6):782-801.
3. Liu F, Kohlmeier S, Wang CY. Wnt signaling and skeletal development. *Cell Signal* 2008; 20(6):999-1009.
4. Chen AE, Ginty DD, Fan CM. Protein kinase A signalling via CREB controls myogenesis induced by Wnt proteins. *Nature* 2005; 433(7023):317-22.
5. Kuhl M, Sheldahl LC, Park M, Miller JR, Moon RT. The Wnt/Ca<sup>2+</sup> pathway: a new vertebrate Wnt signaling pathway takes shape. *Trends Genet* 2000; 16(7):279-83.
6. Logan CY, Nusse R. The Wnt signaling pathway in development and disease. *Annu Rev Cell Dev Biol* 2004; 20:781-810.
7. Mlodzik M. Planar cell polarization: do the same mechanisms regulate *Drosophila* tissue polarity and vertebrate gastrulation? *Trends Genet* 2002; 18(11):564-71.
8. Day TF, Yang Y. Wnt and hedgehog signaling pathways in bone development. *J Bone Joint Surg Am* 2008; 90 Suppl 1:19-24.
9. Hartmann C. A Wnt canon orchestrating osteoblastogenesis. *Trends Cell Biol* 2006; 16(3):151-8.
10. Clevers H. Wnt/beta-catenin signaling in development and disease. *Cell* 2006; 127(3):469-80.
11. Day TF, Guo X, Garrett-Beal L, Yang Y. Wnt/beta-catenin signaling in mesenchymal progenitors controls osteoblast and chondrocyte differentiation during vertebrate skeletogenesis. *Dev Cell* 2005; 8(5):739-50.
12. Glass DA, Bialek P, Ahn JD, Starbuck M, Patel MS, Clevers H et al. Canonical Wnt signaling in differentiated osteoblasts controls osteoclast differentiation. *Dev Cell* 2005; 8(5):751-64.
13. Akiyama H, Lyons JP, Mori-Akiyama Y, Yang X, Zhang R, Zhang Z et al. Interactions between Sox9 and beta-catenin control chondrocyte differentiation. *Genes Dev* 2004; 18(9):1072-87.
14. Hill TP, Spater D, Taketo MM, Birchmeier W, Hartmann C. Canonical Wnt/beta-catenin signaling prevents osteoblasts from differentiating into chondrocytes. *Dev Cell* 2005; 8(5):727-38.
15. Tamamura Y, Otani T, Kanatani N, Koyama E, Kitagaki J, Komori T et al. Developmental regulation of Wnt/beta-catenin signals is required for growth plate assembly, cartilage integrity, and endochondral ossification. *J Biol Chem* 2005; 280(19):19185-95.
16. Fodde R, Smits R. Disease model: familial adenomatous polyposis. *Trends Mol Med* 2001; 7(8):369-73.
17. Robanus-Maandag E, Koelink P, Breukel C, Salvatori D, Jagmohan-Changur S, Bosch C et al. A new conditional *Apc* mutant mouse model for colorectal cancer. *Carcinogenesis* 2010 May;31(5):946-52.

18. Fodde R, Edelmann W, Yang K, van Leeuwen C, Carlson C, Renault B et al. A targeted chain-termination mutation in the mouse *Apc* gene results in multiple intestinal tumors. *Proc Natl Acad Sci U S A* 1994; 91(19):8969-73.
19. Smits R, Kielman MF, Breukel C, Zurcher C, Neufeld K, Jagmohan-Changur S et al. *Apc1638T*: a mouse model delineating critical domains of the adenomatous polyposis coli protein involved in tumorigenesis and development. *Genes Dev* 1999; 13(10):1309-21.
20. Kielman MF, Rindapaa M, Gaspar C, van Poppel N, Breukel C, van Leeuwen S. et al. *Apc* modulates embryonic stem-cell differentiation by controlling the dosage of beta-catenin signaling. *Nat Genet* 2002; 32(4):594-605.
21. Gaspar C, Franken P, Molenaar L, Breukel C, van der Valk M, Smits R et al. A targeted constitutive mutation in the *APC* tumor suppressor gene underlies mammary but not intestinal tumorigenesis. *PLoS Genet* 2009; 5(7):e1000547.
22. Miclea RL, Karperien M, Bosch CA, van der Horst G, van der Valk MA, Kobayashi T et al. Adenomatous polyposis coli-mediated control of beta-catenin is essential for both chondrogenic and osteogenic differentiation of skeletal precursors. *BMC Dev Biol* 2009; 9:26.
23. Schipani E, Ryan HE, Didrickson S, Kobayashi T, Knight M, Johnson RS. Hypoxia in cartilage: HIF-1alpha is essential for chondrocyte growth arrest and survival. *Genes Dev* 2001; 15(21):2865-76.
24. Livak KJ, Schmittgen TD. Analysis of relative gene expression data using real-time quantitative PCR and the 2(-Delta Delta C(T)) Method. *Methods* 2001; 25(4):402-8.
25. Miclea RL, van der Horst G, Robanus-Maandag EC, Löwik CW, Oostdijk W, Wit JM et al. *Apc* bridges the Wnt/beta-catenin to BMP signaling pathway during osteoblast differentiation of KS483 cells. *Exp Cell Res*. 2011; 317(10):1411-21.
26. Albuquerque C, Breukel C, van der Luijt R, Fidalgo P, Lage P, Slors FJ et al. The 'just-right' signaling model: APC somatic mutations are selected based on a specific level of activation of the beta-catenin signaling cascade. *Hum Mol Genet* 2002; 11(13):1549-60.
27. Hilton MJ, Tu X, Cook J, Hu H, Long F. *Ihh* controls cartilage development by antagonizing *Gli3*, but requires additional effectors to regulate osteoblast and vascular development. *Development* 2005; 132(19):4339-51.
28. Long F, Chung UI, Ohba S, McMahon J, Kronenberg HM, McMahon AP. *Ihh* signaling is directly required for the osteoblast lineage in the endochondral skeleton. *Development* 2004; 131(6):1309-18.
29. Maes C, Goossens S, Bartunkova S, Drogat B, Coenegrachts L, Stockmans I et al. Increased skeletal VEGF enhances beta-catenin activity and results in excessively ossified bones. *EMBO J* 2010; 29(2):424-41.
30. Fodde R, Smits R, Hofland N, Kielman M, Meera KP. Mechanisms of APC-driven tumorigenesis: lessons from mouse models. *Cytogenet Cell Genet* 1999; 86(2):105-11.
31. Rokutanda S, Fujita T, Kanatani N, Yoshida CA, Komori H, Liu W et al. Akt regulates skeletal development through GSK3, mTOR, and FoxOs. *Dev Biol* 2009; 328(1):78-93.
32. Schipani E, Lanske B, Hunzelman J, Luz A, Kovacs CS, Lee K et al. Targeted expression of constitutively active receptors for parathyroid hormone and parathyroid hormone-related peptide delays endochondral bone formation and rescues mice that lack parathyroid hormone-related peptide. *Proc Natl Acad Sci U S A* 1997; 94(25):13689-94.

33. Zhu H, Bendall AJ. Dlx5 is a cell autonomous regulator of chondrocyte hypertrophy in mice and functionally substitutes for Dlx6 during endochondral ossification. *PLoS One* 2009; 4(11):e8097.
34. Hardwick JC, Kodach LL, Offerhaus GJ, van den Brink GR. Bone morphogenetic protein signalling in colorectal cancer. *Nat Rev Cancer* 2008; 8(10):806-12.
35. Varga AC, Wrana JL. The disparate role of BMP in stem cell biology. *Oncogene* 2005; 24(37):5713-21.
36. Wozney JM, Rosen V, Celeste AJ, Mitscock LM, Whitters MJ, Kriz RW et al. Novel regulators of bone formation: molecular clones and activities. *Science* 1988; 242(4885):1528-34.
37. Itasaki N, Hoppler S. Crosstalk between Wnt and bone morphogenetic protein signaling: a turbulent relationship. *Dev Dyn* 2010; 239(1):16-33.
38. Gautschi OP, Frey SP, Zellweger R. Bone morphogenetic proteins in clinical applications. *ANZ J Surg* 2007; 77(8):626-31.
39. Tsiridis E, Bhalla A, Ali Z, Gurav N, Heliotis M, Deb S et al. Enhancing the osteoinductive properties of hydroxyapatite by the addition of human mesenchymal stem cells, and recombinant human osteogenic protein-1 (BMP-7) in vitro. *Injury* 2006; 37 Suppl 3:S25-S32.
40. Zhao M, Zhao Z, Koh JT, Jin T, Franceschi RT. Combinatorial gene therapy for bone regeneration: cooperative interactions between adenovirus vectors expressing bone morphogenetic proteins 2, 4, and 7. *J Cell Biochem* 2005; 95(1):1-16.
41. Gaspar C, Fodde R. APC dosage effects in tumorigenesis and stem cell differentiation. *Int J Dev Biol* 2004; 48(5-6):377-86.



# Chapter 4

## **Apc bridges Wnt/ $\beta$ -catenin and BMP signaling during osteoblast differentiation of KS483 cells**

R.L. Miclea<sup>1</sup>, G. van der Horst<sup>2</sup>, E.C. Robanus-Maandag<sup>3</sup>, C.W. Löwik<sup>4</sup>, W. Oostdijk<sup>1</sup>, J.M. Wit<sup>1</sup>, M. Karperien<sup>5</sup>

*<sup>1</sup>Department of Pediatrics, Leiden University Medical Centre (LUMC), Leiden, The Netherlands, <sup>2</sup>Department of Urology, LUMC, Leiden, The Netherlands, <sup>3</sup>Department of Human Genetics, LUMC, Leiden, The Netherlands, <sup>4</sup>Department of Endocrinology and Metabolic Diseases, LUMC, Leiden, The Netherlands, <sup>5</sup>MIRA Institute for Biomedical Technology and Technical Medicine, Department of Tissue Regeneration, University of Twente, Enschede, The Netherlands*

Exp Cell Res. 2011 Jun 10;317(10):1411-21



# Apc bridges Wnt/ $\beta$ -catenin and BMP signaling during osteoblast differentiation of KS483 cells

R.L. Miclea, G. van der Horst, E.C. Robanus-Maandag, C.W. Löwik, W. Oostdijk, J.M. Wit, M. Karperien

## ABSTRACT

The canonical Wnt signaling pathway influences the differentiation of mesenchymal cell lineages in a quantitative and qualitative fashion depending on the dose of  $\beta$ -catenin signaling. Adenomatous polyposis coli (Apc) is the critical intracellular regulator of  $\beta$ -catenin turnover.

To better understand the molecular mechanisms underlying the role of Apc in regulating the differentiation capacity of skeletal progenitor cells, we have knocked down *Apc* in the murine mesenchymal stem cell-like KS483 cells by stable expression of *Apc*-specific small interfering RNA. In routine culture, KSFrt-*Apc*<sub>si</sub> cells displayed a mesenchymal-like spindle shape morphology, exhibited markedly decreased proliferation and increased apoptosis. *Apc* knockdown resulted in upregulation of the Wnt/ $\beta$ -catenin and the BMP/Smad signaling pathways, but osteogenic differentiation was completely inhibited. This effect could be rescued by adding high concentrations of BMP-7 to the differentiation medium. Furthermore, KSFrt-*Apc*<sub>si</sub> cells showed no potential to differentiate into chondrocytes or adipocytes.

These results demonstrate that Apc is essential for the proliferation, survival and differentiation of KS483 cells. *Apc* knockdown blocks the osteogenic differentiation of skeletal progenitor cells, a process that can be overruled by high BMP signaling.



## INTRODUCTION

During endochondral bone formation, skeletal progenitor cells (SPC) arise from mesenchymal cells, transit several differentiation steps to ultimately develop into bone or cartilage (1). Their commitment to one of the two lineages requires a very intricate and tightly controlled crosstalk between transcription factors, cytokines, and growth factors (2). However, the precise molecular interactions that control their lineage commitment and differentiation to mature skeletal cells are not fully understood.

Increasing evidence suggests an important role of the canonical Wnt signaling pathway in the regulation of lineage commitment of SPC (3). In this pathway, in the absence of the Wnt signal, cytoplasmic  $\beta$ -catenin is degraded in the proteasome upon its phosphorylation at specific Ser-Thr residues by a destruction complex consisting of Axin, Adenomatous Polyposis Coli (APC), Glycogen synthase kinase 3 $\beta$  (GSK3 $\beta$ ) and Casein-kinase 1 $\alpha$  (CK1 $\alpha$ ). Wnt growth factors bind to the receptor Frizzled and low-density lipoprotein receptor-related protein-5 or 6 (LRP-5/6) to inactivate this destruction complex, via Dishevelled (DVL). This leads to accumulation of unphosphorylated  $\beta$ -catenin and subsequent translocation into the nucleus. Together with members of the T cell factor/lymphoid enhancer factor (TCF/LEF) family, nuclear  $\beta$ -catenin stimulates transcription of Wnt target genes (4). Up-regulation of  $\beta$ -catenin in bi-potential SPC leads to osteoblast formation, whereas down-regulation favors their commitment to the chondrogenic lineage (5).

Another signaling cascade equally important in the differentiation of SPC is the bone morphogenetic protein (BMP)/Smad pathway which promotes both osteo- and chondrogenesis (6). In this pathway, BMPs bind to and activate BMP type I or II receptors thereby initiating phosphorylation of receptor-regulated Smads (R-Smads) 1, 5, and 8. Phosphorylated active R-Smads form heteromeric complexes with common-partner Smad4 that translocate to the nucleus to regulate the transcription of target genes in cooperation with other transcription factors (7).

Due to the great importance of the Wnt/ $\beta$ -catenin and BMP pathway during both osteogenic and chondrogenic differentiation of SPC, the interaction between these two powerful regulatory pathways has received much attention. For example, it has been shown that BMP-2 upregulates expression of Wnt-3a and  $\beta$ -catenin and that  $\beta$ -catenin is crucial for BMP-induced new bone formation (8;9). However, the BMP signal can also antagonize Wnt in SPC by promoting an interaction between Smad1 and Dvl that restricts  $\beta$ -catenin accumulation (10). These and other data suggest that Wnt and BMP signaling can alternatively synergize or antagonize one another in differentiation of SPC (11;12).

We have recently shown that, by downregulating the canonical Wnt/ $\beta$ -catenin signal, *Apc* is essential for the commitment of SPC to the chondrogenic and osteogenic lineage (13). Moreover, distinct *Apc* mutations unevenly affect the differentiation potential of mouse embryonic stem cells (ES): whereas *Apc* alleles entirely deficient in  $\beta$ -catenin downregulation domains block the differentiation potential of ES, more

hypomorphic alleles which are still able to partially downregulate  $\beta$ -catenin impair the differentiation of ES only to some tissues, e.g. bone and cartilage (14). In cells carrying a hypomorphic Apc mutation, the levels of  $\beta$ -catenin are upregulated only when Apc activity levels are below 2% of normal (14).

To further unravel the subtle role of Apc in the regulation of SPC differentiation, we have knocked down the mouse Apc gene using RNA interference (RNAi) in the murine mesenchymal stem cell-like KS483 cell line. This cell line shows SPC-like characteristics, since it can form osteoblasts, chondrocytes, and adipocytes (15). Our data suggest that Apc knockdown in KS483 cells leads to up-regulation not only of the Wnt/ $\beta$ -catenin, but also of the BMP signaling pathway, further sustaining the interaction of these biological routes during various steps of SPC differentiation. Low levels of Apc inhibited osteoblast, chondrocyte and adipocyte differentiation. Interestingly, the inhibitory effects of Apc knockdown on osteogenic differentiation could be rescued by high levels of BMP-7.

## MATERIALS AND METHODS

### Generation of the KS483 cell lines with stable expression of Apc<sub>si</sub> constructs

To obtain the KSFrt-Apc<sub>si</sub> stable cell line, the *shRNA* plasmid p5H1-Apc<sub>si</sub>, designed to express shRNA targeting the mouse Apc gene, was constructed as described previously (15). To obtain the control, KSFrt-mtApc<sub>si</sub> stable cell line, the *shRNA* plasmid p5H1-mtApc<sub>si</sub> was generated by introducing mismatches at position 7 and 15 of the Apc target sequence. To demonstrate the biological reproducibility of our results, the KSFrt-Apc\*<sub>si</sub> and the KSFrt-mtApc\*<sub>si</sub> cell lines were also generated using the p5H1-Apc\*<sub>si</sub> and the p5H1-mtApc\*<sub>si</sub> plasmid (carrying mismatches at position 5 and 16 of the Apc\*<sub>si</sub> construct), respectively. The target sequences used to specifically silence Apc (Apc<sub>si</sub>, Apc\*<sub>si</sub>) and their corresponding mutant (control) sequences (mtApc<sub>si</sub>, mtApc\*<sub>si</sub>) are shown in Figure 1A. Stable transfections of the 4C3 Frt clone of the KS483 murine host cell line were performed as previously described (15). In this clone, a unique FLP recombinase target (FRT) sequence is introduced in the genome. This site is subsequently used for targeted insertion of the short hair pin vector using FLP-mediated homologous recombination (15).

### Cell culture

KS483 cells were routinely cultured in T75 culture flasks (Greiner Bio-One) as described previously (16). For the KSFrt 4C3 host cell line the medium was supplemented with blasticidin S HCl (2  $\mu$ g/ml; Invitrogen). All stably transfected cell lines were cultured in the presence of hygromycin B (100  $\mu$ g/ml; Invitrogen).

### Immunofluorescence

Immunofluorescence for Apc and  $\beta$ -catenin was performed as described previously with minor modifications (16). In brief, cells were seeded on glass slides (BD Falcon) and either left untreated or treated with Wnt3a (30ng/ml; R&D Systems) for

3hrs. The primary antibodies were rabbit polyclonal anti-Apc (1:500 in NETGEL; Abcam) and rabbit polyclonal anti- $\beta$ -catenin (1:500 in NETGEL; Abcam). The second antibody used was goat anti-rabbit FITC-conjugate (1:250; Sigma). The F-actin cytoskeleton was counterstained using Phalloidin-TRITC (0.33 mg/ml; Sigma). Cells were imaged using the 63 $\times$  objective of an inverted Leica SP2 confocal microscope.

### Western Blot

Approximately  $2 \times 10^7$  cells were either cultured in the control conditions for 24 hrs or with 30ng/ml Wnt3a, rinsed twice with PBS and lysed for 5 min on ice in 400  $\mu$ l of Cell Lysis Buffer (Cell Signaling) and a cocktail of protease inhibitors (Roche). For detection of Apc and  $\beta$ -catenin proteins by Western blot, whole cell lysates were loaded on a 4–20% linear gradient Tris-HCl Gel (BIO-RAD), and transferred onto PVDF membranes (Millipore) by 1 hr electroblotting at 300 mA constant current at RT in blotting buffer (BIO-RAD). Following transfer, the membranes were blocked with 5% nonfat dry milk in TPBS (0.05% Tween 20 in PBS) for 1 hr. Incubation with primary antibodies was performed overnight at 4°C using rabbit polyclonal anti-Apc (1:100; Abcam) or mouse monoclonal anti- $\beta$ -catenin (1:2000; Epitomics) antibodies. Blots were washed 3 times with PBS and incubated with horseradish peroxidase-conjugated secondary antibodies for 1 hr at room temperature. The peroxidase was visualized and quantified by enhanced chemiluminescence using the Molecular Imager Gel Doc XR+ System (BIO-RAD).

### Real-time quantitative PCR

Real-time quantitative PCR was performed using QuantiTect real-time PCR primers (Qiagen) for the detection of the mouse *Apc*, *Ctnnb1*, *Axin2*, *Smad1*, *Smad3*, *Smad4*, and *Bmp7* genes and analyzed as described previously (16).

### Proliferation assay

For proliferation assays, the CellTiter 96<sup>®</sup> AQueous Non-Radioactive Cell Proliferation Assay (Promega) was used. Cells were seeded at a density of 2,500 cells/cm<sup>2</sup>. After 24, 48, 72 and 96 hours, 20  $\mu$ l of MTS [3-(4,5-dimethylthiazol-2-yl)-5-(3-carboxymethoxyphenyl)-2-(4-sulphophenyl)-2H-tetrazolium]] was added to the medium and the mitochondrial activity was measured at 490 nm after 2 hr incubation at 37°C.

### Apoptosis assay

For detection of apoptotic cells, Annexin V staining was performed using Annexin V-FITC (1:250; Bender Med Systems), which specifically binds phosphatidyl serine (PS) residues on the cell membrane, and propidium iodide (PI; Bender Med Systems) at 1 $\mu$ g/ml which binds to DNA once the cell membrane has become permeable. Cells were analyzed by flow cytometry (FACS-Calibur, Becton Dickinson) using the CellQuest program (FACS-Calibur, Becton Dickinson).

### Luciferase transient transfection assays

The KSFrt-*Apc*<sub>si</sub> and KSFrt-mt*Apc*<sub>si</sub> stable cells were seeded at a density of 19,000 cells/cm<sup>2</sup> and 9,500 cells/cm<sup>2</sup>, respectively, in 24-well plates, and transiently trans-

ected with 2  $\mu$ g of the reporter construct (pGL3-(BRE)<sub>2</sub>-Luc, BAT-Luc or pSAR-MT-APC) using Fugene HD transfection reagent (Roche), according to the manufacturer's protocol. To correct for transfection efficiency, 25 ng of Renilla luciferase (pGL4-CAAGS; Promega) was co-transfected. Twenty-four hours after transfection, transfected cells were either left non-stimulated or stimulated for an additional 24 hrs. Luciferase assays were performed as described previously (16).

### Differentiation assays

To induce osteogenic differentiation, the KSFrt-*Apc*<sub>si</sub> and KSFrt-mt*Apc*<sub>si</sub> stable cells were seeded at a density of 24,000 cells/cm<sup>2</sup> and 12,000 cells/cm<sup>2</sup>, respectively, and cultured in the presence or absence of BMP-7 at the concentrations indicated. The medium was changed every 3 to 4 days. At confluence (from Day 4 of culture onward), ascorbic acid (50  $\mu$ g/ml; Merck) and, when nodules appeared (from Day 11 of culture onward),  $\beta$ -glycerol phosphate (5 mM; Sigma) were added to the culture medium. Analysis of the Alkaline Phosphatase activity (at Day 11) and the degree of mineralization (at Day 21) was performed as previously described (17).

To induce chondrogenic differentiation, 300,000 cells were pelleted by centrifugation in a round-bottom-well of a 96-well-plate (Corning) and cultured in 250  $\mu$ l high-glucose DMEM (Gibco), supplemented with 100 U/ml Pen/Strep, 50  $\mu$ g/ml ascorbic acid (Merck), 40  $\mu$ g/ml proline (Sigma), 1 mM Pyruvate, 1:100 ITS + Premix (BD Biosciences). During the first 2 weeks of culture, medium was further enriched with 10 ng/ml TGF $\beta$ 3 (R&D Systems) and 10<sup>-7</sup> M Dexamethasone (Sigma), while beginning with week 3, 500 ng/ml BMP-6 and 5mM  $\beta$ -glycerol-phosphate (Merck) was added to the medium. The medium was replaced every 3 to 4 days. After 6 weeks of culture, pellets were fixed, embedded in paraffin and sectioned. Sections were stained with Toluidine Blue or immunostained for collagen II as previously described (13). Glycosaminoglycan quantification corrected for DNA after 2, 4 and 6 weeks of culture was performed as previously described (16).

To induce adipogenic differentiation, the KSFrt-*Apc*<sub>si</sub> and KSFrt-mt*Apc*<sub>si</sub> stable cells were seeded at a density of 24,000 cells/cm<sup>2</sup> and 12,000 cells/cm<sup>2</sup>, respectively, and cultured in the presence of 25  $\mu$ M Indomethacin after confluence (from Day 4 of culture onward). After 3 weeks of culture, cells were stained with Oil Red O as described previously (17). Quantification of adipocytes was performed by counting adipocytes, defined by the presence of at least 3 lipid droplets per cell from 9 randomly selected fields (3 fields/well) for each group.

### Statistics

All values represent mean  $\pm$  SEM of two or three independent triplicate experiments. Differences were examined by one way analysis of variance (ANOVA). Results were considered significant at  $p < 0.05$ .

## RESULTS

The KSFrt-*Apc*<sub>si</sub> cell line is a valid model for studying the role of *Apc* in SPC differentiation

To study the role of the *Apc* gene in regulating lineage commitment and differentiation of SPC, we generated a cell line with decreased *Apc* expression by RNA interference (RNAi) using the 4C3 Frt clone of the KS483 murine host cell line (18).

Overexpression of *Apc*<sub>si</sub> but not of mt*Apc*<sub>si</sub> decreased wild-type *Apc* protein levels with approximately 50%, suggesting an efficient gene knockdown at the protein level (Figure 1B). KSFrt-*Apc*<sub>si</sub> cells also showed less total  $\beta$ -catenin protein expression in comparison to control mt*Apc*<sub>si</sub> cells in whole cell extracts (Figure 1C). Nevertheless, total  $\beta$ -catenin levels were reduced in both cytoplasmic and nuclear cell fractions (data not shown). Treatment with Wnt3a did not affect the *Apc* expression, but upregulated  $\beta$ -catenin in both KSFrt-*Apc*<sub>si</sub> and KSFrt-mt*Apc*<sub>si</sub> cells.

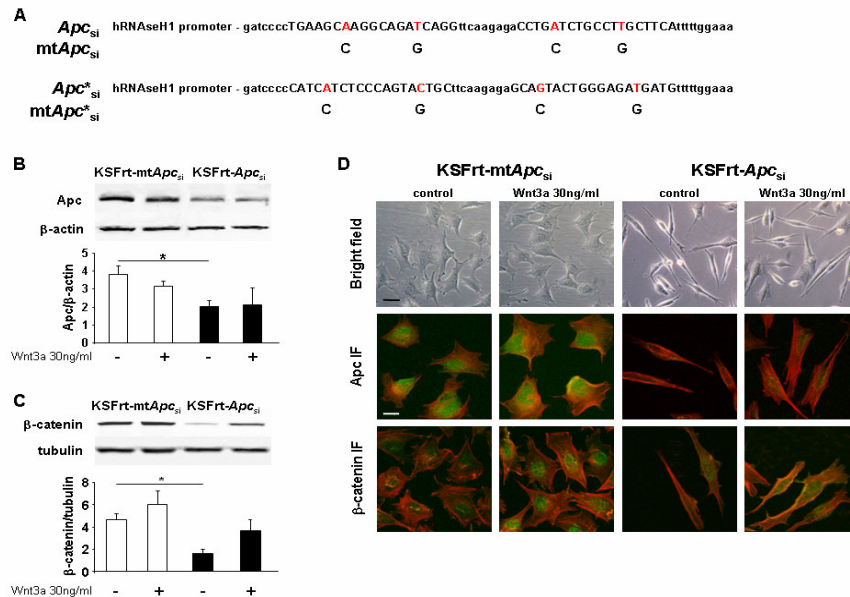


**Figure 1. Morphological and structural characterization of the KSFrt-*Apc*<sub>si</sub> cell line.** (A) The *Apc* target sequence of *Apc*<sub>si</sub>, mt*Apc*<sub>si</sub>, *Apc*<sup>\*</sup><sub>si</sub> and mt*Apc*<sup>\*</sup><sub>si</sub> RNAi vectors driven by the hRNaseH1 promoter used to obtain the KSFrt-*Apc*<sub>si</sub>, KSFrt-mt*Apc*<sub>si</sub>, KSFrt-*Apc*<sup>\*</sup><sub>si</sub> and KSFrt-mt*Apc*<sup>\*</sup><sub>si</sub> cell line, respectively. (B, C) Quantified western blot analysis, performed on total protein lysates, demonstrated that KSFrt-*Apc*<sub>si</sub> cells (black bars) express less *Apc* and  $\beta$ -catenin protein in comparison to control KSFrt-mt*Apc*<sub>si</sub> cells (white bars). (D) Bright field (upper row), IF for *Apc* (green; middle row) and for  $\beta$ -catenin (green; lower row) pictures of the control KSFrt-mt*Apc*<sub>si</sub> and of the KSFrt-*Apc*<sub>si</sub> cells coupled with Phalloidin staining for the F-actin cytoskeleton (red). Note the spindle shape mesenchymal-like morphology of the KSFrt-*Apc*<sub>si</sub> cells, expressing less *Apc* and mostly nuclear  $\beta$ -catenin. Wnt3a (30ng/ml) induced neither morphological nor structural changes in the KSFrt-*Apc*<sub>si</sub> cells. Bar represents 50  $\mu$ m (bright field pictures) or 20  $\mu$ m (IF pictures). \**p* < 0.05.

The morphology of the KSFrt-*Apc*<sub>si</sub> cells was considerably changed into thin, elongated, spindle shape mesenchymal-like cells in contrast to control cells that maintained the polygonal, cuboidal shape of the parental 4C3 cell line (Figure 1D, upper row). Morphology was not influenced by treatment with Wnt3a in neither of the cell lines. To investigate the cellular level and distribution of Apc and  $\beta$ -catenin in the KSFrt-*Apc*<sub>si</sub> cells, we next performed immunofluorescence (IF) analysis coupled with Phalloidin staining for visualizing the F-actin cytoskeleton in non-confluent cultures. IF for Apc confirmed the WB results, indicating overall less Apc expression in KSFrt-*Apc*<sub>si</sub> cells in comparison to control cells (Figure 1D, middle row). Wnt3a affected neither the level of Apc nor its cellular distribution in both cell lines. In control cells,  $\beta$ -catenin was mainly membrane-bound and cytoplasmic, while stimulation with Wnt3a induced  $\beta$ -catenin nuclear translocation (Figure 1D, lower row). In contrast, in the KSFrt-*Apc*<sub>si</sub> cells,  $\beta$ -catenin was mainly present in the nucleus in both non- and Wnt3a-stimulated conditions. Similar results were obtained on confluent cultures of both cell lines (data not shown).

#### Functional characterization of the KSFrt-*Apc*<sub>si</sub> cell line

Proliferation of both KSFrt-*Apc*<sub>si</sub> and KSFrt-*Apc*<sup>\*si</sup> cells was significantly reduced after 24, 48, 72 and 96 hrs of culture in comparison to control cells, as confirmed by MTS proliferation assay ( $p < 0.01$  at all time points; Figure 2A and data not shown). The percentage of apoptotic cells detected by Annexin V staining was significantly increased in the KSFrt-*Apc*<sub>si</sub> cells as compared to control cells (18.02% and 2.73%, respectively,  $p < 0.05$ ; Figure 2B).

We next used the Wnt responsive BAT-Luc reporter construct to evaluate the effect of *Apc* knockdown on Wnt responsiveness (19). In basal conditions, the reporter activity was significantly increased in the KSFrt-*Apc*<sub>si</sub> cells in comparison to control cells ( $p < 0.01$ ; Figure 2C), suggestive for increased endogenous canonical Wnt signaling. Remarkably, the response to Wnt3a was blunted in the KSFrt-*Apc*<sub>si</sub> cell line. This could be due to the lower total  $\beta$ -catenin levels (Figure 1C) and relatively higher percentage of active  $\beta$ -catenin over total  $\beta$ -catenin which already resides in the nucleus of the KSFrt-*Apc*<sub>si</sub> cells even in basal conditions (Figure 1D). We next examined whether *Apc* knockdown could be rescued by transient transfection of an *APC* expression vector, which induces the expression of wild-type APC in the presence of ZnCl<sub>2</sub> (20). As expected, pSAR-MT-APC induced a dose-dependent decrease in BAT-Luc reporter activity in Wnt3a-, but not in non-stimulated control cells. Wild-type APC expression in the KSFrt-*Apc*<sub>si</sub> cells decreased the high basal Wnt-reporter activity dose-dependently (0 $\mu$ M vs. 100 $\mu$ M ZnCl<sub>2</sub>,  $p < 0.05$ ) and rescued the ability of Wnt3a to activate the BAT-Luc reporter indicative for a partial rescue of the knock down phenotype. Upregulation of the established Wnt/ $\beta$ -catenin target gene *Axin2* at the mRNA level further confirmed the increased canonical Wnt signaling in the KSFrt-*Apc*<sub>si</sub> cells ( $p < 0.01$ ; Figure 2D) in line with  $\beta$ -catenin immunofluorescence and BAT-LUC reporter assays (21).

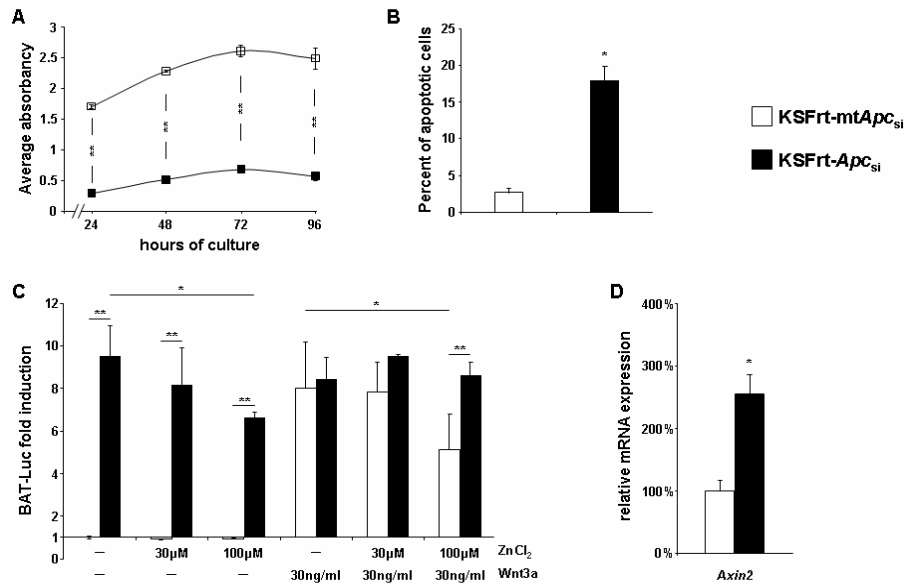


**Figure 2. KSFrt-*Apc*<sub>si</sub> cells display decreased proliferation rate, increased apoptosis and increased Wnt/ $\beta$ -catenin signal transduction.** (A) KSFrt-*Apc*<sub>si</sub> cells (black circles) proliferate significantly less in comparison to control KSFrt-*mtApc*<sub>si</sub> cells (white squares), as measured with an MTS proliferation assay. (B) KSFrt-*Apc*<sub>si</sub> cells (black bar) show significantly increased apoptosis in comparison to control KSFrt-*mtApc*<sub>si</sub> cells (white bar), as determined by Annexin V staining. (C) KSFrt-*mtApc*<sub>si</sub> (white bars) and KSFrt-*Apc*<sub>si</sub> cells (black bars) were transiently co-transfected with BAT-Luc and pSAR-MT-APC. In comparison to control KSFrt-*mtApc*<sub>si</sub> cells, KSFrt-*Apc*<sub>si</sub> cells display increased endogenous BAT-Luc activity that is rescued by inducible expression of wild-type APC dose-dependently. No further increase in BAT-Luc activity is observed in KSFrt-*Apc*<sub>si</sub> cells after stimulation with Wnt3a. Values are expressed as fold induction of firefly luciferase activity of untreated control KSFrt-*mtApc*<sub>si</sub> cells. (D) The relative mRNA expression of *Axin2* in the KSFrt-*Apc*<sub>si</sub> cells (black bar) is higher as compared to KSFrt-*mtApc*<sub>si</sub> cells (white bar). \* $p < 0.05$ , \*\* $p < 0.01$ .

### KSFrt-*Apc*<sub>si</sub> cells display an altered differentiation potential to the chondrogenic, adipogenic and osteogenic lineage

We next examined the multipotency of the KSFrt-*Apc*<sub>si</sub> cells. To determine the potential of KSFrt-*Apc*<sub>si</sub> cells to differentiate into chondrocytes, we cultured them as pellets for 6 weeks. Throughout the chondrogenic differentiation experiment, all KSFrt-*mtApc*<sub>si</sub> pellets remained compact spheres, whereas some of KSFrt-*Apc*<sub>si</sub> gradually lost their spherical shape and others disintegrated. At the end of the culture period, KSFrt-*mtApc*<sub>si</sub> pellets displayed a matrix rich in both Toluidine Blue-positive glycosaminoglycans (GAGs) and Collagen II protein (Figure 3A). In marked contrast, KSFrt-*Apc*<sub>si</sub> cells did not form a cartilage matrix and did not express Collagen II. GAG quantification corrected for DNA in pellets after 2, 4 and 6 weeks of culture confirmed these observations (Figure 3B). At all time points, we detected significantly lower GAG contents in

the KSFrt-*Apc*<sub>si</sub> pellets in comparison to controls ( $p < 0.05$  at 2 weeks,  $p < 0.01$  at 4 and 6 weeks).

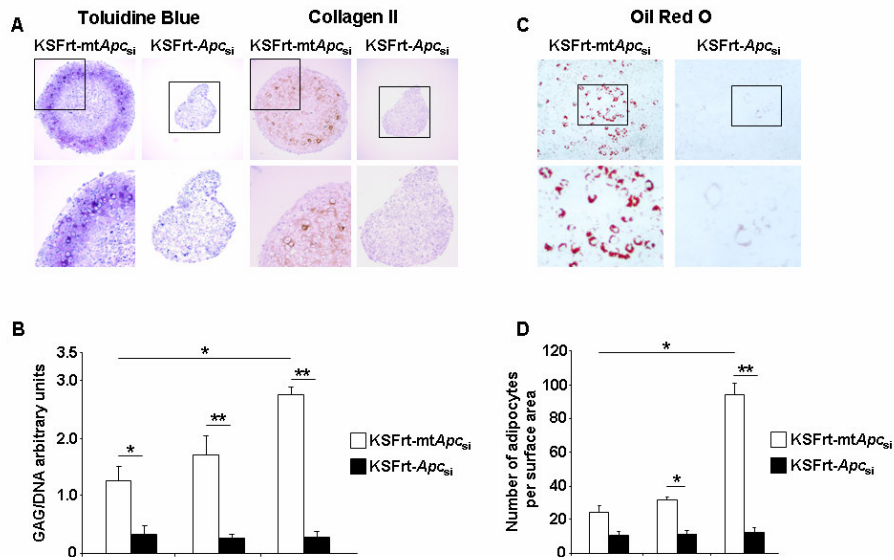


**Figure 3. KSFrt-*Apc*<sub>si</sub> cells display neither chondrogenic nor adipogenic differentiation potential.** (A) KSFrt-*Apc*<sub>si</sub> cells do not differentiate into chondrocytes as demonstrated by the absence of Toluidine Blue staining and Collagen II immunostaining performed after the 6-week-long chondrogenic differentiation protocol. The boxed regions in the pictures of the upper row are magnified in the lower row. (B) Quantification of GAGs corrected for DNA validates the microscopical findings. The GAG content in the KSFrt-mtApc<sub>si</sub> pellets (white bars) increases time dependently, whereas it remains significantly lower in the KSFrt-*Apc*<sub>si</sub> pellets (black bars) at all time points. (C) KSFrt-*Apc*<sub>si</sub> cells do not differentiate into adipocytes as demonstrated by Oil Red O staining performed after the 3-week-long adipogenic differentiation protocol. (D) Adipocyte counting indicates a significantly lower number of adipocytes among the KSFrt-*Apc*<sub>si</sub> cells per surface area (black bars) when compared to KSFrt-mtApc<sub>si</sub> cells. \* $p < 0.05$ , \*\* $p < 0.01$ .

The adipogenic differentiation potential of the KSFrt-*Apc*<sub>si</sub> cells was investigated by performing Oil Red O staining on cells cultured for 1, 2 and 3 weeks in adipogenic medium. After 3 weeks of culture, many of the KSFrt-mtApc<sub>si</sub> cells differentiated into adipocytes containing lipid droplets that positively stained with Oil Red O (Figure 3C). In contrast, differentiation of KSFrt-*Apc*<sub>si</sub> cells into adipocytes was severely impaired. Quantification of the number of adipocytes indicated that after 1, 2 and 3 weeks the number of Oil Red O-positive cells was significantly lower in the KSFrt-*Apc*<sub>si</sub> cells in comparison to controls ( $p < 0.05$  at 2 weeks,  $p < 0.01$  at 3 weeks; Figure 3D).



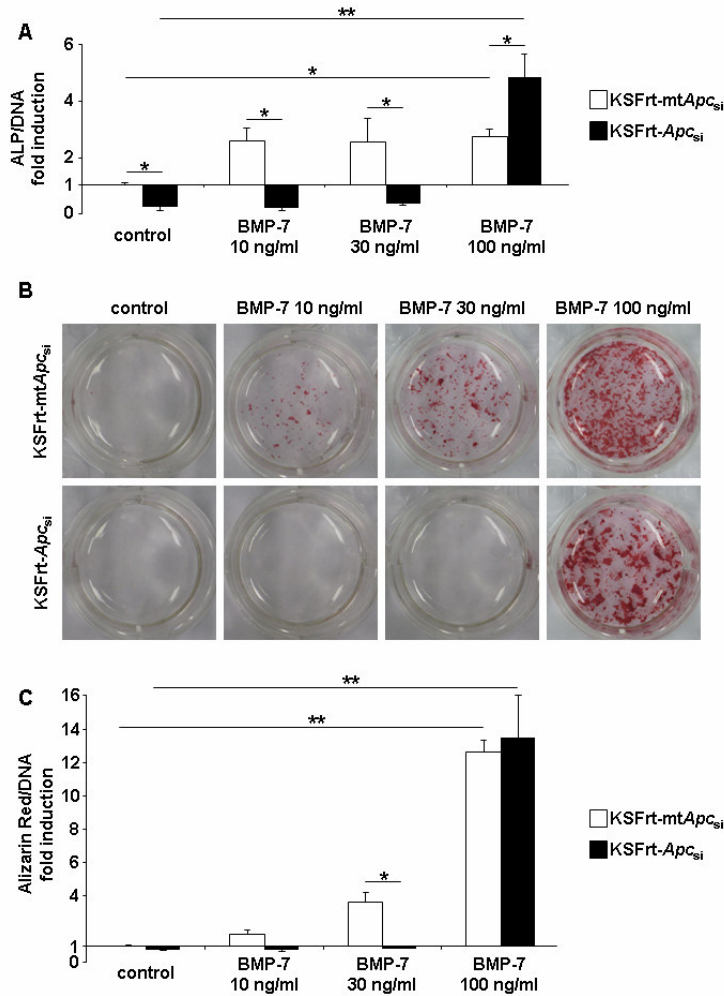


**Figure 4. KSFrt-Apc<sub>si</sub> cells display an impaired osteogenic differentiation potential that can be counteracted by high concentrations of BMP-7.** (A) Alp activity after 11-day-long osteoblast differentiation protocol. In the absence and at low concentrations of BMP-7, KSFrt-Apc<sub>si</sub> cells (black bars) display significantly less Alp activity in comparison to control KSFrt-mtApc<sub>si</sub> cells (white bars). When stimulated with 100 ng/ml BMP-7, KSFrt-Apc<sub>si</sub> cells show significantly increased osteogenic differentiation potential in comparison to control KSFrt-mtApc<sub>si</sub> cells. Values are expressed as fold induction of Alp activity corrected for DNA of untreated control KSFrt-mtApc<sub>si</sub> cells. (B) Representative images of Alizarin Red S-stained cultures after 21-day-long osteoblast differentiation protocol. BMP-7 stimulates the formation of mineralized nodules dose-dependently in control KSFrt-mtApc<sub>si</sub> cells, whereas KSFrt-Apc<sub>si</sub> cells show mineralized nodules only in the presence of high BMP-7 concentrations. (C) Quantification of the amount of Alizarin Red corrected for DNA. When treated with 100 ng/ml BMP-7, KSFrt-Apc<sub>si</sub> cells (black bars) show significantly increased mineral deposition in comparison to control condition. Values are expressed as fold induction of Alizarin Red S content corrected for DNA of untreated control KSFrt-mtApc<sub>si</sub> cells (white bars). \*p < 0.05, \*\*p < 0.01.

To determine the osteogenic potential of KSFrt-*Apc<sub>si</sub>* cells, we performed short-term osteoblast differentiation experiments. Alkaline Phosphatase (ALP) staining and its consequent quantification indicated that, in comparison to control cells, both KSFrt-*Apc<sub>si</sub>* and KSFrt-*Apc<sup>\*</sup><sub>si</sub>* cells display a significantly decreased potential to differentiate into osteoblasts (Figure 4A and data not shown). We next tested whether the inhibition of osteoblastogenesis in the KSFrt-*Apc<sub>si</sub>* cells could be rescued by the addition of pro-osteogenic growth factors like Basic fibroblast growth factor (bFGF), Transforming growth factor, beta 3 (TGF- $\beta$ 3), Parathyroid hormone-related peptide (PTHrP), Insulin-like growth factor 1 (IGF-1), and 2 members of the BMP family, BMP-6 and BMP-7. Of these, only BMP-7 (and, to a lesser extent, BMP-6) could rescue the *Apc<sub>si</sub>*-mediated inhibition of osteogenic differentiation (Figure 4A and data not shown). Osteoblast maturation of KSFrt-*Apc<sub>si</sub>* cells was investigated by alizarin Red S staining after long-term cultures to depict mineralization of the osteoblast nodules. Similar to their controls, neither KSFrt-*Apc<sub>si</sub>* nor KSFrt-*Apc<sup>\*</sup><sub>si</sub>* cells displayed mineralized nodules in the absence of BMP-7 (Figure 4B and data not shown). In contrast to KSFrt-*Apc<sub>si</sub>* cells, low concentrations of BMP-7 (10 and 30 ng/ml) were sufficient to induce matrix mineralization in control cells. Interestingly, high concentrations of BMP-7 (100ng/ml) efficiently induced the formation of alizarin Red S-positive nodules in the KSFrt-*Apc<sub>si</sub>* cells. No statistically significant difference was found when the alizarin Red S staining was quantified between KSFrt-*Apc<sub>si</sub>* and control cells cultured in the presence of 100ng/ml BMP-7 (Figure 4C). However, the osteoblast nodules formed by the KSFrt-*Apc<sub>si</sub>* cells were bigger in comparison to those formed by control cells.

#### Increased BMP signaling in the KSFrt-*Apc<sub>si</sub>* cells

We next assessed the level of BMP signaling in the KSFrt-*Apc<sub>si</sub>* cells by performing transient transfection assays using the BMP-responsive pGL3-(BRE)<sub>2</sub>-Luc reporter construct (22). KSFrt-*Apc<sub>si</sub>* cells displayed significantly increased endogenous levels of BMP signaling in comparison to control KSFrt-*mtApc<sub>si</sub>* cells ( $p < 0.01$ ; Figure 5A). BMP-7 activated the (BRE)<sub>2</sub>-Luc reporter dose-dependently in control cells in contrast to KSFrt-*Apc<sub>si</sub>* cells. In these latter cells, only a high BMP-7 concentration activated the reporter compared to the control condition. The response was blunted in the KSFrt-*Apc<sub>si</sub>* cells compared to KSFrt-*mtApc<sub>si</sub>* cells (0.5-fold vs. 4-fold increase, respectively). Noggin, a potent inhibitor of the BMP signaling pathway (7), managed to decrease both the endogenous and the BMP-7-induced activity of the (BRE)<sub>2</sub>-Luc reporter in the KSFrt-*Apc<sub>si</sub>* cells, suggestive for autocrine stimulation of the BMP signaling pathway for example by increased expression of BMPs. Upregulation of the BMP signaling pathway in the KSFrt-*Apc<sub>si</sub>* cells was further confirmed at the mRNA level by quantitative RT-PCR. *Smad1*, *Smad3*, and *Smad4* were significantly increased in the KSFrt-*Apc<sub>si</sub>* cells ( $p < 0.05$ ; Figure 5B). Interestingly, *Bmp7* showed a 4.4-fold higher expression at the mRNA level in the KSFrt-*Apc<sub>si</sub>* cells in comparison to KSFrt-*mtApc<sub>si</sub>* cells ( $p < 0.01$ ).

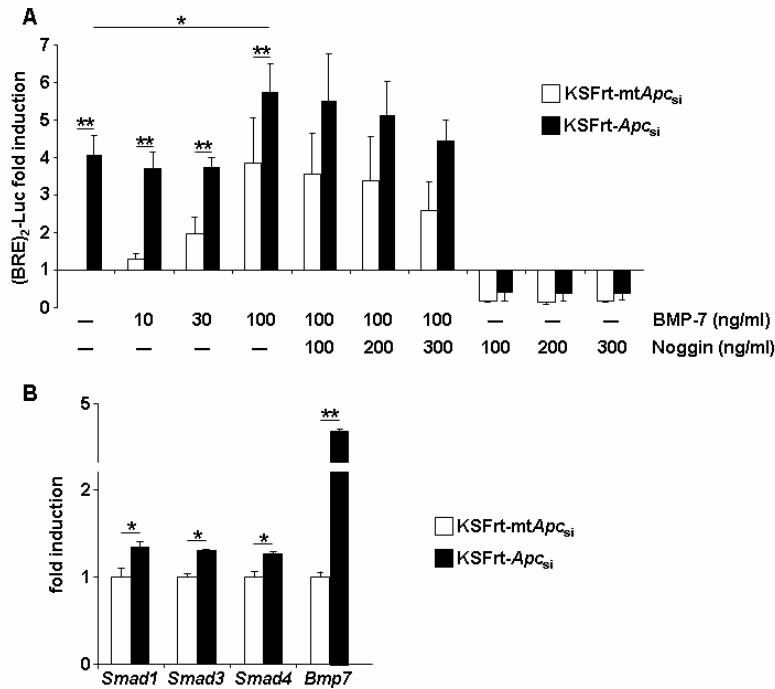


**Figure 5. Increased BMP signaling in the KSFrt-*Apc*<sub>si</sub> cells.** (A) KSFrt-mtApc<sub>si</sub> (white bars) and KSFrt-*Apc*<sub>si</sub> cells (black bars) were transiently transfected with pGL3-(BRE)<sub>2</sub>-Luc. KSFrt-*Apc*<sub>si</sub> cells display increased endogenous (BRE)<sub>2</sub>-Luc activity that is enhanced by treatment with only high concentrations of BMP-7. Noggin inhibits both the endogenous and the BMP-7-induced (BRE)<sub>2</sub>-Luc activity in the KSFrt-*Apc*<sub>si</sub> cells. Values are expressed as fold induction of firefly luciferase activity of untreated control KSFrt-mtApc<sub>si</sub> cells. (B) Significantly increased relative mRNA expression of *Smad1*, *Smad3*, *Smad4*, and *Bmp7* in KSFrt-*Apc*<sub>si</sub> cells (black bars) in comparison to KSFrt-mtApc<sub>si</sub> cells (white bars). \**p* < 0.05, \*\**p* < 0.01.

## DISCUSSION

APC is a multifunctional protein involved in cell adhesion, mitosis, apoptosis, cytoskeletal organization, microtubule assembly, cell fate determination and chromosomal stability, yet it remains mostly investigated as the key intracellular gate-keeper of the canonical Wnt/ $\beta$ -catenin signaling pathway (23-25). In our present study, we demonstrate that Apc is required for proliferation, suppression of apoptosis and differentiation of murine mesenchymal stem cell-like KS483 cells into the osteogenic, chondrogenic and adipogenic lineage. We obtained similar results by using 2 different shRNA sequences targeting *Apc*, while stable transfection of the respective control mutant shRNA plasmids (containing 2 nucleotide mismatches) did not alter the proliferation, survival and differentiation capacity of KS483 cells. This clearly indicates that

our results were the consequence of a bona-fide and specific siRNA effect lowering wild-type Apc expression. This was further confirmed by the partial rescue of BAT-Luc reporter activity by transient transfection of a human APC expression vector. Interestingly, KSFrt-*Apc*<sub>si</sub> cells displayed not only high levels of the canonical Wnt/ $\beta$ -catenin pathway, but also augmented BMP signaling, further sustaining the multifaceted interaction between these two signaling pathways during the differentiation of SPC.

RNAi is a complex biological mechanism during which shRNAs act either by cleavage ("slicing") or by translational repression of their target mRNA (26). KSFrt-*Apc*<sub>si</sub> cells showed decreased Apc expression at the protein level, thereby documenting an efficient Apc knockdown by RNAi (27;28).  $\beta$ -catenin protein expression was also lower in comparison to control cells, suggesting, as has been reported in other cell lines, that low levels of Apc are sufficient to downregulate  $\beta$ -catenin (29). Lower  $\beta$ -catenin expression due to Apc knockdown contrasts observations in tumors, in which Apc inactivation due to deletion or mutation is linked to increased  $\beta$ -catenin expression (24). In contrast to these models, KSFrt-*Apc*<sub>si</sub> still expresses wild type Apc albeit at lower levels. Furthermore, cells carrying hypomorphic Apc mutations show up-regulation of  $\beta$ -catenin levels only when the Apc activity is reduced below 2% of the normal levels (14). Interestingly, the increased activity of the BAT-Luc Wnt responsive construct in the KSFrt-*Apc*<sub>si</sub> cells implies a shift of the inactive/active  $\beta$ -catenin balance in favor of the active fraction. The partial rescue of the *Apc*<sub>si</sub>-induced Wnt activation after transfection with an APC expression vector demonstrates that the upregulation of the Wnt signal in the KSFrt-*Apc*<sub>si</sub> cells is due to Apc knockdown. We recently described that the 4C3 Frt clone of the parental KS483 murine mesenchymal progenitor line can differentiate into osteoblasts, chondrocytes and adipocytes, when cultured in the appropriate conditions and represents a valuable biological tool for the evaluation of gene function both *in vivo* and *in vitro* (15;18;30). Thus, the KSFrt-*Apc*<sub>si</sub> cell line is a reliable model to study the role of Apc in regulating differentiation of SPC (18). It is well established that APC modulates cell shape by organizing the cytoskeleton in particular through stabilization of microtubules (31). The KSFrt-*Apc*<sub>si</sub> cell line developed elongated cellular protrusions, thereby displaying a clearly distinct morphology from the control cells. In agreement with this, upregulation of the canonical Wnt signal has been shown to promote a spindle-like cell morphology (13;32;33).

It is generally accepted that Apc inhibits cell proliferation via  $\beta$ -catenin-dependent and -independent actions, and that inactivation of APC represents the early, initiating event in several malignant diseases (34-36). However, evidence is also available suggesting that APC is essential for cell proliferation (29). Likewise, no consensus regarding the effect of APC on apoptosis has been reached since both stimulation and inhibition of apoptosis by APC have been described (20;37-39). The role of APC in apoptosis, such as observed in the KSFrt-*Apc*<sub>si</sub> can be either  $\beta$ -catenin dependent or independent (23;38). Based on these results, we currently favor the hypothesis that Apc plays opposing roles during development and malignant transformation, by modulating cell shape, proliferation, and survival in a context dependent manner, with distinct consequences in different cell types and at different developmental stages.

The canonical Wnt/ $\beta$ -catenin signaling pathway governs the lineage commitment of bi-potential SPC into osteoblasts or chondrocytes (40). Roughly, it is proposed that

upregulation of this pathway induces the differentiation of SPC into precursors of the osteogenic lineage, whereas its downregulation is needed for chondrogenic differentiation (5). Data available from *in vivo* and *ex vivo* studies indicate that the osteogenic differentiation potential is altered when *Apc* is lacking or mutated, even if the resulting levels of  $\beta$ -catenin are high (13;14). Although being exposed to higher levels of transcriptionally active Wnt and BMP signaling, KSFrt-*Apc<sub>si</sub>* cells display a diminished osteogenic differentiation potential. Similar findings were made in conditional *Apc* knockout mice, in which inactivation of *Apc* in SPCs completely blocked osteoblast and chondrocyte differentiation particular in early stages of skeletogenesis (13). The latter study has also shown that the inhibitory phase in some skeletal elements is followed by accelerated osteoblast formation in later developmental stages (13). Complete inhibition of osteogenesis by knock down of *Apc* appears in contrast with increased BMD and high incidence of osteoma in FAP patients carrying a heterozygous inactivating mutation of *APC* (41). In addition, conditional *Apc* knock out using *Cre* expression under the influence of the *Osteocalcin* promoter, a late marker of osteoblast differentiation, results in increased bone formation and lack of osteoclast formation (42). Therefore we hypothesized that the inhibitory effect on osteoblast differentiation in the KSFrt-*Apc<sub>si</sub>* cells is cell type dependent and may be reversed by environmental factors like exposure to exogenous growth factors.

Interestingly, when the KSFrt-*Apc<sub>si</sub>* cells were exposed to additional high concentrations of BMP-7 and to a lesser extent BMP-6, both potent stimulators of osteogenesis (43), they displayed an increased potential to form osteoblasts in comparison to control cells. Such rescue effect was not observed when using other pro-osteogenic growth factors like bFGF, TGF- $\beta$ 3, PTHrP, IGF-1. One of the potential interpretations is that BMP signaling further activates canonical Wnt signaling, thus it synergistically induces the osteoblast differentiation in KSFrt-*Apc<sub>si</sub>* cells. Our results indicate that *Apc* is essential for the osteogenic differentiation of the KS483 cell line and that the noxious effect of *Apc* knockdown on osteogenesis can be overruled by high BMP signaling induced by BMP-7. Consistently, *in vitro* observations made in C3H10T1/2 cells demonstrate that canonical Wnt signaling itself is not sufficient, but in synergy with BMP signaling it can promote osteoblast differentiation (44).

Both the canonical Wnt and the BMP signaling pathway have been shown to promote osteoblast differentiation, maturation and mineralization (45). However, the complexity of the interactions between these regulatory pathways and the abundance of *in vitro* reports investigating this interrelation in different osteogenic experimental set-ups, complicate its understanding (9;10;44;46-48). The most probable explanation for the wide variety of effects arising upon this interaction is that they represent different aspects of Wnt and BMP functions that are only visible in certain cell types, at specific developmental stages and under particular experimental conditions. Our results add insight to the complexity of interactions between Wnt/ $\beta$ -catenin and BMP signaling during the differentiation of SPC. *In vitro*, BMPs induce Wnt expression (8;49), whereas Wnt signaling induces BMP expression (46;50), suggesting that both Wnt and BMP signaling may jointly regulate each other in osteoblasts. In the KS483 cells, *Apc* knockdown upregulated not only transduction of the Wnt signal, but also the BMP signaling pathway, most likely via up-regulation of *Bmp7* expression. *APC* can

shuttle into and out of the nucleus (51;52), and thus a possible Apc-mediated interaction between Wnt and BMP may occur in any of these two subcellular locations. While in the nucleus the Smad/ $\beta$ -catenin/Lef protein complex regulates many shared target genes (53-55), in the cytoplasm, BMP can either impede or stimulate the canonical Wnt signal via Axin (10;56). Since Apc comprises both Axin and  $\beta$ -catenin binding domains, we speculate that Apc might link the Wnt/ $\beta$ -catenin to BMP signaling pathways during osteoblast differentiation of KS483 cells.

Our present results indicate that Apc is essential for osteogenic, chondrogenic and adipogenic differentiation of the murine mesenchymal-like KS483 cell line which has SPC-like characteristics. Our approach has provided a valuable model in which we demonstrate that levels of functional Apc must be tightly controlled for proper modulation of the transcriptionally active  $\beta$ -catenin and BMP-signaling dosage required for multilineage SPC-differentiation *in vitro*.

## ACKNOWLEDGEMENTS

*We are grateful to Prof. Dr. Peter ten Dijke (Department of Molecular Cell Biology, LUMC, Leiden, The Netherlands) for the pGL3-(BRE)<sub>2</sub>-Luc reporter construct; Dr. Stefano Piccolo (Department of Medical Biotechnologies, University of Padua, Italy) for the BAT-Luc reporter construct; and Prof. Dr. Bert Vogelstein (The Ludwig Center for Cancer Genetics and Therapeutics, Howard Hughes Medical Institute and Sidney Kimmel Cancer Center at the Johns Hopkins Medical Institutions, Baltimore, Maryland, USA) for the pSAR-MT-APC construct. We thank Prof. Dr. Slobodan Vukicevic, Department of Anatomy, School of Medicine, Zagreb, Croatia, for kindly providing BMP-6 and BMP-7 for our study.*

*This work was financially supported by an unrestricted educational grant from IP-SEN FARMACEUTICA BV to RLM.*

## REFERENCES

1. Karsenty G. The complexities of skeletal biology. *Nature* 2003; 423(6937):316-8.
2. Karsenty G, Kronenberg HM, Settembre C. Genetic control of bone formation. *Annu Rev Cell Dev Biol* 2009; 25:629-48.
3. Liu F, Kohlmeier S, Wang CY. Wnt signaling and skeletal development. *Cell Signal* 2008; 20(6):999-1009.
4. Clevers H. Wnt/beta-catenin signaling in development and disease. *Cell* 2006; 127(3):469-80.
5. Hartmann C. A Wnt canon orchestrating osteoblastogenesis. *Trends Cell Biol* 2006; 16(3):151-8.
6. Bessa PC, Casal M, Reis RL. Bone morphogenetic proteins in tissue engineering: the road from the laboratory to the clinic, part I (basic concepts). *J Tissue Eng Regen Med* 2008; 2(1):1-13.
7. ten Dijke P. Bone morphogenetic protein signal transduction in bone. *Curr Med Res Opin* 2006; 22 Suppl 1:57-11.
8. Chen Y, Whetstone HC, Youn A, Nadesan P, Chow EC, Lin AC et al. Beta-catenin signaling pathway is crucial for bone morphogenetic protein 2 to induce new bone formation. *J Biol Chem* 2007; 282(1):526-33.
9. Fischer L, Boland G, Tuan RS. Wnt signaling during BMP-2 stimulation of mesenchymal chondrogenesis. *J Cell Biochem* 2002; 84(4):816-31.
10. Liu Z, Tang Y, Qiu T, Cao X, Clemens TL. A dishevelled-1/Smad1 interaction couples WNT and bone morphogenetic protein signaling pathways in uncommitted bone marrow stromal cells. *J Biol Chem* 2006; 281(25):17156-63.
11. Chen M, Zhu M, Awad H, Li TF, Sheu TJ, Boyce BF et al. Inhibition of beta-catenin signaling causes defects in postnatal cartilage development. *J Cell Sci* 2008; 121(Pt 9):1455-65.
12. Yan Y, Tang D, Chen M, Huang J, Xie R, Jonason JH et al. Axin2 controls bone remodeling through the beta-catenin-BMP signaling pathway in adult mice. *J Cell Sci* 2009; 122(Pt 19):3566-78.
13. Miclea RL, Karperien M, Bosch CA, van der Horst G, van der Valk MA, Kobayashi T et al. Adenomatous polyposis coli-mediated control of beta-catenin is essential for both chondrogenic and osteogenic differentiation of skeletal precursors. *BMC Dev Biol* 2009; 9:26.
14. Kielman MF, Rindapaa M, Gaspar C, van Poppel N, Breukel C, van Leeuwen S et al. Apc modulates embryonic stem-cell differentiation by controlling the dosage of beta-catenin signaling. *Nat Genet* 2002; 32(4):594-605.
15. van der Horst G, van der Werf SM, Farih-Sips H, van Bezooijen RL, Lowik CW, Karperien M. Downregulation of Wnt signaling by increased expression of Dickkopf-1 and -2 is a prerequisite for late-stage osteoblast differentiation of KS483 cells. *J Bone Miner Res* 2005; 20(10):1867-77.

16. Miclea RL, Robanus-Maandag EC, Goeman JJ, Finos L, Bloys H, Löwik CW et al. Inhibition of GSK3- $\beta$  induces loss of the chondrocytic phenotype and cartilage matrix degradation through activation of canonical Wnt signaling. *Osteoarthritis Cartilage* 2011.
17. van der Horst G, Farih-Sips H, Lowik CW, Karperien M. Hedgehog stimulates only osteoblastic differentiation of undifferentiated KS483 cells. *Bone* 2003; 33(6):899-910.
18. van der Horst G, de Rooij KE, Hoogendam J, Sips HCM, Feitsma AL, Que I et al. Functional genomics, drug screening and biomaterial evaluation using mesenchymal progenitor cells. 2010.
19. Maretto S, Cordenonsi M, Dupont S, Braghetta P, Broccoli V, Hassan AB et al. Mapping Wnt/ $\beta$ -catenin signaling during mouse development and in colorectal tumors. *Proc Natl Acad Sci U S A* 2003; 100(6):3299-304.
20. Morin PJ, Vogelstein B, Kinzler KW. Apoptosis and APC in colorectal tumorigenesis. *Proc Natl Acad Sci U S A* 1996; 93(15):7950-4.
21. Jho EH, Zhang T, Domon C, Joo CK, Freund JN, Costantini F. Wnt/ $\beta$ -catenin/Tcf signaling induces the transcription of Axin2, a negative regulator of the signaling pathway. *Mol Cell Biol* 2002; 22(4):1172-83.
22. Korchynskiy O, ten Dijke P. Identification and functional characterization of distinct critically important bone morphogenetic protein-specific response elements in the Id1 promoter. *J Biol Chem* 2002; 277(7):4883-91.
23. Hanson CA, Miller JR. Non-traditional roles for the Adenomatous Polyposis Coli (APC) tumor suppressor protein. *Gene* 2005; 361:1-12.
24. Fodde R. The multiple functions of tumour suppressors: it's all in APC. *Nat Cell Biol* 2003; 5(3):190-2.
25. van Es JH, Giles RH, Clevers HC. The many faces of the tumor suppressor gene APC. *Exp Cell Res* 2001; 264(1):126-34.
26. Petersen CP, Bordeleau ME, Pelletier J, Sharp PA. Short RNAs repress translation after initiation in mammalian cells. *Mol Cell* 2006; 21(4):533-42.
27. Doench JG, Petersen CP, Sharp PA. siRNAs can function as miRNAs. *Genes Dev* 2003; 17(4):438-42.
28. Rao MK, Pham J, Imam JS, MacLean JA, Murali D, Furuta Y et al. Tissue-specific RNAi reveals that WT1 expression in nurse cells controls germ cell survival and spermatogenesis. *Genes Dev* 2006; 20(2):147-52.
29. Schneikert J, Behrens J. Truncated APC is required for cell proliferation and DNA replication. *Int J Cancer* 2006; 119(1):74-9.
30. van der Horst G, Farih-Sips H, Lowik CW, Karperien M. Multiple mechanisms are involved in inhibition of osteoblast differentiation by PTHrP and PTH in KS483 Cells. *J Bone Miner Res* 2005; 20(12):2233-44.
31. Nathke IS. The adenomatous polyposis coli protein: the Achilles heel of the gut epithelium. *Annu Rev Cell Dev Biol* 2004; 20:337-66.
32. Weeraratna AT, Jiang Y, Hostetter G, Rosenblatt K, Duray P, Bittner M et al. Wnt5a signaling directly affects cell motility and invasion of metastatic melanoma. *Cancer Cell* 2002; 1(3):279-88.



33. Haertel-Wiesmann M, Liang Y, Fantl WJ, Williams LT. Regulation of cyclooxygenase-2 and periostin by Wnt-3 in mouse mammary epithelial cells. *J Biol Chem* 2000; 275(41):32046-51.
34. Park KS, Jeon SH, Kim SE, Bahk YY, Holmen SL, Williams BO et al. APC inhibits ERK pathway activation and cellular proliferation induced by RAS. *J Cell Sci* 2006; 119(Pt 5):819-27.
35. Faux MC, Ross JL, Meeker C, Johns T, Ji H, Simpson RJ et al. Restoration of full-length adenomatous polyposis coli (APC) protein in a colon cancer cell line enhances cell adhesion. *J Cell Sci* 2004; 117(Pt 3):427-39.
36. Carson DJ, Santoro IM, Groden J. Isoforms of the APC tumor suppressor and their ability to inhibit cell growth and tumorigenicity. *Oncogene* 2004; 23(42):7144-8.
37. Ahmed Y, Hayashi S, Levine A, Wieschaus E. Regulation of armadillo by a Drosophila APC inhibits neuronal apoptosis during retinal development. *Cell* 1998; 93(7):1171-82.
38. Benchabane H, Ahmed Y. The adenomatous polyposis coli tumor suppressor and Wnt signaling in the regulation of apoptosis. *Adv Exp Med Biol* 2009; 656:75-84.
39. Gaspar C, Fodde R. APC dosage effects in tumorigenesis and stem cell differentiation. *Int J Dev Biol* 2004; 48(5-6):377-86.
40. Hartmann C. Transcriptional networks controlling skeletal development. *Curr Opin Genet Dev* 2009; 19(5):437-43.
41. Miclea RL, Karperien M, Langers AM, Robanus-Maandag EC, van Lierop A, van der Hiel B et al. APC mutations are associated with increased bone mineral density in patients with familial adenomatous polyposis. *J Bone Miner Res* 2010; 25(12):2348-56.
42. Holmen SL, Zylstra CR, Mukherjee A, Sigler RE, Faugere MC, Boussein ML et al. Essential role of beta-catenin in postnatal bone acquisition. *J Biol Chem* 2005; 280(22):21162-8.
43. Lavery K, Hawley S, Swain P, Rooney R, Falb D, Aoui-Ismaïli MH. New insights into BMP-7 mediated osteoblastic differentiation of primary human mesenchymal stem cells. *Bone* 2009; 45(1):27-41.
44. Mbalaviele G, Sheikh S, Stains JP, Salazar VS, Cheng SL, Chen D et al. Beta-catenin and BMP-2 synergize to promote osteoblast differentiation and new bone formation. *J Cell Biochem* 2005; 94(2):403-18.
45. Lian JB, Stein GS, Javed A, van Wijnen AJ, Stein JL, Montecino M et al. Networks and hubs for the transcriptional control of osteoblastogenesis. *Rev Endocr Metab Disord* 2006; 7(1-2):1-16.
46. Bain G, Muller T, Wang X, Papkoff J. Activated beta-catenin induces osteoblast differentiation of C3H10T1/2 cells and participates in BMP2 mediated signal transduction. *Biochem Biophys Res Commun* 2003; 301(1):84-91.
47. Kamiya N, Kobayashi T, Mochida Y, Yu PB, Yamauchi M, Kronenberg HM et al. Wnt Inhibitors Dkk1 and Sost are Downstream Targets of BMP Signaling Through the Type IA Receptor (BMPRIA) in Osteoblasts. *J Bone Miner Res* 2009.
48. Guo X, Wang XF. Signaling cross-talk between TGF-beta/BMP and other pathways. *Cell Res* 2009; 19(1):71-88.
49. Rawadi G, Vayssiere B, Dunn F, Baron R, Roman-Roman S. BMP-2 controls alkaline phosphatase expression and osteoblast mineralization by a Wnt autocrine loop. *J Bone Miner Res* 2003; 18(10):1842-53.

50. Winkler DG, Sutherland MS, Ojala E, Turcott E, Geoghegan JC, Shpektor D et al. Sclerostin inhibition of Wnt-3a-induced C3H10T1/2 cell differentiation is indirect and mediated by bone morphogenetic proteins. *J Biol Chem* 2005; 280(4):2498-502.
51. Henderson BR. Nuclear-cytoplasmic shuttling of APC regulates beta-catenin subcellular localization and turnover. *Nat Cell Biol* 2000; 2(9):653-60.
52. Neufeld KL, White RL. Nuclear and cytoplasmic localizations of the adenomatous polyposis coli protein. *Proc Natl Acad Sci U S A* 1997; 94(7):3034-9.
53. Labbe E, Letamendia A, Attisano L. Association of Smads with lymphoid enhancer binding factor 1/T cell-specific factor mediates cooperative signaling by the transforming growth factor-beta and wnt pathways. *Proc Natl Acad Sci U S A* 2000; 97(15):8358-63.
54. Theil T, Aydin S, Koch S, Grotewold L, Ruther U. Wnt and Bmp signalling cooperatively regulate graded Emx2 expression in the dorsal telencephalon. *Development* 2002; 129(13):3045-54.
55. Hussein SM, Duff EK, Sirard C. Smad4 and beta-catenin co-activators functionally interact with lymphoid-enhancing factor to regulate graded expression of Msx2. *J Biol Chem* 2003; 278(49):48805-14.
56. Tang Y, Liu Z, Zhao L, Clemens TL, Cao X. Smad7 stabilizes beta-catenin binding to E-cadherin complex and promotes cell-cell adhesion. *J Biol Chem* 2008; 283(35):23956-63.



# Chapter 5

## **APC mutations are associated with increased bone mineral density in patients with familial adenomatous polyposis**

R.L. Miclea<sup>1</sup>, M. Karperien<sup>2</sup>, A.M. Langers<sup>3</sup>, E.C. Robanus-Maandag<sup>4</sup>, A. van Lierop<sup>5</sup>, B. van der Hiel<sup>6</sup>, M.P. Stokkel<sup>6</sup>, B.E. Ballieux<sup>7</sup>, W. Oostdijk<sup>1</sup>, J.M. Wit<sup>1</sup>, H.F. Vasen<sup>3</sup>, N.A. Hamdy<sup>5</sup>

<sup>1</sup>Department of Pediatrics, Leiden University Medical Centre (LUMC), Leiden, The Netherlands, <sup>2</sup>MIRA Institute for Biomedical Technology and Technical Medicine, Department of Tissue Regeneration, University of Twente, Enschede, The Netherlands, <sup>3</sup>Department of Gastroenterology, LUMC, Leiden, The Netherlands, <sup>4</sup>Department of Human Genetics, LUMC, Leiden, The Netherlands, <sup>5</sup>Department of Endocrinology and Metabolic Diseases, LUMC, Leiden, The Netherlands, <sup>6</sup>Department of Nuclear Medicine, LUMC, Leiden, The Netherlands, <sup>7</sup>Department of Clinical Chemistry, LUMC, Leiden, The Netherlands

J Bone Miner Res 2010; 25(12):2348-56.



# **APC mutations are associated with increased bone mineral density in patients with familial adenomatous polyposis**

R.L. Miclea, M. Karperien, A.M. Langers, E.C. Robanus-Maandag, A. van Lierop, B. van der Hiel, M.P. Stokkel, B.E. Ballieux, W. Oostdijk, J.M. Wit, H.F. Vasen, N.A. Hamdy

## **ABSTRACT**

The canonical Wnt pathway plays a key regulatory role in osteoblastogenesis and bone mass acquisition through its main effector,  $\beta$ -catenin. Adenomatous polyposis coli (APC) represents the key intracellular gate-keeper of  $\beta$ -catenin turnover and heterozygous germline mutations in the *APC* gene cause familial adenomatous polyposis (FAP). Whether *APC* mutations affect bone mass has not been previously investigated. We conducted a cross-sectional study evaluating skeletal status in FAP patients with a documented *APC* mutation. Twenty-two FAP patients with a mean age of 42 years (54.5% women) were included in this study. Mean BMD Z-scores were significantly increased above normal at all measured sites: lumbar spine ( $p < 0.01$ ), total hip ( $p < 0.01$ ), femoral neck ( $p < 0.05$ ) and trochanter ( $p < 0.01$ ). Z-scores were  $\geq +1$  in 14 patients (63.6%) and  $\geq +2$  in 5 patients (22.7%). Mean values of bone turnover markers were within normal ranges. There was a significant positive correlation between Procollagen type I N-terminal propeptide (P1NP) and  $\beta$ -crosslaps ( $\beta$ -CTX) ( $r = 0.70$ ;  $p < 0.001$ ). Total hip BMD was positively correlated with P1NP ( $r = 0.37$ ;  $p = 0.084$ ),  $\beta$ -CTX ( $r = 0.59$ ;  $p < 0.01$ ) and sclerostin ( $r = 0.56$ ;  $p < 0.01$ ). We demonstrate that FAP patients display a significantly higher than normal mean BMD compared to age- and sex-matched healthy controls in the presence of a balanced bone turnover. Our data suggest a state of “controlled” activation of the Wnt signalling pathway in heterozygous carriers of *APC* mutations, most likely due to upregulation of  $\beta$ -catenin.

## INTRODUCTION

Familial adenomatous polyposis (FAP) is an autosomal dominant syndrome caused by heterozygous germline mutations in the *APC* gene. Occurring in approximately 1:10,000 live births, FAP is characterized by the development of hundreds to thousands of colorectal adenomatous polyps during childhood and adolescence (1). The adenomas inevitably progress to colorectal carcinoma (CRC) at a mean age of 40-50 years, if colectomy is not performed (2). FAP is also associated with an increased risk of extracolonic malignancies (e.g., duodenal, pancreatic, and thyroid cancer) and other pathologic conditions, such as osteomas, dental anomalies, epidermoid cysts, lipomas, desmoid tumors, and congenital hypertrophy of the retinal pigment epithelium (CHRPE) (3). Whereas the majority of FAP patients have a family history of the disease, up to 30% of cases are due to *de novo* mutations in the *APC* gene (4). Genetic analysis identifies gene inactivating mutations within the *APC* gene in more than 70% of cases (1).

The *APC* tumor suppressor gene is located on chromosome 5q21-q22 and consists of 15 exons that encode a large multifunctional protein product (312kDa, 2843 codons), known to be involved in a broad spectrum of cellular processes such as cell cycle regulation, apoptosis, cell adhesion and migration, microtubule assembly, cell fate determination, and chromosomal stability (5). However, *APC*'s main tumor suppressor function is to bind to and to down-regulate the key transducer of the canonical Wnt signaling pathway,  $\beta$ -catenin, thereby acting as a strong negative regulator of the Wnt signaling cascade (6;7). The efficiency of mutant *APC* to downregulate  $\beta$ -catenin is compromised according to the site of the mutation (8). As a result,  $\beta$ -catenin accumulates in the cytoplasm and subsequently translocates into the nucleus, where it stimulates transcription of Wnt target genes leading to increased cell proliferation and decreased apoptosis (6).

Over the past decade, evidence has accumulated about the important role of  $\beta$ -catenin in the regulation of bone mass and in the pathophysiology of a number of skeletal disorders (9). Since *APC* represents a critical regulator of  $\beta$ -catenin levels, it is not surprising that FAP patients carrying mutations in the *APC* gene commonly develop diverse skeletal pathology including osteomas and/or dental anomalies such as supernumerary and impacted teeth (10). Several *in vivo* and *in vitro* studies further support the role of *APC* in both skeletal development and metabolism. Inactivation of *Apc* in skeletal progenitor cells has been shown to lead to an osteosclerotic bone phenotype, due to the formation of highly active osteoblasts (11), whereas inactivation of *Apc* in mature osteoblasts results in an osteopetrotic bone phenotype, due to impaired osteoclast differentiation (12). Interestingly, it has been reported that mice carrying a heterozygous loss-of-function mutation in *Apc* (*Apc*<sup>min/+</sup>) display a significantly increased BMD of the distal femur (13). Taken together, these data strongly imply that *APC* might be involved in the regulation of bone mass by regulating the cytoplasmic levels of  $\beta$ -catenin.

FAP patients carry heterozygous *APC* mutations that result in a constitutively active transduction of  $\beta$ -catenin. We hypothesized, therefore, that FAP may represent a valuable human model for studying the role of the canonical Wnt signaling pathway in bone mass acquisition and maintenance. In this study we addressed the question whether heterozygous mutations in the *APC* gene are associated with alterations in bone mass and/or bone turnover.

## MATERIALS AND METHODS

### Study population

Thirty consecutive FAP patients attending the Outpatient Clinic of the Department of Gastroenterology of the Leiden University Medical Centre (LUMC) for routine follow-up visits over a 6-month calendar period were invited to take part in the study. The inclusion criteria were a clinically established, histologically documented, and genetically confirmed diagnosis of FAP and the willingness of the patient to participate in the study. The only exclusion criterion was the current or past use of any agent known to affect bone metabolism such as bisphosphonates or parathyroid hormone (PTH). The study was approved by the Ethics Committee of the LUMC, and written informed consent was obtained from all patients.

### Demographic and clinical characteristics

Demographic characteristics including age, gender, ethnicity, body weight, height, body mass index (BMI), menopausal status, smoking habits, and alcohol use were documented in all patients. Other data collected were family history of FAP, age at diagnosis, history of colectomy, age at colectomy, extra-colonic manifestations, dental and fracture history, and use of medication. To allow for comparison between different ages and genders, height was expressed as standard deviation score (SDS) corrected for shrinking and secular trend (14).

### BMD measurements

BMD was measured in all patients at the lumbar spine (L1-L4) and at different sites of both hips (total hip, femoral neck, and trochanter) using dual X-ray absorptiometry (DXA) (Hologic QDR-4500, Hologic Inc.). Mean BMD of the left and right hip was used for analysis. Data were expressed as T-scores (number of SDs from the mean value of the sex-matched reference population) and Z-scores (number of SDs from the mean value of the age- and sex-matched reference population) using the NHANES reference values, which are compatible with those of Dutch control populations (15-17). Standard WHO reference values established for BMD measurements were used to define osteopenia ( $-2.5 < T\text{-score} \leq -1$ ) and osteoporosis ( $T\text{-score} \leq -2.5$ ) (18). In our analysis, we considered "low" BMD if  $Z\text{-score} \leq -1$ , "normal" BMD if  $-1 < Z\text{-score} < +1$  and "higher than normal" BMD if  $Z\text{-score} \geq +1$ . The coefficient of variation (CV) of BMD measurements was 1% and the machine was cross-calibrated at regular intervals using a validated phantom.



### **Vertebral fracture assessment (VFA)**

Since vertebral compression fractures may increase lumbar BMD and since these may be clinically silent, we additionally performed vertebral fracture assessment (VFA) to assess the morphology of vertebrae at the lumbar spine (L1–L5). Paired anteroposterior and lateral VFA images were examined by a nuclear medicine physician who was blinded to the DXA results. The Genant's semiquantitative method was used to visually assess abnormal vertebral morphology (AVM) (19). Using this method, grade 1 vertebral deformity (mild) was judged to be present when an anterior, posterior or middle reduction in vertebral height of 20–25% was observed, grade 2 (moderate) when a reduction of 26–40% was observed and grade 3 (severe) when a reduction greater than 40% was observed. Standard paired anteroposterior and lateral radiographs of the thoracic and lumbar spine were performed when AVM was suggested by VFA.

### **Skeletal scintigraphy**

Since scintigraphy is more sensitive than conventional radiographs in the diagnosis of osteomas (20–22) and since the area of uptake on scintigraphy may extend beyond the limits of any radiographic change (22), we used radionuclide imaging to detect this focal bone pathologic condition in our study. Whole body scintigraphy was performed using a standard protocol of images on a dual-headed Toshiba gammacamera (Toshiba CGA 7200, Japan). Anterior and posterior views were acquired 3 hours after injection of 500 MBq (13.5 mCi) of Tc-99m-HDP. Osteomas were considered to be present when a pattern of focally intense tracer uptake surrounded by less prominent increase uptake was visualized. All scintigraphy scans were visually analysed by an independent experienced nuclear medicine physician.

### **Laboratory investigations**

Blood was collected from all patients between 8.00 and 10.00 a.m. after an overnight fast. Serum was used to measure calcium (corrected for an albumin of 42 g/l), phosphate (P), and total alkaline phosphatase (ALP) activity using semi-automated techniques. Serum 25-hydroxyvitamin D (25-OH-D), 1,25-dihydroxyvitamin D (1,25-(OH)<sub>2</sub>-D<sub>3</sub>), PTH, follicle-stimulating hormone (FSH), luteinizing hormone (LH), estrogen (E), testosterone (T), procollagen type I N-terminal propeptide (P1NP), and  $\beta$ -crosslaps ( $\beta$ -CTX) concentrations (respectively markers of bone formation and resorption) were measured using standard radio-immuno-assays (RIA). Vitamin D levels were not corrected for seasonal variation. Vitamin D insufficiency was diagnosed when 25-OH-D concentration was < 50 nmol/l (23). Hypogonadism was defined in men by a serum T concentration < 10 nmol/l and in women by a serum E concentration < 70 pmol/l in the absence of menstrual cycles, associated in both men and women with FSH and LH concentrations > 30 U/l and > 60 U/l, respectively. Additional blood samples were collected at the same time, immediately centrifuged and serum was separated and stored at -80°C for later measurement of sclerostin. This was performed using a solid phase sandwich immunoassay following an in-house protocol on a Sector Imager 2400 platform (Meso Scale Discovery) with a minimum detection limit of 1 pg/ml.

### Statistical analysis

Statistical analysis was performed using the SPSS 16.0 for Windows software package. The number of patients needed to demonstrate a significant effect of *APC* mutations on BMD was statistically determined using a power (1-beta) of 80% and an alpha level of 5%. Under the assumption that the FAP group may demonstrate a 10% increase in BMD, the number of patients needed to be studied to show this effect was calculated to be 20 patients in this single-centre observational cross-sectional study.

All descriptive parameters are expressed as mean  $\pm$  standard deviation (SD) or as numbers and percentages of patients within groups, as appropriate. Categorical variables are presented as frequency and percentage and compared using the Chi-square test. One-sample t-tests were used to compare BMD T- and Z-scores with normal scores. One way ANOVA was used to compare the mean values of several variables between groups. Pearson scores (*r*) were calculated to determine correlation between BMD and different clinical and biochemical variables. A *p* value  $< 0.05$  was considered to be statistically significant.

## RESULTS

### Patients

Of the 30 consecutive FAP patients invited to take part in the study, 4 were not included because a mutation in the *APC* gene could not be identified on DNA analysis, 3 declined to participate in the study and 1 was excluded because of bisphosphonate use. All remaining 22 patients fulfilled the study inclusion criteria and were included in the study.

### Demographic, clinical and genetic characteristics

The demographic, clinical and genetic characteristics of the 22 patients (10 men and 12 women) included in the study are shown in Table 1. Mean age was  $42 \pm 12$  (SD) years. Twenty patients (90.9%) were Caucasian. Four of the 12 women (33.3%) were postmenopausal not using hormone replacement therapy. Mean height SDS was  $-0.50 \pm 1.33$ . Mean BMI was  $27.0 \pm 5.0$  kg/m<sup>2</sup>. None of the patients used excessive alcohol, 7 (31.8%) were former smokers and 6 (27.2%) were smoking an average of 12 cigarettes per day at the time of the study. All patients reported a positive family history for FAP, indicating that none of their mutations were *de novo* mutations. Mean age at diagnosis was 21 years, ranging from 6 to 47 years. All patients but one (95.5%) had undergone prophylactic colectomy at a mean age of  $23 \pm 11$  years. Typical of the FAP syndrome, we documented non-skeletal extra-colonic manifestations in several patients: single or multiple fibroma(s) in 3 patients (13.6%), epidermoid cysts in 4 patients (18.2%), and desmoid tumors in 4 patients (18.2%). Seven patients (31.8%) reported dental anomalies such as impacted teeth (other than third molars), congenitally missing teeth, and/or supernumerary teeth. None of the patients reported a history of low-energy trauma fracture or a clinically manifest vertebral fracture.

Parameters	Values
<b><i>Demographic characteristics</i></b>	
Age (years)*	42 ± 12 (21-60)
Ethnicity (Caucasian/non-Caucasian) †	20 (90.9) / 2 (9.0)
Female gender ‡	12 (54.5)
Menopause#	4 (33.3)
Height (SDS)*	-0.50 ± 1.33 (-2.94-1.71)
Weight (kg)*	79.4 ± 18.3 (42.4-120.9)
Body mass index (kg/m <sup>2</sup> )*	27.0 ± 5.0 (17.9-37.7)
Smoking status (never/former/current) †	9 (40.9) / 7 (31.8) / 6 (27.2)
<b><i>Clinical characteristics</i></b>	
Family history of FAP ‡	22 (100)
Age at diagnosis (years)*	21 ± 10 (6-47)
Colectomy ‡	21 (95.5)
Age at colectomy (years)*	23 ± 11 (13-51)
Fibromas ‡	3 (13.6)
Epidermoid cysts ‡	4 (18.2)
Desmoid tumor ‡	4 (18.2)
Teeth anomalies (current or in the past) †	7 (31.8)
Clinical fractures ‡	0 (0)
<b><i>APC mutation</i></b>	
c.609 insA ‡	1 (4.5)
c.697C>T ‡	1 (4.5)
c.1548G>C ‡	1 (4.5)
c.1744-2A>G splice acceptor defect †	3 (13.6)
c.1958+1_1958+2dupGT ‡	2 (9.0)
c.1972_1975delGAGA ‡	1 (4.5)
c.2805C>A ‡	3 (13.6)
c.2864_2865delAA ‡	2 (9.0)
c.3164_3168delTAATA ‡	1 (4.5)
c.3183_3187delACAAA ‡	1 (4.5)
c.3927_3931delAAAGA ‡	1 (4.5)
c.4069G>T ‡	1 (4.5)
c.4348C>T ‡	2 (9.0)
c.4786delC ‡	2 (9.0)

**Table 1. Demographic, clinical and genetic characteristics of the 22 FAP patients included.** Results are expressed as \*mean ± SD (min-max), †n (%) or #n (valid %).

The 14 different heterozygous mutations in the *APC* gene identified in our study population included 6 deletions, 6 base substitutions, one insertion, and one duplication. Although none of the identified *APC* mutations were located in the same functional domain, most were clustered in exon 15 of the *APC* gene (Figure 1).

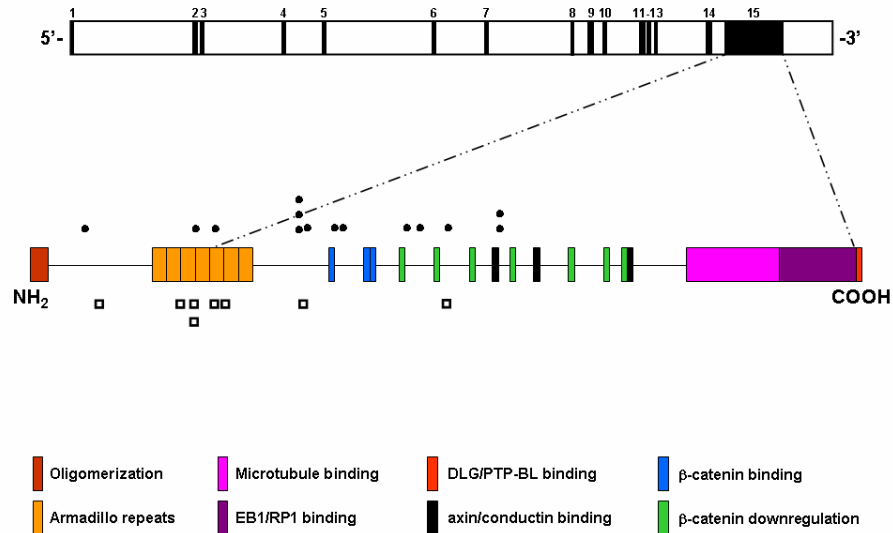


**Figure 1.** Diagram of the *APC* gene (upper bar) comprising 15 exons and the location of the mutations found in our study population (black dots = patients with BMD Z-scores  $\geq +1$ , black squares = patients with BMD Z-scores  $< +1$ ) in relation to the functional domains of the APC protein (lower bar). Of note is the clustering of *APC* mutations found in patients with BMD Z-score  $\geq +1$  among the  $\beta$ -catenin binding/downregulating domains.

### Bone mineral density measurements

BMD data are shown in Table 2 and Figure 2. None of the patients had osteoporosis at any of the sites measured. Osteopenia was present at the lumbar spine in a 58-year-old man (T-score = -1.2) and in a 52-year-old postmenopausal woman (T-score = -2.4), and at the total hip in 2 premenopausal women (T-score = -1.1). None of the patients included in the study had osteopenia at more than one site.

Mean BMD Z-scores were significantly increased above normal (Z-score  $> 0$ ) at all sites measured:  $+0.8 \pm 1.2$  in the lumbar spine ( $p < 0.01$ ),  $+0.7 \pm 1.1$  in the total hip ( $p < 0.01$ ),  $+0.5 \pm 1.0$  in the femoral neck ( $p < 0.05$ ), and  $+1.1 \pm 1.3$  in the trochanter ( $p < 0.01$ ). From the total of 22 patients investigated, 14 patients (63.6%) had BMD Z-scores  $\geq +1$  and 5 patients had a Z-score  $\geq +2$  at one or more sites measured.

### Assessment of vertebral morphology of the lumbar spine

On visual analysis of VFA images of the lumbar spine (L1-L5), mild abnormal vertebral morphology (AVM) was observed in 3 male patients. The AVM observed by VFA was confirmed by standard radiographs in only 2 of the patients in whom it was attributed to vertebral osteochondrosis and degenerative changes respectively. Both these patients had a history of back pain and a normal lumbar BMD. AVM observed on VFA was not confirmed by standard radiography in the 3<sup>rd</sup> patient who had a lumbar BMD Z-score  $> +2$ . The finding of higher than normal Z-scores on lumbar BMD assessment

was thus deemed to be reliable. There was no statistically significant demographic, clinical and laboratory difference between patients with and without AVM.

<b>Bone mineral density</b>	<b>Mean <math>\pm</math> SD (min-max)</b>
<b><i>Lumbar spine (L1-L4)</i></b>	
g/cm <sup>2</sup>	1.123 $\pm$ 0.168 (0.790-1.460)
T-score	+0.5 $\pm$ 1.4 (-2.4-3.4)
Z-score	+0.8 $\pm$ 1.2 (-1.5-3.6)**
<b><i>Total hip</i></b>	
g/cm <sup>2</sup>	1.051 $\pm$ 0.194 (0.811-1.508)
T-score	+0.4 $\pm$ 1.2 (-1.0-3.2)
Z-score	+0.7 $\pm$ 1.1 (-1.0-3.2)**
<b><i>Femoral neck</i></b>	
g/cm <sup>2</sup>	0.899 $\pm$ 0.161 (0.695-1.280)
T-score	+0.0 $\pm$ 1.2 (-1.4-2.6)
Z-score	+0.5 $\pm$ 1.0 (-1.3-2.6)*
<b><i>Trochanter</i></b>	
g/cm <sup>2</sup>	0.841 $\pm$ 0.177 (0.629-1.242)
T-score	+0.9 $\pm$ 1.3 (-0.7-3.7)**
Z-score	+1.1 $\pm$ 1.3 (-0.7-3.7)**

**Table 2. BMD measurements of the 22 FAP patients included.** \*p<0.05, \*\*p<0.01 one sample t-test compared to normal scores

### **Skeletal scintigraphy**

Single or multiple foci of increased radioisotope tracer uptake, consistent with the presence of an osteoma, were observed in 13 patients (59.0%). Mean number of foci was 1.85  $\pm$  0.55 per patient. The most common localization of osteomas was craniofacial, where 10 patients (76.9%) demonstrated single or multiple foci of increased tracer uptake, particularly in the mandible or maxilla. One patient displayed scintigraphic signs of osteoma in the knees, 1 in both the mandible and the clavicle and 1 in a cervical vertebra. There was no statistically significant difference in mean age between patients with or without osteoma(s) (39  $\pm$  13 years vs. 45  $\pm$  8 years; p = 0.238). There was a trend of an association between the presence of teeth anomalies and scintigraphic evidence for osteoma(s) (odds ratio = 4.1; 95%CI, 0.5 to 28.8; p = 0.083).

### **Laboratory investigations**

Mean laboratory values of all parameters investigated were within the normal laboratory reference ranges (Table 3). Of the 12 patients (60%) with 25-OH-D insufficiency, 2 had increased PTH concentrations in the presence of normal BMD in both the lumbar spine and the hips. None of the patients studied had evidence for hypogonadism, except for the 4 postmenopausal women.

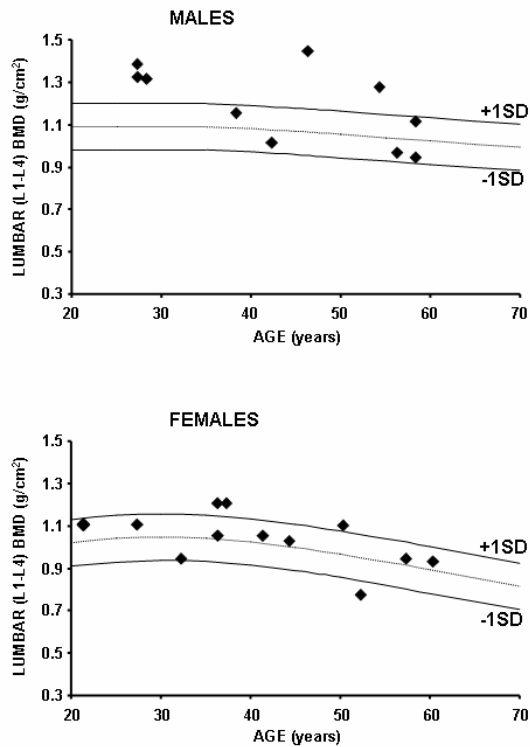


**Figure 2.** Lumbar BMD values in all FAP patients included in the study plotted against the NHANES normative data (upper graph - males, lower graph - females).

None of the patients included in the study had serum ALP activity above normal. Since both markers of bone turnover P1NP and  $\beta$ -CTX display different reference values according to gender and menopausal status, we expressed the measured values of these 2 bone turnover markers as a multiple of the upper limit of the normal reference (X ULN) (24-27). While mean P1NP was normal for the whole population ( $0.72 \pm 0.28$  X ULN), 5 patients (22.7%) had a P1NP value above the ULN. Two of these patients exhibited normal BMD, while the other 3 had higher than normal BMD. Similarly, mean  $\beta$ -CTX was normal for the whole population ( $0.60 \pm 0.37$  X ULN), with only 2 patients (9%) having  $\beta$ -CTX values above the ULN in the presence of higher than normal BMD. Interestingly, these 2 patients also had P1NP values above the ULN. Mean sclerostin ( $n = 20$ ) was  $38.32 \pm 23.33$  pg/ml, with 1 patient (5%) showing a concentration above the upper limit of the reference range (10.5-71.3 pg/ml). This patient showed higher than normal BMD at the lumbar spine and total hip, as well as levels of P1NP and  $\beta$ -CTX levels above the ULN.

Parameters	Mean $\pm$ SD (min-max)	Reference values
Corrected Ca for Alb	2.23 $\pm$ 0.09 (2.12-2.57)	2.15-2.55
P	1.14 $\pm$ 0.16 (0.83-1.49)	0.9-1.5
25-OH-D	52.5 $\pm$ 16.3 (27-78)	50-120
1,25-(OH) <sub>2</sub> -D3	94.5 $\pm$ 36.0 (30-174)	40-140
PTH	4.8 $\pm$ 2.0 (0.4-8.9)	1.5-8
ALP	73.6 $\pm$ 23.1 (36.2-118.3)	40-120
P1NP		
whole group (*ULN)	0.72 $\pm$ 0.28 (0.26-1.29)	
men + premenop. women	46.5 $\pm$ 15.7 (19.3-76.3)	<59
postmenop. women	31.4 $\pm$ 9.8 (19.8-42.7)	<76
$\beta$ -CTX		
whole group (*ULN)	0.60 $\pm$ 0.37 (0.16-1.81)	
men < 50 years	0.545 $\pm$ 0.294 (0.27-1.06)	<0.584
men 50 - 70 years	0.312 $\pm$ 0.087 (0.18-0.37)	<0.704
men > 70 years	NA	<0.854
women < 50 years	0.335 $\pm$ 0.142 (0.16-0.56)	<0.573
women > 50 years	0.294 $\pm$ 0.150 (0.17-0.51)	<1.008
Sclerostin (n=20)	38.32 $\pm$ 23.33 (23.1-129.3)	10.5-71.3

**Table 3. Laboratory investigations of the 22 FAP patients included.** Key: Ca, Calcium (mmol/l); Alb, Albumin; P, Phosphate (mmol/l); 25-OH-D, 25-hydroxyvitamin D (nmol/l); 1,25-(OH)<sub>2</sub>-D3, 1,25-dihydroxyvitamin D3 (pmol/l); PTH, parathyroid hormone (pmol/l); ALP, Alkaline Phosphatase (U/l); P1NP, procollagen type 1 amino-terminal propeptide (ng/ml); ULN, upper limit of normal;  $\beta$ -CTX, beta-crosslaps (ng/ml); Sclerostin (pg/ml).

### Correlations between markers of bone turnover and BMD

P1NP was significantly correlated with  $\beta$ -CTX ( $r^2 = 0.49$ ;  $p < 0.001$ ), and lumbar BMD was significantly correlated with total hip BMD ( $r^2 = 0.53$ ;  $p < 0.001$ ). Total hip BMD further correlated with  $\beta$ -CTX ( $r^2 = 0.34$ ;  $p < 0.01$ ) and with sclerostin ( $r^2 = 0.31$ ;  $p < 0.01$ ) and lumbar BMD correlated with sclerostin ( $r^2 = 0.24$ ;  $p < 0.05$ ). Although not reaching statistical significance we also found a trend towards a correlation of P1NP with total hip BMD ( $r^2 = 0.13$ ;  $p = 0.084$ ) and with sclerostin ( $r^2 = 0.16$ ,  $p = 0.068$ ).

### Potential determinants of increased BMD in FAP patients

To find possible explanations for the increased mean BMD observed in our study population, we took a closer look at the subgroup of patients characterized by BMD Z-scores  $\geq +1$  at one or more sites measured ( $n = 14$ ). None of the patients had any particular anthropometric, physical activity, lifestyle, dietary or pharmacological factors that might have contributed to an increase in BMD. Patients with a Z-score  $\geq +1$  showed a significant correlation between lumbar BMD and total hip BMD ( $r^2 = 0.36$ ;  $p < 0.05$ ), and between P1NP and  $\beta$ -CTX concentrations ( $r^2 = 0.58$ ;  $p < 0.01$ ). Lumbar BMD significantly correlated with sclerostin concentrations ( $r^2 = 0.37$ ;  $p < 0.05$ ), and total hip BMD correlated with P1NP ( $r^2 = 0.41$ ;  $p < 0.05$ ),  $\beta$ -CTX ( $r^2 = 0.60$ ;  $p < 0.01$ ) and sclerostin concentrations ( $r^2 = 0.47$ ;  $p < 0.05$ ).

There was no significant difference between patients with Z-scores  $\geq +1$  and the remainder of the patients included in our study in any demographic, clinical or laboratory characteristics (Table 4). There was also no significant difference between the P1NP- $\beta$ -CTX regression lines when comparing these 2 groups (Figure 3).

Characteristic	Z-score $\geq +1$	Z-score $< +1$	P value
<b>Demographic</b>			
Number of patients	14	8	
Age (years)*	40 $\pm$ 11	45 $\pm$ 12	0.377
Caucasian ethnicity <sup>‡</sup>	13 (92.8)	7 (87.5)	0.674
Female gender <sup>‡</sup>	6 (42.8)	6 (75)	0.145
Menopause <sup>#</sup>	2 (33.3)	2 (33.3)	0.346
Height (SDS)*	-0.2 $\pm$ 1.0	-1.0 $\pm$ 1.7	0.196
Body mass index (kg/m <sup>2</sup> )*	27.5 $\pm$ 4.5	26.0 $\pm$ 6.0	0.513
<b>Clinical</b>			
Family history of FAP <sup>‡</sup>	14 (100)	8 (100)	-
Age at diagnosis (years)*	20 $\pm$ 9	24 $\pm$ 12	0.462
Colectomy <sup>‡</sup>	13 (92.8)	8 (100)	0.439
Age at colectomy (years)*	22 $\pm$ 11	26 $\pm$ 10	0.477
Fibromas <sup>‡</sup>	2 (14.2)	1 (12.5)	0.907
Epidermoid cysts <sup>‡</sup>	3 (21.4)	1 (12.5)	0.601
Desmoid tumor <sup>‡</sup>	4 (28.5)	0 (0)	0.095
Teeth anomalies <sup>‡</sup>	3 (21.4)	4 (50)	0.166
Osteomas by scintigraphy <sup>‡</sup>	8 (57.1)	5 (62.5)	0.806
Abnormal vertebral morphology <sup>‡</sup>	2 (14.2)	0 (0)	0.262
<b>Serum biochemistry</b>			
Corrected Ca for Alb*	2.25 $\pm$ 0.10	2.21 $\pm$ 0.04	0.368
P*	1.13 $\pm$ 0.17	1.15 $\pm$ 0.16	0.836
25-OH-D*	54.6 $\pm$ 15.5	48.8 $\pm$ 18.2	0.440
PTH*	4.83 $\pm$ 2.12	4.96 $\pm$ 1.96	0.890
ALP*	74.5 $\pm$ 26.0	72.0 $\pm$ 18.4	0.808
P1NP*	0.73 $\pm$ 0.30	0.70 $\pm$ 0.26	0.835
$\beta$ -CTX*	0.65 $\pm$ 0.44	0.51 $\pm$ 0.20	0.425
Sclerostin*	40.8 $\pm$ 29.3	34.4 $\pm$ 9.6	0.561

**Table 4. Demographic, clinical and biochemical characteristics of patients grouped according to BMD Z-score values.** Results are expressed as \*mean  $\pm$  SD (min-max), <sup>‡</sup>n (%), <sup>#</sup>n (valid %). Key: Ca, Calcium (mmol/l); Alb, Albumin; P, Phosphate (mmol/l); 25-OH-D, 25-hydroxyvitamin D (nmol/l); PTH, parathyroid hormone (pmol/l); ALP, Alkaline Phosphatase (U/l); P1NP, procollagen type 1 amino-terminal propeptide (\*ULN);  $\beta$ -CTX, beta-crosslaps (\*ULN); ULN, upper limit of normal; Sclerostin (pg/ml).



Interestingly, mutations found in patients with BMD Z-score  $\geq +1$  were predominantly located among the  $\beta$ -catenin binding/downregulating domains, while the majority of the mutations found in patients with BMD Z-score  $< +1$  were found among the Armadillo repeats of the APC protein.

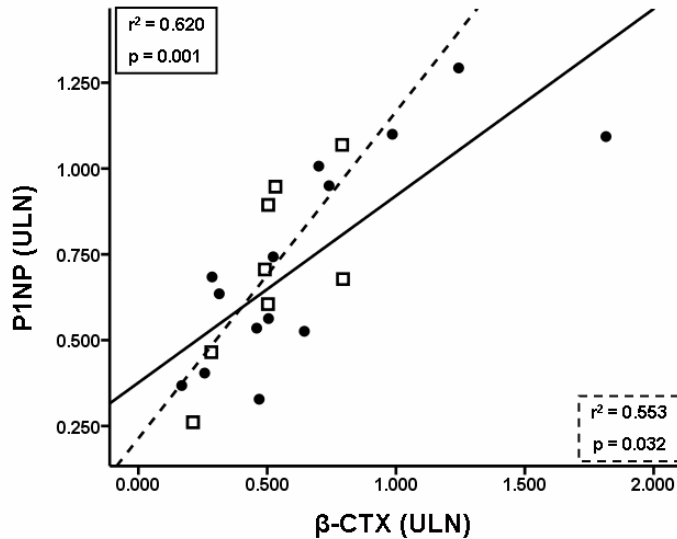


**Figure 3. Correlations between P1NP (ULN) and  $\beta$ -CTX (ULN) fitted to the linear model.** Black dots indicate patients ( $n = 14$ ; 63.6%) with BMD Z-scores  $\geq +1$  at one or more sites measured, and empty black squares indicate the rest of the patients ( $n = 8$ ; 36.3%). The continuous fit line indicates correlation for the “higher than normal” BMD group (BMD Z-scores  $\geq +1$  at one or more sites measured), with its correlation coefficient and  $p$  value in the upper left corner of the graph. The dotted fit line indicates correlation for the other patients, with their correlation coefficient and  $p$  value in the lower right corner of the graph.

## DISCUSSION

To our knowledge this is the first systematic evaluation of bone and mineral metabolism in FAP patients carrying heterozygous mutations in the APC gene. Our data show that these patients display a statistically significant higher mean BMD than age- and sex-matched controls. Seventeen of the 22 patients studied (77.3%) had consistently higher BMD values than the mean for age and sex-matched controls (Z-score  $> 0$ ), 14 patients (63.6%) had Z-scores  $\geq +1$  and 5 patients (27.2%) had Z-scores  $\geq +2$  at one or more sites measured. Our only inclusion criterion for the study was a clinical, histological and genetically confirmed FAP, and our sole exclusion criterion was the use of bone modulating agents that may positively influence bone mass. FAP patients were thus included in the study regardless of age, gender or severity of disease manifesta-

tions. Although heterogeneous, our study population was representative of FAP patients, since all clinical findings (colonic and extracolonic manifestations) were present in proportions previously reported in other FAP cohorts (1;28). In our study population, mean P1NP and  $\beta$ -CTX concentrations were within the normal ranges and were significantly positively correlated. Both these markers were also positively correlated with BMD. These results suggest that heterozygous inactivating *APC* mutations have a moderately positive effect on bone mass accrual, by a mechanism probably involving decreased  $\beta$ -catenin degradation. In keeping with published literature (reviewed in 1), we also observed a high prevalence of focal bone pathology, such as osteomas and teeth anomalies, in our study population. Whereas a positive correlation was found between the prevalence of these two focal pathologies, we detected no correlation between these anomalies and increased BMD. This finding suggests that the two phenotypes observed, the increased BMD on one hand, and the focal bone pathology on the other hand, are likely to occur as a result of independent molecular mechanisms.

It is well established that the canonical Wnt signaling pathway plays a key regulatory role in osteoblastogenesis and in bone mass accrual (29). Activation of this signaling cascade promotes osteoblast differentiation from progenitor cells and enhances bone mass acquisition via  $\beta$ -catenin, while suppression of this pathway results in bone loss. Alteration of several intracellular and extracellular controllers of the levels of transduced Wnt/ $\beta$ -catenin signaling has indeed been linked to disturbed skeletal homeostasis (30-34). Using murine conditional genetic models, we and others have shown that *Apc* is involved in the regulation of both prenatal and postnatal bone mass accrual by regulating the levels of Wnt/ $\beta$ -catenin signaling (11;12). Our present study confirms findings from these *in vivo* animal studies by demonstrating that heterozygous mutations in the *APC* gene are associated with a higher than normal bone mass in a majority of FAP patients.

However, not all FAP patients included in our study displayed an increased BMD, implying that different mutations in the *APC* gene may have distinct effects on bone mass acquisition. Interestingly, in our study population, the *APC* mutations found in patients with increased BMD were mostly located among the  $\beta$ -catenin binding/downregulating domains, suggesting that the heterozygous loss of  $\beta$ -catenin-regulating activity is likely to have a positive effect on BMD. Alternatively, an effect of *APC* on BMD may be balanced by patient-specific environmental and/or (epi)genetic factors. It is likely that due to the relative small size of our study we were unable to detect specific effects of different *APC* mutations on BMD. Which particular *APC* mutation has the most beneficial effect on BMD remains thus to be elucidated. As observed in conditional heterozygous *Apc* mutant mice (11;12), FAP patients display an average height similar to that of the general population, suggesting that one functional *APC* allele is sufficient for normal longitudinal bone growth.

In our study population, increased BMD was associated with coupled increases in the concentrations of biochemical markers of bone formation and resorption, albeit the mean remaining within the normal laboratory reference ranges. Higher BMD than normal could thus not be explained by an imbalance between bone resorption and bone formation. Inhibition of sclerostin by mechanical stimulation or following treatment of osteoporosis with intermittent PTH has been demonstrated to have positive

effects on bone mass (35;36). However, mean serum sclerostin was increased in the FAP patients we studied, and was significantly positively correlated with BMD. Sclerostin normally antagonizes the canonical Wnt signaling pathway by binding to the Wnt co-receptors LRP5 and LRP6 (37). The increase in sclerostin we observed might therefore be interpreted as a negative feedback mechanism to prevent further bone mass accrual. This notion is in agreement with *in vivo* data indicating that heterozygous *Apc*<sup>min/+</sup> mice display high sclerostin transcript levels in the tibia associated with increased BMD (13).

Osteomas are benign, slow-growing osteogenic lesions, usually affecting the jaws and flat bones of the calvaria. They are present in 46–93% of FAP patients, an incidence 4 to 20 times higher than in control groups (3–16%) (38–40). In keeping with previous studies (2), osteomas were predominantly located in the upper and/or lower mandible in our patients, and their presence was positively correlated with the presence of teeth anomalies (41;42). Patients with scintigraphic evidence of osteoma(s) were on average younger than those without osteomas, albeit non-statistically significantly. This observation is in keeping with previous reports indicating that osteomas are more prevalent in young FAP patients (1). However, it is well documented that osteomas may resolve spontaneously (43;44), so that due to the cross-sectional design of our study we cannot exclude the possibility that some of the patients without any present sign of osteoma(s) may have had this pathology in the past.

In the present study, we found no difference in BMD between patients with and without focal bone pathology, and no correlation between increased BMD and focal bone pathology. These findings suggest that, in FAP patients, osteomas and teeth anomalies are likely to develop due to local mechanisms, whereas the positive effect of the *APC* mutations on BMD is likely to be systemic. A local mechanism, such as loss of heterozygosity (LOH), has indeed been described in colonic, duodenal and desmoid tumors in FAP patients (45). To our knowledge, there are no available data on genetic analysis of osteomas from FAP patients. We hypothesize that somatic inactivation of the second *APC* allele may be responsible for the occurrence of focal bone pathology, while the systemic BMD increase may be attributed to the  $\beta$ -catenin activation secondary to heterozygous *APC* mutations.

In recent years, the Wnt/ $\beta$ -catenin signaling pathway has undoubtedly emerged as a pivotal regulator of bone formation prenatally, during growth and throughout adulthood. We document here for the first time that FAP individuals carrying heterozygous *APC* mutations, resulting in activation of the canonical Wnt signaling pathway, display significantly higher mean BMD compared to age- and sex-matched healthy controls in the presence of a balanced bone turnover. Whether increased bone mass accrual is sustained over the years, and whether this higher BMD than normal may reduce age-related fracture risk remains to be established by long-term follow-up studies in FAP patients. Whereas our data may not thus have direct clinical implications to FAP patients, they do add to the volume of evidence regarding the important role of the canonical Wnt signaling pathway in the regulation of bone mass. That our findings in FAP patients may be relevant is indeed supported by their analogy to similar data reported in relatives of patients with sclerosteosis, who carry heterozygous mutations in the *SOST* gene, another negative regulator of the canonical Wnt signaling

pathway (46). These individuals are asymptomatic, lack the characteristic “high bone mass phenotype” of their homozygous relatives, but do display consistently increased BMD values than the mean of age and sex-matched controls, either within the high normal range or clearly above it, but reaching Z-scores  $\geq +2$  in only a minority of cases. Findings from these two human genetic models suggest a state of “controlled” activation of the Wnt signalling pathway in heterozygous carriers of *SOST* or *APC* mutations that may be exploited in the identification of potentially attractive therapeutic targets in the treatment of osteoporosis.

## **ACKNOWLEDGMENTS**

*We are grateful to Dr. Ron Wolterbeek (Department of Medical Statistics, LUMC) for statistical advice and to Dr. Carli Tops (Department of Clinical Genetics, LUMC) for APC mutation analysis of patients included in the study.*

*This work was financially supported by an unrestricted educational grant from IP-SEN FARMACEUTICA BV to RLM.*

## REFERENCES

1. Vasen HF, Moslein G, Alonso A, Aretz S, Bernstein I, Bertario L et al. Guidelines for the clinical management of familial adenomatous polyposis (FAP). *Gut* 2008; 57(5):704-13.
2. Nieuwenhuis MH, Vasen HF. Correlations between mutation site in APC and phenotype of familial adenomatous polyposis (FAP): a review of the literature. *Crit Rev Oncol Hematol* 2007; 61(2):153-61.
3. Groen EJ, Roos A, Muntinghe FL, Enting RH, de Vries J, Kleibeuker JH et al. Extra-intestinal manifestations of familial adenomatous polyposis. *Ann Surg Oncol* 2008; 15(9):2439-50.
4. Burt RW. Colon cancer screening. *Gastroenterology* 2000; 119(3):837-53.
5. Fodde R. The multiple functions of tumour suppressors: it's all in APC. *Nat Cell Biol* 2003; 5(3):190-2.
6. Korinek V, Barker N, Morin PJ, van Wichen D, de Weger R, Kinzler KW et al. Constitutive transcriptional activation by a beta-catenin-Tcf complex in APC-/- colon carcinoma. *Science* 1997; 275(5307):1784-7.
7. Morin PJ, Sparks AB, Korinek V, Barker N, Clevers H, Vogelstein B et al. Activation of beta-catenin-Tcf signaling in colon cancer by mutations in beta-catenin or APC. *Science* 1997; 275(5307):1787-90.
8. Polakis P. Wnt signaling and cancer. *Genes Dev* 2000; 14(15):1837-51.
9. Macsai CE, Foster BK, Xian CJ. Roles of Wnt signalling in bone growth, remodelling, skeletal disorders and fracture repair. *J Cell Physiol* 2008; 215(3):578-87.
10. Wijn MA, Keller JJ, Giardiello FM, Brand HS. Oral and maxillofacial manifestations of familial adenomatous polyposis. *Oral Dis* 2007; 13(4):360-5.
11. Miclea RL, Karperien M, Bosch CA, van der Horst G, van der Valk MA, Kobayashi T et al. Adenomatous polyposis coli-mediated control of beta-catenin is essential for both chondrogenic and osteogenic differentiation of skeletal precursors. *BMC Dev Biol* 2009; 9:26.
12. Holmen SL, Zylstra CR, Mukherjee A, Sigler RE, Faugere MC, Bouxsein ML et al. Essential role of beta-catenin in postnatal bone acquisition. *J Biol Chem* 2005; 280(22):21162-8.
13. Su Q, Pun S, Pennypacker B, Winkelmann C, Flores OA, Glantschnig H et al. Evaluation of bone phenotype in mice carrying adenomatous polyposis coli (APCmin) gene mutation. *J Bone Miner Res* 22[S1], 166. 2007.
14. Niewenweg R, Smit ML, Walenkamp MJ, Wit JM. Adult height corrected for shrinking and secular trend. *Ann Hum Biol* 2003; 30(5):563-9.
15. Wahner HW, Looker A, Dunn WL, Walters LC, Hauser MF, Novak C. Quality control of bone densitometry in a national health survey (NHANES III) using three mobile examination centers. *J Bone Miner Res* 1994; 9(6):951-60.
16. Genant HK, Grampp S, Gluer CC, Faulkner KG, Jergas M, Engelke K et al. Universal standardization for dual x-ray absorptiometry: patient and phantom cross-calibration results. *J Bone Miner Res* 1994; 9(10):1503-14.

17. Staal KP, Roos JC, Manoliu RA, Kostense PJ, Lips P. Variations in diagnostic performances of dual-energy X-ray absorptiometry in the northwest of The Netherlands. *Osteoporos Int* 2004; 15(4):335-44.
18. Assessment of fracture risk and its application to screening for postmenopausal osteoporosis. Report of a WHO Study Group. *World Health Organ Tech Rep Ser* 1994; 843:1-129.
19. Genant HK, Wu CY, Van Kuijk C, Nevitt MC. Vertebral fracture assessment using a semi-quantitative technique. *J Bone Miner Res* 1993; 8(9):1137-48.
20. Swee RG, McLeod RA, Beabout JW. Osteoid osteoma. Detection, diagnosis, and localization. *Radiology* 1979; 130(1):117-23.
21. Smith FW, Gilday DL. Scintigraphic appearances of osteoid osteoma. *Radiology* 1980; 137(1 Pt 1):191-5.
22. Omojola MF, Cockshott WP, Beatty EG. Osteoid osteoma: an evaluation of diagnostic modalities. *Clin Radiol* 1981; 32(2):199-204.
23. Roux C, Bischoff-Ferrari HA, Papapoulos SE, de Papp AE, West JA, Bouillon R. New insights into the role of vitamin D and calcium in osteoporosis management: an expert roundtable discussion. *Curr Med Res Opin* 2008; 24(5):1363-70.
24. Meijer WG, van der Veer E, Jager PL, van der Jagt EJ, Piers BA, Kema IP et al. Bone metastases in carcinoid tumors: clinical features, imaging characteristics, and markers of bone metabolism. *J Nucl Med* 2003; 44(2):184-91.
25. Garnero P, Sornay-Rendu E, Claustrat B, Delmas PD. Biochemical markers of bone turnover, endogenous hormones and the risk of fractures in postmenopausal women: the OFELY study. *J Bone Miner Res* 2000; 15(8):1526-36.
26. Garnero P, Borel O, Delmas PD. Evaluation of a fully automated serum assay for C-terminal cross-linking telopeptide of type I collagen in osteoporosis. *Clin Chem* 2001; 47(4):694-702.
27. Okabe R, Nakatsuka K, Inaba M, Miki T, Naka H, Masaki H et al. Clinical evaluation of the Elecsys beta-CrossLaps serum assay, a new assay for degradation products of type I collagen C-telopeptides. *Clin Chem* 2001; 47(8):1410-4.
28. Bertario L, Russo A, Sala P, Varesco L, Giarola M, Mondini P et al. Multiple approach to the exploration of genotype-phenotype correlations in familial adenomatous polyposis. *J Clin Oncol* 2003; 21(9):1698-707.
29. Pitters E, Boudin E, Van Hul W. Wnt signaling: a win for bone. *Arch Biochem Biophys* 2008; 473(2):112-6.
30. Gong Y, Slee RB, Fukai N, Rawadi G, Roman-Roman S, Reginato AM et al. LDL receptor-related protein 5 (LRP5) affects bone accrual and eye development. *Cell* 2001; 107(4):513-23.
31. Little RD, Carulli JP, Del Mastro RG, Dupuis J, Osborne M, Folz C et al. A mutation in the LDL receptor-related protein 5 gene results in the autosomal dominant high-bone-mass trait. *Am J Hum Genet* 2002; 70(1):11-9.
32. Morvan F, Boulukos K, Clement-Lacroix P, Roman RS, Suc-Royer I, Vayssiere B et al. Deletion of a single allele of the Dkk1 gene leads to an increase in bone formation and bone mass. *J Bone Miner Res* 2006; 21(6):934-45.
33. van Bezooijen RL, Roelen BA, Visser A, van der Wee-Pals L, de Wilt E, Karperien M et al. Sclerostin is an osteocyte-expressed negative regulator of bone formation, but not a classical BMP antagonist. *J Exp Med* 2004; 199(6):805-14.

34. Bodine PV, Zhao W, Kharode YP, Bex FJ, Lambert AJ, Goad MB et al. The Wnt antagonist secreted frizzled-related protein-1 is a negative regulator of trabecular bone formation in adult mice. *Mol Endocrinol* 2004; 18(5):1222-37.
35. Robling AG, Niziolek PJ, Baldrige LA, Condon KW, Allen MR, Alam I et al. Mechanical stimulation of bone in vivo reduces osteocyte expression of Sost/sclerostin. *J Biol Chem* 2008; 283(9):5866-75.
36. Keller H, Kneissel M. SOST is a target gene for PTH in bone. *Bone* 2005; 37(2):148-58.
37. van Bezooijen RL, Bronckers AL, Gortzak RA, Hogendoorn PC, van der Wee-Pals L, Balemans W et al. Sclerostin in mineralized matrices and van Buchem disease. *J Dent Res* 2009; 88(6):569-74.
38. Dunlop MG, Farrington SM, Bubb VJ, Cunningham C, Wright M, Curtis LJ et al. Extracolonic features of familial adenomatous polyposis in patients with sporadic colorectal cancer. *Br J Cancer* 1996; 74(11):1789-95.
39. Ullbro C, Alm T, Ericson S, Koch G, Schioler R. Occult radiopaque jaw lesions in familial adenomatous polyposis. *Swed Dent J* 1990; 14(5):201-12.
40. Thakker N, Davies R, Horner K, Armstrong J, Clancy T, Guy S et al. The dental phenotype in familial adenomatous polyposis: diagnostic application of a weighted scoring system for changes on dental panoramic radiographs. *J Med Genet* 1995; 32(6):458-64.
41. Ida M, Nakamura T, Utsunomiya J. Osteomatous changes and tooth abnormalities found in the jaw of patients with adenomatosis coli. *Oral Surg Oral Med Oral Pathol* 1981; 52(1):2-11.
42. Utsunomiya J, Nakamura T. The occult osteomatous changes in the mandible in patients with familial polyposis coli. *Br J Surg* 1975; 62(1):45-51.
43. Kitsoulis P, Mantellos G, Vlychou M. Osteoid osteoma. *Acta Orthop Belg* 2006; 72(2):119-25.
44. Simm RJ. The natural history of osteoid osteoma. *Aust N Z J Surg* 1975; 45(4):412-5.
45. Latchford A, Volikos E, Johnson V, Rogers P, Suraweera N, Tomlinson I et al. APC mutations in FAP-associated desmoid tumours are non-random but not 'just right'. *Hum Mol Genet* 2007; 16(1):78-82.
46. Gardner JC, van Bezooijen RL, Mervis B, Hamdy NA, Lowik CW, Hamersma H et al. Bone mineral density in sclerosteosis; affected individuals and gene carriers. *J Clin Endocrinol Metab* 2005; 90(12):6392-5.

# Chapter 6

## **Inhibition of Gsk3 $\beta$ in cartilage induces osteoarthritic features through activation of the canonical Wnt signaling pathway**

R.L. Miclea<sup>1</sup>, M. Siebelt<sup>2</sup>, L. Finos<sup>3</sup>, J.J. Goeman<sup>3</sup>, C.W. Löwik<sup>4</sup>, W. Oostdijk<sup>1</sup>, H. Weinans<sup>2</sup>, J.M. Wit<sup>1</sup>, E.C. Robanus-Maandag<sup>5</sup>, M. Karperien<sup>6</sup>

<sup>1</sup>*Department of Pediatrics, Leiden University Medical Centre (LUMC), Leiden, The Netherlands,* <sup>2</sup>*Department of Orthopaedics, Erasmus University Medical Center, Rotterdam, The Netherlands,* <sup>3</sup>*Department of Medical Statistics, LUMC, Leiden, The Netherlands,* <sup>4</sup>*Department of Endocrinology and Metabolic Diseases, LUMC, Leiden, The Netherlands,* <sup>5</sup>*Department of Human Genetics, LUMC, Leiden, The Netherlands,* <sup>6</sup>*MIRA Institute for Biomedical Technology and Technical Medicine, University of Twente, Department of Tissue Regeneration, Enschede, The Netherlands*

Osteoarthritis Cartilage 2011





# Inhibition of Gsk3 $\beta$ in cartilage induces osteoarthritic features through activation of the canonical Wnt signaling pathway

R.L. Miclea, M. Siebelt, L. Finos, J.J. Goeman, C.W. Löwik, W. Oostdijk, H. Weinans, J.M. Wit, E.C. Robanus-Maandag, M. Karperien

## ABSTRACT

In the past years, the canonical Wnt/ $\beta$ -catenin signaling pathway has emerged as a critical regulator of cartilage development and homeostasis. In this pathway, glycogen synthase kinase-3 $\beta$  (GSK3 $\beta$ ) down-regulates transduction of the canonical Wnt signal by promoting degradation of  $\beta$ -catenin. In this study we wanted to further investigate the role of Gsk3 $\beta$  in cartilage maintenance. Therefore, we have treated chondrocytes *ex vivo* and *in vivo* with GIN, a selective GSK3 $\beta$  inhibitor.

In E17.5 fetal mouse metatarsals, GIN treatment resulted in loss of expression of cartilage markers and decreased chondrocyte proliferation from day 1 onward. Late (3 days) effects of GIN included cartilage matrix degradation and increased apoptosis. Prolonged (7 days) GIN treatment resulted in resorption of the metatarsal. These changes were confirmed by microarray analysis showing a decrease in expression of typical chondrocyte markers and induction of expression of proteinases involved in cartilage matrix degradation. An intra-articular injection of GIN in rat knee joints induced nuclear accumulation of  $\beta$ -catenin in chondrocytes 72 hours later. Three intra-articular GIN injections with a two days interval were associated with surface fibrillation, a decrease in glycosaminoglycan expression and chondrocyte hypocellularity 6 weeks later.

These results suggest that, by down-regulating  $\beta$ -catenin, Gsk3 $\beta$  preserves the chondrocytic phenotype, and is involved in maintenance of the cartilage extracellular matrix. Short term  $\beta$ -catenin upregulation in cartilage secondary to Gsk3 $\beta$  inhibition may be sufficient to induce osteoarthritis-like features *in vivo*.

## INTRODUCTION

Differentiated chondrocytes maintain their phenotype via synthesis of cartilage-specific extracellular matrix (ECM) molecules including collagen type II and sulfated proteoglycans, like aggrecan (1). Chondrocytes easily lose essential characteristics when they are removed from their natural environment and cultured *in vitro* or expanded for the purpose of cartilage tissue engineering (1;2). Chondrocyte dedifferentiation also occurs in the presence of retinoic acid, nitric oxide, or proinflammatory cytokines like interleukin (IL)-1 $\beta$  and TNF- $\alpha$ , as well as in osteoarthritis (OA) (2).

We and others have shown that both constitutive up- or down-regulation of the canonical Wnt pathway negatively influences cartilage development and maintenance resulting in OA-like features. This suggests that a tight regulation of this signaling cascade is crucial throughout the chondrocyte life-cycle (3-6). In this pathway, in the absence of a Wnt signal, a destruction complex comprising Axin (Conductin) and Adenomatous polyposis coli (APC) mediates the phosphorylation of  $\beta$ -catenin by GSK3 $\beta$ , which induces degradation of cytosolic  $\beta$ -catenin in the proteasome. Binding of Wnt to its transmembrane receptor Frizzled results in activation of Dishevelled. This is followed by reduction of GSK3 $\beta$  activity and accumulation of cytoplasmic  $\beta$ -catenin. Upon its nuclear translocation,  $\beta$ -catenin will function as a co-factor of TCF/LEF transcription factors to induce expression of Wnt target genes (6). GSK3 $\beta$  is constitutively active and, unlike many kinases that are activated following stimulus-dependent phosphorylation, it becomes inactive following phosphorylation (7). Studies reported so far indicate that Gsk3 $\beta$  activity is required for both chondrocyte and osteoblast differentiation and thus for endochondral bone development (8). However, no data is available regarding the role of GSK3 $\beta$  in maintenance of the chondrocytic phenotype.

To better understand the role of Gsk3 $\beta$  in regulation of the chondrocyte life cycle, we inactivated this kinase *ex vivo* and *in vivo* by using 3-[9-Fluoro-2-(piperidine-1-carbonyl)-1,2,3,4-tetrahydro-[1,4]diazepino[6,7,1-hi]indol-7-yl]-4-imidazo[1,2-a]pyridin-3-yl-pyrrole-2,5-dione, a selective and potent GSK3 $\beta$  inhibitor, in this manuscript further referred to as GIN (9). Our results imply that Gsk3 $\beta$  activity is crucial for maintenance of the chondrocytic phenotype and for the integrity of cartilage ECM, mainly by down-regulating the canonical Wnt signaling pathway. The cartilage phenotypic changes induced by GIN bear similarities to some of the clinical features commonly observed in OA.

## **MATERIALS AND METHODS**

### **KS483 cell culture, immunofluorescence for $\beta$ -catenin, transient transfection assays**

Routine culture of KS483 cells in T75 culture flasks (Greiner Bio-One), immunofluorescence for  $\beta$ -catenin and transient transfection assays were performed as previously described (10).

### ***Ex vivo* experiments**

The three middle metatarsals were dissected from E17.5 Swiss Albino mouse embryos. Explants isolated from different animals were randomly distributed and individually cultured in 500  $\mu$ l  $\alpha$ -MEM (Invitrogen) medium containing 10% FCS (Invitrogen), 100 U Pen/Strep (Invitrogen) and 1% GlutaMax (Invitrogen). After an equilibration period of 48 hours, metatarsals were challenged with vehicle or GIN as described in the results section. All *ex vivo* experiments were approved by the ethical committee of the Leiden University Medical Center and complied with national laws relating to the conduct of animal experiments.

### **Proliferation and apoptosis assays**

Chondrocyte proliferation was assessed by immunohistochemistry (IHC) for proliferating cell nuclear antigen (PCNA) according to manufacturer's protocol (Santa Cruz Biotechnology). Chondrocyte apoptosis was determined by the TUNEL reaction (Promega), as previously described (11). For statistical analysis a number of N = 3 independent samples were used and each experiment was repeated at least once.

### **Histology, Immunohistochemistry, In situ hybridization**

Histology, IHC, and in situ hybridization (ISH) were performed as previously described (5).

### **Quantification of glycosaminoglycans**

The glycosaminoglycan (GAG) content in N = 3 whole metatarsals per condition was quantified related to the amount of DNA using the Blyscan Sulfated GAG Assay kit (Biocolor) according to manufacturer's protocol. Experiments were repeated at least once.

### **Gene expression profiling**

For each condition, RNA was isolated from N = 15 whole metatarsals, checked for quality, amplified and labeled as previously described (12). Labeled cRNA was further used for the hybridization to Affymetrix GeneChip<sup>®</sup> Mouse Genome 430A 2.0 Array according to the manufacturer's protocol. The raw and normalized data are deposited on the website of the Department of Tissue Regeneration of the Twente University Institute for Biomedical Technology (<http://tr.tnw.utwente.nl>).

### **Microarray data analysis**

To evaluate the large number of genes and to find gene expression trends and noteworthy signaling pathways that are involved in the GIN-mediated effects, we used principal component analysis (13). Using a cut-off value of 2 for the expression fold change, a list of 316 differentially expressed genes (225 down- and 91 up-regulated) was generated and used for subsequent analysis (Table 1 and 2).

Functional annotation of the differentially expressed genes identified by the PCA analysis was performed using the DAVID bioinformatics database and the Gene Ontology (GO) terms to describe their (extra)cellular location (GO\_CC), molecular functions (GO\_MF), and the biological processes (GO\_BP) in which they are involved (14-16). Enrichment of GO functional groups was determined to be meaningful when the number of probe sets in our list that mapped to a specific GO term was greater than 2 with a p-value  $\leq 0.001$ .

Validation of the microarray analysis was performed by real-time quantitative PCR as previously described (12).

### ***In vivo* experiments**

All *in vivo* experiments were approved by the ethical committee of the Erasmus University Medical Center and complied with national laws relating to the conduct of animal experiments. Thirteen-week-old male Wistar rats (400-450 g) were housed under standard laboratory conditions (temperature 24°C, 12-hour light-dark cycle) with food and water *ad libitum*. The animals were acclimatized to the laboratory environment for 3 weeks before the start of the experiments.

### **GIN treatment**

In a dose-finding study (n=4), the effect of an intra-articular injection of 100  $\mu$ l GIN dissolved in PBS at concentrations of  $3 \cdot 10^{-7}$  M,  $10^{-6}$  M,  $3 \cdot 10^{-6}$  M, and  $10^{-5}$  M in the knee joint was investigated.

In a second experiment, 8 rats were injected intra-articularly at day 1, 3 and 5 with 100  $\mu$ l  $10^{-5}$  M GIN. Four rats were injected with GIN in the left knee, the remaining 4 were injected in the right knee. Contralateral joints served as controls and were injected with vehicle. All animals were scanned using contrast-enhanced microCT (CECT) before GIN injection (t = 0) and during follow up as previously described (17). Rats were sacrificed at the times indicated in the text.

### **Microscopical analysis and quantification**

IHC for  $\beta$ -catenin coupled with Alcian Blue (AB) counterstaining for GAGs was carried out as previously described (5). Quantification of the AB staining was performed using Image-Pro Plus software, version 7.0.

### **Statistical analysis**

All values represent median and range for experiments when  $N \leq 4$  and mean and 95% confidence interval (CI) when  $N \geq 5$ . The paired t-test, the univariate general linear model using simple contrasts and parameter estimates and one-way ANOVA were used

to assess the data, as appropriate. *P* values less than 0.05 were considered significant. Statistical analysis was performed using SPSS v16.0 (SPSS).

## RESULTS

### Inhibition of Gsk3 $\beta$ through GIN results in activation of the canonical Wnt signaling pathway *in vitro* and *ex vivo*

We first performed transient transfection experiments in mesenchymal-like KS483 cells using the Wnt-responsive BAT-Luc reporter vector (10;18). As expected, GIN induced a dose-dependent increase in luciferase activity, with a maximum response at  $10^{-7}$  M (Figure 1A). At higher concentrations, the luciferase activity decreased, presumably due to toxic effects (Figure 1A and data not shown). Furthermore, GIN was significantly more potent in inducing the Wnt reporter construct than LiCl, another established inhibitor of GSK3 $\beta$ . Activation of the Wnt reporter construct by  $10^{-7}$  M GIN was accompanied by  $\beta$ -catenin accumulation and nuclear translocation as confirmed by immunofluorescence (Figure 1B). The overall level of  $\beta$ -catenin was notably increased in cells treated with GIN when compared to LiCl (50 mM) or Wnt3a (50 ng/ml) (Figure 1B).

We next investigated the effect of GIN on fetal mouse metatarsals, which represent an established model for studying the chondrocyte life cycle *ex vivo* (19). After incubation for 3 days, GIN dose-dependently increased the levels of  $\beta$ -catenin as revealed by IHC (Figure 1C). Metatarsals treated with either  $10^{-7}$  M or  $10^{-6}$  M GIN displayed  $\beta$ -catenin staining mainly in the nuclei, indicating an efficient activation of the canonical Wnt signal. The latter concentration resulted in immunohistochemically detectable nuclear  $\beta$ -catenin expression in almost all chondrocytes. Strikingly, metatarsals treated with  $10^{-6}$  M GIN displayed a much fainter AB counterstaining in comparison to controls, indicative for loss of GAGs. Additional morphological analysis revealed no evidence of cell death, cell shrinkage, picnotic nuclei, blebbing of the cytoplasm or necrosis. Subsequent experiments using the fetal mouse metatarsal *ex vivo* culture model were performed with  $10^{-6}$  M GIN.

### GIN inhibits chondrocyte proliferation and increases cartilage apoptosis

We assessed the effect of GIN on chondrocyte proliferation using IHC for PCNA. The percentage of proliferating cells was smaller in the GIN-treated group compared to controls at all time points examined (Figure 2A-E). Chondrocyte proliferation was significantly inhibited both at d1 (11.3% vs. 25.9%,  $p = 0.048$ ) and at d3 (7.6% vs. 27.8%,  $p = 0.014$ ). TUNEL staining in combination with histological evaluation was used to assess chondrocyte apoptosis. GIN did not have an effect on TUNEL positivity at 6h, d1 and d3 (Figure 2F-J). Only after prolonged GIN treatment (d7), TUNEL staining was significantly increased (22.9% vs. 6.0%,  $p = 0.043$ ). At d7, TUNEL-positive cells were predominantly identified among the hypertrophic chondrocytes in controls. In contrast, TUNEL-positive cells were also observed among the resting and proliferative chondrocytes in

the GIN-treated group. Based on histological evaluation, TUNEL-positive cells underwent apoptosis.

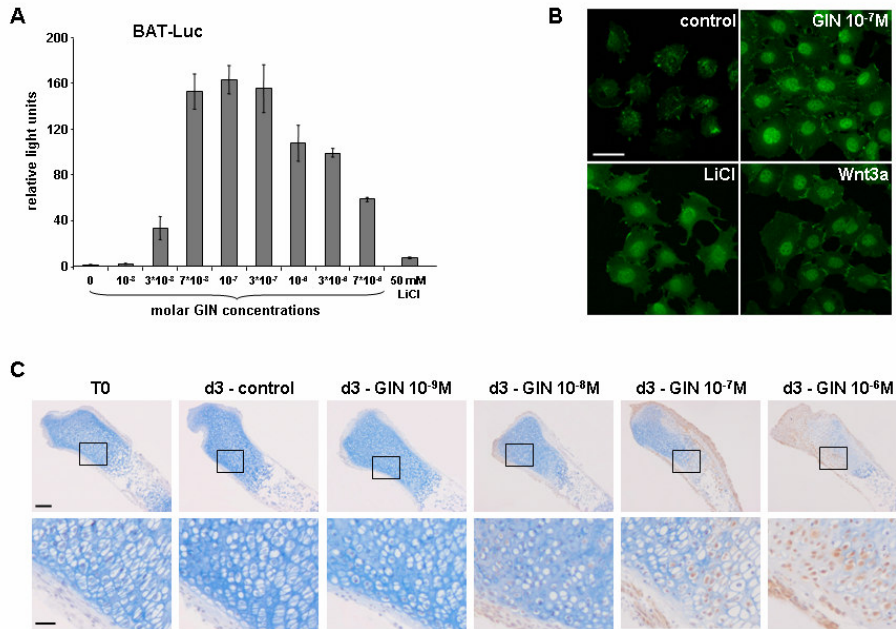


**Figure 1. GIN activates the canonical Wnt signaling pathway via  $\beta$ -catenin.** (A) GIN activated a transiently transfected Wnt reporter construct in KS483 cells dose-dependently. Values represent the mean and 95% CI (error bars) of  $N = 9$  luciferase observations corrected for renilla luciferase. (B) Representative images showing the effect of GIN ( $10^{-7}$ M), LiCl (50mM) and Wnt3A (50ng/ml) on  $\beta$ -catenin localization in KS483 cells as revealed by immunofluorescence. Out of the three Wnt activators, GIN was most effective in stabilizing and inducing nuclear translocation of  $\beta$ -catenin. Scale bar =  $10\mu\text{m}$ . (C) Representative images showing  $\beta$ -catenin IHC combined with AB staining on longitudinal sections of E17.5 murine metatarsals treated for 3 days with the indicated concentrations of GIN. In this experimental set-up,  $10^{-6}$ M GIN induces nuclear  $\beta$ -catenin translocation in almost all cells without any sign of toxicity. Note the progressive decrease in the intensity of the AB staining. The boxed regions in the upper row pictures are magnified in the lower row pictures. Scale bars =  $100\mu\text{m}$  (upper row),  $25\mu\text{m}$  (lower row).

### Inhibition of Gsk3 $\beta$ induces degradation of cartilage matrix and loss of the chondrocytic phenotype *ex vivo*

We investigated the effect of GIN at the cellular level by IHC analysis for  $\beta$ -catenin, collagen type II and X, and ISH analysis for *Col2a1* and *Col10a1*. No microscopical differences between vehicle- and GIN-treated metatarsals were observed at 6h (data not shown).  $\beta$ -catenin expression at the start of the experiment and in the control metatarsals at d1, d3 and d7 was restricted to the cytoplasm of a minority of perichondrial and periosteal cells (Figure 3A<sub>i</sub>, A<sub>iii</sub>, A<sub>v</sub>). We first noticed a clear increase in the level of nuclear  $\beta$ -catenin after 1 day of GIN treatment (Figure 3A<sub>ii</sub>).  $\beta$ -catenin accumulation was observed at d3 and d7 as well (Figure 3A<sub>iv</sub>, A<sub>vi</sub>). The level of nuclear  $\beta$ -catenin was

inversely correlated with the intensity of the AB counterstaining (Figure 3A-A<sub>vi</sub>). GIN treatment progressively decreased the GAG content in the ECM, with a near complete loss of GAGs at d7 (Figure 3F). GIN did not have an effect on mineral deposition and ossification of the metatarsals (data not shown).

Additional microscopical analysis revealed *Col2a1* mRNA and collagen type II protein expression in the resting, proliferative and prehypertrophic chondrocytes, and their matrix, respectively, at all time points in the controls (Figure 3B, B<sub>i</sub>, B<sub>iii</sub>, B<sub>v</sub>, C, C<sub>i</sub>, C<sub>iii</sub>, C<sub>v</sub>). GIN treatment for 1 day resulted in a considerable inhibition of the mRNA expression of this chondrocyte marker, whereas its protein expression was not changed (Figure 3B<sub>ii</sub>, C<sub>ii</sub>). At d3, most of the chondrocytes in the GIN-treated metatarsals, although surrounded by a matrix rich in collagen type II, failed to express *Col2a1* (Figure 3B<sub>iv</sub>, C<sub>iv</sub>). At d7, neither *Col2a1* nor collagen type II expression was found in the GIN-treated metatarsals (Figure 3B<sub>vi</sub>, C<sub>vi</sub>).

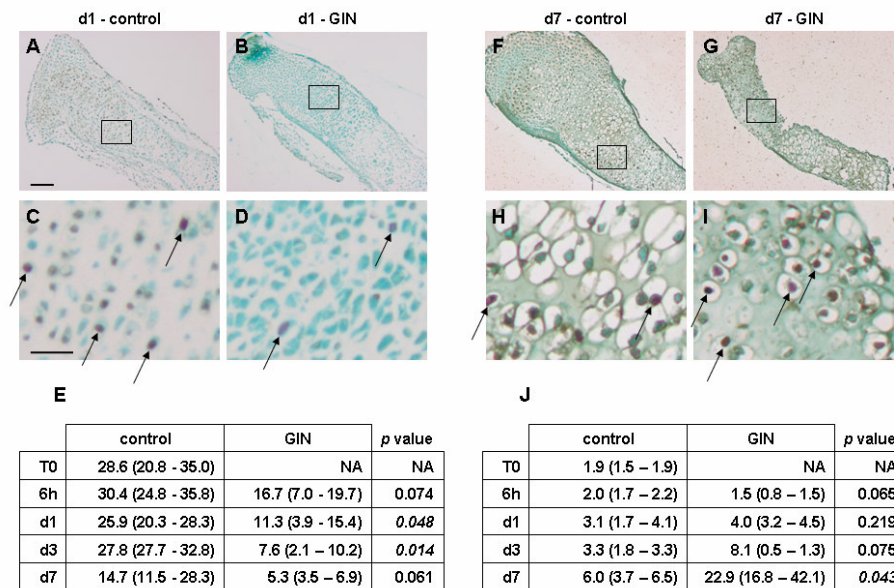


**Figure 2. GIN inhibits chondrocyte proliferation and augments cartilage apoptosis.** (A-D) Representative images showing PCNA IHC on metatarsals treated with vehicle (A, C) or GIN (B, D) for 1 day. Note that the number of the PCNA-positive nuclei (brown) is decreased in the GIN-treated metatarsal. (E) Quantification in N = 3 independent samples of the PCNA-positive nuclei (examples indicated by black arrows in C, D) indicates significant inhibition of chondrocyte proliferation upon GIN treatment at d1 and d3. PCNA positive cells were counted on a midsagittal tissue section. Each field contained at least 500 cells and data are expressed as median (range) % of PCNA positive cells from total number of cells. (F-I) Representative pictures of metatarsals cultured in control (F, H) or GIN-enriched (G, I) medium for 7 days after TUNEL staining. Note that the number of the TUNEL-positive nuclei (brown) is increased in the GIN-treated metatarsal. (J) Quantification in N = 3 independent samples of the TUNEL-positive nuclei (examples indicated by black arrows in H, I) indicates significantly more chondrocyte apoptosis upon prolonged GIN treatment (d7). Quantification and data expression as in (E). (C, D, H, I) High magnification pictures of the boxed regions in A, B, F, and G, respectively. Scale bars: 100 μm (A, B, F, G), 25 μm (C, D, H, I).



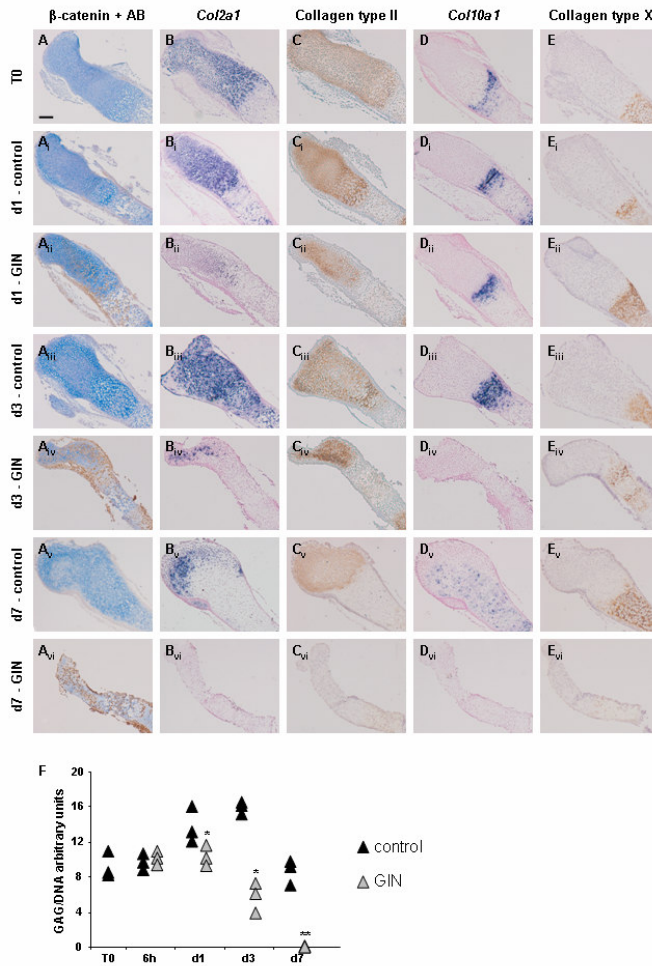


**Figure 3. GIN induces loss of the chondrocytic phenotype *ex vivo*.** Representative pictures of (A-A<sub>vi</sub>)  $\beta$ -catenin immunostaining combined with AB staining, (B-B<sub>vi</sub>) *Col2a1* mRNA expression, (C-C<sub>vi</sub>) Collagen type II immunostaining, (D-D<sub>vi</sub>) *Col10a1* mRNA expression, and (E-E<sub>vi</sub>) Collagen type X immunostaining, on consecutive longitudinal sections of E17.5 mouse metatarsals (N = 3 independent samples) isolated at the indicated time points. B-catenin-positive chondrocytes lose *Col2a1* expression upon GIN treatment already at d1. Chondrocyte marker expression at the mRNA level is inhibited after 3-day-long GIN treatment. Chondrocytes exposed to GIN for 7 days fail to express specific markers at both mRNA and protein level. Scale bar: 100  $\mu$ m. (F) Quantification of GAGs corrected for DNA (N = 3 independent samples) validates the microscopical findings. \*p = 0.023 (d1), \*p = 0.016 (d3), \*\*p = 0.008 (d7), all GIN vs. same time point untreated. Data are expressed in arbitrary GAG/DNA units (black triangles - controls, grey triangles - GIN treated samples).

Furthermore, control metatarsals displayed *Col10a1* and collagen type X expression in the hypertrophic zone (Figure 3D, D<sub>i</sub>, D<sub>iii</sub>, D<sub>v</sub>, E, E<sub>i</sub>, E<sub>iii</sub>, E<sub>v</sub>). At d1, there were no differences in the expression of this mature chondrocyte marker between the control and the GIN-treated group, neither at the mRNA nor at the protein level (Figure 3D<sub>ii</sub>, E<sub>ii</sub>). At d3, GIN-treated explants displayed no *Col10a1* expression, whereas collagen type X was still present in the ECM (Figure 3D<sub>iv</sub>, E<sub>iv</sub>). Ultimately, at d7, GIN induced a complete absence of both *Col10a1* and collagen type X (Figure 3D<sub>vi</sub>, E<sub>vi</sub>).

### Microarray analysis confirms GIN's proteolytic effects on cartilage

To further examine the effects of GIN on gene expression patterns in the fetal mouse metatarsal model, we performed cDNA microarray analysis on mRNA isolated from GIN-treated and control explants at T0, 6h, d1 and d3. We particularly designed our microarray analysis as such since GIN-treated metatarsals at d7 showed only aggravated features of the ones observed at d3. Furthermore, the increased apoptosis at d7 would have jeopardized the specificity of the results and mainly revealed differentially expressed genes related to cell death, an indirect effect of GIN treatment.

According to GO\_CC terms, the vast majority of the 316 differentially expressed genes (225 down- and 91 up-regulated) encoded proteins that are active in the ECM (Figure 4A). Classification according to GO\_MF and GO\_BP terms is represented in Figure 4B and 4C, respectively. The large number of up-regulated genes and the fact that they did not categorize under any GO terms related to cell death suggested that our microarray data efficiently revealed biological effects caused by GIN treatment and not by toxicity.

In consistence with the microscopical findings indicating significant cartilage matrix degradation, we found among the 91 up-regulated genes numerous transcripts encoding established proteinases: Matrix metalloproteinase 9 (*Mmp9*), *Mmp10*, *Mmp11*, and HtrA serine peptidase 1 (*Htra1*). Given the role of GSK3 $\beta$  in canonical Wnt signaling, the microarray data showed evidence for a Wnt/ $\beta$ -catenin signature as evidenced by the upregulation of established direct targets of the  $\beta$ -catenin/TCF4 complex, like Axin2 and adenomatous polyposis coli down-regulated 1 (*Apcdd1*). Microarray and pathway analysis did not reveal clear signatures of changes in other signaling pathways, such as Hedgehog and FGF. Furthermore, several cartilage ECM proteins were identified among the 225 down-regulated genes: unique cartilage matrix-associated protein (*Ucma*), matrilin 1 (*Matn1*), *Matn3*, *Matn4*, hyaluronan and proteoglycan link protein 1 (*Hapln1*), collagen, type XI, alpha 1 (*Col11a1*), epiphycan (*Epyc*), fibromodulin (*Fmod*), matrix Gla protein (*Mgp*), *Col14a1*, and (*Col9a3*). In the list of repressed genes, we also found transcripts known to encode non-cartilaginous matrix proteins like osteomodulin (*Omd*), osteoglycin (*Ogn*), microfibrillar-associated protein 4 (*Mfap4*), tenomodulin (*Tnmd*), asporin (*Aspn*), and fibulin7 (*Fbln7*), suggesting a more complex effect of the GIN treatment on the extracellular matrix.

To independently validate the results of the microarray analysis, 16 genes were selected for confirmation by quantitative real-time RT-PCR analysis. For the transcriptional analysis we therefore isolated RNA from a separate experiment that mirrored the one used to generate the microarray data. Four of these 16 genes are known to be involved in chondrocyte differentiation and cartilage maintenance (*Sox9*, *Col2a1*, *Acan*

and *Col10a1*), 4 are members of the canonical Wnt signaling pathway (*Axin1*, *Axin2*, *Gsk3b* and *Ctnnb1*), and 8 encode proteinases known to regulate maintenance and degradation of the ECM (*Mmp2*, *Mmp3*, *Mmp9*, *Mmp13*, *Adams4*, *Adams5*, *Hyal1* and *Ctsk*). We found a similar expression pattern of the analyzed genes, indicating that our microarray data specifically corresponded to actual gene expression patterns (Figure 5).

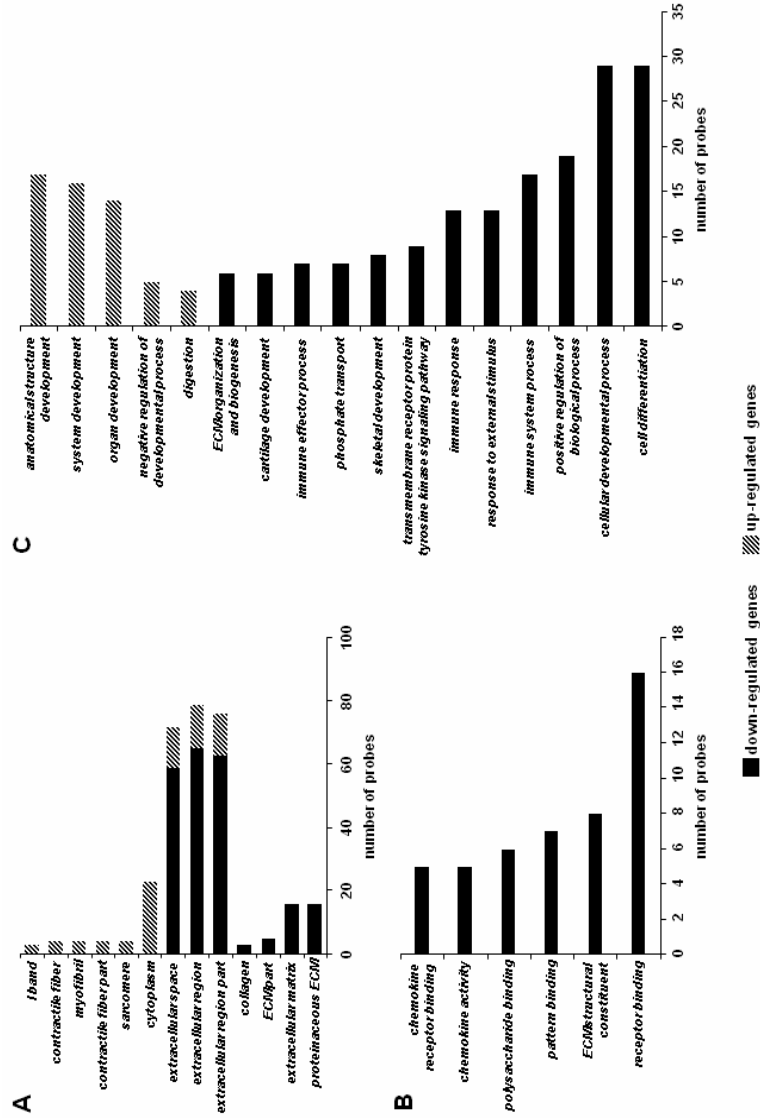


**Figure 4. Functional annotation of the GIN-modulated genes according to GO terms.** Functional annotation according to GO\_CC (A), GO\_MIF (B) and GO\_BP (C) terms was used to determine the enrichment of the differentially expressed transcripts indicated by PC1.

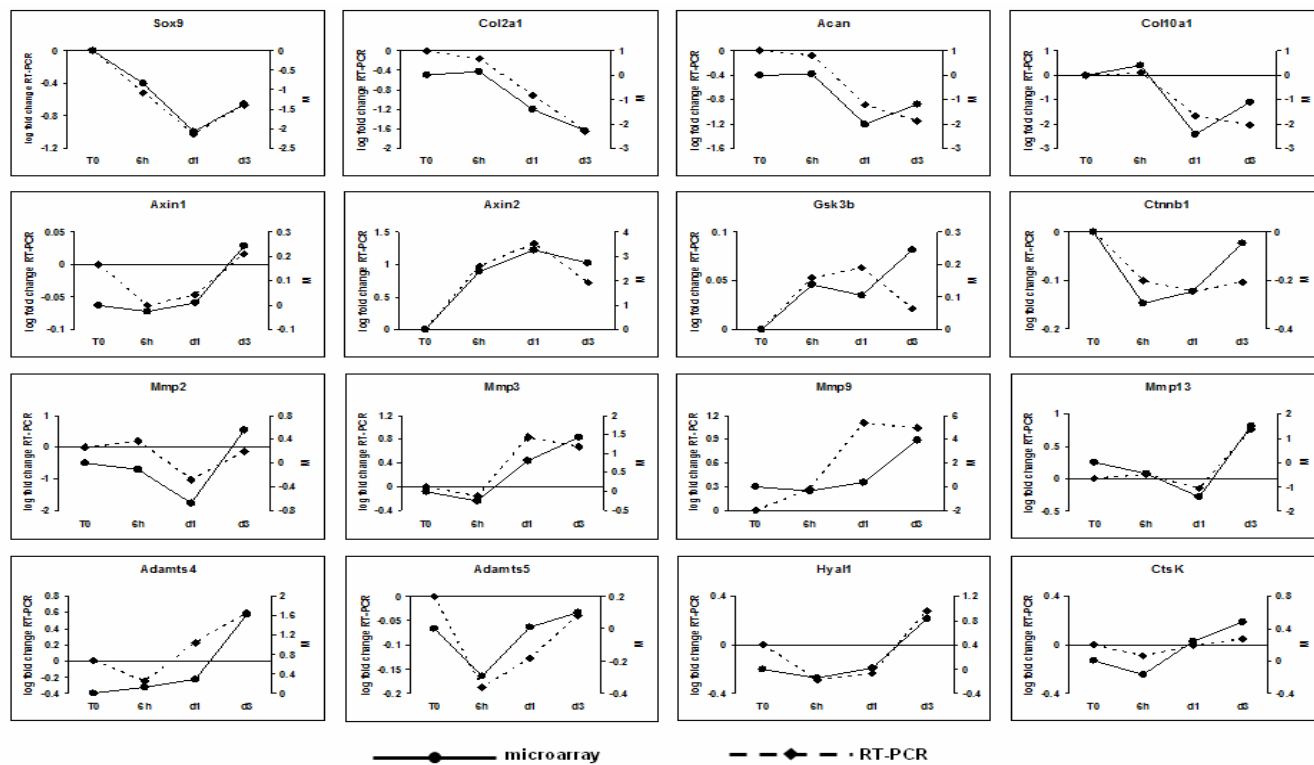


**Figure 5. Quantitative Real-Time RT-PCR validates the microarray data.** Correlation between qPCR and microarray results for *Sox9*, *Col2a1*, *Acan*, *Col10a1*, *Axin1*, *Axin2*, *Gsk3b*, *Ctnnb1*, *Mmp2*, *Mmp3*, *Mmp9*, *Mmp13*, *Adamts4*, *Adamts5*, *Hyal1*, and *CtsK*. The primary y-axis (left) indicates the RT-PCR results as normalized fold change on a log-scale. The secondary y-axis (right) indicates the microarray results as the log-differential expression ratios (M). Data are expressed as the mean of N = 6 metatarsals (qPCR) and N = 15 metatarsals (microarray).

### GIN induces OA-like effects *in vivo*

We next investigated whether GIN can induce the same biological effects in an *in vivo* experimental model. In an initial experiment, we observed 72 hours after GIN injection nuclear translocation of  $\beta$ -catenin in a dose-dependent fashion in rat knee articular chondrocytes, whereas vehicle treatment did not induce a change in  $\beta$ -catenin expression in the control joints (Figure 6A, A<sub>i</sub>, B, B<sub>i</sub> and data not shown). Virtually all articular chondrocytes treated with the highest GIN concentration ( $10^{-5}$  M) showed nuclear  $\beta$ -catenin expression, yet they did not display any morphological changes or alterations of their ECM. We did not detect  $\beta$ -catenin up-regulation in other tissues such as synovium, tendons, or bone at the examined time point, nor evidence of inflammation.

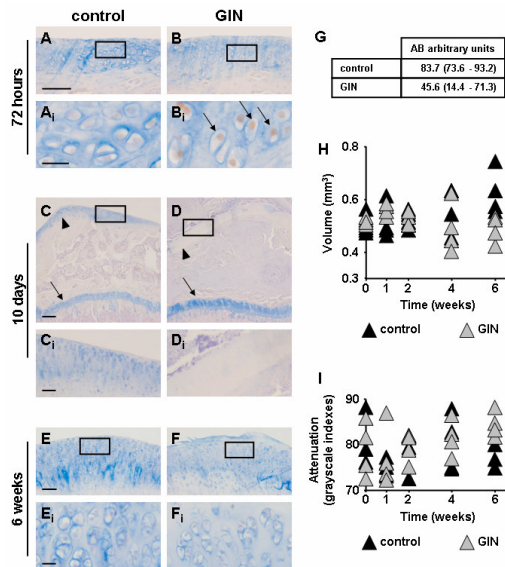


**Figure 6. GIN induces OA-like effects in rat articular cartilage.** (A, B) Representative pictures of  $\beta$ -catenin IHC combined with AB staining on longitudinal mid-sagittal sections of tibial plateaus 72 hours after injection with vehicle (A) or  $10^{-5}$  M GIN (B). Seventy-two hours after GIN injection there is  $\beta$ -catenin up-regulation (arrows in B<sub>i</sub>). (C, D) Representative pictures of AB staining on longitudinal mid-sagittal sections of proximal tibias 10 days after injection with vehicle (C) or  $10^{-5}$  M GIN (D) indicate massive ECM degradation only in the GIN-treated articular cartilage (arrowheads). GP cartilage is unaffected in both conditions (arrows). (E, F) Representative pictures of  $\beta$ -catenin IHC combined with AB staining on longitudinal mid-sagittal sections of tibial plateaus 6 weeks after injection with vehicle (E) or  $10^{-5}$  M GIN (F). Short term GIN treatment does not lead to  $\beta$ -catenin up-regulation 6-weeks-later, but induces OA-like morphological changes of the articular cartilage. (A<sub>i</sub>, B<sub>i</sub>, C<sub>i</sub>, D<sub>i</sub>, E<sub>i</sub>, F<sub>i</sub>) High magnification pictures of the boxed regions in A, B, C, D, E and F, respectively. (G) Quantification of the intensity of the AB staining, at 6 weeks, in the control and GIN-treated knees (N = 4 independent samples) showing less GAGs in the treated samples. Data are expressed as median (range) AB arbitrary units, p = 0.050. (H, I) Quantification of volume and attenuation measurements from CECT-data (N = 4 independent samples) (black triangles - controls, grey triangles - GIN treated samples). Scale bars: 200  $\mu$ m (A, B, C, D, E, F), 20  $\mu$ m (A<sub>i</sub>, B<sub>i</sub>, E<sub>i</sub>, F<sub>i</sub>), 300  $\mu$ m (C, D).

In a second experiment, we injected  $10^{-5}$ M GIN on day 1, 3 and 5. Four rats (“early” group) displayed signs of severe acute inflammation of the GIN-treated knee beginning at day 7 and these animals were therefore sacrificed already at day 10. No difference in  $\beta$ -catenin expression was observed between the GIN-treated and control knees of these animals (data not shown). In the vehicle-injected knee, the surface of the AC was smooth, the matrix was densely stained with AB and showed no signs of degeneration (Figure 6C, C<sub>i</sub>). Besides displaying histological signs of inflammation (intra-articular infiltration of neutrophils and macrophages, synoviocyte hyperplasia, fibrin exudation etc.), the GIN-treated knees in the “early” group displayed intensely degraded AC, containing almost no GAGs, as indicated by absence of AB staining (Figure 6D, D<sub>i</sub> and data not shown) in each of the 4 animals.

The other 4 rats (“late” group) from this experiment were sacrificed after 6 weeks and again showed no difference in the  $\beta$ -catenin expression pattern between the GIN-treated knee and controls (Figure 6E, E<sub>i</sub>, F, F<sub>i</sub>). Whereas no morphological changes were observed in the control knees of the “late” group, GIN-treated samples from all 4 rats displayed superficial fibrillation of AC, focal hypocellularity of chondrocytes, and reduced AB staining. Quantification of the intensity of the AB staining revealed significantly less staining in the cartilage of GIN-treated knees in comparison to contralateral control knees (Figure 6G,  $p=0.05$ ).

Although not statistically significant, CECT analysis of condylar cartilage revealed a trend in reduction of cartilage volume as well as GAG-depletion (expressed by increased attenuation) in the GIN-treated knee joints in comparison to control knees (Figure 6H, I).

## DISCUSSION

Here we show that Gsk3 $\beta$ , by controlling the canonical Wnt signaling pathway, is critical for maintenance of the chondrocytic phenotype. Inhibition of Gsk3 $\beta$  in chondrocytes *ex vivo* leads to loss of cartilage markers expression, induces matrix degradation by stimulating the expression of Mmps, inhibits chondrocyte proliferation and, most likely as a consequence of these effects, induces chondrocyte apoptosis. In addition, we demonstrate that transient inhibition of Gsk3 $\beta$ , following three intra-articular injections of GIN in rat knees during 1 week is associated with the appearance of OA-like features 6-weeks later. In agreement with our results, recent findings suggest that upregulation of  $\beta$ -catenin through induction of proteasomal degradation of Gsk3 $\beta$  in chondrocytes initiates early events of OA, while inhibition of Gsk3 $\beta$  may block chondrogenesis (20;21).

Besides the canonical Wnt pathway, GSK3 $\beta$  also regulates signal transduction of the Hedgehog (Hh) and Fibroblast growth factor (Fgf) family of secreted proteins (22;23). Given that both Hh and Fgf growth factors play important roles in the chondrocyte life cycle, we searched in our microarray results for possible target genes of these proteins among the list of transcripts differentially regulated by GIN (24;25). Only PR domain containing 1, with ZNF domain (*Prdm1*) matched this criterion, acting down-

stream of a sequential Wnt and Fgf signaling cascade (26). Our microarray expression data indicated that GIN treatment up-regulated the canonical Wnt target genes *Axin2* and *Apcdd1*, transcripts that have previously been shown to be induced only by Wnt and not by Fgf signaling (27-29). The protein products of *Axin2* and *Naked cuticle homolog 2*, both of which are upregulated in the microarray, are both renowned antagonists of the canonical Wnt signal. They have been shown to participate in negative feedback regulation of  $\beta$ -catenin activity (30-32). Taken together, these findings suggest that the intense cartilage matrix degeneration as well as the loss of the chondrocytic phenotype following GIN treatment occurred, at least in our experimental set-up, mainly due and can be explained by the activation of the Wnt/ $\beta$ -catenin pathway, although we cannot exclude minor roles of other signaling pathways in which GSK3 $\beta$  is known to be implicated nor of minor off-target effects of GIN.

Previously, we and others have reported that continuous exposure of chondrocytes to extensive levels of  $\beta$ -catenin *in vivo* induces loss of the chondrocytic phenotype as evidenced by the loss in expression of typical chondrocyte markers (5;6). Microarray analysis of GIN-treated metatarsals confirmed and extended this observation. Furthermore, our microscopical analysis suggests that GIN not only induced an enhanced degradation of the ECM, but also inhibited the expression of several ECM constituents in a time-dependent manner. Noteworthy, in the metatarsal experiments the loss of expression of typical cartilage markers at the mRNA level was observed before protein degradation was noticeable. GIN treatment inhibited the expression of genes encoding collagenous (*Col9a3*, *Col11a1*, and *Col14a1*), and non-collagenous ECM proteins (*Ucma*, *Matn1*, *Matn3*, *Matn4*, *Hapln1*, *Fmod*, *Mgp*), as well as proteoglycans (*Epyc*). In addition, GIN stimulated the expression of proteinases *Mmp9*, *Mmp10*, *Mmp11*, and *Htra1*, which promote ECM degradation, suggesting that the loss of tissue integrity observed in the treated metatarsals is due not only to a loss of the links between the collagenous and the non-collagenous proteins in the matrix, but also to active matrix degradation.

Decreased chondrocyte proliferation, augmented apoptosis, loss of the chondrocytic phenotype and degradation of ECM together characterize the “degradative phase” of OA, the most common form of arthritis (33). These pathological phenomena were observed after up-regulated canonical Wnt signaling by GIN-treatment in our experimental set-ups *ex vivo* and *in vivo*, in agreement with recent data suggesting a link between excess signaling through the Wnt/ $\beta$ -catenin pathway and OA (6). Moreover, many genes reportedly induced in OA cartilage were up-regulated by GIN treatment: *Mmp9*, *Mmp10*, *Mmp11*, *Axin2*, *Htra1*, angiopoietin-like 2 (*Angptl2*), and met proto-oncogene (*Met*) (2;34-38). *Htra1*, which is increased several-fold in joint cartilage of OA patients, promotes degeneration of cartilage (36;39), while *Met*, besides contributing to the altered metabolism during OA, also stimulates osteophyte development (40). *Serping1*, previously reported to be repressed in OA, and *Matn3*, whose inactivation leads to higher incidence of OA, were both down-regulated by GIN (41;42). In addition, inactivation of *Frzb*, another transcript repressed by GIN treatment, renders joints more susceptible for osteoarthritic changes (43).

Our results suggest that treatment with GIN can induce cartilage degeneration of rat AC after 3 intra-articular injections of GIN with a two days interval. We observed two distinct phenotypes, most likely explained by a difference in retention time of GIN

in the knee joint: a severe form with acute inflammation associated with resorption already 10 days after the first injection a milder phenotype. The potent catabolic effects of GIN on cartilage may have caused rapid and excessive cartilage degradation. These degradation products may have triggered an acute form of inflammation through the release of for example collagen type II fragments. In animals with the milder phenotype, microscopical analysis demonstrated the presence of the first signs of OA-like changes such as surface fibrillation, focal chondrocyte hypocellularity and a decrease in GAG staining in GIN-treated knees but not in the contralateral control knees 6-weeks after the last GIN-injection. CECT analysis revealed a trend of less cartilage volume and more attenuation, indicative for GAG loss in the GIN treated animals; however this observation did not reach significance. In contrast to the increased  $\beta$ -catenin expression in AC present 3 days after GIN injection, we did not detect increased  $\beta$ -catenin staining 6 weeks after GIN injection nor did we find evidence for nuclear  $\beta$ -catenin accumulation in the synovium, tendons or bone at each of the analysed time points. This suggests that a transient rise in  $\beta$ -catenin in AC may be sufficient to trigger development of OA-like features, an observation that extends findings in conditional constitutive mice carrying a stabilized, oncogenic variant of  $\beta$ -catenin, which also develop OA (4). Although we did not find evidence for increased  $\beta$ -catenin accumulation in other joint tissues besides cartilage at the examined time points, we cannot exclude that GIN-injection has resulted in a more rapid and transient rise of  $\beta$ -catenin in these tissues which was normalized 72 hours after the injection. This may have also contributed to the observed pathology. Furthermore, we cannot exclude that the mild cartilage phenotype was due to a milder form of inflammation in the first weeks after injection. However, given the clear evidence of increased nuclear  $\beta$ -catenin accumulation in AC 72 hours after GIN injection and the consistency of the *in vivo* findings with the phenotypic changes and effects on gene expression of GIN in our *ex vivo* cartilage explant model, we favor the hypothesis that these first indications of cartilage degeneration were due to a transient rise in  $\beta$ -catenin in AC triggering cartilage catabolism and changes in the chondrocyte phenotype.

Abnormally regulated GSK3 $\beta$  has been associated with many pathological conditions like Alzheimer's disease, mood disorders, diabetes and cancer (7). However, a direct link between GSK3 $\beta$  and the pathophysiology of OA has not yet been reported. Since in our experimental set-ups the GIN-induced effects reflect some of the pathological findings normally seen in osteoarthritic chondrocytes, we speculate that Gsk3 $\beta$  plays a role in the pathophysiology of this degenerative cartilage disease as well, most likely by regulating the levels of  $\beta$ -catenin. Whether pharmacological modulation of Gsk3 $\beta$  might represent a potential novel therapeutical approach for the management of OA remains to be elucidated.

## ACKNOWLEDGEMENTS

*This work was financially supported by an unrestricted educational grant from IP-SEN FARMACEUTICA BV to RLM that we gratefully acknowledge.*



## **CONTRIBUTIONS**

*Conception and design: RLM, MK; Collection of data: RLM, MS; Analysis and interpretation of the data: RLM, MS, LF, JIG, HW, JMW, ECR-M, MK; Drafting of the article: RLM; Critical revision of the article for important intellectual content: RLM, MS, LF, JIG, CWL, WO, HW, JMW, ECR-M, MK; Final approval of the article: RLM, MS, LF, JIG, CWL, WO, HW, JMW, ECR-M, MK; Statistical expertise: LF, JIG.*

**Table 1. List of GIN-down-regulated genes identified by PCA with a minimal fold change < -2.**

<b>Gene symbol</b>	<b>Affymetrix code</b>	<b>Fold change</b>
Adipoq	1422651_at	-5.14
Ucma	1428994_s_at	-4.74
Cxcl5	1419728_at	-4.32
Chrdl1	1434201_at	-4.27
Abi3bp	1427053_at	-4.13
Cytl1	1456793_at	-3.99
Ecrq4	1460049_s_at	-3.96
G0s2	1448700_at	-3.86
Srpx	1451939_a_at	-3.83
Abi3bp	1427054_s_at	-3.82
Mia1	1419608_a_at	-3.79
Cfd	1417867_at	-3.75
Islr	1418450_at	-3.67
Frzb	1416658_at	-3.65
Omd	1418745_at	-3.63
Ecrq4	1423261_at	-3.63
Ogn	1419662_at	-3.58
Frzb	1448424_at	-3.56
Ucma	1428993_at	-3.51
Cyp7b1	1421074_at	-3.42
Depdc6	1451348_at	-3.42
Ogn	1419663_at	-3.36
Hp	1448881_at	-3.25
Lpl	1431056_a_at	-3.23
Wwp2	1456714_at	-3.21
Pdcd4	1418840_at	-3.18
Penk1	1427038_at	-3.12
Lcn2	1427747_a_at	-3.11
Ptx3	1418666_at	-3.11
Angptl1	1455224_at	-3.09
Steap4	1460197_a_at	-3.09
Angpt1	1439066_at	-3.08
Calml4	1424713_at	-3.07
Lect1	1460258_at	-3.05
Lpl	1415904_at	-3.04
Matn1	1418477_at	-3.02
Susd5	1437387_at	-3.02
Hapln1	1421633_a_at	-2.99
Fgf7	1438405_at	-2.96
Mettl7a1	1434150_a_at	-2.96
Chrdl1	1421295_at	-2.96
Wwp2	1457499_at	-2.95

Hapln1	1426294_at	-2.93
5033414K04Rik	1436999_at	-2.92
Prlr	1441102_at	-2.92
Pdcd4	1456393_at	-2.92
Hapln1	1426295_at	-2.9
Sdpr	1416779_at	-2.9
Scin	1450276_a_at	-2.89
Plscr2	1448961_at	-2.85
Cxcl14	1418457_at	-2.85
BB144871	1436453_at	-2.85
Depdc6	1428622_at	-2.81
Mfap4	1424010_at	-2.81
Cyp7b1	1421075_s_at	-2.8
Matn3	1422148_at	-2.79
Gas2	1450112_a_at	-2.77
Depdc6	1443579_s_at	-2.76
6330403K07Rik	1426766_at	-2.76
Rspo3	1455607_at	-2.76
Al646023	1456878_at	-2.75
Mup1	1420465_s_at	-2.73
Col11a1	1449154_at	-2.73
Wwp2	1438482_at	-2.73
Efcab1	1455074_at	-2.72
Peg3	1417356_at	-2.7
Prlr	1448556_at	-2.7
Wwp2	1448145_at	-2.69
Meg3	1436713_s_at	-2.69
Vcam1	1448162_at	-2.67
Scara5	1451204_at	-2.67
Chrdl1	1456722_at	-2.66
Prlr	1437397_at	-2.63
Vnn1	1418486_at	-2.63
Lbp	1448550_at	-2.62
Peg3	1417355_at	-2.62
Agtr1a	1436739_at	-2.61
Adhfe1	1424393_s_at	-2.6
Pdlim2	1423946_at	-2.58
S100b	1434342_at	-2.58
Fxyd3	1418374_at	-2.56
Rora	1457177_at	-2.56
Hapln1	1438020_at	-2.54
Rian	1428055_at	-2.53
Slc1a3	1426340_at	-2.52
Ppp1r3c	1433691_at	-2.52
Fry	1456480_at	-2.51

---

Sorbs2	1437197_at	-2.5
Meg3	1452905_at	-2.5
Matn4	1418464_at	-2.5
Scrg1	1420764_at	-2.49
Hapln1	1458109_at	-2.48
Meg3	1428764_at	-2.47
Gda	1435748_at	-2.47
Fibin	1419376_at	-2.47
Cmtm5	1430600_at	-2.47
Mgp	1448416_at	-2.47
Kcnt2	1459971_at	-2.46
Angpt1	1421421_at	-2.46
Nope	1416474_at	-2.46
Kcnt2	1440030_at	-2.46
Sdpr	1416778_at	-2.43
Angpt1	1421441_at	-2.43
Efcab1	1454198_a_at	-2.42
Epyc	1421114_a_at	-2.42
Wwp2	1448146_at	-2.41
Gpr27	1434848_at	-2.41
Zim1	1421405_at	-2.4
Matn3	1455948_x_at	-2.39
Mup3	1426154_s_at	-2.39
Sec16b	1450734_at	-2.38
Epha3	1455426_at	-2.37
Sema3d	1453148_at	-2.37
Fmod	1437685_x_at	-2.36
Hhip	1421426_at	-2.36
Tox	1425483_at	-2.36
Pak3	1435486_at	-2.35
Car3	1449434_at	-2.35
1110006E14Rik	1431094_at	-2.35
Sdr39u1	1459269_at	-2.35
Fgf7	1422243_at	-2.35
Hcfc1r1	1428406_s_at	-2.34
Copg2	1445268_at	-2.34
Msr1	1448061_at	-2.34
Fmod	1456084_x_at	-2.33
Sorbs2	1441624_at	-2.32
Clec11a	1418796_at	-2.32
S3-12	1418595_at	-2.32
Prlr	1425853_s_at	-2.31
Peg3	1433924_at	-2.31
Ly6c1	1421571_a_at	-2.31
Car3	1460256_at	-2.31

Gnas	1444767_at	-2.29
Col14a1	1427168_a_at	-2.28
Ifi27	1426278_at	-2.28
Afap1l2	1436870_s_at	-2.28
Depdc6	1453571_at	-2.27
Mfap5	1418454_at	-2.27
Aldh6a1	1448104_at	-2.27
Sdpr	1443832_s_at	-2.26
Papola	1419032_at	-2.26
Kctd4	1420537_at	-2.25
Papss2	1421989_s_at	-2.25
Aff3	1433939_at	-2.24
Cxcl1	1419209_at	-2.24
Fzd4	1419301_at	-2.23
Rnf144b	1439153_at	-2.23
Pparg	1420715_a_at	-2.23
Rarres2	1428538_s_at	-2.22
Serping1	1416625_at	-2.22
C3	1423954_at	-2.21
Lilrb4	1420394_s_at	-2.21
Rspo2	1455893_at	-2.21
Tnmd	1417979_at	-2.21
Csgalnact1	1452365_at	-2.2
Maf	1447849_s_at	-2.2
Aspn	1416652_at	-2.2
Rgs5	1417466_at	-2.2
Fmod	1415939_at	-2.2
6530401D17Rik	1451679_at	-2.2
Pak3	1437318_at	-2.19
Efemp1	1427183_at	-2.18
Cybrd1	1460604_at	-2.18
Olfml1	1455663_at	-2.18
Fmod	1437718_x_at	-2.18
Gtl2	1429257_at	-2.18
9530019H20Rik	1458113_at	-2.17
Scara3	1427020_at	-2.17
Zfpm2	1449314_at	-2.17
Pira6	1420464_s_at	-2.17
Crispld1	1423352_at	-2.17
Papss2	1421987_at	-2.17
Cxcl12	1448823_at	-2.17
Susd5	1438636_s_at	-2.17
S100b	1419383_at	-2.16
Klhl24	1451793_at	-2.16
Ptgis	1448816_at	-2.15

---

Nope	1416473_a_at	-2.15
Akr1c14	1418979_at	-2.15
Hs6st2	1450047_at	-2.15
Tox	1446950_at	-2.15
2310050P20Rik	1453841_at	-2.14
Mest	1423294_at	-2.14
Hcfc1r1	1428405_at	-2.14
Mettl7a1	1454858_x_at	-2.14
Mirg	1457030_at	-2.13
Mme	1455961_at	-2.12
N4bp2l1	1417707_at	-2.12
Lcp1	1415983_at	-2.12
B230217C12Rik	1428568_at	-2.12
Ccl9	1417936_at	-2.12
Agtr2	1415832_at	-2.12
Ccl9	1448898_at	-2.11
Ptprc	1422124_a_at	-2.11
Meg3	1428765_at	-2.1
Gda	1435749_at	-2.1
Itgbl1	1425039_at	-2.1
Gstt1	1418186_at	-2.1
Hhip	1437933_at	-2.09
Mettl7a1	1434151_at	-2.08
Apoc1	1417561_at	-2.08
Itih5	1429159_at	-2.08
Papola	1419033_at	-2.08
Lrrc17	1429679_at	-2.07
Aff3	1441172_at	-2.06
LOC552901	1458505_at	-2.06
Fxyd1	1421374_a_at	-2.06
Smoc2	1431362_a_at	-2.06
Fgfr3	1421841_at	-2.06
Vkorc1	1452770_at	-2.06
Meg3	1429256_at	-2.05
Klhl24	1438519_at	-2.05
Col9a3	1460693_a_at	-2.04
Epha3	1425575_at	-2.04
Ttc30b	1423672_at	-2.04
AI449310	1455452_x_at	-2.03
Mme	1422975_at	-2.03
Tox	1445612_at	-2.02
Ctgf	1416953_at	-2.02
Col11a1	1418599_at	-2.02
Ebf3	1460666_a_at	-2.02
Mxd4	1434378_a_at	-2.01

Chapter 6

---

Arhgap20	1429918_at	-2.01
Lsp1	1417756_a_at	-2.01
Fbln7	1460412_at	-2.01

**Table 2. List of GIN-up-regulated genes identified by PCA with a minimal fold change > +2.**

<b>Gene symbol</b>	<b>Affymetrix code</b>	<b>Fold change</b>
Cadps	1448955_s_at	4.55
Mmp10	1420450_at	4.44
Dsp	1435494_s_at	4.42
Dsp	1435493_at	4.26
Ened	1429637_at	4.02
Inhbb	1426858_at	3.72
Ened	1416805_at	3.67
Mmp11	1417234_at	3.61
Apcdd1	1454822_x_at	3.5
1810011O10Rik	1435595_at	3.47
Prdm1	1420425_at	3.45
Snca	1436853_a_at	3.44
Il11	1449982_at	3.43
Apcdd1	1449070_x_at	3.41
Nkd2	1434275_at	3.38
LOC624112	1440815_x_at	3.25
Apcdd1	1418382_at	3.25
1810011O10Rik	1451415_at	3.19
Cadps	1444488_at	3.17
Axin2	1436845_at	3.09
Adcy1	1456487_at	3.08
Plekhg4	1457145_at	3.06
Nkd2	1419466_at	3.06
Krt39	1437440_at	3.03
Fhod3	1435551_at	2.93
Tmem8	1418344_at	2.92
Sema4f	1439768_x_at	2.91
Snca	1418493_a_at	2.84
Apcdd1	1418383_at	2.83
4921509J17Rik	1429106_at	2.8
Cxcr6	1425832_a_at	2.77
Nkd2	1419465_at	2.75
Myh1	1427868_x_at	2.74
Ccl8	1419684_at	2.73
Cps1	1455540_at	2.71
Notum	1451857_a_at	2.71
Gnai1	1454959_s_at	2.69
4921509J17Rik	1439093_at	2.66
Htr2b	1422125_at	2.61
Gnai1	1434440_at	2.61
Met	1434447_at	2.6
Mmp9	1448291_at	2.46



Myh1	1427520_a_at	2.46
Ccbe1	1437385_at	2.46
Mmp9	1416298_at	2.45
Ndp	1449251_at	2.43
Cadps	1458298_at	2.42
Rcan1	1416600_a_at	2.4
Stmn4	1418105_at	2.38
Twist2	1448925_at	2.37
Hspa4l	1418253_a_at	2.34
Ampd3	1422573_at	2.34
Rcan1	1416601_a_at	2.31
Cxcr6	1422812_at	2.3
Htra1	1438251_x_at	2.3
Tec	1460204_at	2.28
Mafb	1451715_at	2.27
Angptl2	1455090_at	2.27
Angptl2	1421002_at	2.26
Tnc	1456344_at	2.25
Masp1	1425985_s_at	2.25
Angptl2	1450085_at	2.23
Mafb	1451716_at	2.22
Krt19	1417156_at	2.21
Msc	1418417_at	2.21
Arl4c	1454788_at	2.21
Htra1	1416749_at	2.2
Ankrd1	1420992_at	2.19
Dio2	1418937_at	2.18
Cryab	1434369_a_at	2.17
AI425999	1435657_at	2.16
Gsta2	1421040_a_at	2.16
2210408K08Rik	1437087_at	2.15
Cryab	1416455_a_at	2.15
Ppargc1a	1434099_at	2.11
Gnai1	1427510_at	2.1
Pla2g7	1430700_a_at	2.09
2310076G05Rik	1442077_at	2.09
Pmepa1	1452295_at	2.07
Gsta2	1421041_s_at	2.07
Bex1	1448595_a_at	2.06
Ppargc1a	1456395_at	2.05
4631422O05Rik	1428861_at	2.05
Chst1	1449147_at	2.05
Vash2	1451105_at	2.04
Hspa4l	1458385_at	2.04
Ankrd1	1420991_at	2.04

Gsk3 $\beta$  inhibition promotes cartilage degradation

---

Lcp2	1418641_at	2.03
Slco5a1	1440874_at	2.03
Hmgn3	1459040_at	2.02
Mex3b	1437152_at	2.02

## REFERENCES

1. Pacifici M, Koyama E, Iwamoto M. Mechanisms of synovial joint and articular cartilage formation: recent advances, but many lingering mysteries. *Birth Defects Res C Embryo Today* 2005; 75(3):237-48.
2. Aigner T, Zien A, Gehrsitz A, Gebhard PM, McKenna L. Anabolic and catabolic gene expression pattern analysis in normal versus osteoarthritic cartilage using complementary DNA-array technology. *Arthritis Rheum* 2001; 44(12):2777-89.
3. Zhu M, Chen M, Zuscik M, Wu Q, Wang YJ, Rosier RN et al. Inhibition of beta-catenin signaling in articular chondrocytes results in articular cartilage destruction. *Arthritis Rheum* 2008; 58(7):2053-64.
4. Zhu M, Tang D, Wu Q, Hao S, Chen M, Xie C et al. Activation of beta-catenin signaling in articular chondrocytes leads to osteoarthritis-like phenotype in adult beta-catenin conditional activation mice. *J Bone Miner Res* 2009; 24(1):12-21.
5. Miclea RL, Karperien M, Bosch CA, van der Horst G, van der Valk MA, Kobayashi T et al. Adenomatous polyposis coli-mediated control of beta-catenin is essential for both chondrogenic and osteogenic differentiation of skeletal precursors. *BMC Dev Biol* 2009; 9(1):26.
6. Chun JS, Oh H, Yang S, Park M. Wnt signaling in cartilage development and degeneration. *BMB Rep* 2008; 41(7):485-94.
7. Doble BW, Woodgett JR. GSK-3: tricks of the trade for a multi-tasking kinase. *J Cell Sci* 2003; 116(Pt 7):1175-86.
8. Kapadia RM, Guntur AR, Reinhold MI, Naski MC. Glycogen synthase kinase 3 controls endochondral bone development: contribution of fibroblast growth factor 18. *Dev Biol* 2005; 285(2):496-507.
9. Engler TA, Henry JR, Malhotra S, Cunningham B, Furness K, Brozinick J et al. Substituted 3-imidazo[1,2-a]pyridin-3-yl- 4-(1,2,3,4-tetrahydro-[1,4]diazepino-[6,7,1-hi]indol-7-yl)pyrrole-2,5-diones as highly selective and potent inhibitors of glycogen synthase kinase-3. *J Med Chem* 2004; 47(16):3934-7.
10. van der Horst G, van der Werf SM, Farih-Sips H, van Bezooijen RL, Lowik CW, Karperien M. Downregulation of Wnt signaling by increased expression of Dickkopf-1 and -2 is a prerequisite for late-stage osteoblast differentiation of KS483 cells. *J Bone Miner Res* 2005; 20(10):1867-77.
11. Smink JJ, Buchholz IM, Hamers N, van Tilburg CM, Christis C, Sakkars RJ et al. Short-term glucocorticoid treatment of piglets causes changes in growth plate morphology and angiogenesis. *Osteoarthritis Cartilage* 2003; 11(12):864-71.
12. Hoogendam J, Parlevliet E, Miclea R, Lowik CW, Wit JM, Karperien M. Novel early target genes of parathyroid hormone-related peptide in chondrocytes. *Endocrinology* 2006; 147(6):3141-52.
13. Jonnalagadda S, Srinivasan R. Principal components analysis based methodology to identify differentially expressed genes in time-course microarray data. *BMC Bioinformatics* 2008; 9:267.

14. Huang da W, Sherman BT, Lempicki RA. Systematic and integrative analysis of large gene lists using DAVID bioinformatics resources. *Nat Protoc* 2009; 4(1):44-57.
15. Dennis G, Jr., Sherman BT, Hosack DA, Yang J, Gao W, Lane HC et al. DAVID: Database for Annotation, Visualization, and Integrated Discovery. *Genome Biol* 2003; 4(5):3.
16. Ashburner M, Ball CA, Blake JA, Botstein D, Butler H, Cherry JM et al. Gene ontology: tool for the unification of biology. The Gene Ontology Consortium. *Nat Genet* 2000; 25(1):25-9.
17. Palmer AW, Guldberg RE, Levenston ME. Analysis of cartilage matrix fixed charge density and three-dimensional morphology via contrast-enhanced microcomputed tomography. *Proc Natl Acad Sci U S A* 2006; 103(51):19255-60.
18. Cai Y, Mohseny AB, Karperien M, Hogendoorn PC, Zhou G, Cleton-Jansen AM. Inactive Wnt/beta-catenin pathway in conventional high-grade osteosarcoma. *J Pathol* 2010; 220(1):24-33.
19. Mushtaq T, Bijman P, Ahmed SF, Farquharson C. Insulin-like growth factor-I augments chondrocyte hypertrophy and reverses glucocorticoid-mediated growth retardation in fetal mice metatarsal cultures. *Endocrinology* 2004; 145(5):2478-86.
20. Wu Q, Huang JH, Sampson ER, Kim KO, Zuscik MJ, O'Keefe RJ et al. Smurf2 induces degradation of GSK-3beta and upregulates beta-catenin in chondrocytes: a potential mechanism for Smurf2-induced degeneration of articular cartilage. *Exp Cell Res* 2009; 315(14):2386-98.
21. Choi YA, Kang SS, Jin EJ. BMP-2 treatment of C3H10T1/2 mesenchymal cells blocks MMP-9 activity during chondrocyte commitment. *Cell Biol Int* 2009; 33(8):887-92.
22. Takenaka K, Kise Y, Miki H. GSK3beta positively regulates Hedgehog signaling through Sufu in mammalian cells. *Biochem Biophys Res Commun* 2007; 353(2):501-8.
23. Katoh M, Katoh M. Cross-talk of WNT and FGF signaling pathways at GSK3beta to regulate beta-catenin and SNAIL signaling cascades. *Cancer Biol Ther* 2006; 5(9):1059-64.
24. Day TF, Yang Y. Wnt and hedgehog signaling pathways in bone development. *J Bone Joint Surg Am* 2008; 90 Suppl 1:19-24.
25. Ornitz DM. FGF signaling in the developing endochondral skeleton. *Cytokine Growth Factor Rev* 2005; 16(2):205-13.
26. Mercader N, Fischer S, Neumann CJ. Prdm1 acts downstream of a sequential RA, Wnt and Fgf signaling cascade during zebrafish forelimb induction. *Development* 2006; 133(15):2805-15.
27. ten Berge D, Brugmann SA, Helms JA, Nusse R. Wnt and FGF signals interact to coordinate growth with cell fate specification during limb development. *Development* 2008; 135(19):3247-57.
28. Rousset R, Mack JA, Wharton KA, Jr., Axelrod JD, Cadigan KM, Fish MP et al. Naked cuticle targets dishevelled to antagonize Wnt signal transduction. *Genes Dev* 2001; 15(6):658-71.
29. Jukkola T, Sinjushina N, Partanen J. Drapc1 expression during mouse embryonic development. *Gene Expr Patterns* 2004; 4(6):755-62.
30. Zeng W, Wharton KA, Jr., Mack JA, Wang K, Gadbow M, Suyama K et al. naked cuticle encodes an inducible antagonist of Wnt signalling. *Nature* 2000; 403(6771):789-95.
31. Moon RT, Bowerman B, Boutros M, Perrimon N. The promise and perils of Wnt signaling through beta-catenin. *Science* 2002; 296(5573):1644-6.

32. Jho EH, Zhang T, Domon C, Joo CK, Freund JN, Costantini F. Wnt/beta-catenin/Tcf signaling induces the transcription of Axin2, a negative regulator of the signaling pathway. *Mol Cell Biol* 2002; 22(4):1172-83.
33. Sandell LJ, Aigner T. Articular cartilage and changes in arthritis. An introduction: cell biology of osteoarthritis. *Arthritis Res* 2001; 3(2):107-13.
34. Mohtai M, Smith RL, Schurman DJ, Tsuji Y, Torti FM, Hutchinson NI et al. Expression of 92-kD type IV collagenase/gelatinase (gelatinase B) in osteoarthritic cartilage and its induction in normal human articular cartilage by interleukin 1. *J Clin Invest* 1993; 92(1):179-85.
35. Pfander D, Cramer T, Weseloh G, Pullig O, Schuppan D, Bauer M et al. Hepatocyte growth factor in human osteoarthritic cartilage. *Osteoarthritis Cartilage* 1999; 7(6):548-59.
36. Tsuchiya A, Yano M, Tocharus J, Kojima H, Fukumoto M, Kawaichi M et al. Expression of mouse HtrA1 serine protease in normal bone and cartilage and its upregulation in joint cartilage damaged by experimental arthritis. *Bone* 2005; 37(3):323-36.
37. Meng J, Ma X, Ma D, Xu C. Microarray analysis of differential gene expression in temporomandibular joint condylar cartilage after experimentally induced osteoarthritis. *Osteoarthritis Cartilage* 2005; 13(12):1115-25.
38. Velasco J, Zarrabeitia MT, Prieto JR, Perez-Castrillon JL, Perez-Aguilar MD, Perez-Nunez MI et al. Wnt pathway genes in osteoporosis and osteoarthritis: differential expression and genetic association study. *Osteoporos Int* 2009.
39. Hu SI, Carozza M, Klein M, Nantermet P, Luk D, Crowl RM. Human HtrA, an evolutionarily conserved serine protease identified as a differentially expressed gene product in osteoarthritic cartilage. *J Biol Chem* 1998; 273(51):34406-12.
40. Dankbar B, Neugebauer K, Wunrau C, Tibesku CO, Skwara A, Pap T et al. Hepatocyte growth factor induction of macrophage chemoattractant protein-1 and osteophyte-inducing factors in osteoarthritis. *J Orthop Res* 2007; 25(5):569-77.
41. van der Weyden L, Wei L, Luo J, Yang X, Birk DE, Adams DJ et al. Functional knockout of the matrilin-3 gene causes premature chondrocyte maturation to hypertrophy and increases bone mineral density and osteoarthritis. *Am J Pathol* 2006; 169(2):515-27.
42. Gebauer M, Saas J, Haag J, Dietz U, Takigawa M, Bartnik E et al. Repression of anti-proliferative factor Tob1 in osteoarthritic cartilage. *Arthritis Res Ther* 2005; 7(2):R274-R284.
43. Lories RJ, Peeters J, Bakker A, Tylzanowski P, Derese I, Schrooten J et al. Articular cartilage and biomechanical properties of the long bones in Frzb-knockout mice. *Arthritis Rheum* 2007; 56(12):4095-103.

# **Chapter 7**

**Summary, conclusions,  
directions for future research**



## SUMMARY AND CONCLUSIONS

The interaction of Wnt proteins with their receptors and identification of Wnt signaling antagonists have been the foci of many studies and review articles (1-3). These studies show that canonical Wnt signaling is a very complex biological pathway, consisting of a large number of genes, receptors, agonists and antagonists, which bind to each other in many different combinations to elicit a large number of responses in a variety of cells and tissues. Many studies have now identified that the Wnt signaling pathway has a crucial role in growth plate biology, bone formation and skeletal remodeling (4-13). Most of these data were based on observations made in animal models in which the main effector of the canonical Wnt signaling,  $\beta$ -catenin, is either forcedly expressed or inactivated. Still at the time of the start of our studies, the cellular mechanisms by which canonical Wnt signaling controls skeletal development and maintenance via wild-type  $\beta$ -catenin were largely unknown. No reports were available on the role of Apc in regulation of skeletal precursor cell (SPC) differentiation via control of  $\beta$ -catenin. In addition, no studies had been reported on the possible beneficial effect of human APC mutations on bone mass, while only a few reports were published investigating the function of Gsk3 $\beta$  in cartilage maintenance (14). The experiments described in this thesis were designed in order to improve our understanding of the role of proteins acting up-stream of  $\beta$ -catenin during skeletal development and maintenance. Our findings and conclusions indicate that Apc and GSK3 $\beta$ , the two master intracellular regulators of the levels of transduced canonical Wnt signaling, fulfill major roles in the regulation of chondrocyte and osteoblast biology and pathology by adjusting the protein level of  $\beta$ -catenin.

The *Cre/loxP* system is a tool for tissue-specific knockout of those genes which cannot be investigated in differentiated tissues because of their early embryonic lethality using conventional knockouts (15). We initially used this genetic system to investigate whether Apc is involved in lineage commitment of SPCs by generating conditional knockout mice lacking functional Apc in *Col2a1*-expressing cells (16). Our data indicate that the *Col2a1* promoter is suitable for this study, since *Cre*-mediated recombination starts very early (E9.5) in SPCs that have not yet committed to the chondrogenic or the osteogenic lineage, consistent with previous findings in other *Col2a1-Cre* lines (17;18). Lack of functional Apc resulted in a pleiotropic skeletal cell phenotype. In the vast majority of SPCs, loss of functional Apc led to a strongly increased  $\beta$ -catenin level, resulting in the formation of an undifferentiated mesenchymal cell, with no differentiation potential for both osteogenic and chondrogenic lineages. When the inhibitory effect of a strongly increased  $\beta$ -catenin level in the skeletal precursors was reduced, highly active osteoblasts arose. Strong repression of  $\beta$ -catenin in these precursors was required for chondrogenesis. Our data presented in **chapter 2** indicate that a tight Apc-mediated control of  $\beta$ -catenin levels is essential for differentiation of skeletal precursors as well as for the maintenance of a chondrocytic phenotype in a spatio-temporal regulated manner.



We continued our expedition in unraveling the role of *Apc* in skeletal development by generating compound conditional *Col2a1-Cre;Apc<sup>15lox/1638N</sup>* and *Col2a1-Cre;Apc<sup>15lox/1572T</sup>* mutant embryos. Distinct levels of Wnt/ $\beta$ -catenin signaling in the two types of embryos differentially affected the chondrogenic and osteogenic differentiation of SPCs. Relatively high levels of  $\beta$ -catenin in the SPCs of *Col2a1-Cre;Apc<sup>15lox/1638N</sup>* embryos led to a complete blockade of both chondrocyte and osteoblast formation, while intermediate levels of  $\beta$ -catenin in the SPC of *Col2a1-Cre;Apc<sup>15lox/1572T</sup>* embryos led to regional-specific modulation of SPC differentiation. Whereas sclerotomal SPCs expressing *Apc <sup>$\Delta$ 15/1572T</sup>* failed to differentiate into chondrocytes and osteoblasts, in the inferior mandible and long bones these cells differentiated into highly active osteoblasts. Gradients of soluble growth factors regulate many developmental processes such as tissue organization, patterning and segmentation (19). By generating conditional compound *Col2a1-Cre;Apc<sup>15lox/1638N</sup>* and *Col2a1-Cre;Apc<sup>15lox/1572T</sup>* transgenic mice, we prove in **chapter 3** that different *Apc* mutations resulting in different levels of canonical Wnt signaling have distinct effects on the differentiation of SPC. This implies that a tight regulation of the dosage of functional *Apc* is directive for the lineage commitment of SPC via modulation of  $\beta$ -catenin.

To be able to mechanistically analyze the role of *Apc* in the regulation of SPC differentiation into chondrocytes and osteoblasts, we next knocked down the mouse *Apc* gene using RNA interference (RNAi) in the murine mesenchymal stem cell-like KS483 cell line (20). This cell line has SPC-like characteristics, since it can form osteoblasts, chondrocytes, and adipocytes (21). Our results indicated that *Apc* is required for proliferation, suppression of apoptosis and for differentiation of murine mesenchymal stem cell-like KS483 cells into the osteogenic, chondrogenic and adipogenic lineage. *Apc* knockdown led to up-regulation not only of the Wnt/ $\beta$ -catenin, but also of the BMP signaling pathway, further sustaining the interaction of these biological routes during various steps of SPC differentiation. Interestingly, the inhibitory effects of *Apc* knockdown on osteogenic differentiation could be rescued by high levels of exogenous BMP-7. It is noteworthy to mention that we obtained similar results by using 2 different shRNA sequences targeting *Apc*, while stable transfection of the respective control mutant shRNA plasmids (containing 2 nucleotide mismatches) did not alter the proliferation, survival and differentiation capacity of KS483 cells. This clearly indicates that our results were the consequence of a bona-fide and specific siRNA effect lowering wild-type *Apc* expression. Partial rescue of the Wnt-responsive BAT-Luc reporter activity by transient transfection of a human *APC* expression vector further confirmed these observations. Our approach described in **chapter 4** provides a valuable model demonstrating that levels of functional *Apc* must be tightly controlled for proper modulation of the transcriptionally active  $\beta$ -catenin and BMP-signaling dosage required for multi-lineage SPC-differentiation *in vitro*.

To further analyze the role of *APC* in the skeleton and thereby to complete our *in vivo* and *in vitro* mouse studies, we next performed the first cross-sectional, population-based study documenting a detailed assessment of bone and mineral metabolism in familial adenomatous polyposis (FAP) patients carrying heterozygous mutations in the *APC* gene (22). Our results indicated that FAP patients display a statistically significantly higher mean BMD in comparison with age and sex matched controls. In our

study population mean P1NP (marker of bone formation) and mean  $\beta$ -CTX (marker of bone resorption) concentrations were within the normal ranges and were significantly positively correlated. Furthermore, both these markers were positively correlated with bone mineral density (BMD). Our data described in **chapter 5** suggest a state of “controlled” activation of the Wnt signalling pathway in heterozygous carriers of *APC* mutations, most likely due to upregulation of  $\beta$ -catenin resulting in a higher than normal BMD. Our findings in FAP patients are sustained by data reported in relatives of patients with sclerosteosis, who carry heterozygous mutations in the *SOST* gene, another negative regulator of the canonical Wnt signaling pathway (23). Findings from these two human genetic models may be exploited in the identification of potentially attractive therapeutic targets in the treatment of osteoporosis.

Studies reported so far indicate that Gsk3 $\beta$  activity is required for both chondrocyte and osteoblast differentiation and thus for endochondral bone development (24). However, no data was available regarding the role of Gsk3 $\beta$  in maintenance of the chondrocytic phenotype. To investigate this we finally treated chondrocytes *ex vivo* and *in vivo* with GIN, a selective GSK3 $\beta$  inhibitor (25). Gsk3 $\beta$ , by controlling the canonical Wnt signaling pathway, was critical for maintenance of the chondrocytic phenotype. Inhibition of Gsk3 $\beta$  in fetal mouse metatarsals led to loss of cartilage markers expression, induced matrix degradation by stimulating the expression of Mmps, inhibited chondrocyte proliferation and, most likely as a consequence of these effects, induced chondrocyte apoptosis. In addition, transient inhibition of Gsk3 $\beta$ , following three intra-articular injections of GIN in rat knees during one week was associated with the appearance of osteoarthritis (OA)-like features six weeks later. In agreement with our results, recent findings suggest that upregulation of  $\beta$ -catenin through induction of proteasomal degradation of Gsk3 $\beta$  in chondrocytes initiates early events of OA, while inhibition of Gsk3 $\beta$  may block chondrogenesis (26;27). Abnormally regulated GSK3 $\beta$  has been associated with many pathological conditions like Alzheimer’s disease, mood disorders, diabetes and cancer (28). However, a direct link between GSK3 $\beta$  and the pathophysiology of OA has not yet been reported. Since in our experimental set-ups described in **chapter 6** the GIN-induced effects reflect some of the pathological findings normally seen in osteoarthritic chondrocytes, we speculate that Gsk3 $\beta$  plays a role in the pathophysiology of this degenerative cartilage disease as well, most likely by regulating the levels of  $\beta$ -catenin.

## DIRECTIONS FOR FUTURE RESEARCH

Our *in vivo* results obtained in the conditional *Apc* mutant mice indicate that a tight regulation of the levels of  $\beta$ -catenin by *Apc* is crucial during skeletal development. An important drawback of our studies is that we cannot exactly indicate the timeslot when the regulation of SPC differentiation by *Apc* begins during embryogenesis and how this expands in subsequent developmental stages. Developing an inducible conditional mouse line carrying both a tissue- and time-specific *Apc* inactivation will enable us to more precisely unravel the role of *Apc* during distinct steps of SPC differentiation

into chondrocytes and osteoblasts. Nevertheless, performing *in vitro* differentiation experiments, for instance by using mouse embryonic fibroblasts from  $Apc^{+/15lox}$ ,  $Apc^{15lox/15lox}$ ,  $Apc^{+/1638N}$ ,  $Apc^{+/1572T}$ ,  $Apc^{15lox/1638N}$  and  $Apc^{15lox/1572T}$  mice infected with Cre-lentiviruses could provide a more quantifiable approach to investigate the regulation of SPC differentiation by Apc.

In our cross-sectional, population-based study, we demonstrated that FAP patients display a significantly higher than normal mean BMD compared to age- and sex-matched healthy controls in the presence of a balanced bone turnover. Whether increased bone mass accrual is sustained over the years, and whether this higher BMD than normal may reduce age-related fracture risk remains to be established by long-term follow-up studies in FAP patients.

Our *in vivo* results from the GIN-treated rat knees suggest that Gsk3 $\beta$  inhibition can induce cartilage degeneration of rat articular cartilage after 3 intra-articular injections of GIN with a two days interval. It will be interesting to test whether the mild phenotypic effects resembling early stages of OA would result in more exaggerated effects in a longer follow-up time. Nevertheless our results indicate that  $\beta$ -catenin upregulation in cartilage secondary to Gsk3 $\beta$  inhibition is sufficient to induce OA-like features *in vivo*, thereby providing a valid model for the study of OA. Whether pharmacological modulation of Gsk3 $\beta$  might represent a potential novel therapeutical approach for the management of OA remains to be elucidated.

## REFERENCES

1. Cadigan KM, Nusse R. Wnt signaling: a common theme in animal development. *Genes Dev* 1997; 11(24):3286-305.
2. Johnson ML, Rajamannan N. Diseases of Wnt signaling. *Rev Endocr Metab Disord* 2006; 7(1-2):41-9.
3. Miller JR. The Wnts. *Genome Biol* 2002; 3(1):REVIEWS3001.
4. Baron R, Rawadi G. Wnt signaling and the regulation of bone mass. *Curr Osteoporos Rep* 2007; 5(2):73-80.
5. Chun JS, Oh H, Yang S, Park M. Wnt signaling in cartilage development and degeneration. *BMB Rep* 2008; 41(7):485-94.
6. Church V, Nohno T, Linker C, Marcelle C, Francis-West P. Wnt regulation of chondrocyte differentiation. *J Cell Sci* 2002; 115(Pt 24):4809-18.
7. Corr M. Wnt-beta-catenin signaling in the pathogenesis of osteoarthritis. *Nat Clin Pract Rheumatol* 2008; 4(10):550-6.
8. Hartmann C. A Wnt canon orchestrating osteoblastogenesis. *Trends Cell Biol* 2006; 16(3):151-8.
9. Hartmann C. Skeletal development--Wnts are in control. *Mol Cells* 2007; 24(2):177-84.
10. Krishnan V, Bryant HU, MacDougald OA. Regulation of bone mass by Wnt signaling. *J Clin Invest* 2006; 116(5):1202-9.
11. Liu F, Kohlmeier S, Wang CY. Wnt signaling and skeletal development. *Cell Signal* 2008; 20(6):999-1009.
12. Luyten FP, Tylzanowski P, Lories RJ. Wnt signaling and osteoarthritis. *Bone* 2009; 44(4):522-7.
13. Piters E, Boudin E, van Hul W. Wnt signaling: a win for bone. *Arch Biochem Biophys* 2008; 473(2):112-6.
14. Kapadia RM, Guntur AR, Reinhold MI, Naski MC. Glycogen synthase kinase 3 controls endochondral bone development: contribution of fibroblast growth factor 18. *Dev Biol* 2005; 285(2):496-507.
15. Nagy A. Cre recombinase: the universal reagent for genome tailoring. *Genesis* 2000; 26(2):99-109.
16. Miclea RL, Karperien M, Bosch CA, van der Horst G, van der Valk MA, Kobayashi T et al. Adenomatous polyposis coli-mediated control of beta-catenin is essential for both chondrogenic and osteogenic differentiation of skeletal precursors. *BMC Dev Biol* 2009; 9:26.
17. Long F, Chung UI, Ohba S, McMahon J, Kronenberg HM, McMahon AP. Ihh signaling is directly required for the osteoblast lineage in the endochondral skeleton. *Development* 2004; 131(6):1309-18.

18. Day TF, Guo X, Garrett-Beal L, Yang Y. Wnt/beta-catenin signaling in mesenchymal progenitors controls osteoblast and chondrocyte differentiation during vertebrate skeletogenesis. *Dev Cell* 2005; 8(5):739-50.
19. Gaspar C, Fodde R. APC dosage effects in tumorigenesis and stem cell differentiation. *Int J Dev Biol* 2004; 48(5-6):377-86.
20. Miclea RL, van der Horst G, Robanus-Maandag EC, Lowik CW, Oostdijk W, Wit JM et al. Apc bridges Wnt/beta-catenin and BMP signaling during osteoblast differentiation of KS483 cells. *Exp Cell Res*. 2011 Jun 10;317(10):1411-21.
21. van der Horst G, van der Werf SM, Farih-Sips H, van Bezooijen RL, Lowik CW, Karperien M. Downregulation of Wnt signaling by increased expression of Dickkopf-1 and -2 is a prerequisite for late-stage osteoblast differentiation of KS483 cells. *J Bone Miner Res* 2005; 20(10):1867-77.
22. Miclea RL, Karperien M, Langers AM, Robanus-Maandag EC, van Lierop A, van der Hiel B et al. APC mutations are associated with increased bone mineral density in patients with familial adenomatous polyposis. *J Bone Miner Res* 2010; 25(12):2348-56.
23. Gardner JC, van Bezooijen RL, Mervis B, Hamdy NA, Lowik CW, Hamersma H et al. Bone mineral density in sclerosteosis; affected individuals and gene carriers. *J Clin Endocrinol Metab* 2005; 90(12):6392-5.
24. Kapadia RM, Guntur AR, Reinhold MI, Naski MC. Glycogen synthase kinase 3 controls endochondral bone development: contribution of fibroblast growth factor 18. *Dev Biol* 2005; 285(2):496-507.
25. Miclea RL, Robanus-Maandag EC, Goeman JJ, Finos L, Bloys H, Löwik CW et al. Inhibition of Gsk3 $\beta$  in cartilage induces osteoarthritic features through activation of the canonical Wnt signaling pathway. *Osteoarthritis and cartilage* 2011.
26. Wu Q, Huang JH, Sampson ER, Kim KO, Zuscik MJ, O'Keefe RJ et al. Smurf2 induces degradation of GSK-3 $\beta$  and upregulates beta-catenin in chondrocytes: a potential mechanism for Smurf2-induced degeneration of articular cartilage. *Exp Cell Res* 2009; 315(14):2386-98.
27. Choi YA, Kang SS, Jin EJ. BMP-2 treatment of C3H10T1/2 mesenchymal cells blocks MMP-9 activity during chondrocyte commitment. *Cell Biol Int* 2009; 33(8):887-92.
28. Doble BW, Woodgett JR. GSK-3: tricks of the trade for a multi-tasking kinase. *J Cell Sci* 2003; 116(Pt 7):1175-86.





## **Samenvatting**





## SAMENVATTING

Het skelet bestaat uit ongeveer 200 botten en 300 gewrichten die het lichaam ondersteunen en zijn vorm geven. Het bestaat uit twee delen: het axiale skelet (schedel, wervelkolom en ribbenkast) en het appendiculaire skelet (pijpbeneden, sleutelbeneden, schouderbladen en bekkenbeneden). Het skelet zorgt voor lengtegroei, ondersteuning van de verschillende lichaamsdelen, voor mineraal huishouding, voor bescherming van onze organen en samen met de spieren voor beweging. Het skelet is een levend weefsel, dat tijdens het hele leven voortdurend wordt vernieuwd. Drie verschillende celtypen zijn hiervoor verantwoordelijk: chondrocyten (voor kraakbeen-aanmaak), osteoblasten (voor botaanmaak) en osteoclasten (voor kraakbeen- en bot-resorptie).

Voor een gezond skelet is gedurende verschillende levensfasen een precieze regulatie tussen de aanmaak en afbraak van bot en kraakbeen van zeer groot belang. Deze regulatie wordt grotendeels uitgevoerd door hormonen en groeifactoren. Hormonen zijn regulerende stoffen, die in hormoonklieren geproduceerd worden en via het bloed stromen naar de plaats waar ze werkzaam zijn. Het groeihormoon (GH), de schildklierhormonen en de geslachtshormonen zijn de belangrijkste hormonen tijdens de ontwikkeling en onderhoud van het skelet. Groeifactoren zijn eiwitten die door bepaalde cellen worden gemaakt en in hun directe omgeving hun effect op andere cellen uitvoeren. Groeifactoren die een cruciale rol spelen in het skelet zijn: Insulin-like Growth Factor (IGF)-I en -II, Fibroblast Growth Factor (FGF), Parathormone-related Peptide (PTHrP), Indian Hedgehog (IHH) en leden van de Wnt-familie van groeifactoren.

Wijkt de groei van het skelet af van normaal, dan spreekt men over een groei-stoornis. Slechts in een minderheid van de kinderen met een groei-stoornis kan de oorzaak definitief worden vastgesteld en zelfs bij een bekende oorzaak is een causale behandeling meestal niet beschikbaar. Momenteel is voor enige groepen kinderen met korte gestalte behandeling met GH injecties beschikbaar, maar het effect van GH varieert sterk per kind. Recent is daarnaast biosynthetisch IGF-I beschikbaar gekomen voor kinderen met een IGF-I tekort. Korte gestalte in de kindertijd, adolescentie en volwassenheid kan psychologische, sociale, educatieve en professionele gevolgen hebben. Vandaar dat er een grote behoefte is aan nieuwe diagnostische instrumenten en behandelingsvormen voor patiënten die niet van de momenteel beschikbare therapie kunnen profiteren. Ook daarom wordt veel onderzoek gedaan om de invloed van verschillende groeifactoren in skeletontwikkeling beter te begrijpen.

Een gewricht wordt in de regel gevormd door twee botten waarvan de uiteinden zijn bekleed met articulaire kraakbeen. Dit kraakbeen is spiegelglad en maakt samen met het intra-articulaire vocht een soepele beweging mogelijk. Daarbij is het articulaire kraakbeen erg elastisch, zodat het schokken kan opvangen zoals die bijvoorbeeld optreden bij lopen. Omdat articulaire kraakbeen avasculair is, is het nogal kwetsbaar en herstelt het slecht na het optreden van beschadiging. De laag van articulaire kraakbeen bij kinderen is relatief dik en deze neemt naarmate wij ouder worden langzaam af.

Wanneer het kraakbeen beschadigd raakt bij bijvoorbeeld een ongeval of herhaaldelijke blessures, zal uiteindelijk de soepele werking van het gewricht verloren gaan en kan de meest voorkomende gewrichtsaandoening, artrose, ontstaan.

Tussen het twintigste en dertigste levensjaar bereiken de botten hun maximale massa (piek-bot-massa). Voor een goede botopbouw zijn hoogwaardige voeding met voldoende vitamine D en calcium, lichaamsbeweging en zonlicht van belang. In de vierde of vijfde decade begint de botmassa af te nemen. Dit is het gevolg van toegenomen botafbraak door osteoclasten en verminderde botvorming door osteoblasten. Wanneer de botafbraak groter wordt dan de botaanmaak ontstaat botontkalking, oftewel osteoporose. Deze skeletziekte wordt gekarakteriseerd door een lage botmassa en het verlies van botstructuur. Osteoporose leidt tot een verhoogde kans op botbreuken, kleiner en krommer worden, orgaanlachten en evenwichtsverlies. Vrijwel alle geneesmiddelen die beschikbaar zijn voor de behandeling van osteoporose hebben anti-resorptieve effecten, waardoor ze de activiteit van de osteoclasten remmen. Deze geneesmiddelen verminderen het risico op fracturen, maar ze leiden niet tot een significante toename van de botmassa. Omdat verschillende groeifactoren de activiteit van osteoblasten en daarmee de botaanmaak kunnen stimuleren, bestaat er een grote interesse om hun precieze effecten in het botweefsel te begrijpen.

Fundamentele inzichten in de regulatie van skeletontwikkeling, groei, en bot- en kraakbeenmetabolisme verbeteren ons begrip in deze processen en verhogen daarmee de kans om alternatieve geneesmiddelen te vinden voor de behandeling van groeistoornissen, osteoporose en artrose. Wnt signalering is een zeer complexe biologische signaleringsroute, bestaande uit een groot aantal groeifactoren, receptoren en remmers, die aan elkaar binden in veel verschillende combinaties. Wnt signalering kan een groot aantal reacties uitvoeren in een verscheidenheid aan cellen en weefsels. De Wnt groeifactoren zijn hierdoor betrokken bij een breed scala aan ontwikkelingsprocessen. Daarnaast spelen zij een centrale rol in stamcelvernieuwing en proliferatie in verschillende weefsels zoals dikke darm, huid, en haarfollikels. In de laatste decennia hebben vele studies vastgesteld dat Wnt signalering een cruciale rol speelt in skeletontwikkeling en -onderhoud.

Tot nu toe zijn er 19 Wnt groeifactoren geïdentificeerd. Deze kunnen tenminste drie signaleringsroutes activeren: de canonische Wnt /  $\beta$ -catenine route, de Wnt/ $\text{Ca}^{2+}$  en de Wnt / vlakke polariteitsroute. Hiervan is de canonische Wnt /  $\beta$ -catenine route het beste begrepen. Deze signaleringsroute remt de differentiatie van chondrocyten, terwijl het de differentiatie van osteoblasten stimuleert. Echter, studies hebben aangetoond dat de niveaus van  $\beta$ -catenine zorgvuldig gereguleerd moeten worden. Te veel Wnt /  $\beta$ -catenine signalering interfereert met het differentiatiepotentieel van cellen. APC (adenomatosis polyposis coli) en GSK3 $\beta$  (glycogen synthase kinase 3 $\beta$ ) zijn twee intracellulaire eiwitten, die de hoeveelheid functioneel  $\beta$ -catenine in de kern bepalen. Hiermee kunnen ze het resulterende niveau van het Wnt signaal beïnvloeden. Een grondigere kennis van de functies van deze twee eiwitten zal ons helpen om het werkingsmechanisme van de Wnt /  $\beta$ -catenine signaleringsroute tijdens skeletontwikkeling en -onderhoud beter te kunnen begrijpen. In dit proefschrift hebben we de functies van Apc en Gsk3 $\beta$  in de complexe Wnt /  $\beta$ -catenine signaleringsroute tijdens skeletontwikkeling en -onderhoud verder uitgediept.

Tijdens de skeletontwikkeling zijn de eiwitniveaus van  $\beta$ -catenine in de canonische Wnt signaleringsroute doorslaggevend voor de differentiatie van skeletvoorlopercellen (SVC) in osteoblasten en chondrocyten. Om te onderzoeken of Apc ook betrokken is in deze processen hebben we de skeletontwikkeling van proefdiermuizen zonder functioneel Apc in SVCn bestudeerd. Deze muizen laten een sterk verhoogde canonisch Wnt signalering zien in hun skelet als gevolg van een functioneel verlies van Apc. Muizen waarin beide kopieën van het Apc gen uitgeschakeld zijn, stierven perinataal en toonden een sterk aangetaste botontwikkeling. Al hun lange botten waren misvormd en misten hun structurele integriteit. De meerderheid van de SVCn zonder functioneel Apc kon niet in chondrocyten of osteoblasten differentiëren. Echter, de SVCn in de proximale ribben waren in staat om aan het schadelijke effect van functioneel Apc verlies te ontsnappen en vormden zeer actieve osteoblasten. Apc inactivatie in chondrocyten was geassocieerd met dedifferentiatie van deze cellen. Onze resultaten in **hoofdstuk 2** bevestigen dat een strakke Apc-gemedieerde controle van de  $\beta$ -catenine niveaus essentieel is voor de differentiatie van SVCn. Daarnaast is Apc nodig voor het behoud van de chondrocyteïgenschappen in de reeds gevormde chondrocyten.

Tot op heden zijn alleen de aan / uit effecten van  $\beta$ -catenine op de differentiatie van SVCn onderzocht. Er zijn geen studies beschikbaar over de effecten van gemiddelde  $\beta$ -catenine niveaus tijdens de skeletontwikkeling. Apc staat bekend als de belangrijkste intracellulaire regulator van de dosering van transcriptioneel actief  $\beta$ -catenine. Om het effect van verschillende  $\beta$ -catenine doseringen op SVCn te kunnen onderzoeken, hebben we Apc mutante muizen gegenereerd met een conditioneel mutant allel ( $Apc^{15lox}$ ) en een hypomorphisch (minder functioneel) Apc mutant allel ( $Apc^{1638N}$  of  $Apc^{1572T}$ ). Dit resulteerde in verschillende niveaus van canonische Wnt signalering. Een relatief sterke toename van  $\beta$ -catenine in de SVCn van  $Col2a1-Cre; Apc^{15lox/1638N}$  embryo's leidde tot een volledige remming van kraakbeen- en botvorming. Een matig toegenomen niveau van  $\beta$ -catenine in de SVCn van  $Col2a1-Cre; Apc^{15lox/1572T}$  embryo's resulteerde in de vorming van zeer actieve osteoblasten, geen osteoclasten en vroegrijpe mineralisatie. Zo laten we in **hoofdstuk 3** zien dat een nauwkeurige dosering van de Wnt /  $\beta$ -catenine signalering door Apc nodig is voor de differentiatie van de SVCn.

Om een beter inzicht te krijgen in de moleculaire mechanismen waarmee Apc de differentiatie van SVCn beïnvloedt, hebben we de expressie van Apc in de muis mesenchymale stamcel-achtige KS483 cellijn verminderd. Gekweekte  $KS483-Apc_{si}$  cellen vertoonden een mesenchymaal-achtige morfologie, een sterk verminderde proliferatie en verhoogde apoptose. Hoewel de verlaging van het Apc eiwit in opregulatie van de Wnt /  $\beta$ -catenine en BMP / Smad signalering resulteerde, werd de osteogene differentiatie compleet geremd. Dit remmende effect kon worden opgeheven door toevoeging van hoge concentraties van BMP-7 in het differentiatie-medium. Daarnaast waren  $KS483-Apc_{si}$  cellen niet in staat om te differentiëren in chondrocyten of adipocyten. We tonen in **hoofdstuk 4** aan dat Apc essentieel is voor de proliferatie, overleving en differentiatie van KS483 cellen. Verlaging van Apc eiwit expressie blokkeert de osteogene differentiatie, een proces dat tegengegaan kan worden door verhoogde BMP signalering.

Humane heterozygote mutaties in het APC gen veroorzaken een erfelijke, uiteindelijk maligne, aandoening, waarbij honderden poliepen in de dikke darm voorkomen.

Deze ziekte staat bekend onder de naam familiale adenomateuze polyposis (FAP). Of *APC* mutaties een invloed op de botmassa hebben in de mens was niet bekend. Om dit te onderzoeken, hebben we een cross-sectionele studie uitgevoerd in FAP patiënten met een gedocumenteerde *APC* mutatie. Onze resultaten toonden aan dat deze patiënten een significant hogere botmassa hebben in vergelijking met gezonde controles. Ons enige inclusiecriteria voor deelname aan de studie was een bevestigd FAP syndroom, en ons enige exclusiecriteria was het gebruik van botmassamodulerende geneesmiddelen. FAP patiënten werden dus opgenomen in deze studie, ongeacht leeftijd, geslacht of de ernst van de ziekteverschijnselen. Onze studiepopulatie, weliswaar heterogeen, was representatief voor FAP patiënten, omdat alle klinische bevindingen aanwezig waren in verhoudingen die in andere FAP cohorten eerder zijn gemeld. Onze resultaten, beschreven in **hoofdstuk 5**, suggereren dat heterozygote *APC* mutaties een positief effect hebben op de botmassa, hoogst waarschijnlijk door verhoogde expressie van  $\beta$ -catenine.

De canonische Wnt /  $\beta$ -catenine signaleringsroute is bekend ook voor zijn functie in kraakbeenonderhoud. Omdat GSK3 $\beta$  een belangrijk Wnt-regulerend eiwit is wilden we nagaan wat de precieze rol van dit eiwit in kraakbeen is. Daarom hebben we chondrocyten *ex vivo* en *in vivo* met GIN behandeld, een selectieve GSK3 $\beta$  remmer. Efficiënte GSK3 $\beta$  remming werd gevalideerd door dosis-afhankelijke verhoging van de canonische Wnt signaleringsroute via  $\beta$ -catenine. In foetale muis middenvoetsbeentjes, resulteerde GIN behandeling in verlies van expressie van kraakbeengenen en verminderde chondrocytproliferatie. Late (3 dagen) effecten van GIN waren degradatie van de kraakbeenmatrix en een verhoogde apoptose, terwijl langdurige (7 dagen) GIN behandeling resulteerde in resorptie van het middenvoetsbeentje. Deze veranderingen werden bevestigd door middel van genexpressie-analyse, die een daling liet zien in de expressie van typische kraakbeen genen en inductie van de expressie van proteasen betrokken bij kraakbeenmatrixdegradatie. Intra-artculaire injectie van GIN in kniegewrichten van ratten veroorzaakte nucleaire accumulatie van  $\beta$ -catenine in chondrocyt-kernen. Dit ging gepaard met kraakbeenafbraak, oppervlaktefibrillatie en chondrocythypocellulariteit. Onze resultaten beschreven in **hoofdstuk 6** bewijzen dat GSK3 $\beta$  in het behoud van het chondrocyte fenotype en kraakbeenmatrix betrokken is door het verlaging van  $\beta$ -catenine. Bovendien kan remming van GSK3 $\beta$  in chondrocyten worden gebruikt om artrose-achtige functies *in vivo* te induceren.

Tenslotte zijn in **hoofdstuk 7** de bevindingen van dit proefschrift samengevat. Ook worden in dit hoofdstuk potentiële toekomstige onderzoeklijnen genoemd om de functie van *Apc* en GSK3 $\beta$  tijdens skeletontwikkeling en -onderhoud nog beter te kunnen begrijpen.





## List of publications





## LIST OF PUBLICATIONS

Miclea RL, Robanus-Maandag EC, Goeman JJ, Finos L, Bloys H, Oostdijk W, Löwik CW, Wit JM, Karperien M – *Inhibition of Gsk3 $\beta$  in cartilage induces osteoarthritic features through activation of the canonical Wnt signaling pathway*. Osteoarthritis Cartilage, 2011 Aug 27. [Epub ahead of print].

Miclea RL, van der Horst G, Robanus-Maandag EC, Lowik CW, Oostdijk W, Wit JM, Karperien M – *Apc bridges Wnt/ $\beta$ -catenin and BMP signaling during osteoblast differentiation of KS483 cells*. Exp Cell Res. 2011 Jun 10;317(10):1411-21

Miclea RL, Karperien M, Langers AM, Robanus-Maandag EC, van Lierop A, van der Hiel B, Stokkel MP, Ballieux BE, Oostdijk W, Wit JM, Vasen HF, Hamdy NA – *APC mutations are associated with increased bone mineral density in patients with familial adenomatous polyposis*. J Bone Miner Res. 2010 Dec;25(12):2624-32

Miclea RL, Karperien M, Bosch CA, van der Horst G, van der Valk MA, Kobayashi T, Kronenberg HM, Rawadi G, Akçakaya P, Lowik CW, Fodde R, Wit JM, Robanus-Maandag EC – *Adenomatous polyposis coli-mediated control of  $\beta$ -catenin is essential for both chondrogenic and osteogenic differentiation of skeletal precursors*. BMC Dev Biol. 2009 Apr;9(1):26

Miclea RL, Phillip M, Sävendahl L, Wit JM – *The 7th ESPE Growth Plate Working Group Symposium – EUROGROP June 27th 2007, Helsinki, Finland*. Pediatr Endocrinol Rev. 2007 Dec;5(2):680-5

Hendriks J, Miclea RL, Schotel R, Karperien M, Riesle J, van Blitterswijk CA – *Primary chondrocytes enhanced their cartilage tissue formation when co-cultured with dermal fibroblasts, 3T3 fibroblasts and embryonic stem cells*. Soft Matter. 2010 Mar 6:5080-5088

Hoogendam J, Parlevliet E, Miclea R, Löwik CW, Wit JM, Karperien M – *Novel early target genes of PTHrP in chondrocytes*. Endocrinology. 2006 Jun;147(6):3141-52

Miclea RL, Robanus-Maandag EC, Lowik CW, Oostdijk W, Fodde R, Wit JM, Karperien M – *Adenomatous polyposis coli-gene dosage controls  $\beta$ -catenin-mediated differentiation of skeletal precursors*. Manuscript in preparation.



## **Curriculum vitae**



## **CURRICULUM VITAE**

The author of this thesis was born on May 24<sup>th</sup>, 1979 in Oradea, Romania. He attended secondary school at the “Mihai Eminescu” high school in Oradea, where he got his Romanian Bacalaureate diploma in June 1998. He then started his study in Medicine at the “Iuliu Hațieganu” University of Medicine and Pharmacy in Cluj-Napoca, Romania, where he received his MD diploma in September 2004. During his medical study he performed a 3-months research project at the subdivision of Pediatric Endocrinology of the Leiden University Medical Center (LUMC) under the supervision of Prof. Dr. J. M. Wit and Dr. M. Karperien investigating possibilities to enhance the differentiation of KS483 cells into chondrocytes. From March 2005 until May 2010 he performed research for his present PhD project at the subdivision of Pediatric Endocrinology of the LUMC under the supervision of Prof. Dr. J. M. Wit, Dr. M. Karperien and Dr. E. C. Robanus-Maandag. For the research he conducted during his PhD program he received several fellowships and awards: in 2005 a Short Time Research Fellowship from the European Society for Pediatric Endocrinology (ESPE, Lyon, FR); in 2006 a Travel Award from the ESPE (Rotterdam, NL); in 2007 a Young Investigator Award from the European Calcified Tissue Society (ECTS, Copenhagen, DK); in 2008 a Travel Award from the ECTS (Barcelona, Spain). He began his training in radiology in May 2010 in the LUMC, under the supervision of Prof. Dr. J. L. Bloem.



## **Dankwoord**





## DANKWOORD

It takes only two to tango but it surely takes a hundred to finalize a PhD thesis. If you are reading these lines you most likely have contributed directly or indirectly to this thesis. Therefore thank you! I will be forever grateful to you all! I would like to use this opportunity to personally thank some of you.

My promotor, Prof. Dr. Jan Maarten Wit. Jan Maarten, thank you very much for the opportunity you gave me to conduct a PhD study under your supervision. Your scientific enthusiasm and curiosity have inspired me throughout the years! You gave me a lot of freedom in my research, yet you were always carefully guiding and encouraging what turned out to be a rewarding project.

My co-promotor, Dr. Marcel Karperien. Marcel, I have learned so much from you (too much to be named here), for which I express my deepest gratitude. In the first years from close by, later from Twente, you always stimulated me to get the most from my experiments. The foundation of this thesis lays in your ideas.

My co-promotor, Dr. Els Robanus-Maandag. Els, many thanks for “adopting” me after Marcel left for Twente. Your accuracy and critical point-of-view have always had a positive effect on the interpretation of my results.

Dr. Neveen Hamdy, thank you for supervising the BOMFAP study with your great experience in clinical research.

Dr. Wilma Oostdijk, thank you for your interest in my project and for your constructive feedback.

I'd like to thank my *Kinder-ENDO* research colleagues Hermine, Joyce, Remco and Sandy, who ensured that I was constantly engaged and entertained along the way. Special thanks to Jakomijn for initiating me in the bio-medical research lab.

I thank my office mates, Geertje and Jimmy for their contribution to the cheerful, yet productive atmosphere we had the luck to work in.

I would like to thank the people from the ENDO-lab for their support and *gezelligheid*. Annemiek, Antoon, Chris, Christel, Claudia, Edwin, Eric, Gabri, Guido, Hanna, Henny, Henry, Ineke, Isabel, Ivo, Janna, Janny, Judith, Karien, Laura, Maggy, Martiene, Patrick, Petra, Thomas, Rutger, Trea, Vicky have all made me feel at home in the ENDO-lab although I was a *kinder-AIO*. Special thanks to Hetty for familiarizing me with several molecular biology techniques and to Lianne for her histological expertise.

I am grateful to Prof. Dr. Clemens Löwik, Prof. Dr. Hans Romijn and Prof. Dr. Jan Smit for their valuable comments and hospitality.

I would like to definitely acknowledge all the FAP patients that volunteered to participate in the BOMFAP study as well as Prof. Dr. Hans Vasen for helpful discussions during the course of this clinical study.

I am indebted to Dr. Livio Finos, Dr. Jelle Goeman and Dr. Ron Wolterbeek for their statistical expertise that has indubitably contributed to the coherence of this thesis.

Thanks to the secretaries of the Pediatrics department for their assistance, especially Mirjam Vollebregt, who always provided a prompt answer to my administrative dilemmas.

My appreciation also goes to my two Bachelor students that I had the chance to supervise. Both Celia and Pinar impressed me with their determination, that I'm sure will help them a lot in their future careers.

I'd also like to thank my two paranymphs, Jeroen and Michel. I am very happy to have such friends besides me on this memorable day. I hope you both feel the same.

*În final aș dori să mă adresez familiei mele fără de care această carte ar fi fost infinit mai săracă. Socrilor mei le mulțumesc pentru suportul și bunătatea lor cu care ne înconjoară de peste țări și de aproape.*

*Nico, Dinu, Alex, Roxi, Tușa, Iulia și Muși, deși departe, unii nedrept de departe, dragostea voastră m-a ajutat, poate fără să știți, să duc la bun sfârșit acest proiect.*

*Părinților mei le voi fi mereu îndatorat. Mami și Tati, m-ați ajutat să mă ridic iar apoi m-ați încurajat să îmi urmez drumul ce-l doresc în viață, deși asta a însemnat să mă vedeți plecat. Căldura și dragostea voastră necondiționată m-au sprijinit și impulsionat mereu.*

*Sara, îngerașul meu, sper să îți placă acum albastrul copertei și să fii mândră de tati peste ani când sper să vrei să citești câteva rânduri din această teză. În prezența ta, tot restul devine nesemnificativ.*

*Cristina, ești farul meu pe furtună și pe cer senin, dimineața și seara, ieri și mâine. Îți dai seama că la câtă apă e în Olanda, fără lumina ta m-aș fi rătăcit demult. Îți mulțumesc pentru că ești. Te iubesc din tot sufletul meu!*

